Development of Antimicrobial Impregnated Catheter Coatings to Prevent Uropathogenic *Escherichia coli* Infections

Kelly Laura Capper-Parkin

A thesis submitted in partial fulfilment of the requirements of

Sheffield Hallam University

for the degree of Doctor of Philosophy

October 2023

Candidate declaration

I hereby declare that:

1. I have not been enrolled for another award of the University, or other academic or professional organisation, whilst undertaking my research degree.

2. None of the material contained in the thesis has been used in any other submission for an academic award.

3. I am aware of and understand the University's policy on plagiarism and certify that this thesis is my own work. The use of all published or other sources of material consulted have been properly and fully acknowledged.

4. The work undertaken towards the thesis has been conducted in accordance with the SHU Principles of Integrity in Research and the SHU Research Ethics Policy.

5. The word count of the thesis is 37608 words

Name	Kelly Capper-Parkin
Date	16th October 2023
Award	PhD
Research Institute	Biomolecular Sciences Research Centre/ I2RI
Director of Studies	Dr Sarah Forbes

Abstract

Background: Urinary catheters are an essential medical device, used in the management of urinary incontinence and retention. However, catheters provide an abiotic surface upon which bacteria may colonise and form biofilms recalcitrant to immune clearance and antibiotic therapy. The incidence of catheter associated urinary tract infection (CAUTI) is a significant burden for healthcare systems, with uropathogenic *Escherichia coli* (UPEC) posing as one of the most common causative pathogens. The development of an effective anti-infective catheter coating which could prevent biofilm formation upon the catheter surface would be therefore have significant impact on improving the quality of life for catheterised patients.

Methods: Presented here is a study into the development of potential antimicrobial containing sol-gel coatings to prevent UPEC colonisation and biofilm formation. Broad spectrum biocides and quorum sensing inhibitors (QSI) were evaluated for their potential as anti-infective coating agents both independently and in pairwise combinations to assess synergistic antimicrobial and cytotoxic activity. The impact of long-term biocide/QSI exposure on the bacterial transcriptome and proteome was determined and correlated to changes in bacterial susceptibility impacting overall coating efficacy. Biocides and QSIs were incorporated into a novel sol-gel coating system. Anti-biofilm potential was determined within a continuous culture drip flow reactor model and elution of antimicrobials from the sol-gel coating was determined via mass spectrometry.

Results: Biocides and QSIs often displayed synergistic antibiofilm activity. The most promising initial combination of biocide and QSI was PHMB with cinnamaldehyde with regards to high antimicrobial activity and low cytotoxicity, however following incorporation into a sol-gel coating and evaluation in a drip flow model, silver nitrate with cinnamaldehyde demonstrated the best efficacy at reducing of biofilm formation. Long-term exposure to the test biocides and QSI led to a high number of changes within the transcriptome, frequently associated with regulation of motility associated genes, however this was not mirrored in the proteomics data, where fewer significantly differentially expressed proteins were observed. Regarding release of the test agents from the sol-gel coating, the elution of silver nitrate was rapid compared to the elution of BAC which did not elute readily from the coating.

Conclusions: In the development of an antimicrobial impregnated catheter coating to prevent UPEC infection, the combination of silver nitrate with cinnamaldehyde demonstrates promise. The combination of silver nitrate with cinnamaldehyde was found to be synergistically antimicrobial, both antimicrobials elute from the coating, rapidly in the case of silver nitrate and slower in the case of cinnamaldehyde, and it was shown to reduce the biofilm formed within a continuous culture drip flow reactor model.

Acknowledgements

A huge thank you to my fantastic supervisors. I have grown so much through this PhD, and it is down to you all and your support. Dr Sarah Forbes, my DoS who has been a fantastic supervisor and mentor over the past 4+ years, always there to help whenever I have needed it in all situations. Dr Tim Nichol, who has answered so many questions of mine, has always been helpful and so patient with me and the endless stream of mass spec issues I have had over the years. Thanks to Dr Mel Lacey, who has helped me to broaden my experience and all the extracurricular activities you have roped me in to. Professor Tom Smith, whose knowledge seems endless and whose insightful questions have broadened my knowledge.

Thank you so much to everyone who started with me in 2019! You have all been so supportive over the years, the best team anyone could have around them. To all the BMRC PhD students, thank you! There have been some challenges over the years, but from the camaraderie of the covid times to the laughs in the office and the unwavering support throughout, thank you!

Thanks to my family, who have always encouraged my love of science since I was little. Thanks for your interest and patience as I have worked to explain what I am now doing to you. I'd hope you have a good idea what I do now.

Possibly the biggest thank you goes to Sam. Your seemingly never-ending patience with me over these years, for carrying me when times have been tough and for just simply being amazing. Thank you!

Contents

List of Figures

List of Tables

List of Abbreviations

Term	Definition
*	$p \leq 0.05$
**	$p \leq 0.01$
***	$p \leq 0.001$
****	$p \leq 0.0001$
AHL	Acyl-homoserine lactone
AI-2	Autoinducer 2
AMR	Antimicrobial resistance
AU	Artificial urine
BAC	Benzalkonium chloride
BSMC	Bladder smooth muscle cells
CAUTI	Catheter associated urinary tract infections
CFU	Colony forming units
CV	Crystal violet
DFR	Drip Flow Biofilm Reactor
DPD	4,5-dihydroxy-2,3-pentandione
EC958	UPEC strain EC958
EMEM	Eagles' minimum essential medium
EPS	Extracellular polymeric substance
FBS	Foetal bovine serum
FC	Fold change
F-DPD	4-fluoro-5-hydroxypentane-2,3-dione
FDR	False discovery rate
FIC	Fractional Inhibitory concentration
FICI	Fractional Inhibitory concentration index
Furanone-C30	(z)-4-bromo-5(bromomethylene)-2(5H)-furanone
GFP	Green fluorescent protein
HCAI	Healthcare associated infections
HUEPC	Human uroepithelial cells
IBC	Intracellular bacterial communities
ICP-MS	Inductively coupled plasma – mass spectrometry
IPA	Isopropyl alcohol
L929	Mouse fibroblast cells of the cell line L929
LC-MS	Liquid chromatography mass spectrometry
LOD	Limit of detection
LOQ	Limit of quantitation
MBC	Minimum bactericidal concentration
MBEC	Minimum biofilm eradication concentration
MHA	Mueller Hinton Agar
MHB	Mueller Hinton Broth
MIC	Minimum inhibitory concentration
MTMS	Trimethoxymethylsilane
MTT	3-(4,5-dimethylthiazol-2-yl)-2,5-diphenyltetrazolium bromide
PBS	Phosphate buffered saline
PDMS	Polydimethylsiloxane
PHMB	Polyhexamethylene biguanide

QS	Quorum sensing
QSI	Quorum sensing inhibitor
TEOS	Tetraethyl orthosilicate
TMOS	Tetramethyl orthosilicate
UPEC	Uropathogenic *Escherichia coli*
UTI	Urinary tract infection

1.
General Introduction

1.1.Introduction.

Antimicrobial coated medical devices are widespread throughout the medical field. However, the selection of antimicrobial resistant bacterial populations is a common cause for device failure. In order to fully evaluate the long-term anti-infective potential of any medical device coating we need to understand how bacteria will respond to the antimicrobial over time. Urinary catheters are one of the most commonly used medical device, however, long-term catheterisation comes with a significant risk of infection. An antimicrobial catheter coating which prevents microbial colonisation of the catheter surface could be effective in reducing the incidence of catheter associated urinary tract infections (CAUTI) and significantly contribute towards improved patient health.

Previous work has characterised the effects of long-term exposure of a panel eight uropathogenic *Escherichia coli* strains to 7 proposed anti-infective catheter coating agents, including four biocides and three quorum sensing inhibitors. Changes in antimicrobial susceptibility, growth, biofilm formation and relative pathogenicity were evaluated after long-term antimicrobial exposure at sub-lethal concentrations. To correlate changes in phenotype with genotype, genome sequencing and RNA-sequencing was performed. Variant analysis and differential gene expression analysis revealed the selection of mutations and changes in gene expression after biocide exposure (Henly, 2019).

In this current work we expand upon these previous findings by including proteomic analysis of the antimicrobial adapted UPEC isolates to further understand the mechanisms that govern antimicrobial adaptation. We evaluated synergistic antimicrobial, antibiofilm and cytotoxic activity of our biocides and QSIs to allow us to identify appropriate combinations of antimicrobials to take forward into a sol-gel based anti-infective catheter coating formulation. The growth inhibitory, bactericidal, and anti-biofilm properties of our sol-gel coatings was determined in batch and continuous culture systems. Elution profiles of antimicrobials from the sol-gel was determined by mass spectrometry.

1.2. Catheter associated urinary tract infections.

Urinary catheterisation is a common medical intervention for draining the bladder in healthcare settings and in the wider community. Catheterisation is used to aid both management of incontinence and urinary retention as a result of neurological conditions, bladder dysfunction, in the care of immobile or less mobile patients, and to aid in surgery (Nicolle, 2014; Feneley, Hopley and Wells, 2015). Long-term catheterisation is typically achieved through the use of the Foley catheter (Figure 1.1). The catheter is inserted into the bladder through the urethra and held in place by inflation of a balloon (Feneley, Hopley and Wells, 2015). Other catheter designs include the suprapubic catheter or intermittent catheters. There is some evidence to suggest that intermittent catheters have lower incidence of urinary tract infections (UTI) compared to long term catheterisation, however much more research is required to confirm this (Kinnear *et al.*, 2020).

Asymptomatic bacteriuria is common in catheterised patients and is not treated as a CAUTI unless it progresses with other indications of infection, such as a fever and positive urine cultures (Lo *et al.*, 2014). Urinary tract infections account for 36% of health care associated infections (HCAIs) and CAUTIs account for an average of 80% of nosocomial UTIs (Jacobsen *et al.*, 2008) with a range of 67% to 97% occurrence in general hospital admissions and ICUs respectively (Parker *et al.*, 2017). 70-80% of complicated UTIs in the United States are associated with the presence of an indwelling catheter (Flores-Mireles *et al.*, 2015). Risk of infection increases with each day of catheterisation (Letica-Kriegel *et al.*, 2019) and can lead to a wide range of complications including: obstruction of the catheter, bladder stones, prostatitis, pyelonephritis and bacteraemia (Nicolle, 2014). Bacteraemia as a result of CAUTI is the outcome in 1-4% of cases (Saint and Chenoweth, 2003) and is associated with a 30%-40% mortality rate (Melzer and Welch, 2013). CAUTIs are a significant burden on healthcare systems worldwide and incur significant costs. The annual cost of CAUTI for the NHS is estimated to be between £1 - 2.5 billion (Feneley, Hopley and Wells, 2015). In the USA, it is estimated that a case of CAUTI costs from $876 – $10,197 per patient dependent upon severity of infection (Hollenbeak and Schilling, 2018).

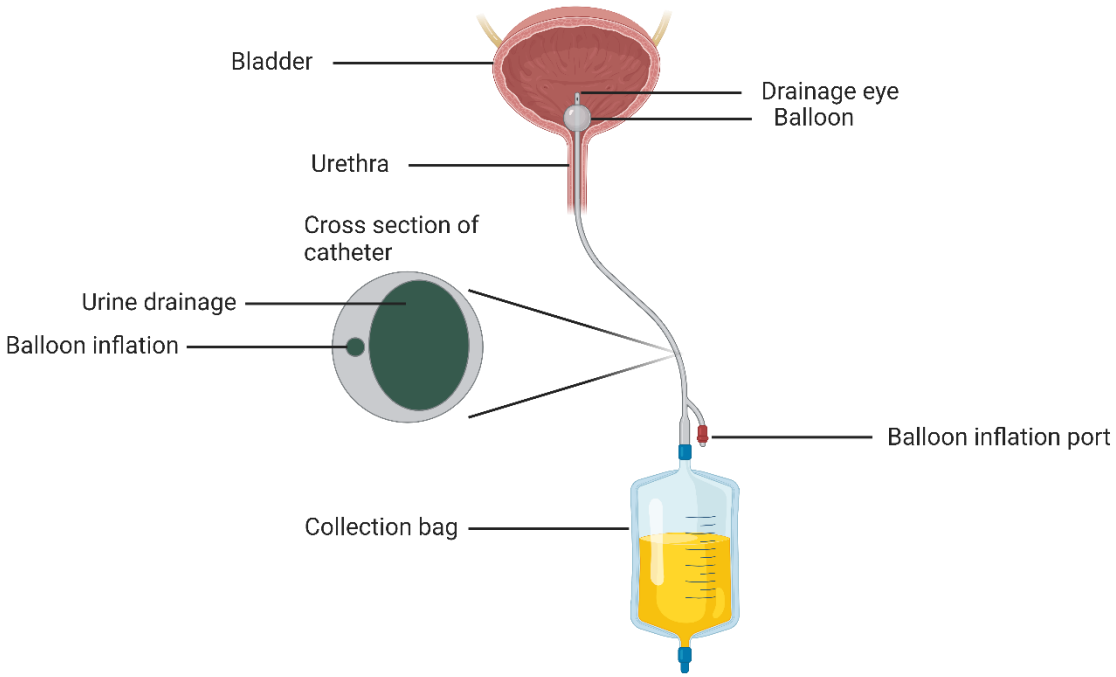

Figure 1.1. Foley catheter held in place within the bladder by inflation of the balloon. Cross section of the catheter shows the larger drainage hole and the opening through which the balloon is inflated.

There are many microbial species associated with CAUTI including, but not limited to; *Escherichia coli, Proteus* spp. including *P. mirabilis* and *P. vulgaris, Pseudomonas aeruginosa, Klebsiella* spp. including *K. pneumoniae, Enterococcus* spp. including *E. faecalis*, *Staphylococcus* spp. including *S. aureus* and *S. epidermidis, Citrobacter freundii, Providentia rettgeri* and *Candida* spp. including *C. albicans* (Nicolle, 2014; Mandakhalikar, Chua and Tambyah, 2016; Cortese *et al.*, 2018). Despite the plethora of potential infectious agents that may cause CAUTI, the most prevalent species contributing to this infection is uropathogenic *Escherichia coli* (UPEC).

1.3. Uropathogenic Escherichia coli.

UPEC is the most common causative organism of UTIs, is responsible for up to 75% of uncomplicated UTIs and 65% of complicated UTIs (Flores-Mireles *et al.*, 2015). *E. coli* is the most commonly isolated organism (43%) from bacteraemic episodes following catheterisation (Melzer and Welch, 2013; Nicolle, 2014). Virulence factors associated

with UPEC include those facilitating biofilm formation and infection such as adhesins, iron acquisition systems and secretion of toxins, however, there is wide heterogeneity across UPEC strains (Tartof *et al.*, 2005; Jacobsen *et al.*, 2008; Totsika *et al.*, 2011; Kakkanat *et al.*, 2017).

Sequence type (ST) 131 is the most commonly isolated UPEC strain and is disseminated globally (Tartof *et al.*, 2005; Totsika *et al.*, 2011). EC958 is representative of ST131; a multidrug resistant UPEC strain originally isolated from a UTI patient in the northwest of England (Totsika *et al.*, 2011; Forde *et al.*, 2014). It is an extended spectrum β-lactamase (ESBL) producing, fluoroquinolone resistant strain and carries virulence associated genes including adhesins, autotransporters and iron receptors (Forde *et al.*, 2014). Another key strain is CFT073, a pyelonephritic strain of UPEC which is highly cytotoxic (Mobley *et al.*, 1990). Both EC958 and CFT073 express similar virulence factors and form mature biofilms (Totsika *et al.*, 2011).

1.3.1. Biofilm formation

The formation of biofilms is potentially the most predominant challenge associated with UPEC infections. Bacterial biofilms are communities of bacteria within a self-secreted extracellular polymeric substance, providing bacteria with protection from host defences and antimicrobials. Biofilms also provide support for a community of bacteria with multiple phenotypes through the generation of distinct gradients of nutrients and oxygen allowing the growth of species with diverse metabolic requirements. Biofilms frequently contain a sub-population of dormant cells, known as persisters, cells that exist in a low metabolic activity state. Persisters are known to exhibit low antimicrobial susceptibility and are attributed with recalcitrant infections (López, Vlamakis and Kolter, 2010). Biofilms are a key aspect of the pathogenesis of UPEC and can form on the external surface or intraluminally within the catheter. During infections biofilms have also been shown to establish on the surface or within host cells as intracellular biofilm communities (IBC) (Terlizzi, Gribaudo and Maffei, 2017). Biofilms are a key aspect of most chronic bacterial infections due to their recalcitrance to antibiotic therapy (Stewart and Costerton, 2001).

Biofilm formation can be divided into 5 stages, see Figure 1.2. Initiation of biofilm formation is dependent upon expression of motility associated genes including flagella,

which allow the bacteria to reach the surface, overcome and repulsive electrostatic or van der Waals forces and reversibly attach to an underlying conditioning film or abiotic surface (Pratt and Kolter, 1998). Surface adhesins, including fimbriae and pili are then involved in permanent attachment to the surface/host cell. Once attached to the surface microcolonies form and cells begin to secrete an extracellular polymeric substance of proteins, polysaccharides and DNA which surrounds the bacteria forming mature biofilms (López, Vlamakis and Kolter, 2010). Individual cells or small sections of the biofilm break off or disperse from the mature biofilm and colonise new sections of the catheter or urinary tract.

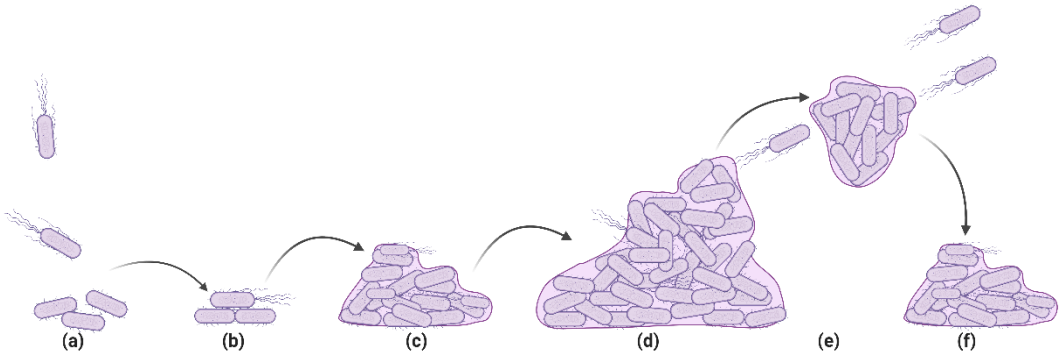

Figure 1.2. Depiction of biofilm formation. (a) Bacterial cells land on the surface/cell membrane with reversible attachment, followed by (b) irreversible adhesion of cells to the surface. (c) Biofilms then mature with secretion of extra polymeric substances (EPS) eventually forming (d) a mature biofilm with different cellular phenotypes present within the oxygen and nutrient gradients of the biofilm. (e) Dispersal of biofilm from mature biofilm occurs through release of individual cells or sections of the biofilm breaking off to (f) form new biofilms elsewhere. Figure created with BioRender.com.

1.3.2. Biofilms and pathogenesis

UPEC biofilms may become established on the catheter surface or within the lumen, potentially impairing drainage of the catheter. The presence of persister cells within the biofilm provide a reservoir of bacteria for subsequent infection. Additionally, UPEC have been shown to exhibit a biofilm phenotype via the formation of IBC within the host cells of the urinary tract, helping to evade immune detection and allowing persistence of an infection. These IBCs may contain as many as 10^5 bacteria per cell, this is often a source

of recurrent UTI (Terlizzi, Gribaudo and Maffei, 2017). The structure of the biofilm aids the recalcitrance to antimicrobial therapy. A mature biofilm has a complex structure which provides an effective barrier to antimicrobials, preventing the antimicrobial from reaching its target, and the density of the biofilm can create areas of oxygen and nutrient gradients, affecting the phenotypes of the of the bacteria within (Orazi and O'Toole, 2019).

The main challenge in prevention of recurrent UPEC infections is to prevent biofilm formation, thereby increasing the effectiveness of any implemented antibiotic therapy. Once biofilms form there is the establishment of persister populations, which withstand antibiotic treatment and allow the re-activation of UPEC infection in the host once therapy has concluded.

1.4. Existing methods of CAUTI prevention.

Currently the most effective method to reduce the incidence of CAUTI is to focus on the reduction of unnecessary catheter usage and to implement appropriate hygiene procedures when handling catheters (Parker *et al.*, 2017). Where a catheter is required, behavioural changes are the second line of defence, including close monitoring of the patient, staff training on infection prevention, increased regularity of changing the catheter, cleaning the area around the site of insertion and use of closed drainage systems (Lo *et al.*, 2014). Despite a robust approach to catheter care by healthcare providers, the problem of CAUTI still remains and is one of the largest contributors towards healthcare associated infection. In order to further reduce infection rates, research has focused on the development of effective anti-infective catheter coatings.

Anti-infective catheter coatings currently in use across global healthcare settings include Nitrofurazone impregnated (ReleaseNF, Rochester Medical) and silver coated (Lubri-Sil and Bardex IC, Bard Care). These have been used in clinical settings with mixed outcomes (Johnson, Kuskowski and Wilt, 2006; Menezes *et al.*, 2019) and are not currently recommended for use by the NHS due to insufficient evidence of their benefit versus the additional cost (Loveday *et al.*, 2014). A Cochrane review of catheter usage concluded that silver alloy catheters did not reduce the burden of CAUTI, nitrofurazone impregnated catheters increased discomfort for patients and the best approach is to

reduce the number of unnecessary catheterisations (Lam *et al.*, 2014). Whilst numerous anti-infective catheter coatings have shown promise in *in vitro* studies, there is concern that antimicrobial activity will be short lived in practice either due to elution of the active agent from the coating over time (Johnson, Johnston and Kuskowski, 2012), due to blockage of antimicrobial activity as the catheter becomes coated in host proteins post insertion, or due to the selection of microbial populations with reduced antimicrobial susceptibility as they become exposed to sub-lethal concentrations of antimicrobial as it is released from the catheter (Mandakhalikar, Chua and Tambyah, 2016; Singha, Locklin and Handa, 2017; Anjum *et al.*, 2018; Majeed *et al.*, 2019; Andersen and Flores-Mireles, 2020; Werneburg, 2022). There are further concerns over the cytotoxicity of coating agents, as concentrations required to prevent microbial colonisation over long-periods of time may cause cytotoxic effects within the urinary tract. Due to the lack of anti-infective catheter coatings that display prolonged antimicrobial efficacy and low cytotoxicity there has been an active search for new approaches. A more recent consideration is to use quorum sensing inhibitors to prevent biofilm establishment on the catheter surface.

1.5. Quorum sensing and inhibitors

Quorum sensing (QS) is a density dependent chemical communication system found across all bacteria. Small molecules known as autoinducers, are secreted by bacteria into the environment, upon detection by neighbouring cells they are internalised and elicit a change in gene expression dependent upon reaching a threshold concentration.

One of the most common QS mechanisms of bacteria uses the autoinducer acyl-homoserine lactone (AHL) (Papenfort and Bassler, 2016). *E. coli* do not have an AHL synthase gene; however, they do express a homologue of the *luxR* AHL receptor gene – *sdiA*, and modulate gene expression as a result of exposure to external AHLs which may occur during a mixed species infection (Houdt *et al.*, 2006).

Figure 1.3 shows the mechanism of AHL mediated quorum sensing in *E. coli*. SdiA has a C-terminal DNA binding domain and N-terminal autoinducer binding domain, which is capable of binding to different structured AHLs. Binding of the AHL to the autoinducer

(AI) binding domain allows dimerisation of the SdiA molecule which then modulates transcription regulation (Yao *et al.*, 2006).

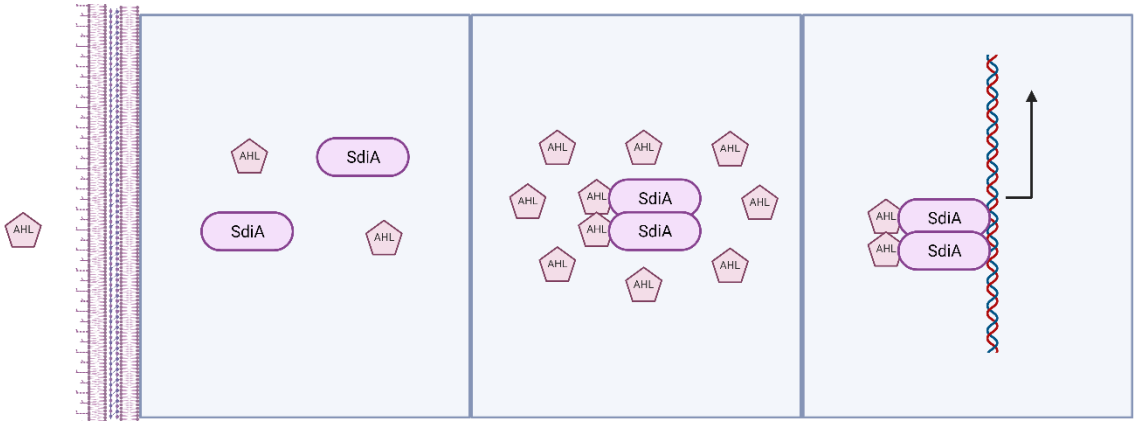

Figure 1.3. AHL mediates quorum sensing in *E. coli.* *E. coli* do not express an AHL synthase, however they do expresses a LuxR homologue – SdiA. AHL dissolves through the membrane freely and above threshold concentrations, binds to SdiA. The AHL-SdiA complex binds to the DNA at lux boxes and modulates transcription of specific genes. Figure created in Biorender.

The main quorum sensing mechanism in *E. coli* uses autoinducer-2 (AI-2). The AI-2 signalling system is composed of the transporter complex *lsrACDB*, the repressor *lsrR*, and signal kinase *lsrK*. LuxS is a 4,5-dihydroxy-2,3-pentanedione (DPD) synthase, DPD then spontaneously cyclises to form the AI-2 molecule recognised by the cell (Li *et al.*, 2007). Figure 1.4 shows the mechanism of AI-2 signalling in *E. coli*. AI-2 is released from the cell and accumulates until a threshold limit is reached, where it is then internalised via the transporter complex. Within the cell it is phosphorylated by LsrK, phospho-AI-2 then inhibits the repression of gene expression by LsrR (Li *et al.*, 2007). AI-2 has been shown to induce biofilm formation in *E. coli* through *mqsR,* a regulator gene which induces expression of genes associated with chemotaxis, flagellar synthesis and motility (González Barrios *et al.*, 2006).

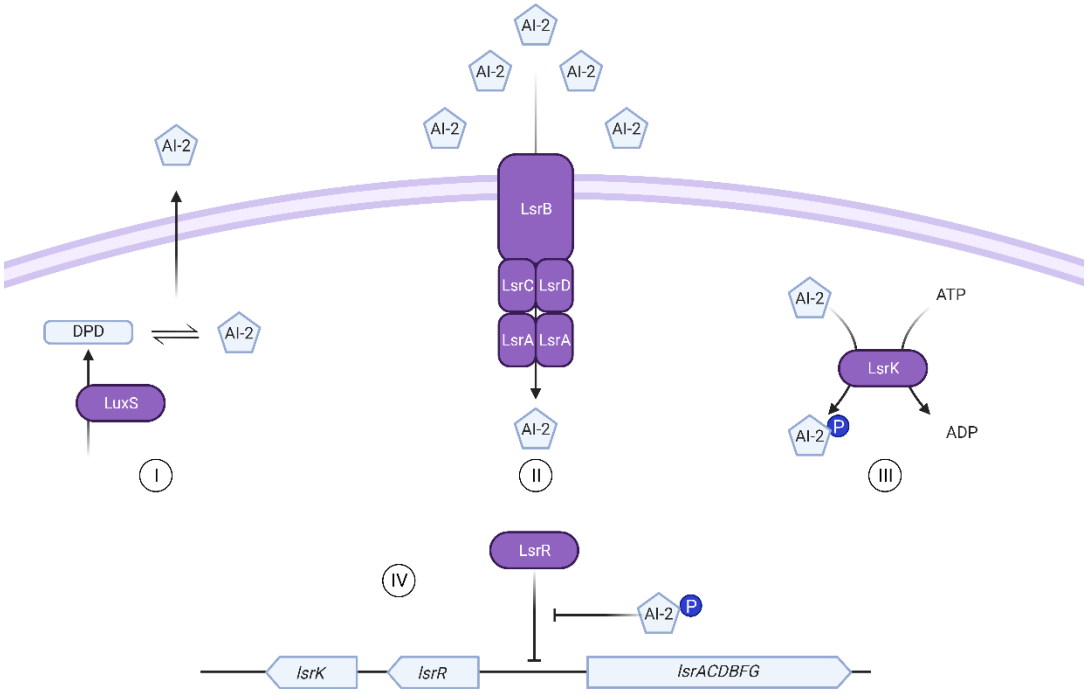

Figure 1.4. AI-2 signalling of E. coli. LuxS is a DPD synthase, DPD spontaneously cyclises into the general structure of AI-2. Once threshold limit is reached of AI-2 externally of the cell it is internalised via the Lsr transporter complex, within the cell it is phosphorylated by LsrK. Phospho-AI-2 inhibits the inhibition of the *lsr* operon by LsrR. Figure created in Biorender.

1.5.1. Quorum sensing inhibitors

Quorum sensing allows the cell density dependent regulation of gene expression in bacteria. Many genes modulated as a response to quorum sensing are associated with virulence factors and biofilm formation (Guo *et al.*, 2013; Papenfort and Bassler, 2016; Rubini *et al.*, 2020). Use of quorum sensing inhibitors (QSIs) are a novel strategy to prevent infection through disruption of the virulence phenotype without killing the bacteria, reducing the chance of resistance developing as the selective pressure is lower (Guo *et al.*, 2013). Quorum sensing inhibitors are characterised as anti-pathogenic drugs which may target either generation of the signal, the signal receptor, or the signal molecule itself (Rasmussen and Givskov, 2006). Detection of novel QSI is often through the screening of analogues of autoinducers in combination with genetic reporter systems (Rasmussen and Givskov, 2006; Styles *et al.*, 2020). Antimicrobial molecules have also been found to have QSI properties at sub inhibitory concentrations, of particular interest to this thesis is cinnamaldehyde (Niu, Afre and Gilbert, 2006).

1.5.2. Cinnamaldehyde

The main component of cinnamon essential oil is *trans*-cinnamaldehyde (Zhang *et al.*, 2016). The *sdiA* gene of *E. coli* encodes an AHL receptor with similar structure and function to LuxR and activation is possible with a large number of AHL based autoinducers (Yao *et al.*, 2006; Styles *et al.*, 2020). Although the exact mechanism of quorum sensing inhibition in *E. coli* by cinnamaldehyde has not been elucidated, it has been investigated within *Vibrio* spp. It has been proposed that the α,β unsaturated carbonyl of cinnamaldehyde binds to the nucleophilic amino acid side chains of LuxR, thereby reducing the ability of LuxR to bind to the DNA (Brackman *et al.*, 2008, 2011).

Cinnamaldehyde has also been demonstrated to reduce surface adhesin expression and biofilm formation in *E. coli* in a number of studies (Niu and Gilbert, 2004; Amalaradjou *et al.*, 2010; Amalaradjou, Narayanan and Venkitanarayanan, 2011; Kot *et al.*, 2015). At high concentrations cinnamaldehyde has antimicrobial properties which include morphological changes to the membrane and permeabilization leading to leakage of proteins and DNA (Zhang *et al.*, 2016), inhibition of ATP and ATPases and inhibition of cell division via inhibition of FtsZ (Doyle and Stephens, 2019).

1.5.3. Furanone-C30

Brominated furanones, derived from the algae *Delisea pulchra* and synthetically produced, have been demonstrated to interrupt quorum sensing in bacteria (Brackman and Coenye, 2015). In Gram-negative bacteria, furanones at subinhibitory concentrations have been shown to negatively impact or inhibit biofilm formation (Ren, Sims and Wood, 2001; Hentzer *et al.*, 2002; Janssens *et al.*, 2008). *E. coli* biofilms were thinner, contained fewer water channels and had a higher proportion of dead cells within when treated with sub-inhibitory concentrations of (*5Z*)-4-bromo-5-(bromomethylene)-3-butyl-2(*5H*)-furanone (furanone-C30) (Ren, Sims and Wood, 2001).

Quorum sensing inhibition by brominated furanones is also known to be mediated through the AHL signalling system. Furanone compounds compete with AHLs to bind to

LuxR, inducing a conformational change which increases the degradation of the LuxR-furanone complex (Hentzer *et al.*, 2002; Manefield *et al.*, 2002). LuxS suppression by furanone derived compounds has been observed in Gram-positive bacteria, unlike for Gram-negative bacteria the outcome was an increase in biofilm formation (Kuehl *et al.*, 2009). Furanones have been observed to inhibit quorum sensing via the AI-2 pathway in *V. harveyi*, however, the mechanisms of this are not yet clear, but it has been suggested that this may be achieved by the same mechanism as observed in the LuxS suppression in Gram-positive bacteria (Ren, Sims and Wood, 2001).

1.5.4. F-DPD

Auto-inducer 2 (AI-2) molecules are derived from 4,5-dihydroxy-2,3-pentanedione (DPD) which spontaneously cyclises to form AI-2 (Guo *et al.*, 2013). Analogues of DPD have been investigated as inhibitors of AI-2 based QS including the use of isobutyl-DPD, phenyl-DPD (Roy *et al.*, 2013) and 4-fluoro-DPD (F-DPD) (Henly *et al.*, 2021). Suggested mechanisms of DPD analogue interruption of QS include that phospho-DPD analogues may competitively bind to LsrR without activating the receptor (Roy *et al.*, 2013).

1.6. Biocides

Biocides are broad spectrum antimicrobials which have multiple bacteriostatic and bactericidal modes of action. A potential benefit of using biocides in a catheter coating is the lack of a single selective pressure upon the bacteria meaning that potential mutations leading to resistance are less likely to occur. Despite this, there have been several reports of bacteria becoming less susceptible to certain biocides after exposure at sub-lethal concentrations, suggested to be due to the selection of resistant mutants or induced phenotypic adaptations. These changes may be transient and revert once the selective pressure is removed or they may be sustained. Additionally, there is concern that exposure to sub-lethal concentrations of biocide may induce changes in susceptibility to third party agents, including antibiotics, owing to the selection of mutations in shared target sites or through the induction of broad defence mechanisms (Henly *et al.*, 2019; Westfall *et al.*, 2019; Merchel Piovesan Pereira, Wang and Tagkopoulos, 2020, 2021).

1.6.1. PHMB

Polyhexamethylene biguanide (PHMB) is a polymer of biguanide groups interlinked with hexamethylene chains in 2-40 repeats (Allen, White and Morby, 2006; Rembe *et al.*, 2016). Longer polymer lengths are correlated with higher antimicrobial activity (Gilbert and Moore, 2005; Allen, White and Morby, 2006). PHMB interacts with the membranes of bacterial cells, via displacement of Ca^{2+} ions and binding to lipopolysaccharides, leading to formation of immobile and inflexible lipid rafts resulting in membrane fissures and intracellular leakage and eventual cell lysis due to membrane precipitation at high concentrations (Gilbert and Moore, 2005). Shorter polymers more readily gain access into the cytoplasm where it has been shown to condense DNA (Sowlati-Hashjin, Carbone and Karttunen, 2020).

1.6.2. BAC

Benzalkonium chloride is an amphoteric surfactant with a variable chain length ranging from 8-18 carbons. It interrupts the lipid layers of cells leading to leakage of components. At low concentrations it is associated with loss of osmolarity and leakage of key ions and at higher concentrations it solubilises the membranes. The proposed mechanism is that the positive nitrogen atom within the molecule interacts with the phospholipid head groups and subsequently the tail inserts itself into the membrane core. The insertion of BAC into the membrane results in a loss of the hydrophobic region found between the two layers of the membrane, leading to dysfunction of the proteins within and eventually leading to cell lysis (Gilbert and Moore, 2005).

1.6.3. Silver nitrate

Silver ions are commonly used biocides. Silver ions interact with the sulfhydryl (thiol) groups of proteins, leading to inactivation of enzymes and inhibiting cell function, damaging the cell envelope and inhibiting growth (Furr *et al.*, 1994; Woo *et al.*, 2008). Silver has been associated with cytoplasmic membrane shrinkage to the extent of detachment from the cell wall (Feng *et al.*, 2000). Increased permeability of the membrane due to silver is associated with dysregulation of membrane potential

(Majeed *et al.*, 2019). Silver has also been observed in condensed DNA, further inhibiting cell replication (Feng *et al.*, 2000).

1.6.4. Triclosan

Triclosan is a chlorinated phenolic compound which is used commonly in cleaning products, and has been detected within the blood, milk and urine of humans due to general daily exposure (Calafat *et al.*, 2008; Kim *et al.*, 2011; Alfhili and Lee, 2019). Triclosan binds to the enoyl-acyl carrier protein reductase, FabI, halting fatty acid synthesis (Levy, McMurry and Oethinger, 1998; Stewart *et al.*, 1999; Russell, 2004). Inhibition of fatty acids leads to membrane damage, destabilisation and leakage (Russell, 2004).

1.7.Sol-gel

Sol-gel technology has been in use for decades, it is a relatively simple process that is based upon the hydrolysis and condensation reactions within a colloidal suspension (the sol) to polymerise into a gel structure that when dried onto a surface, which can be used as a coating (Jones, 1989). Benefits to using sol-gel technology include the low processing temperatures, use of liquid precursors and simple processing (Wang and Bierwagen, 2009). Many aspects of sol-gel synthesis can be tuned to create the optimum coating through modification of pH, temperature, catalyst used, ratio of water, aging time, drying time and choice of molecular precursors (Jones, 1989; Brinker *et al.*, 1992; Wang and Bierwagen, 2009; Owens *et al.*, 2016; Rivero and Goicoechea, 2016).

Silicon alkoxide based sol-gel coatings have been investigated in a number of studies for biomedical purposes. They have been used in the delivery of antimicrobials with good biocompatibility (Adams *et al.*, 2009; Jaiswal, McHale and Duffy, 2012; Owens *et al.*, 2016; Nichol *et al.*, 2021). In a comparison with poly(hydroxyethymethacrylate) (pHEMA) and poly(ethylene glycol) (PEG) as coatings containing the above biocides and QSIs, the silicon alkoxide based sol-gel was observed to have the highest biocompatibility (Henly, 2019).

1.8. Aims and objectives of the thesis

The overall aim of this thesis is to develop and demonstrate the efficacy of a non-cytotoxic antimicrobial urinary catheter coating to prevent the formation of UPEC biofilms on the catheter surface through combination of biocides and QSIs within a sol-gel coating.

1. The first aim of this thesis is a continuation of Henly's (2019) work on the adaptation of EC958 following long-term exposure to biocides and QSIs by investigation of induced transcriptomic and proteomic changes. We further consider how these changes relate to phenotypic alterations that may impact long-term coating efficacy (Chapter 2).
2. The second aim was to develop an effective antimicrobial catheter coating through the following 3 objectives.

   (i) Profiling the elution of each antimicrobial from the sol-gel coating over the period of a week via mass spectrometry (Chapter 3).

   (ii) Evaluation of synergistic bacteriostatic, bactericidal, and anti-biofilm activity of biocides and QSIs and identification of acceptable cytotoxicity of the effective antimicrobial combinations (Chapter 4).

   (iii) Validation of the anti-biofilm efficacy of the biocide and QSI containing sol-gel coating in a drip flow reactor model (Chapter 5).

2.
Bacterial Adaptation to Biocides and Quorum Sensing Inhibitors – Transcriptomics and Proteomics

Passaging of bacterial isolates in the presence of biocides, phenotypic analysis of generated isolates and early transcriptomic analysis of QSI passaged isolates was performed by Emma Henly et al and have been published in:

> Henly, E. L., Dowling, J. A. R., Maingay, J. B., Lacey, M. M., Smith, T. J., & Forbes, S. (2019). Biocide Exposure Induces Changes in Susceptibility, Pathogenicity, and Biofilm Formation in Uropathogenic Escherichia coli. Antimicrobial Agents and Chemotherapy, 63(3). https://doi.org/10.1128/AAC.01892-18

and

> Henly, E. L., Norris, K., Rawson, K., Zoulias, N., Jaques, L., Chirila, P. G., Parkin, K. L., Kadirvel, M., Whiteoak, C., Smith, T. J., Lacey, M. M., & Forbes, S. (2021). Impact of long-term quorum sensing inhibition on uropathogenic Escherichia coli. Journal of Antimicrobial Chemotherapy, dkaa517. https://doi.org/10.1093/jac/dkaa517

and

> Henly, E. L. (2019). Antimicrobial Adaptation in Uropathogenic Escherichia coli. (Doctoral Thesis) Sheffield Hallam University.

Proteomics experiments were performed by Khoa Pham of the biOMICS Facility, Faculty of Science Mass Spectrometry Centre, University of Sheffield.

2.1.Abstract

Background: Anti-infective coating strategies for implantable medical devices are becoming widespread across the medical field. Concerns have however been raised wide-spread use of these coatings may promote the selection of antimicrobial resistant bacterial populations or induce changes in individual strains resulting in altered phenotypic characteristics potentially impacting resistance and pathogenicity.

Methods: To assess this, uropathogenic *E. coli* strain EC958 was passaged twelve times in the presence or absence of sub-lethal concentrations of the biocides (polyhexamethylene biguanide (PHMB), benzalkonium chloride (BAC), silver nitrate and triclosan) or quorum sensing inhibitors (*trans*-cinnamaldehyde, (z)-4-bromo-5(bromomethylene)-2(5H)-furanone (furanone-C30) and F-DPD). Change in phenotype and antimicrobial susceptibility profiles were compared to a control passaged on an antimicrobial free media. Genome sequencing with variant analysis and RNA-sequencing with differential gene expression analysis was completed previously in *E. coli* EC958, see Henly (2019). In this chapter, further investigation into the changes within the transcriptome was performed by gene ontology analysis and assessment of differential protein expression was determined via mass spectrometry.

Results: A high number of genes were differentially regulated in response to long-term exposure to the antimicrobials when compared to the passaged control. A change in biofilm formation was observed for the majority of the antimicrobial adapted isolates and within the transcript data genes related to chemotaxis and locomotion were overrepresented in PHMB, BAC, cinnamaldehyde and furanone-C30 exposed isolates. However, a much smaller number of proteins were significantly differentially expressed. Cinnamaldehyde resulted in the highest number of differentially expressed proteins, including many involved in chemotaxis which were over expressed which could be associated with the observed increase in biofilm formation.

No proteins were differentially expressed following exposure to F-DPD, where the only phenotypic change was a reduction in biofilm formation on a catheter surface. However, triclosan also had no differentially expressed proteins, but had significant increases in resistance to triclosan, cross resistance to nitrofurantoin, increased biofilm formation on a polystyrene plate, reduced biofilm formation on a catheter and reduced pathogenicity. There were instances of a lack of concordance between the transcript

and protein data, with instances of a number of proteins differentially expressed which were oppositely expressed in the transcriptomic data. This is likely due to substantial variation in protein profiles between biological replicates during proteomic analysis.

Conclusions: Long-term exposure to each biocide and QSI led to a unique phenotype, and a unique combination of differentially expressed genes and proteins. Genes associated with motility were over-represented by down regulated genes in PHMB, BAC, cinnamaldehyde and F-DPD conditions. However, changes in protein expression were much fewer; no differentially expressed proteins were observed following long-term exposure to triclosan and F-DPD, whereas a high number of proteins were differentially expressed by the cinnamaldehyde exposed strain.

2.2.Introduction

Uropathogenic *E. coli* (UPEC) are a significant causative organism of catheter associated urinary tract infections (CAUTI) (Flores-Mireles *et al.*, 2015). One key strain of UPEC is EC958 which has been identified in urinary tract infections across the globe and harbours multiple antibiotic resistance genes and multiple virulence factors including adhesins, autotransporters and iron receptors (Totsika *et al.*, 2011; Forde *et al.*, 2014).

Antimicrobial resistance (AMR) is an urgent global issue with an estimated 4.95 million deaths in 2019, with *E. coli* identified as one of the key pathogens contributing towards these mortality rates (Murray *et al.*, 2022). UPEC, including EC958, carry their antibiotic resistance genes within a plasmid which has potential for conjugal transfer between strains and species allowing the dissemination of antibiotic resistance throughout a microbial community (Totsika *et al.*, 2011). The spread of antibiotic resistance is promoted through wide-spread antibiotic use, providing a selective environment for resistant microbial pathogens. The use of biocides as alternative anti-infective agents to antibiotics has been suggested to reduce the chance of resistance developing, due to the multiple target sites of action of the biocides. However, resistance against biocides has been observed previously and there have been cases of cross-resistance occurring towards other antimicrobials including clinically relevant antibiotics (Blair *et al.*, 2015; Cowley *et al.*, 2015; Forbes *et al.*, 2015; Singha, Locklin and Handa, 2017; Kampf, 2018). Alternative anti-virulence agents such as quorum sensing inhibitors (QSIs) are presumed to be less likely to lead to antimicrobial resistance since they do not exert a selective pressure on the survival of the bacteria and instead may act through modulation of virulence only (Høiby *et al.*, 2010).

In a previous investigation, UPEC isolate EC958 was repeatedly exposed to the biocides (polyhexamethylene biguanide (PHMB), benzalkonium chloride (BAC), silver nitrate and triclosan) and QSIs (*trans*-cinnamaldehyde, (z)-4-bromo-5(bromomethylene)-2(5H)-furanone (furanone-C30) and 4-fluoro-5-hydroxypentane-2,3-dione (F-DPD) over twelve passages. The resultant changes to the phenotype (summarised in Table 2.1), genotype and transcriptome were analysed (Henly, 2019; Henly *et al.*, 2019, 2021).

Decreases in susceptibility to the exposed antimicrobial were observed following exposure to PHMB (MIC and MBC only), cinnamaldehyde and furanone-C30, for all other

biocides there was an increase in resistance to the test antimicrobial whilst no susceptibility change was observed following exposure to F-DPD. Only triclosan demonstrated induced cross-resistance to an antibiotic, which was towards nitrofurantoin. Reductions in pathogenicity were observed following exposure to PHMB, BAC, triclosan and furanone-C30 and biofilm formation varied, dependent upon the isolate and antimicrobial (Table 2.1). A number of genome mutations were observed in biocide adapted UPEC isolates, including some which were observed following exposure to all antimicrobials. RNA-sequencing indicated that a large number of genes were differentially regulated after biocide exposure, as discussed in Henly (2019).

Table 2.1. Summary of phenotypic changes in EC958 observed following long-term exposure to biocides and QSIs.

Phenotypic assay	PHMB	BAC	Silver nitrate	Triclosan	Cinnamaldehyde	Furanone-C30	F-DPD
MIC fold change	-0.2	2	2	260	-2	-3	-
MBC fold change	-0.9	-	16	8	-5	-2	-
MBEC fold change	42.4	4	1.3	125	-2	-2	-
Cross resistance	-	-	-	Nitrofurantoin resistance	-	-	-
Biofilm formation – plate	-	Increase	-	Increase	Increase	Increase	-
Biofilm formation – catheter	Decrease	-	-	Decrease	-	Decrease	Decrease
Pathogenicity	Decrease	Decrease	-	Decrease	-	Decrease	-
BSM cell invasion	-	Increase	-	-	-	-	-

Data originally published in (Henly, 2019; Henly *et al.*, 2019, 2021)*. "-" indicates no significant change.*

2.2.1. Aims of this chapter

Previous work into characterisation of long-term biocide and QSI exposure in EC958 outlined alternations in the phenotype, genome and transcriptome. This chapter further investigates the transcriptomic changes through interrogation of the biological function of these genes through gene ontology analysis. Furthermore, proteomic profiles were determined after biocide exposure through mass spectrometry and comparisons of the transcriptome to the proteome were made. Identification of the differentially expressed proteins and the potential correlations to the phenotypic data are discussed.

2.3.Methods

2.3.1. Bacterial strains and long-term biocide exposure

All chemicals were sourced from Sigma Aldrich, UK, unless stated otherwise. Bacteria were cultured in Mueller Hinton broth (MHB) or on Mueller Hinton agar (MHA) and incubated under aerobic conditions at 37°C overnight before use unless otherwise stated.

UPEC strain EC958 was exposed to PHMB (Vantocil, Lonza, UK), BAC, silver nitrate (Alfa Aesar, UK), triclosan, cinnamaldehyde, furanone-C30 (synthesised in house as described in Guo et al. (2009)) and F-DPD at 5x MBC concentration in a well in the centre of an agar plate providing a diffusion gradient prior to incubation for 2 days at 37°C. The closest biomass to the well was passaged onto a fresh test plate containing an equivalent antimicrobial gradient, this was repeated over 12 passages. Bacteria were archived in 50% glycerol at -80°C for future use (Henly *et al.*, 2019, 2021).

2.3.2. Transcriptomics

RNA sequencing and identification of significantly up or down regulated genes is described in (Henly, 2019).

Lists of genes which were identified as significantly differentially regulated were uploaded to PANTHER (v18.0, http://www.pantherdb.org/, Mi et al., 2019). The statistical overrepresentation test was selected and compared to the reference genome of *E. coli*, with annotation by the gene ontology (GO) data sets of biological process, molecular function, and cellular component. Test type was Fisher's Exact with calculation of the false discovery rate (FDR). The statistical overrepresentation test compares the number of genes from the differentially regulated list within a GO term to the number of genes expected within that GO term from the reference genome. Statistically significant GO terms ($p \leq 0.05$ and $FDR \leq 0.05$) were identified of genes which were overrepresented (higher number of genes within that term represented than expected) and underrepresented (lower number of genes represented in the differentially expressed list compared to the whole genome within a single GO term).

2.3.3. Proteomics

Protein extraction was performed on overnight cultures diluted 1:100 and grown to mid-log phase (OD_{600} of 0.4). Cells were then pelleted and washed 3 times in 3ml of ice-cold phosphate buffered saline (PBS, Gibco). Cells were resuspended in 5ml extraction buffer (5% SDS in 50mM Tris (pH 7, Fisher Chemical) with 1% protease inhibitor cocktail and 50 µg/ml lysozyme) and incubated on ice for 15 minutes prior to sonication at 40% amplitude in 6 x 30 second bursts. Protein was precipitated in 1:1:8 solution of cell lysate: trichloroacetic acid (6.1N): acetone (Fisher Chemical) and incubated at -20^{o}C for 1 hour. Protein was pelleted at 16,000 x g, washed three times in 1 ml acetone and dissolved in 2 ml rehydration buffer (5% SDS/50mM Tris (pH 7) with 1% protease inhibitor). Protein was quantified using a bicinchoninic acid (BCA) assay as per kit instructions (Pierce™ BCA Protein Assay Kit, ThermoScientific).

Protein analysis was completed by the biOMICS Facility, University of Sheffield. Briefly, 15 µg of protein was prepared for analysis by the S-trap technique followed by trypsin digestion at 47^{o}C for 2 hours. Samples were run on an Orbitrap Elite MS coupled with a nano-HPLC Ultimate 3000 system, samples were run over a 155-minute HPLC gradient, and the 20 most abundant ions were selected for MS/MS analysis. MS data was analysed in Maxquant V1.6.10.43 with reference to the *E. coli* O25b_H4 protein database for protein identification and quantitation of protein abundances. Data was then submitted to Perseus V1.6.15.0 for statistical analysis. Protein abundance was normalised to the median of each sample and missing values were imputated. Heatmaps of expression and principal component analysis of all samples were performed. Pairwise comparisons of antimicrobial exposed conditions compared to the passaged control were performed with t-test analysis and cut offs of $\alpha = 0.05$ and FDR = 0.05 to identify proteins with significantly different expression.

2.4.Results

Uropathogenic *E. coli* strain EC958 was exposed to the biocides (PHMB, BAC, silver nitrate or triclosan) or QSIs (cinnamaldehyde, furanone-C30 or F-DPD) over the course of 12 passages on solid media, and the transcriptomic and proteomic changes were compared to a control strain passaged in the absence of any antimicrobial.

Pairwise comparisons of the EC958 antimicrobial exposed and passaged control strains identified genes which were differentially expressed. The results and discussion of specific genes were documented by Henly (2019). Identification of changes in biological process, molecular function and cellular component was performed through gene ontology based analysis for each biocide and QSI using PANTHERdb (Mi *et al.*, 2019).

Differential expression analysis of the protein profiles after antimicrobial exposure were also performed through mass spectrometry. Principle component analysis (Figure 2.1) and hierarchical clustering of the proteins from each isolate (Figure 2.2) suggests that the cinnamaldehyde exposed isolate has the most significantly altered proteome. The control, PHMB and BAC exposed isolates cluster independently, whereas the silver nitrate, triclosan, furanone-C30 and F-DPD exposed conditions are more dispersed and overlap.

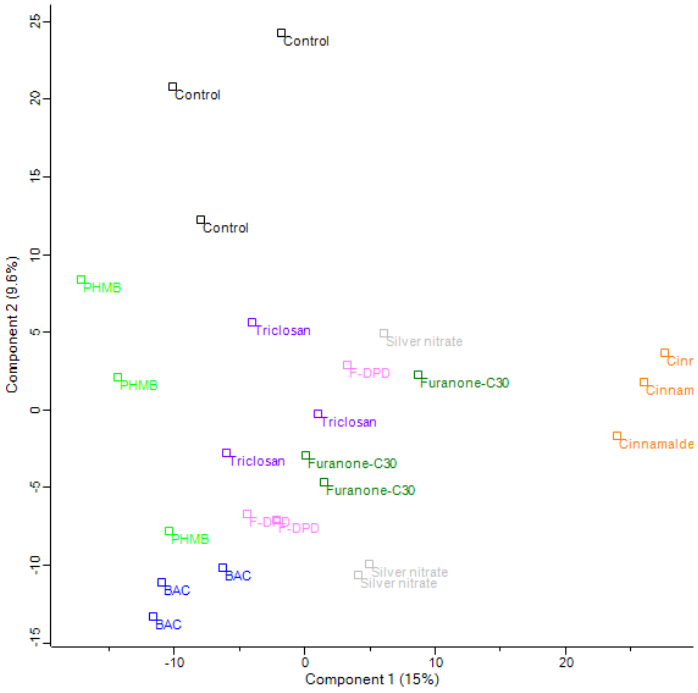

Figure 2.1 . Principal component analysis of differential protein expression of all passaged conditions.

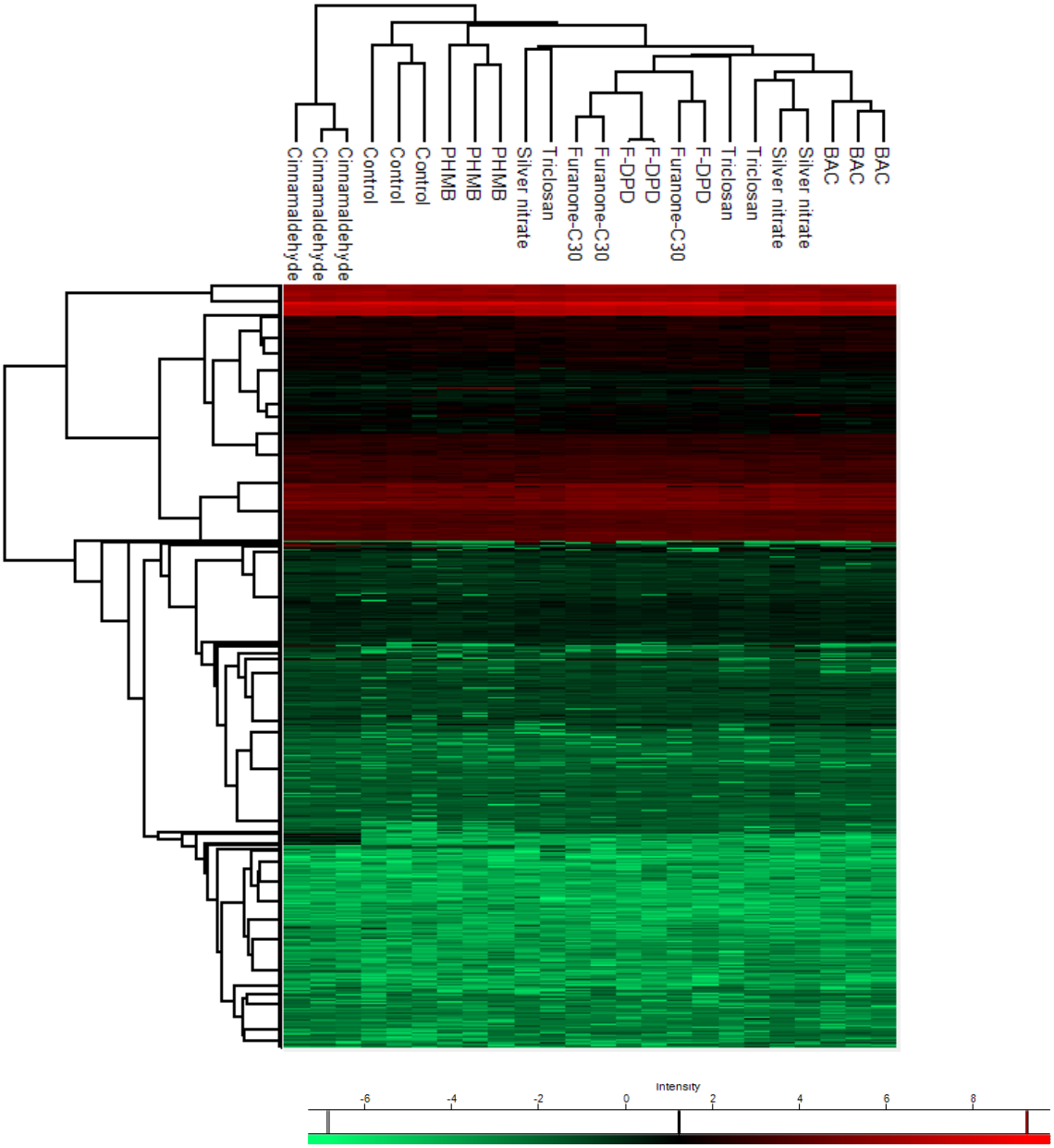

Figure 2.2. Heatmap analysis of protein expression and hierarchical clustering of proteins and conditions. Row and column trees created based upon the Euclidean distance pre-processed with k-means based upon the Log_2 fold change of protein expression.

2.4.1. Transcriptomic and proteomic changes following PMHB exposure

Long-term exposure to PHMB led differential expression of 405 genes, of these 284 were mapped to GO terms within PANTHER. Within the GO terms, groups of potential interest include over representation of genes associated with chemotaxis (GO:0006935) and cytoskeletal motor activity (GO:0003774) and a significant down-regulation of genes associated with the bacterial-type flagellum (GO:000j9288).Terms relating to nucleic acid activity including nucleic acid metabolic process (GO:0090304) and catalytic activity acting on a nucleic acid (GO:0022804) were underrepresented (Table 2.2).

A single protein was identified as significantly differentially expressed following PHMB exposure, this was a phosphogluconate dehydratase Edd, with a Log_2 fold change of +2.47 ($p < 0.001$), which is responsible for dehydration of D-gluconate 6-phosphate into 2-dehydro-3-deoxy-D-gluconate 6-phosphate as part of the gluconate metabolic pathway within *E. coli* (Zablotny & Fraenkel, 1967) (Figure 2.3).

Table 2.2. Summary of GO biological process, molecular function, and cellular component groups over- or under-represented following exposure to PHMB.

GO biological process		Number of genes	Fold enrichment	p-value
Cellular process	GO:0009987	239	1.28	1.23×10^{-11}
Organic acid metabolic process	GO:0006082	63	1.7	4.89×10^{-5}
Catabolic process	GO:0009056	64	1.84	3.74×10^{-6}
Galactarate metabolic process	GO:0019580	6	15.46	3.22×10^{-5}
Localization	GO:0051179	86	1.79	8.42×10^{-8}
Chemotaxis	GO:0006935	14	5.85	1.14×10^{-6}
Organic substance transport	GO:0071702	66	2.11	1.85×10^{-8}
Glutamine family amino acid metabolic process	GO:0009064	12	3.26	7.73×10^{-4}
Alpha-amino acid catabolic process	GO:1901606	14	3.09	4.50×10^{-4}
Sulphate assimilation	GO:0000103	6	10.31	1.49×10^{-4}
Locomotion	GO:0040011	14	5.85	1.14×10^{-6}
Amide catabolic process	GO:0043605	7	8.33	1.11×10^{-4}
Glyoxylate metabolic process	GO:0046487	7	7.73	1.57×10^{-4}
Tricarboxylic acid cycle	GO:0006099	10	5.15	9.68×10^{-5}
Cell motility	GO:0048870	14	3.38	2.02×10^{-4}
Nitrogen compound transport	GO:0071705	36	1.95	2.47×10^{-4}
Organic cyclic compound metabolic process	GO:1901360	33	0.56	1.25×10^{-4}
Organic substance biosynthetic process	GO:1901576	28	0.49	6.57×10^{-6}
Nucleic acid metabolic process	GO:0090304	16	0.48	9.70×10^{-5}
Macromolecule biosynthetic process	GO:0009059	10	0.37	2.64×10^{-4}
GO Molecular function				
Cytoskeletal motor activity	GO:0003774	6	11.6	9.44×10^{-5}
Transporter activity	GO:0005215	62	1.71	4.37×10^{-5}
Active transmembrane transporter activity	GO:0022804	36	2.04	1.06×10^{-4}
Catalytic activity, acting on a nucleic acid	GO:0140640	4	0.21	5.30×10^{-5}
GO Cellular component				
Cellular anatomical entity	GO:0110165	220	1.15	4.74×10^{-4}
Cell projection	GO:0042995	15	3.31	1.46×10^{-4}
Bacterial-type flagellum	GO:0009288	13	6.09	1.93×10^{-6}
ATP-binding cassette (ABC) transporter complex, substrate-binding subunit-containing	GO:0055052	29	3.01	6.61×10^{-7}
Intracellular organelle	GO:0043229	0	< 0.01	2.27×10^{-4}

Only parent groups and select subgroups shown, some groups have multiple subgroups within them, not shown.

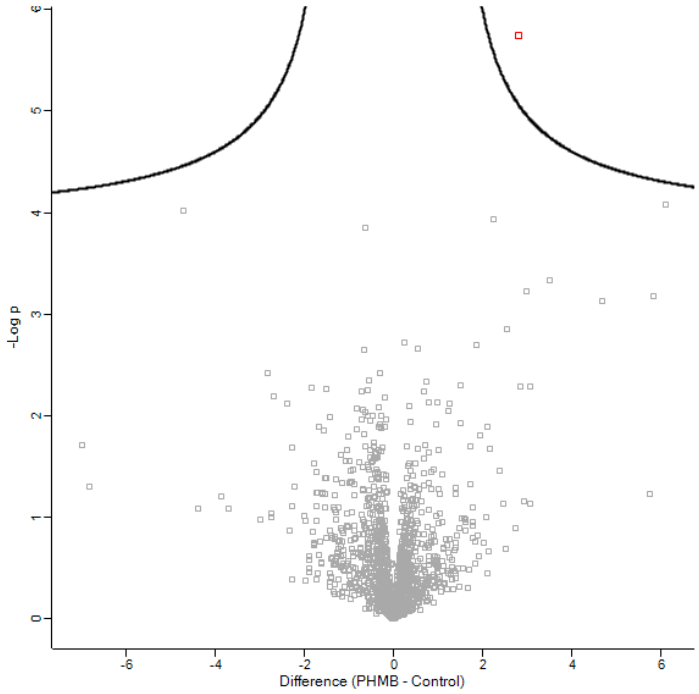

Figure 2.3. Volcano plot of protein expression of EC958 passaged in the presence or absence of PHMB compared to passaged control strain. Cut offs determined by two-sided t-test with a false discovery rate of 0.05 and a s0 value of 0.1. Significantly differentially expressed proteins identified by red squares.

2.4.2. Transcriptomic and proteomic changes following BAC exposure

Following exposure to BAC, 352 genes were differentially expressed. This included genes associated with locomotion (GO:0040011), cell motility (GO:0048870) and the bacterial-type flagellum motor and secretion (GO:0120100 and GO:0120102) which were predominantly down regulated (Appendix, Table 8.2). Whereas genes associated with nucleic acid metabolic processes (GO:0090304), DNA binding (GO:0003677) and catalytic activity acting on a nucleic acid (GO:0140640) were all underrepresented (Table 2.3).

Following long-term exposure to BAC, 21 proteins were over expressed and 11 under expressed compared to the passaged control (Figure 2.4). The highest over expressed proteins were 2-oxoglutarate reductase SerA, deoxyribonucleoside regulator YjhU and acetyl-coenzyme A synthetase Acs. The most under-expressed proteins were NADH-quinone oxidoreductase subunit NuoH, phosphatase NudJ and uronate isomerase UxaC, (Table 2.4).

Table 2.3. Summary of GO biological process, molecular function and cellular component groups over- or under-represented following exposure to BAC.

GO biological process		Number of genes	Fold enrichment	p-value
Cellular process	GO:0009987	237	1.25	1.37×10^{-9}
Organonitrogen compound metabolic process	GO:1901564	91	1.43	3.54×10^{-4}
Small molecule catabolic process	GO:0044282	39	1.82	5.84×10^{-4}
Amide metabolic process	GO:0043603	43	2.9	2.68×10^{-9}
Cell motility	GO:0048870	24	5.72	2.23×10^{-10}
Regulation of response to external stimulus	GO:0032101	6	8.32	3.58×10^{-4}
Protein secretion by the type III secretion system	GO:0030254	6	10.17	1.61×10^{-4}
Purine-containing compound metabolic process	GO:0072521	19	2.5	6.87×10^{-4}
Locomotion	GO:0040011	23	9.48	1.77×10^{-13}
Response to external stimulus	GO:0009605	28	2.27	$1.24E \times 10^{-4}$
Reactive nitrogen species metabolic process	GO:2001057	11	5.59	2.37×10^{-5}
Peptide metabolic process	GO:0006518	27	2.88	3.53×10^{-6}
Organelle organization	GO:0006996	30	3.27	9.01×10^{-8}
Cellular component biogenesis	GO:0044085	42	1.73	8.04×10^{-4}
Nucleobase metabolic process	GO:0009112	11	3.29	1.20×10^{-3}
Protein-containing complex organization	GO:0043933	28	2.37	7.72×10^{-5}
Nucleic acid metabolic process	GO:0090304	10	0.3	1.72×10^{-6}
GO Molecular function				
Cytoskeletal motor activity	GO:0003774	6	11.44	1.02×10^{-4}
rRNA binding	GO:0019843	22	5.5	2.36×10^{-9}
Structural molecule activity	GO:0005198	27	5.49	3.35×10^{-11}
DNA binding	GO:0003677	15	0.43	1.41×10^{-4}
Catalytic activity, acting on a nucleic acid	GO:0140640	3	0.15	6.17×10^{-6}
GO Cellular component				
Organelle	GO:0043226	49	4.27	6.26×10^{-16}
Bacterial-type flagellum motor	GO:0120100	5	12.71	2.90×10^{-4}
Protein-containing complex	GO:0032991	99	1.61	7.69×10^{-7}
Type III protein secretion system complex	GO:0030257	6	10.17	1.61×10^{-4}
Bacterial-type flagellum secretion apparatus	GO:0120102	6	10.17	1.61×10^{-4}
Intracellular organelle	GO:0043229	29	3.11	3.64×10^{-7}
Large ribosomal subunit	GO:0015934	14	6.28	5.88×10^{-7}

Only parent groups shown, some groups have multiple subgroups within them. Number of genes is the number of significantly differentially expressed between conditions.

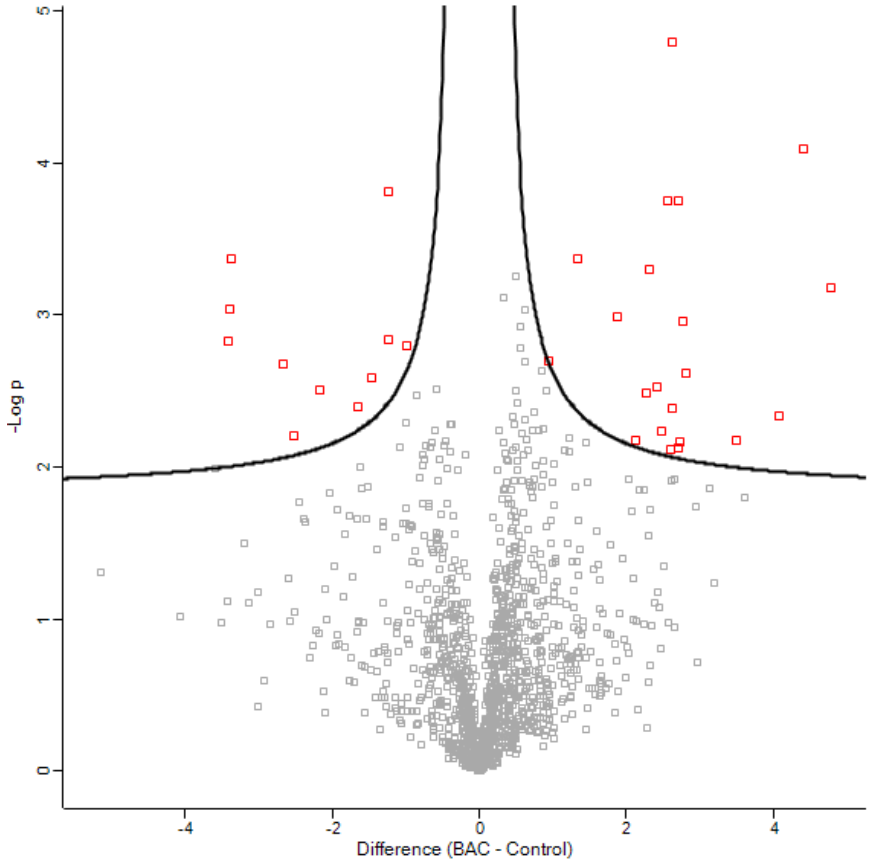

Figure 2.4. Volcano plot of protein expression of EC958 passaged in the presence of BAC compared to a passaged control strain. Cut offs determined by two-sided t-test with a false discovery rate of 0.05 and a s0 value of 0.1. Significantly differentially expressed proteins identified by red squares.

Table 2.4. All proteins differentially expressed in EC958 following long-term exposure to BAC.

Protein	Gene	Log_2 fold change	p-value
Over-expressed			
2-oxoglutarate reductase	*serA*	4.77	6.60×10^{-4}
Deoxyribonucleoside regulator	*yjhU*	4.41	7.94×10^{-5}
Acetyl-coenzyme A synthetase	*acs*	4.08	4.52×10^{-3}
GTP cyclohydrolase 1	*folE*	3.49	6.60×10^{-3}
L-serine dehydratase	*sdaA*	2.81	2.40×10^{-3}
Cytochrome bd-I ubiquinol oxidase subunit 2	*cydB*	2.75	1.10×10^{-3}
4-aminobutyrate aminotransferase	*gabT*	2.72	6.70×10^{-3}
Ribosome maturation factor RimP	*rimP*	2.70	1.74×10^{-4}
Ribosomal RNA large subunit methyltransferase F	*rlmF*	2.70	7.34×10^{-3}
Isocitrase	*aceA*	2.62	4.10×10^{-3}
Exodeoxyribonuclease 7 large subunit	*xseA*	2.62	1.58×10^{-5}
Flavodoxin	*fldA*	2.59	7.50×10^{-3}
Enamine/imine deaminase	*tdcF*	2.55	1.75×10^{-4}
Aldehyde dehydrogenase	*aldB*	2.47	5.79×10^{-3}
Ribosomal silencing factor RsfS	*rsfS*	2.40	2.95×10^{-3}
Cystathionine gamma-synthase	*metB*	2.30	4.94×10^{-4}
PTS IIA-like nitrogen regulatory protein PtsN	*ptsN*	2.26	3.25×10^{-3}
DUF3748 domain-containing protein	*yidR*	2.12	6.63×10^{-3}
UPF0227 protein YcfP	*ycfP*	1.88	1.03×10^{-3}
SDR family oxidoreductase	*yeeZ*	1.33	4.18×10^{-4}
Chorismate synthase	*aroC*	0.94	1.97×10^{-3}
Under-expressed			
NADH-quinone oxidoreductase subunit H	*nuoH*	-3.42	1.58×10^{-3}
Phosphatase NudJ	*nudJ*	-3.39	1.44×10^{-3}
Uronate isomerase	*uxaC*	-3.37	1.46×10^{-3}
Uncharacterized protein	WLH_00626	-2.68	9.12×10^{-4}
Ribosome association toxin RatA	*ratA*	-2.53	4.26×10^{-4}
Hydrogenase maturation factor	*hypD*	-2.19	2.08×10^{-3}
Mechanosensitive ion channel family protein	EWT59_09455	-1.66	6.11×10^{-3}
Maltodextrin-binding protein	*malE*	-1.47	3.04×10^{-3}
UPF0441 protein YgiB	*ygiB*	-1.25	4.00×10^{-3}
Uncharacterized protein	WLH_04693	-1.24	2.58×10^{-3}
Ribosome-binding factor A	*rbfA*	-1.00	1.53×10^{-4}

Protein identified by Maxquant and Perseus to identify proteins which were significantly differentially expressed.

2.4.3. Transcriptomic and proteomic changes following silver nitrate exposure

Silver nitrate exposure led to a significant change in the differential expression of 366 genes compared to the passaged control. GO terms which were over-represented included different metabolic processes (glutamate (GO:0006536), aldaric acid (GO:0019577) and galactarate (GO:0019580)). Whereas terms including lipid biosynthetic processes and catalytic activity acting on nucleic acids (GO: 0140640) were significantly under-represented (Table 2.5).

A total of 5 proteins were differently expressed following exposure to silver nitrate (Figure 2.5). Four proteins were significantly over expressed 50S ribosomal protein L23 RplW, deoxyribonucleoside regulator YjhU, sugar kinase YeiI and exodeoxyribonuclease 7 XseA and one was under expressed NADH-quinone oxidoreductase subunit H NuoH, see Table 2.6.

Table 2.5. Summary of GO biological process, molecular function, and cellular component groups over- or under-represented following exposure to silver nitrate.

GO biological process		Number of genes	Fold enrichment	p-value
Cellular process	GO:0009987	218	1.3	3.93×10^{-12}
Glutamate metabolic process	GO:0006536	8	8.11	3.52×10^{-5}
Aldaric acid metabolic process	GO:0019577	7	17.22	3.40×10^{-6}
Galactarate metabolic process	GO:0019580	6	17.22	1.80×10^{-5}
Monocarboxylic acid metabolic process	GO:0032787	33	2.37	1.24×10^{-5}
Aspartate family amino acid catabolic process	GO:0009068	7	5.48	7.59×10^{-4}
Gamma-aminobutyric acid catabolic process	GO:0009450	4	11.48	1.43×10^{-3}
Nucleoside monophosphate metabolic process	GO:0009123	11	3.79	3.95×10^{-4}
Ribose phosphate metabolic process	GO:0019693	14	2.91	7.24×10^{-4}
Localization	GO:0051179	77	1.79	4.38×10^{-7}
Glyoxylate metabolic process	GO:0046487	8	9.84	1.20×10^{-5}
Generation of precursor metabolites and energy	GO:0006091	32	2.87	3.46×10^{-7}
Organic acid transport	GO:0015849	21	2.38	4.79×10^{-4}
Nitrogen compound transport	GO:0071705	34	2.05	1.71×10^{-4}
Macromolecule metabolic process	GO:0043170	33	0.55	4.49×10^{-5}
Lipid biosynthetic process	GO:0008610	0	< 0.01	5.65×10^{-4}
GO Molecular function				
Lyase activity	GO:0016829	27	2.36	1.07×10^{-4}
Transporter activity	GO:0005215	59	1.81	1.06×10^{-5}
Oxidoreductase activity	GO:0016491	46	1.81	1.31×10^{-4}
Catalytic activity, acting on a nucleic acid	GO:0140640	3	0.17	4.12×10^{-5}
GO Cellular component				
Cellular anatomical entity	GO:0110165	200	1.16	2.35×10^{-4}
Cell periphery	GO:0071944	105	1.29	2.40×10^{-3}

Only parent groups shown, some groups have multiple subgroups within them. Number of genes is the number of significantly differentially expressed between conditions.

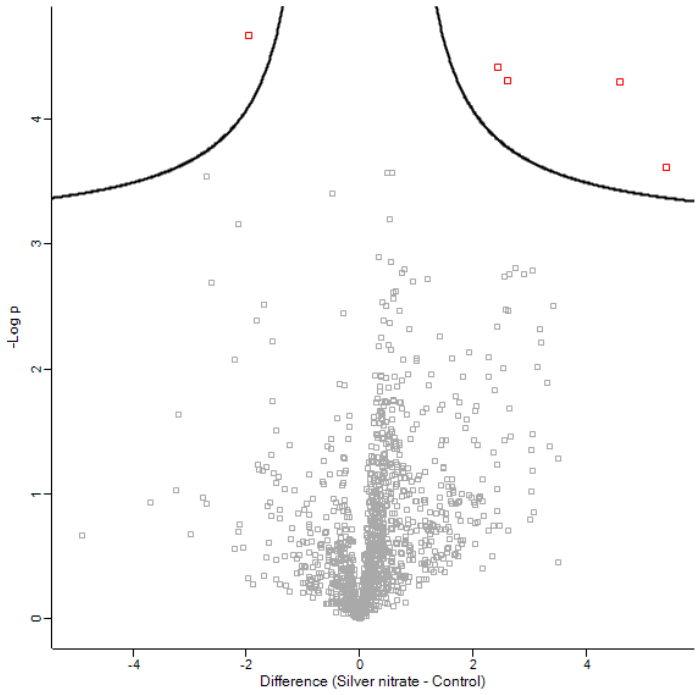

Figure 2.5. Volcano plot of protein expression compared between silver nitrate exposed and passaged control strain of EC958. Cut offs determined by two-sided t-test with a false discovery rate of 0.05 and a s0 value of 0.1. Significantly differentially expressed proteins identified by red squares.

Table 2.6. Differentially expressed proteins following passaging in the presence of silver nitrate.

Protein name	Gene	Fold change	P-value
Over expressed			
50S ribosomal protein L23	*rplW*	5.41	2.42×10^{-4}
Deoxyribonucleoside regulator	EWT59_12660 (*yjhU*)	4.59	5.02×10^{-5}
Sugar kinase	EWT59_25460 (*yeiI*)	2.61	4.86×10^{-5}
Exodeoxyribonuclease 7 large subunit	*xseA*	2.43	3.81×10^{-5}
Under expressed			
NADH-quinone oxidoreductase subunit H	*nuoH*	-1.97	2.11×10^{-5}

2.4.4. Transcriptomic and proteomic changes following triclosan exposure

Following long-term exposure to triclosan, 172 genes were significantly upregulated, and 155 genes were significantly downregulated. GO terms including localisation (GO:0051179), cytochrome metabolic processes (GO:1903604) and carbohydrate transport (GO:0008643) were overrepresented and terms of nucleic acid metabolic processes (GO: 0140640) and catalytic activity acting on a nucleic acid (GO:0090304) were under-represented (Table 2.7). No proteins were significantly differentially expressed following multiple passages in the presence of triclosan (Figure 2.6).

Table 2.7. Summary of GO biological process, molecular function, and cellular component groups over- or under-represented following exposure to triclosan.

GO biological process		**Number of genes**	**Fold enrichment**	**raw p-value**
Cellular process	GO:0009987	198	1.29	2.29×10^{-10}
Organonitrogen compound metabolic process	GO:1901564	74	1.43	1.27×10^{-3}
Amide catabolic process	GO:0043605	8	11.55	4.37×10^{-6}
Localization	GO:0051179	68	1.72	8.11×10^{-6}
Cytochrome metabolic process	GO:1903604	5	18.77	6.49×10^{-5}
Monocarboxylic acid metabolic process	GO:0032787	34	2.66	6.04×10^{-7}
Glycolate metabolic process	GO:0009441	5	13.41	1.88×10^{-4}
Thiosulfate transport	GO:0015709	4	12.51	1.05×10^{-3}
Sulphate assimilation	GO:0000103	5	10.43	4.36×10^{-4}
Cellular component assembly	GO:0022607	29	2.01	5.59×10^{-4}
Cellular aldehyde metabolic process	GO:0006081	10	3.68	8.35×10^{-4}
Ornithine metabolic process	GO:0006591	5	9.38	6.28×10^{-4}
Aldehyde catabolic process	GO:0046185	6	5.93	1.23×10^{-3}
Generation of precursor metabolites and energy	GO:0006091	26	2.54	3.86×10^{-5}
Carbohydrate transport	GO:0008643	20	2.91	4.84×10^{-5}
Nucleic acid metabolic process	GO:0090304	10	0.36	1.80×10^{-4}
GO Molecular function				
Catalytic activity, acting on a nucleic acid	GO:0140640	1	0.06	3.73×10^{-6}
GO Cellular component				
Cellular anatomical entity	GO:0110165	189	1.19	1.37×10^{-5}

Only parent groups shown, some groups have multiple subgroups within them. Number of genes is the number of significantly differentially expressed between conditions.

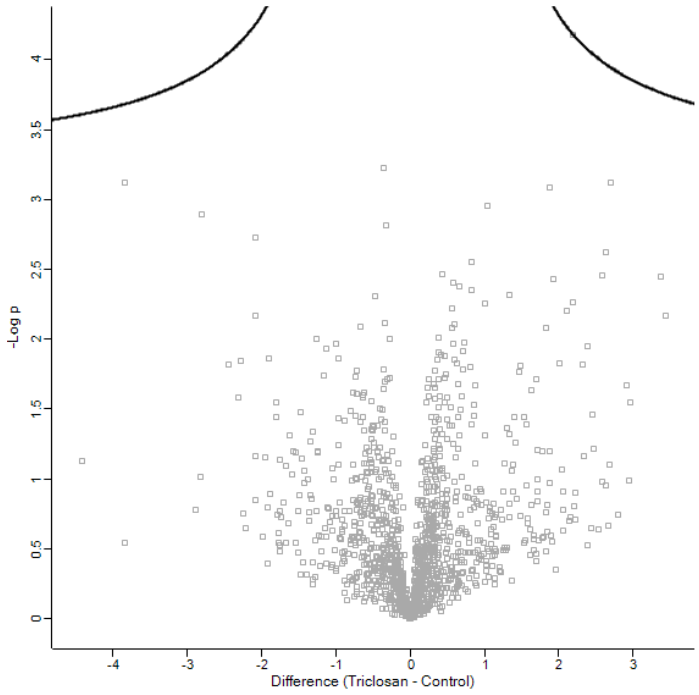

Figure 2.6. Volcano plot of differences in protein expression between EC958 passaged in the presence or absence of triclosan. No proteins were significantly differentially expressed. Cut offs determined by two-sided t-test with a false discovery rate of 0.05 and a s0 value of 0.1. Significantly differentially expressed proteins identified by red squares.

2.4.5. Transcriptomic and proteomic changes following cinnamaldehyde exposure

Long-term exposure to cinnamaldehyde led to the most numerous differentially regulated genes and differentially expressed proteins of all conditions tested. 368 genes were upregulated, and 329 genes downregulated. GO term analysis showed that locomotion (GO:0040011), cell motility (GO:0048870) and intracellular anatomical structure (GO:0005622) were overrepresented, and DNA recombination (GO:0006310) was underrepresented (Table 2.8)

Cinnamaldehyde saw the largest number of differently expressed proteins with a total of 64 proteins over expressed and 9 under-expressed (Figure 2.7). The highest overexpression was observed for methyl-accepting chemotaxis protein (Tsr), flagellar hook-filament junction protein 1 (FlgK) and chemotaxis protein A (CheA). The most under expressed proteins were phosphatase NudJ, NADH-quinone oxidoreductase subunit H (NuoH) and ECA polysaccharide chain length modulation protein (WzzE), see Table 2.9.

Table 2.8. Summary of GO biological process, molecular function, and cellular component groups over- or under-represented following exposure to cinnamaldehyde.

GO biological process		**Number of genes**	**Fold enrichment**	**raw p-value**
Cellular process	GO:0009987	386	1.2	9.70×10^{-10}
Locomotion	GO:0040011	18	4.37	3.21×10^{-6}
Reactive nitrogen species metabolic process	GO:2001057	15	4.49	1.67×10^{-5}
Cell motility	GO:0048870	20	2.81	1.67×10^{-4}
DNA recombination	GO:0006310	2	0.14	3.99×10^{-4}
GO Molecular function				
Binding	GO:0005488	347	1.21	1.03×10^{-7}
Catalytic activity	GO:0003824	276	1.21	5.89×10^{-5}
GO Cellular component				
Cellular anatomical entity	GO:0110165	382	1.16	1.25×10^{-6}
Methyl accepting chemotaxis protein complex	GO:0098561	6	7.7	9.10×10^{-4}
Organelle	GO:0043226	41	2.1	3.91×10^{-5}
Intracellular anatomical structure	GO:0005622	210	1.26	1.42×10^{-4}

Only parent groups shown, some groups have multiple subgroups within them. Number of genes is the number of significantly differentially expressed between conditions.

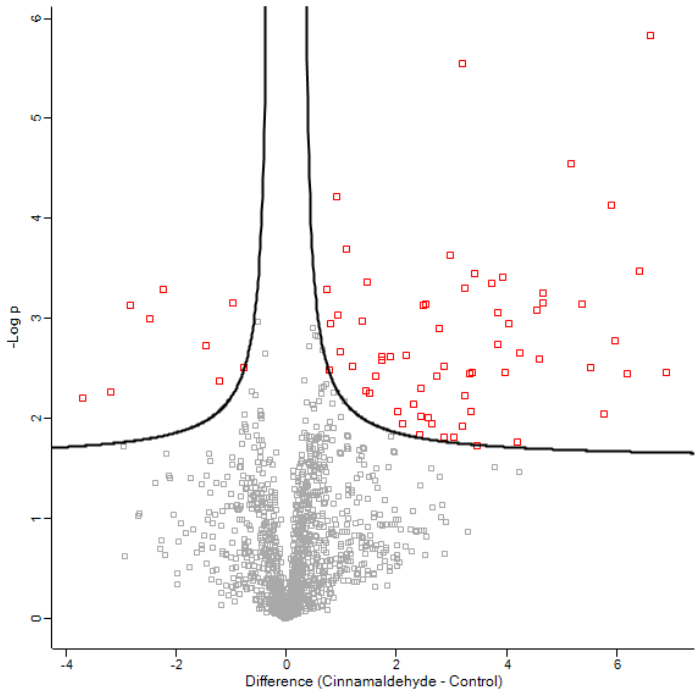

Figure 2.7. Volcano plot showing the differentially expressed proteins between EC958 passaged in the presence or absence of cinnamaldehyde. A total of 73 proteins were differentially expressed. Cut offs determined by two-sided t-test with a false discovery rate of 0.05 and a s0 value of 0.1. Significantly differentially expressed proteins identified by red squares.

Table 2.9. Proteins which were differentially expressed following long-term exposure to cinnamaldehyde.

Protein	Gene	Log2 Fold change	P value
Over expressed proteins			
Methyl-accepting chemotaxis protein Tsr	*tsr*	6.89	3.41×10^{-3}
Flagellar hook-associated protein 1	*flgK*	6.61	1.46×10^{-6}
Chemotaxis protein CheA	*cheA*	6.40	3.27×10^{-4}
Methyl-accepting chemotaxis protein II	*tar*	6.18	3.53×10^{-3}
50S ribosomal protein L23	*rplW*	5.96	1.64×10^{-3}
Flagellar hook-associated protein 2	*fliD*	5.90	7.30×10^{-5}
Flagellin	*fliC*	5.76	8.81×10^{-3}
Flagellar protein FliL	*fliL*	5.52	3.05×10^{-3}
Chemotaxis protein CheY	*cheY*	5.36	7.03×10^{-4}
Chemotaxis protein CheW	*cheW*	5.17	2.82×10^{-5}
Acid stress chaperone HdeA	*hdeA*	4.65	5.51×10^{-4}
Flagellar L-ring protein	*flgH*	4.64	6.94×10^{-4}
Flagellar motor switch protein FliM	*fliM*	4.58	2.49×10^{-3}
Flagellar hook-filament junction protein FlgL	*flgL*	4.55	8.07×10^{-4}
Flagellar P-ring protein	*flgI*	4.23	2.16×10^{-3}
Alcohol dehydrogenase AdhP	*adhP*	4.18	1.70×10^{-2}
Chemotaxis protein methyltransferase	*cheR*	4.04	1.09×10^{-3}
Flagellar basal-body rod protein FlgC	*flgC*	3.97	3.43×10^{-3}
Uncharacterized protein	*ybaY*	3.91	3.83×10^{-4}
Protein-glutamate methylesterase/protein-glutamine glutaminase	*cheB*	3.84	8.59×10^{-4}
Acetyl-coenzyme A synthetase	*acs*	3.84	1.79×10^{-3}
Isocitrase	*aceA*	3.73	4.41×10^{-4}
Flagellar M-ring protein	*fliF*	3.46	1.82×10^{-2}
RNA polymerase sigma factor FliA	*fliA*	3.41	3.49×10^{-4}
Ribosomal RNA small subunit methyltransferase E	*rsmE*	3.36	3.37×10^{-3}
GTP cyclohydrolase 1	*folE*	3.35	8.40×10^{-3}
4-aminobutyrate aminotransferase GabT	*gabT*	3.33	3.48×10^{-3}
Transcription factor MAF1	WLH_00667	3.24	4.91×10^{-4}
Lipopolysaccharide export system ATP-binding protein LptB	*lptB*	3.24	5.79×10^{-3}
Dihydroneopterin triphosphate 2-epimerase	*folX*	3.19	1.19×10^{-2}
Succinylornithine transaminase	*astC*	3.18	2.75×10^{-6}
Glyceraldehyde-3-phosphate dehydrogenase	*gap*	3.02	1.52×10^{-2}
Ribosome maturation factor RimP	*rimP*	2.97	2.30×10^{-4}
PTS IIA-like nitrogen regulatory protein PtsN	*ptsN*	2.85	2.93×10^{-3}
Phosphoesterase	*yfcE*	2.85	1.53×10^{-2}
Citrate synthase	*prpC*	2.76	1.25×10^{-3}
Ubiquinone biosynthesis accessory factor UbiT	*ubiT*	2.72	3.69×10^{-3}
Iron uptake system component EfeO	*efeO*	2.64	1.12×10^{-2}
ClpXP protease specificity-enhancing factor	*sspB*	2.56	9.68×10^{-3}
Malate synthase	*aceB*	2.53	7.13×10^{-4}
Nucleoid-associated protein YbaB	*ybaB*	2.49	7.24×10^{-4}
LysM peptidoglycan-binding domain-containing protein	EWT59_02020	2.45	9.48×10^{-3}
Ribosomal silencing factor RsfS	*rsfS*	2.43	4.89×10^{-3}

Protein	Gene	Log2 Fold change	P value
DUF3313 domain-containing protein	*ydcL*	2.41	1.44×10^{-2}
Aldo/keto reductase family oxidoreductase	EWT59_04710	2.29	7.11×10^{-3}
Sugar kinase	*yeiI*	2.18	2.30×10^{-3}
Phospholipase A1	*pldA*	2.10	1.12×10^{-2}
Curved DNA-binding protein	*cbpA*	2.01	8.43×10^{-3}
L-lysine 6-monooxygenase LucD	*iucD*	1.87	2.38×10^{-3}
Hydrolase	*ycaC*	1.72	2.59×10^{-3}
Protein/nucleic acid deglycase HchA	*hchA*	1.72	2.36×10^{-3}
Aldehyde dehydrogenase	*aldB*	1.62	3.68×10^{-3}
Cystine ABC transporter substrate-binding protein	*tcyJ*	1.51	5.44×10^{-3}
Glutaredoxin	*grxC*	1.45	4.33×10^{-4}
Cold shock-like protein CspC	*cspC*	1.43	5.20×10^{-3}
molybdate ABC transporter periplasmic binding protein	*modA*	1.37	1.04×10^{-3}
Uncharacterized protein	*yfaZ*	1.20	2.98×10^{-3}
N-acetylmuramoyl-L-alanine amidase	*amiC*	1.09	2.02×10^{-4}
N-acetylglucosamine-6-phosphate deacetylase	*nagA*	0.97	2.10×10^{-3}
Putative selenium delivery protein YdfZ	*ydfZ*	0.93	9.23×10^{-4}
Glucokinase	*glk*	0.90	5.90×10^{-5}
L-threonine 3-dehydrogenase	*tdh*	0.80	1.11×10^{-3}
Citrate synthase	*gltA*	0.77	3.20×10^{-3}
33 kDa chaperonin	*hslO*	0.73	5.06×10^{-4}
Under expressed proteins			
Phosphatase NudJ	*nudJ*	-3.71	6.13×10^{-3}
NADH-quinone oxidoreductase subunit H	*nuoH*	-3.20	5.34×10^{-3}
ECA polysaccharide chain length modulation protein	*wzzE*	-2.84	7.30×10^{-4}
Ribulose-phosphate 3-epimerase	*rpe*	-2.49	9.78×10^{-4}
Thiol:disulfide interchange protein	*dsbG*	-2.25	5.07×10^{-4}
Ribosome association toxin RatA	*ratA*	-1.47	1.86×10^{-3}
Probable septum site-determining protein MinC	*minC*	-1.21	4.20×10^{-3}
Alanine transaminase	*alaC*	-0.97	6.92×10^{-4}
Formate dehydrogenase iron-sulfur subunit	*fdxH*	-0.77	3.08×10^{-3}

2.4.6. Transcriptomic and proteomic changes following furanone-C30 exposure

Exposure to furanone-C30 led to upregulation of 122 genes and downregulation of 98 genes, overrepresented GO terms included sulfate transport (GO:0008272) and mRNA binding (GO:0003729). No GO terms were underrepresented (Table 2.10). Long-term exposure to furanone-C30 led to an increase in expression of 4 proteins (YbeD, YjhU, RimP and XseA) and under expression of one protein (Rpe; Figure 2.8 and Table 2.11).

Table 2.10. Summary of GO biological process, molecular function, and cellular component groups over- or under-represented following exposure to triclosan.

GO biological process		**Number of genes**	**fold enrichment**	**raw p-value**
Cellular process	GO:0009987	141	1.34	2.11×10^{-10}
Sulphate transport	GO:0008272	4	15.69	4.00×10^{-4}
Amide metabolic process	GO:0043603	39	4.74	2.66×10^{-15}
Cellular component assembly	GO:0022607	26	2.63	1.02×10^{-5}
Ribosomal large subunit biogenesis	GO:0042273	12	10.29	1.88×10^{-8}
Glyoxylate metabolic process	GO:0046487	5	9.8	3.93×10^{-4}
Reactive nitrogen species metabolic process	GO:2001057	8	7.32	3.89×10^{-5}
GO Molecular function				
Nitrite reductase activity	GO:0098809	4	21.96	1.61×10^{-4}
Binding	GO:0005488	119	1.27	5.41×10^{-5}
Structural molecule activity	GO:0005198	31	11.35	2.80×10^{-21}
mRNA binding	GO:0003729	7	8.35	5.98×10^{-5}
GO Cellular component				
Cellular anatomical entity	GO:0110165	132	1.22	4.26×10^{-5}
Organelle	GO:0043226	34	5.33	1.07×10^{-14}
Large ribosomal subunit	GO:0015934	17	13.72	4.30×10^{-13}

Only parent groups shown, some groups have multiple subgroups within them. Number of genes is the number of significantly differentially expressed between conditions.

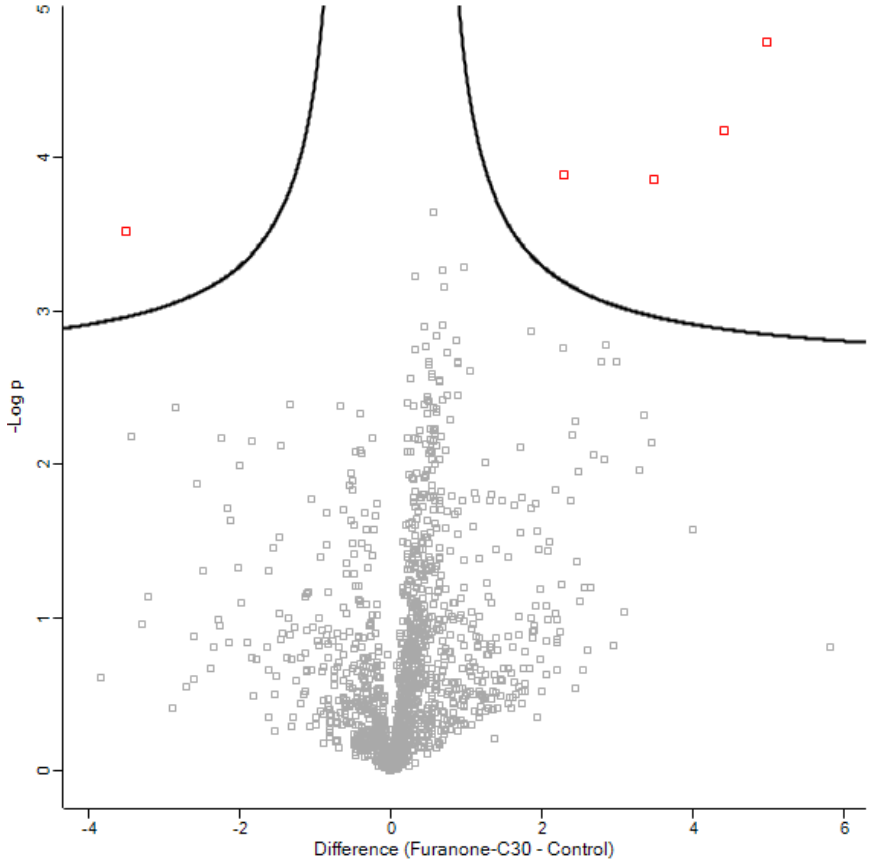

Figure 2.8. Volcano plot showing the differentially expressed proteins between EC958 passaged in the presence or absence of furanone-C30. Cut offs determined by two-sided t-test with a false discovery rate of 0.05 and a s0 value of 0.1. Significantly differentially expressed proteins identified by red squares.

Table 2.11. List of proteins which were differentially expressed following long-term exposure to furanone-C30.

Protein name	Gene	Fold change	P-value
Over expressed			
UPF0250 protein YbeD	*ybeD*	4.95	1.73×10^{-5}
Deoxyribonucleoside regulator	*yjhU*	4.39	6.57×10^{-5}
Ribosome maturation factor RimP	*rimP*	3.47	1.37×10^{-4}
Exodeoxyribonuclease 7 large subunit	*xseA*	2.29	1.28×10^{-4}
Under expressed			
Ribulose-phosphate 3-epimerase	*rpe*	-3.51	2.99×10^{-4}

2.4.7. Transcriptomic and proteomic changes following F-DPD exposure

F-DPD exposure led to differential expression of 267 genes.. GO term analysis indicated cell motility (GO:0048870) and response to stimulus (GO:0050896) were significantly overrepresented. The GO term organic cyclic compound metabolic process (GO:1901360) was the only term to be underrepresented (Table 2.12). Finally, there were no significantly differentially expressed proteins following long-term exposure of F-DPD (Figure 2.9).

Table 2.12. Summary of GO biological process, molecular function, and cellular component groups over- or under-represented following exposure to F-DPD.

GO biological process		Number of genes	Fold enrichment	p-value
Cell motility	GO:0048870	21	9.18	3.43×10^{-13}
Regulation of response to stimulus	GO:0048583	6	7.3	3.77×10^{-4}
Regulation of protein modification process	GO:0031399	4	18.65	2.44×10^{-4}
Intracellular pH elevation	GO:0051454	4	15.99	3.73×10^{-4}
Protein secretion by the type III secretion system	GO:0030254	5	15.54	7.15×10^{-5}
Response to stimulus	GO:0050896	61	1.7	1.20×10^{-5}
Cell projection organization	GO:0030030	12	4.3	4.99×10^{-5}
Organic cyclic compound metabolic process	GO:1901360	15	0.46	3.65×10^{-4}
GO Molecular function				
Cytoskeletal motor activity	GO:0003774	6	20.98	3.67×10^{-6}
GO Cellular component				
Organelle	GO:0043226	25	4	1.15×10^{-8}
Bacterial-type flagellum motor	GO:0120100	5	23.31	1.79×10^{-5}
Methyl accepting chemotaxis protein complex	GO:0098561	6	23.98	2.16×10^{-6}
Type III protein secretion system complex	GO:0030257	5	15.54	7.1×10^{-5}
Bacterial-type flagellum secretion apparatus	GO:0120102	5	15.54	7.15×10^{-5}

Only parent groups shown, some groups have multiple subgroups within them. Number of genes is the number of significantly differentially expressed between conditions.

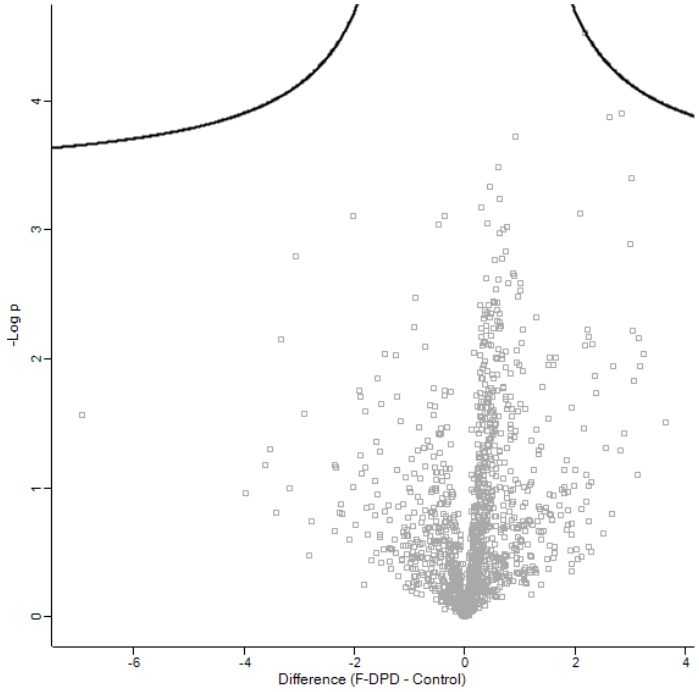

Figure 2.9. Volcano plot showing the differentially expressed proteins between EC958 passaged in the presence or absence of F-DPD. Cut offs determined by two-sided t-test with a false discovery rate of 0.05 and a s0 value of 0.1. Significantly differentially expressed proteins identified by red squares.

2.5. Discussion

Bacterial adaptation to antimicrobials resulting in the development of antimicrobial resistance or causing phenotypic adaptations impacting pathogenic potential is a global concern (Murray *et al.*, 2022). The potential for development of resistance against the primary antimicrobial and cross-resistance to third party antimicrobials such as clinically relevant antibiotics is therefore of great interest within the research field. Investigated here was a continuation of the work by Henly (2019). We performed an investigation into the transcriptomic and proteomic changes in uropathogenic *E. coli* strain EC958 after exposure to PHMB, BAC, silver nitrate, triclosan, cinnamaldehyde, furanone-C30 and F-DPD. This led to identification of a wide range of biological, cellular and molecular processes which were over or underrepresented as determined through gene ontology analysis of differentially expressed genes. Furthermore, significant changes in the expression of specific proteins were identified following biocide and QSI exposure via mass spectrometry.

2.5.1. PHMB

Phenotypic changes as a result of PHMB exposure led to a reduction in the minimum inhibitory (MIC) and bactericidal concentrations (MBC), reduction in biofilm formation on a catheter surface and reduced pathogenicity in a *Galleria mellonella* model. However, the minimum biofilm eradication concentration (MBEC) was significantly increased (Henly *et al.*, 2019).

Gene ontology analysis of the transcriptomic data identified that genes associated with bacterial-type flagellum-dependent cell motility (GO:0071973) and locomotion (GO:0040011) were statistically over-represented. As discussed in Henly (2019), genes within these terms, including *acs, cheZ, dppA, flgC,G,H, flhA, fliF,G,H,K,M,N,O,P, malE* and *rbsB* were all significantly down-regulated in their expression following PHMB exposure. This reduction in motility could be theorised to be associated with the observed decrease biofilm formation where motility is involved in the initial surface contact, attachment and expansion of the biofilm (Pratt and Kolter, 1998). However, from the proteomic analysis, no proteins associated with flagellum or locomotion were differentially expressed.

There was only one protein which was significantly increased in expression following PHMB exposure, the phosphogluconate dehydrogenase, Edd ($Log_2FC = 2.5$), however this gene showed a reduction in transcription in the RNAseq data (Log_2 fold change = -1.22). Previous investigations have shown that the overexpression of Edd, could lead to accumulation of 2-keto-3-deoxy-6-phosphagluconate during the Entner-Doudoroff pathway, this has been shown to have an inhibitory effect on the growth of *E. coli* (Fuhrman *et al.*, 1998) which may also contribute to the reduction in biofilm formation and pathogenicity previously observed.

2.5.2. BAC

Phenotypic changes which were observed following long-term exposure to BAC included an increase in the MIC and MBEC, increase in biofilm formation on a plate-based assay and an increase in cell invasion, however there was a decrease in the relative pathogenicity (Henly *et al.*, 2019). GO term analysis of the significantly differentially expressed genes indicated that terms associated with cell motility (GO:0048870), locomotion (GO:0040011) and the bacterial type flagellum motor (GO:0120100) were all overrepresented and these were predominantly by genes which were down regulated (see Appendix Table 8.2). This is contradictory to the expected outcome, as a reduction in the expression of motility associated genes would be expected to be associated with a reduction in biofilm formation (Pratt and Kolter, 1998).

Only two of the differentially expressed proteins were also differentially expressed within the transcriptomic data: acetyl-coenzyme A synthetase *acs* (RNA: $Log_2FC = 1.12$. $p < 0.001$, protein: $Log_2FC = 4.075$, $p = 0.005$) and 30S ribosome binding factor, *rbfA* (RNA: $Log_2FC = -1.5$, $p < 0.001$, protein: $Log_2FC = -1.001$, $p = 0.002$). Acs has been associated with acetylation of chemotaxis protein CheY, which is responsible for switching the rotational direction of the flagellar motor and was shown to have reduced chemotactic responses to stimuli when it is not acetylated (Barak and Eisenbach, 2001). The increase in Acs expression could be a mechanism behind increased biofilm formation, by an increasing the acetylation of CheY and chemotaxis. The 30Sribosome binding factor, *rbfA*, is a cold shock protein which has no obvious connection to the phenotypes observed here, a depletion in the expression of *rbfA* is associated with an

increase in accumulation of immature 16S rRNA which could lead to a stalling of translation (Shajani et al., 2011).

The deoxyribonucleoside regulator YjhU was significantly increased in protein expression as a result of long-term exposure to BAC. Previously, increased expression of this transcription factor has been correlated with a reduction in motility and a decrease in expression of motility associated genes within *E. coli* (Kim, Lee and Ryu, 2013). The overexpression of the protein may be involved in the regulation of the motility associated genes observed in our isolate.

There was an increase in the expression of PTS IIA-like nitrogen regulatory protein (PtsN). Increased expression of PtsN has been previously associated with reduction in cell envelope stress through reduced expression of multiple cell envelope stress response associated proteins including extra cytoplasmic function sigma factor (σ^E), periplasmic protein (CpxP) and the BaeSR two component system (Hayden and Ades, 2008). This is contradictory to the increases in the MIC and MBEC observed following long-term exposure to BAC where a reduction in the envelope stress response would likely lead to increased susceptibility to membrane active compounds such as BAC (Gilbert and Moore, 2005).

In contrast, ribosome associated toxin (RatA) was under expressed in BAC exposed conditions. It has 100% similarity to PasT found in CFT073 which is associated with increased stress tolerance, colonisation of mouse urinary tracts and persister cell formation (Norton and Mulvey, 2012). Following long-term exposure to BAC, there was reduced pathogenicity in a *G. mellonella* wax worm model which could be theorised to be associated with RatA reduction as could our observed decrease in BAC susceptibility due to increased stress tolerance.

NADH-quinone oxidoreductase subunit H (NuoH) showed the largest reduction in protein expression following exposure to BAC (Log_2FC = -3.42). Within the transcriptomic analysis, *nuoH* was not significantly differentially regulated however subunit F (*nuoF)* was down regulated (Log_2FC = -1.19). NADH-quinone oxidoreductase is involved in the respiratory chain and has proton transport functionality in *E. coli*. Subunit H is an intermembrane component which is involved in ubiquinone binding and subunit F is the catalytic dehydrogenase site for NADH of the enzyme (Leif *et al.*, 1995; Friedrich,

1998). Down regulation of *nuo* genes has been observed previously as a result of long-term BAC exposure (Forbes *et al.*, 2019). However, the impacts of this regulation on the observed phenotype are unclear as reduced expression and down regulation of genes associated with respiration would be expected to reduce growth rates thus overall biofilm formation, which is in contrast to what was observed in the current investigation.

2.5.3. Silver nitrate

Following long-term exposure to silver nitrate, increases in the MIC, MBC and MBEC of EC958 were observed (Henly *et al.*, 2019). A total of 366 genes were differentially regulated compared to a passaged control, however only 5 proteins were significantly differentially expressed.

NADH-quinone oxidoreductase subunit H (NuoH) protein expression was reduced following passaging in the presence of silver nitrate. As mentioned with regards to BAC exposure, the NADH-quinone oxidoreductase is associated with the electron transport chain of *E. coli*, involved in pumping protons into the periplasmic space (Friedrich, 1998). Previous work has identified that *nuo* genes are down regulated in response to acute exposure to silver ions (Saulou-Bérion *et al.*, 2015). The prolonged exposure to silver ions of silver nitrate could have led to a suppression of NuoH. Silver inhibits the respiratory chain of *E. coli*, through targeting the cytochromes a and b, and flavoproteins (Bragg and Rainnie, 1974). Subunit F of the NADH-quinone oxidoreductase protein contains a flavin mononucleotide (Leif *et al.*, 1995) which could be a target of silver nitrate. Due to this targeting of the respiratory chain by silver nitrate, over representation of the GO terms aerobic respiration (GO:0009060), cellular respiration (GO:0045333) transmembrane transporter activity (GO:0022857) was observed following silver nitrate exposure and 17/25 genes within cellular respiration were up regulated (Appendix Table 8.3) this could potentially be due to the bacteria compensating for the suppression of some aspects of the respiration chain by increasing expression of other genes.

Expression of YjhU was increased following long-term exposure to silver nitrate. There was no change in biofilm formation as a result of silver nitrate exposure, however there were increases in the minimum inhibitory, bactericidal and biofilm eradication concentrations. Upregulation of *yjhU* has been previously observed to be correlated not

only with increases in biofilm formation but also increased antimicrobial resistance (Kim, Lee and Ryu, 2013), which may explain the decreased silver susceptibility observed in our isolate.

2.5.4. Triclosan

Prolonged exposure to triclosan led to an increase in the MIC, MBC and MBEC of EC958. Biofilm formation on a polystyrene plate also increase, whereas biofilm formation on a catheter surface decreased, as did pathogenicity. Triclosan exposure also led to cross resistance to nitrofurantoin (Henly *et al.*, 2019). 327 genes were differentially regulated following long-term exposure to triclosan, despite these significant changes, there were no significantly differentially expressed proteins.

From the transcriptomic data, there was overrepresentation of genes associated with transport (GO:0006818), this has also been observed in a previous study in UPEC strain CFT073 upon exposure to triclosan (Ligowska-Marzęta *et al.*, 2019). Sulphur transport associated genes were also upregulated in CFT073 by triclosan exposure, which is similar to what was observed in the current investigation with an overrepresentation of genes associate with sulphate assimilation (GO:0000103), of which these genes were largely upregulated (appendix Table 8.4). The reasons for this increase in sulphur related gene expression after triclosan exposure however remain unclear (Ligowska-Marzęta *et al.*, 2019).

Previous work into the genomic changes in our triclosan exposed isolate revealed a mutation in *fabI* (Henly, 2019) which has been identified multiple times as the mechanism by which bacteria develop resistance to triclosan, this has been observed in multiple studies and explains the elevated MIC, MBC and MBEC after triclosan exposure (Levy, McMurry and Oethinger, 1998; Stewart *et al.*, 1999; Henly, 2019).

2.5.5. Cinnamaldehyde

Long-term exposure to cinnamaldehyde led to a reduced susceptibility of EC958 at MIC, MBC and MBEC, however there was an increase in biofilm formation in plate-based assays (Henly *et al.*, 2021). Cinnamaldehyde exposure led to the highest number of

significantly differentially expressed proteins: 64 proteins were over expressed and 9 were under expressed.

Increased expression of proteins associated with chemotaxis (Tar, Tsr, and CheA,B,R,W,Y) and the flagella (FliA,C,D,H,L,M and FlgC,F,I,K,L) was observed following long-term exposure to cinnamaldehyde. This increase in the expression of motility related proteins could be associated with the increase in biofilm formation, as motility is involved to overcome repulsive forces, provide the initial surface contact facilitating attachment and allow expansion of the biofilm (Pratt and Kolter, 1998). The highest increase in relative protein expression was in methyl-accepting chemotaxis serine sensing protein, Tsr ($Log_2FC = 6.89$), which is associated with chemotaxis towards AI-2 through the binding of Tsr to the AI-2 receptor LsrB (Hegde *et al.*, 2011). Tsr, Tar and CheY have also all been shown to be involved in the auto aggregation of *E. coli* in the presence of AI-2 (Laganenka, Colin and Sourjik, 2016) and CheY may be acetylated by acetyl-coenzyme A synthetase (RNA: $Log_2FC = 1.5$, protein: $Log_2FC = 3.8$) which leads to the switching on of the tumbling chemotactic method, switching the rotation of FliM from anticlockwise to clockwise and is involved in repellence and attraction to stimuli (Barak and Eisenbach, 2001). Together, this suggests a potential rationale behind the increase in biofilm formation on a plate-based assay; there is increased expression of proteins towards AI-2 which would increase the number of cells initially attaching and forming a biofilm. It could be hypothesised that long-term exposure to cinnamaldehyde, which inhibits quorum sensing within *E. coli* through both AHL (SdiA) based and AI-2 systems (Brackman *et al.*, 2008, 2011), could result in increases in proteins of QS associated pathways to compensate for this sustained repression.

2.5.6. Furanone-C30

Long-term exposure to furanone-C30 resulted in a reduction in MIC, MBC and MBEC, biofilm formation on a catheter surface and pathogenicity, however there was an increase in biofilm formation on a plate-based assay (Henly *et al.*, 2021).

Genes associated with the RNA binding (GO:0003723) were overrepresented and all associated genes were downregulated in response to long-term exposure to furanone-C30. Genes within the overrepresented group of Translation (GO:0006412) were also

predominantly down regulated. Suggesting that long-term exposure to furanone-C30 could have caused an overall reduction on impact on the translation of the cell, reducing growth rate and potentially impacting biofilm formation.

Structurally related compounds to furanone-C30 have been investigated as potential inhibitors of AI-2 communication, it has been shown to impact the expression of chemotaxis and flagellar biosynthesis (Ren *et al.*, 2004). However, there was no over or under representation of chemotaxis and flagellum associated genes in this investigation after furanone-C30 exposure.

Four proteins were significantly over expressed as a result of long-term furanone-C30 exposure, YbeD, YjhU, RimP and XseA and Rpe was under expressed. Transcriptional regulator YjhU was also over expressed following both BAC and silver nitrate long-term exposure, the expression of which has been observed to be correlated with a reduction in motility and antimicrobial susceptibility in response to exposure to volatile organic compounds (Kim, Lee and Ryu, 2013) which is in contrast to the observed reduction in MIC, MBC and MBEC in our isolate but would support a lower level of biofilm formation and reduced pathogenicity.

Exodeoxyribonuclease 7 large subunit XseA was also over expressed following exposure to BAC and silver nitrate, and ribosome maturation factor RimP (which binds to the 30S ribosomal subunit and acts as a chaperone (Nord *et al.*, 2009; Sashital *et al.*, 2014)) was also over expressed following exposure to BAC and cinnamaldehyde. However, there is no obvious links to the resultant phenotypes. Similarly, ribulose-phosphate 3-epimerase (Rpe, which is involved in the pentose phosphate pathway, converting ribulose 5-phosphate into xylose 5 phosphate (Sobota and Imlay, 2011)) was also under expressed in cinnamaldehyde exposed strains, but there are no clear links between the observed phenotypes and the pattern of protein expression.

2.5.7. F-DPD

Long-term exposure to F-DPD led to no change in antimicrobial susceptibility but did result in a decrease in biofilm formation on a catheter surface only (Henly *et al.*, 2021). GO term analysis revealed overrepresentation of bacterial-type flagellum-dependent cell motility (GO:0001539) and chemotaxis (GO: 0006935) and the genes within these

groups were downregulated (*aer*, *cheA, B, R, W, Y, Z*, *flgC, G, H, J*, *flhA, B, fliD, F, G, H, K, M, N, O, P, S, motA, tar* and *tsr*). As discussed with regards to Cinnamaldehyde (section 2.5.5), these genes have been associated with the formation of biofilms and the movement towards AI-2 (Laganenka, Colin and Sourjik, 2016). The downregulation of these genes could be associated with a reduction in motility and hence a reduction in biofilm formation (Pratt and Kolter, 1998). However, no proteins were identified as significantly differentially expressed within this analysis.

2.6. Conclusions

Long-term exposure to each antimicrobial led to a unique combination of phenotypic responses, changes in transcriptomic regulation and protein expression for each biocide and QSI tested. Of particular note is the comparatively small number of proteins differentially expressed compared to the differential gene regulation. We also observed occasions where there was a visible change in phenotype with no identifiable change in protein expression. This may be due to variation between biological replicates within the proteomic data, as can be seen in the dendrogram, where there is unclear clustering of samples from the same conditions which would have been expected, particularly within the controls. To address this, there should be additional replicates undertaken to increase the power of the statistical analysis. Alternatively, a targeted approach to investigate the expression of specific proteins may also be used.

With regards to the development of an antimicrobial catheter coating, there appears to be a number of potential transcriptional and translational routes through which long-term antimicrobial exposure may induce phenotypic changes in UPEC to occur. These may lead to a change in susceptibility, biofilm growth and relative pathogenicity and should be taken into account when determining an effective anti-infective coating for urinary catheters.

3.
Sol-gel coatings for delivery of biocides and quorum sensing inhibitors

3.1.Abstract

Background: Commercially available anti-infective silver hydrogel or nitrofurazone impregnated catheters have demonstrated limited efficacy in clinical practice. This is theorised to be due to issues with elution rates resulting in a limited window of activity as well as the potential selection for antimicrobial resistant microbial populations. In the development of a successful anti-infective catheter coating the release of the active agents should ideally provide antimicrobial protection for a prolonged period of time and maintain release at concentrations high enough to prevent selection of resistance whilst not exhibiting host cytotoxicity.

Methods: In this chapter biocides and quorum sensing inhibitors (QSIs) were incorporated into a novel silica-based hybrid sol-gel formulation at either 2 mg/ml or 10 mg/ml concentration. The amount of antimicrobial eluted from the coating was quantified by LC-MS for PHMB, BAC, triclosan and cinnamaldehyde, ICP-MS for silver nitrate and investigated by both ICP-MS and GC-MS for furanone-C30. In addition to this, the efficacy of the eluted biocide or QSI was assessed by disc diffusion assay against a panel of clinical UPEC isolates either in their native state, or those which had been passaged 12 times in the presence of the test biocide or QSI to determine if bacteria may become insusceptible to coating agents over time.

Results: Regarding the elution profiles, in order of time to complete elution, silver nitrate eluted most rapidly from the coating, followed by PHMB, cinnamaldehyde, triclosan and finally BAC which did not elute effectively. The lack of elution from the BAC coating correlated with the lack of a zone of microbial inhibition in the disc diffusion assays. Silver nitrate demonstrated large zones of microbial inhibition, which correlates with a sudden release of silver ions from the sol-gel coating upon submersion/placing on the agar. Triclosan showed slower sustained release indicating a potentially longer-term antimicrobial efficacy as a coating agent.

Conclusions: Detection and quantitation methods were evaluated for PHMB, BAC, silver nitrate, triclosan and cinnamaldehyde, whereas further development is required for quantitation of furanone-C30 elution from the sol-gel coating. The release profile differs by antimicrobial, with silver nitrate demonstrating rapid release and very low release from BAC incorporated coatings.

3.2.Introduction

Modern healthcare relies heavily on implantable medical devices; however, such devices are prone to microbial contamination of the device surface largely during implantation. The development of anti-infective surfaces is a challenge for all indwelling medical devices due to issues with long-term activity and potential host cytotoxicity. Urinary catheters are colonised by bacteria which form recalcitrant biofilms leading to catheter associated urinary tract infections (CAUTI) which are challenging to treat. Commercially available anti-infective catheter coatings include nitrofurazone impregnated (ReleaseNF®, Rochester Medical) and silver based (Lubri-Sil® and Bardex IC®, Bard Care) which release their active agent from the coating into the surroundings to prevent colonisation by uropathogens have been developed. These coatings have however been shown to have little to no net benefit to patients in clinical practice (Johnson, Johnston and Kuskowski, 2012; Lam *et al.*, 2014). There is significant research into the development of anti-infective catheter coatings, which has been reviewed extensively: Singha, Locklin and Handa, (2017), Cortese et al., (2018), Andersen and Flores-Mireles, (2019), Ramstedt et al., (2019), and Dai, Gao and Duan, (2023) and highlights the multiple attributes of the coating that need to be considered when evaluating its overall efficacy.

An effective catheter coating should prevent the initial microbial colonisation of the catheter surface whilst maintaining a suitably high concentration of antimicrobial to prevent selection of resistant microbial populations (Buhmann *et al.*, 2016). In the previous chapter the effects of the biocides (PHMB, BAC, silver nitrate and triclosan) and the QSIs (*trans*-cinnamaldehyde and furanone-C30) were assessed for their ability to induce changes in transcriptomic and proteomic profiles in UPEC EC958 following long term exposure. In this chapter the release of these antimicrobial compounds from a proposed silica-based hybrid sol-gel coating technology is presented. An understanding of the release profiles could lead to optimisation of the coating to prolong release at a sustained and suitable concentration to prevent infection whilst minimising the risk of selection for resistance and cytotoxicity.

Sol-gel technology is a research field which is well used within the materials industry. Sol-gel based materials are formed from a precursor colloidal suspension of molecules (the sol) which, through the addition of an acidic or basic solvent-based catalyst,

polymerise through a series of hydrolysis and condensation reactions to form a gel like structure. This sol-gel in solution form can then be used to coat surfaces and upon evaporation of the solvent dries into a solid thin film coating (Jones, 1989).

Sol-gel technology has been used in a wide range of applications as there is a wide range of conditions and configurations which can be optimised, from the make up of the precursor solution to the pH of the catalyst and how the sol-gel is cured can all impact the final outcome (Owens *et al.*, 2016). There is significant research into the use of sol-gel technology in the prevention of corrosion and biofouling (Figueira, 2020). However, there has been some research into the biomedical applications of this technology including as scaffolds in tissue regeneration, delivery of biomolecules and as sensing devices, all summarised in Owens et al., (2016), additionally in the formation of antimicrobial textiles (Rivero and Goicoechea, 2016).

The potential applications of sol-gel technology are vast, as are those based upon silicon alkoxides, used here. The specific sol-gel formulation used within this study has been used previously to deliver gentamicin from hydroxyapatite-coated titanium orthopaedic prostheses and was shown to eradicate relevant bacterial strains *in vitro* and were successful in lowering infection rates in rat models (Nichol *et al.*, 2021). The benefit of using sol-gel technology is the ability to have precise control over the properties of the gels through optimisation of many factors, from the water content, the pH of the catalyst solution and the composition of the precursor solutions (Jones, 1989; Brinker, C and Scherer, George, 1990).

An anti-infective urinary catheter coating should deliver an effective concentration of the antimicrobial into the surroundings at a level which is high enough to maintain inhibition of the bacteria without exerting a selection pressure, yet low enough as to not lead to cytotoxicity. To quantify the release, mass spectrometry techniques were used throughout this chapter. The detection methods used were dependent on the antimicrobial tested.

3.2.1. Aims of this chapter

This chapter aimed to quantify the elution of antimicrobial from a silica-based hybrid sol-gel coating and assess the antimicrobial activity of this coating in a disc diffusion based assay in UPEC before and after repeated exposure to biocides and QSIs.

3.3.Methods

All chemicals were sourced from Sigma Aldrich, UK, unless otherwise stated.

3.3.1. Sol-gel production and antimicrobial incorporation

The silica-based hybrid sol-gel was prepared by mixing 0.5 ml of tetraethyl orthosilicate (TEOS), 1 ml tetramethyl orthosilicate (TMOS) and 2.18 ml anhydrous isopropanol for 5 minutes at room temperature. To this, 1 ml Trimethoxymethylsilane (MTMS) was added slowly, followed by dropwise addition of 2.35 ml of acid/solvent mix (total acid/solvent catalyst was composed of 2.18 ml anhydrous isopropyl alcohol and 2.5 ml 0.07M nitric acid). Polydimethylsiloxane (0.65ct, molecular weight 162, PDMS) was added slowly (4 additions of 50 µl before the remaining acid/solvent mix was added dropwise and stirred for 10 minutes followed by dropwise addition of 2.4 ml 0.07M nitric acid. The solution was stirred for 72 hours prior to use as in Nichol et al., (2021).

Antimicrobial stocks of PHMB (Lonza, UK), BAC, silver nitrate (Alfa Aesar, UK) and *trans*-cinnamaldehyde, were diluted to working concentrations in water. Triclosan and (z)-4-bromo-5(bromomethylene)-2(5H)-furanone) (furanone-C30; synthesised in house as described in Guo, *et al* (2009)) were diluted to working stock concentrations in 5% v/v ethanol. Antimicrobials were prepared at either 20 mg/ml or 100 mg/ml concentration and added to the sol-gel just prior to coating at a 1:10 dilution (100 µl antimicrobial stock to 900 µl sol-gel). Either square 22x22mm coverslips, or circular 6mm diameter coverslips were coated by the antimicrobial/sol-gel, coverslips were cleaned with an Azo wipe before 10 µl of antimicrobial/sol-gel was spread across the surface with the aid of the pipette tip. Antimicrobial/sol-gel coverslips were left to dry overnight and stored in the fridge until use.

3.3.2. Elution of antimicrobials from sol-gel coated coverslips.

Prepared antimicrobial/sol-gel square glass coverslips at 0 mg/ml, 2 mg/ml and 10 mg/ml concentrations were placed one per well into a six well plate and submerged in 3 ml of 0.1M ammonium acetate (pH 7.2). The entire contents of the well were removed and stored at -20^{o}C, this was the 0 hour collection. The coverslips were then submerged with 3 ml of fresh 0.1 M ammonium acetate and incubated at 37^{o}C, 30 RPM. At each time point, the entire contents of the well were removed, stored at -20^{o}C and replaced

with 3 ml of fresh ammonium acetate. Time points were 0, 1, 6, 24, 48, 72 and 168 hours. Samples were warmed to room temperature and vortexed to mix before transfer to vials for analysis.

3.3.3. Quantitation of PHMB

Initial detection of PHMB was through direct injection of diluted samples at 10 µg/ml in 0.1M ammonium acetate (pH 7.2) into 6420 Triple Quad LCMS mass spectrometer (Agilent Technologies). Standards of PHMB were prepared from a stock of known concentration (200 mg/ml) diluted in ammonium acetate between 0.125 µg/ml and 20 µg/ml. Samples were analysed on a 1260 Infinity II HPLC system coupled to the 6420 Triple Quad LCMS mass spectrometer and controlled by MassHunter Workstation Data Acquisition system (v10.1) and qualitative analysis software (v8.0, Agilent). Samples were run though a Luna 5µm C18 column (1x150mm, 100Å, Phenomenex), under an isocratic condition of 80% H2O with 0.1% formic acid and 20% acetonitrile with 0.1% formic acid at a flow rate of 0.1ml/minute. Injection volume was 10 µl, draw speed of 200 µl/min and eject speed at 400 µl/min, followed by a 10 second needle wash in 60% methanol/40% H_2O. Detection of PHMB was under MS2 selected ion monitoring (SIM) mode for the ions *m/z* = 184 and *m/z* = 367 with the following settings: “unit” resolution, dwell time of 200 ms, 135 v fragmentor energy, 4 v cell accelerator voltage and positive ion mode. The ions of interest eluted from the column at 1.79 minutes. A standard curve based on the peak height at 1.79 minutes retention time was created and the concentration of the samples was determined from this.

3.3.4. Quantitation of BAC

BAC was quantified using the same LC-MS instrumentation set up as in 3.3.3. The column used was an X-Bridge Amide 5 µm, 4.5 x 150 mm (Agilent) and isocratic separation of 80% acetonitrile with 0.1% formic acid and 20% ammonium acetate (0.1M, pH 3.3), with a flow rate of 0.5 ml/minute. Mass spectrometry detection of BAC was by multiple reaction monitoring (MRM) scan type with precursor ions of *m/z* = 304 and *m/z* = 332 representative of benzyldimethyldodecylammonium chloride (C_{12}-BAC) and benzyldimethyltetradecylammonium chloride (C_{14}-BAC) respectively, with detection of the product ion *m/z* = 91 representative of the benzene ring of BAC common to both

C_{12}-BAC and C_{14}-BAC. MS resolution was set to unit with a dwell time of 200 ms, fragmentor voltage of 135 v, collision energy of 30 V and cell accelerator of 4 v, in positive ion mode. Standard curves were produced between 0.0625 – 10 µg/ml.

3.3.5. Quantitation of silver nitrate

The release of silver ions from the silver nitrate containing sol-gel was quantified by inductively coupled plasma mass spectrometry (ICP-MS, NexION, Perkin Elmer). Samples and standards (TraceCert 1mg/L in nitric acid) were diluted in 1% nitric acid before analysis. Both silver isotopes (^{107}Ag and ^{109}Ag) were quantified in triplicate per reading and a standard curve for each isotope was created, the sum of the concentration of each isotope within the sample was used to determine the total silver ion concentration within the sample (Syngistix v1.0, Perkin Elmer).

3.3.6. Quantitation of triclosan

Triclosan was quantified by detection of three ions of *m/z* = 287, 289 and 291, identified by direct injection of the samples. Quantification was achieved by LC-MS using the same system and C18 column as for quantitation in 3.3.3. The injection volume was 10 µl and separation was through isocratic conditions of 90% acetonitrile with 0.1% formic acid and 10% H_2O with 0.1% formic acid for a total of 10 minute run time. MS2 SIM scan type was used to identify the three ions, all with unit resolution, 200 ms dwell time, fragmentor voltage at 135 v and cell accelerator voltage at 4 v in negative ion mode. A total of all three ions eluted at 2.05 minutes and standards between 0.1 and 50 µg/ml were used to form a standard curve for quantitation.

3.3.7. Quantitation of cinnamaldehyde

LC-MS quantification of cinnamaldehyde was carried out using the same system and column as in section 3.3.3. with 5 µl injection of sample or standards, followed by a 10 second flush in 60% methanol and separation was in the C18 column at a flow rate of 0.1 ml/min. Solvent A was H_2O with 0.1% formic acid, solvent B was acetonitrile with 0.1% formic acid. Initial conditions were 99.5% A, held for 1 minute, before ramping to 90% B by 10 minutes, held for 3 minutes and reduced back to 0.5% B over 1 minute and

held until a total run time of 25 minutes. Detection of cinnamaldehyde was by MS2 SIM scan to identify the ion *m/z* = 133, using unit resolution, dwell time of 200 ms, fragmentor voltage of 100 v and cell accelerator voltage of 3 v, in positive ion mode. Cinnamaldehyde eluted from the column at 17.2 minutes and a standard curve was produced from standards in the range of 0.125 – 10 µg/ml.

3.3.8. Quantitation of furanone-C30.

Both ICP-MS and GC-MS were trialled for quantitation of furanone-C30. ICP-MS detection of bromine from a standard solution (QMX) and known furanone-C30 concentrations were diluted in 1% nitric acid and run through the same system as used for silver nitrate quantitation (section 3.3.5, Syngistix software v3.2). Detection of both common bromine ions (^{79}Br and ^{81}Br) were detected. For GC-MS detection, samples were extracted in 500 µl diethyl ether. Samples and standards were injected by the 7693 autosampler (Agilent), at a volume of 1 µl, run through an RTX-5 column in a 7890A GC system and detected by the 5975C VL MSD with triple axis detector (Agilent) to identify the key ion at *m/z* = 253.8. Column temperature was initially 80^{o}C, held for 3 minute before rising to 250 ^{o}C at a rate of 50^{o}C/second, held for 5 minutes before cooling with a 3 minute post run time.

3.3.9. Sol-gel disc diffusion assays

Six UPEC clinical strains (EC1, EC2, EC11, EC26, EC28 and EC34) previously isolated from urinary tract infections (UTIs) (Stepping Hill Hospital, Stockport, UK) and two laboratory characterised UPEC stains (EC958 and CFT073) were used in this work (Henly *et al.*, 2019, 2021). Previously, each strain had been passaged twelve times in the presence of the biocides or QSIs used here and stored within glycerol stocks at -80^{o}C until analysis (Henly, 2019; Henly *et al.*, 2019, 2021). Bacteria were cultured in Mueller Hinton broth (MHB) or on Mueller Hinton agar (MHA) (Sigma Aldrich, UK) and incubated under aerobic conditions at 37^{o}C overnight before use.

Overnight cultures were diluted to an OD_{600} of 0.008 and spread onto a MHA plate. Antimicrobial incorporated sol-gel discs prepared as described in 3.3.1. were placed on

top of the lawn of bacteria, sol-gel side down, and incubated for 24 hours at 37^{o}C. The zone of inhibition surrounding the discs was measured in mm.

3.3.10. Data analysis

The percentage of antimicrobial eluted from the sol-gel coating was based on the assumption of a homogenous incorporation of the antimicrobial within the sol-gel prior to coating, leading to a theoretical maximum concentration of 20 µg of available antimicrobial in 2 mg/ml coatings, and 100 µg of available antimicrobial in 10 mg/ml coatings. The concentration of the eluate was quantified by the methods above and used to calculate the mean cumulative amount released into the ammonium acetate based on the mean. Standard curves were extrapolated by linear regression. Comparison of the storage conditions for BAC samples was performed by linear regression analysis within GraphPad Prism (v8.1.1.). Comparisons of exposed strains and unexposed strains following sol-gel disc diffusion assays was by student two-tailed t-tests for each strain. Graphs and all data analysis were produced in GraphPad Prism (v 8.1.).

3.4.Results

Biocides (PHMB, BAC, silver nitrate and triclosan) and QSIs (*trans*-cinnamaldehyde and furanone-C30) were incorporated into a silica-based hybrid sol-gel coating. The total amount of biocide or QSI eluted from the coating was quantified and the antimicrobial properties of these coatings were assessed by disc diffusion assays.

3.4.1. Elution of antimicrobials from the sol-gel coating

Each antimicrobial was incorporated into the sol-gel at a concentration of either 2 mg/ml or 10 mg/ml. Samples of eluate were taken at time points over the course of one week and the concentration of the eluate quantified by different mass spectrometry methods, dependent upon the antimicrobial.

3.4.1.1. Elution of PHMB

Eluate from PHMB containing sol-gel coatings was analysed by LC-MS and quantified by detection of the main ion of *m/z* = 184, representative of the repeating hexamethylene biguanide unit. From 10 mg/ml PHMB containing sol-gel there is higher initial elution and all available PHMB had eluted within 48 hours (106 µg ± 9.1 SD), whereas where PHMB was incorporated into the sol-gel at 2 mg/ml it continued to elute for up to a week with a maximum elution of 19.2 µg ± 4.1 SD (Figure 3.1). Initial elution of PHMB was rapid for both concentrations tested, this slowed for 10 mg/ml samples and was and sustained for 2 mg/ml samples.

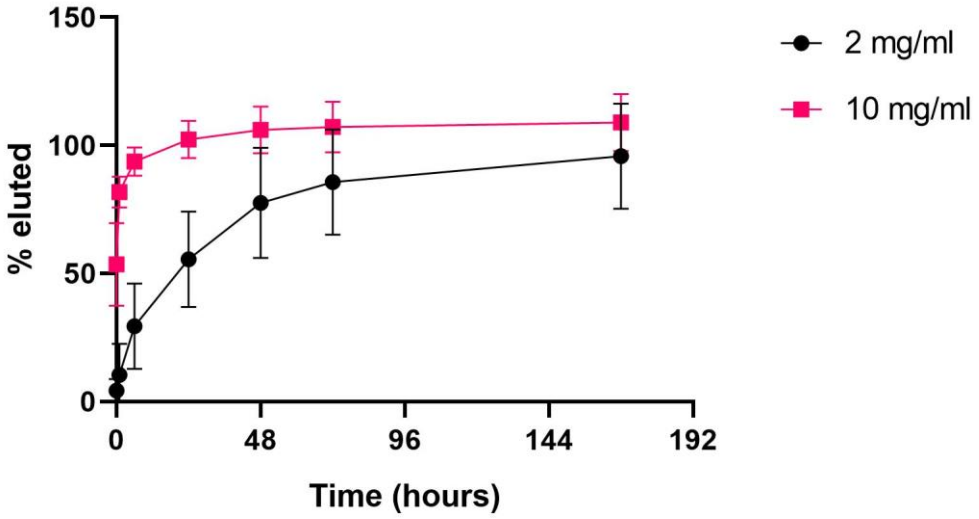

Figure 3.1. Percentage of PHMB eluted from sol-gel coated coverslips into 0.1 M ammonium acetate (pH 7.2) for up to 1 week. Eluate was quantified by LC-MS/MS detection of *m/z* = 184 from sol-gel coatings containing either 2 mg/ml or 10 mg/ml PHMB. N = 3 and error bars represent ± standard deviation.

Quantitation of PHMB by detection of the *m/z* = 184 ion was a linear interaction between 0.125 and 25 µg/ml. Example standard curve presented in Figure 3.2.

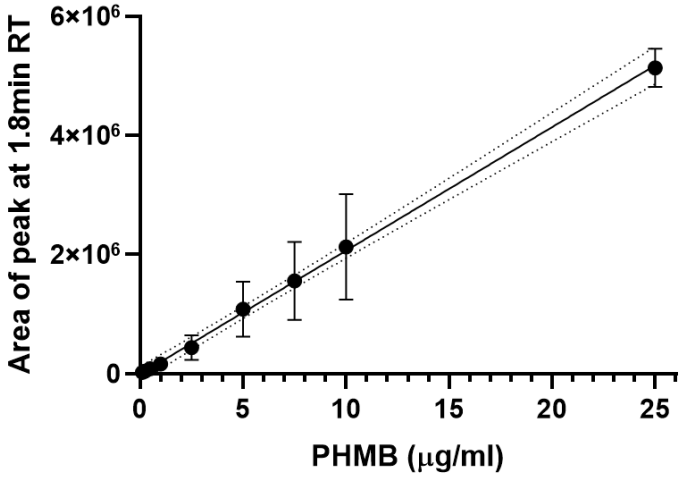

Figure 3.2. Example standard curve for quantitation of PHMB based upon detection of m/z = 184 and 367 by LC-MS/MS. N = 6 (run at the start and end of samples run), error bars represent ± standard deviation and dotted lines represent the 95% confidence intervals of the curve. Equation of the line: y= 207528x – 10847, r^2 = 0.9286.

3.4.1.2. Elution of BAC

BAC was quantified by the detected by LC-MS detection of the product ion *m/z* = 91 from both C_{12}-BAC and C_{14}-BAC precursor ions. Over the course of a week, very little BAC eluted from the coating, up to a maximum of 1.5% (1.5 µg) from the 10 mg/ml coating and 0.12% (0.2 µg) from the 2 mg/ml coating (Figure 3.3). With so little eluting from the coating, the stability of BAC was assessed by running multiple standards either fresh, stored at room temperature or stored in the fridge for 72 hours, there was no significant difference in the standard curves produced (linear regression analysis of comparison of slopes p = 0.3912 and intercepts p = 0.6034, pooled equation: y = 75575 x – 6072, Figure 3.4).

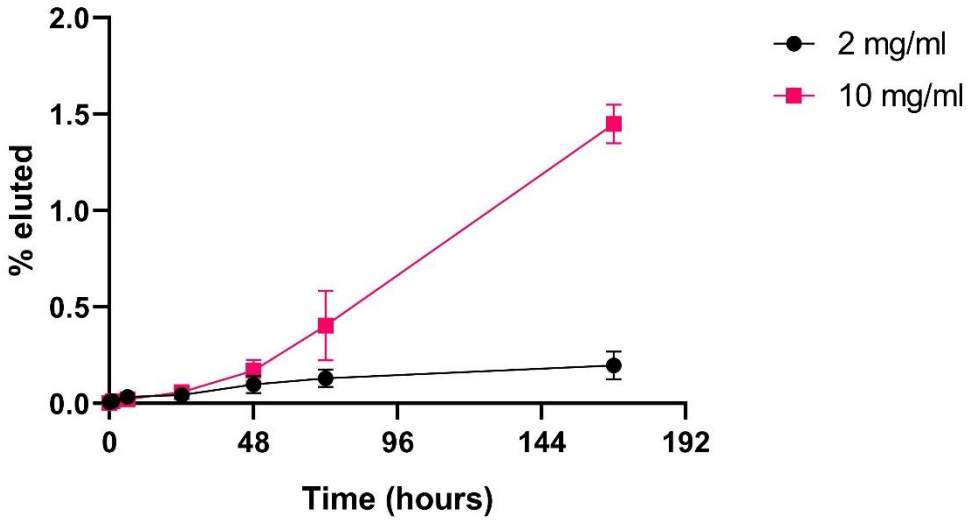

Figure 3.3. Percentage of available BAC within a sol-gel coating eluted into ammonium acetate (pH 7.2) over the course of a week. Eluate was quantified by LC-MS detection of product ion *m/z* = 91 from sol-gel coatings containing BAC at either 2 mg/ml or 10 mg/ml. N = 3 and error bars represent ± 1 standard deviation.

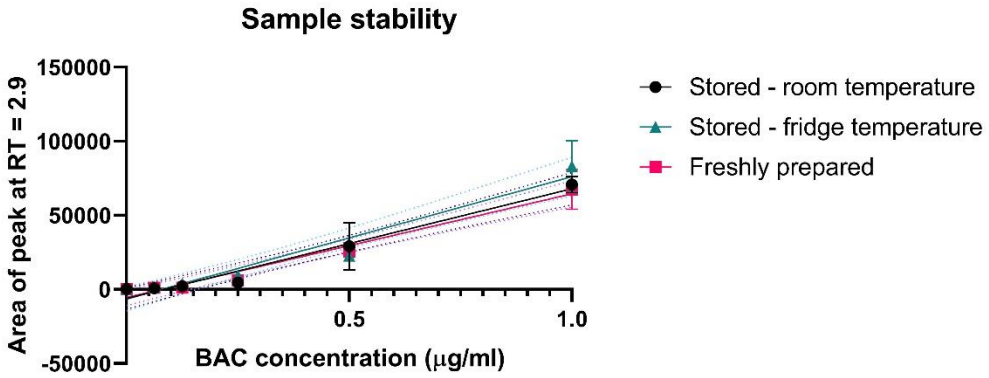

Figure 3.4. Comparison on standards stored under different conditions: 72 hours at room temperature, fridge temperature or made up fresh the same day. There is no significant differences between the slopes (p = 0.3912) or the intercepts (p = 0.6034) as calculated by comparison of slopes and intercepts within GraphPad Prism (8.1.1). Room temperature: y = 74090x – 6187, r^2 = 0.9347, fridge: y = 82582x -6528, r^2 = 0.9193 fresh: y = 69973x -5492, r^2 = 0.9471. Dotted lines represent the 95% confidence intervals.

3.4.1.3. Elution of silver nitrate

Elution of silver nitrate was quantified by ICP-MS detection of the silver ions within the eluate. Silver nitrate eluted rapidly from the sol-gel coating; within 24 hours the rate of elution had stabilised (Figure 3.5). Immediately, at 0 hours, 1.4 µg of silver was released from the 2 mg/ml silver nitrate coating and 9.7 µg from the 10 mg/ml silver nitrate coating.

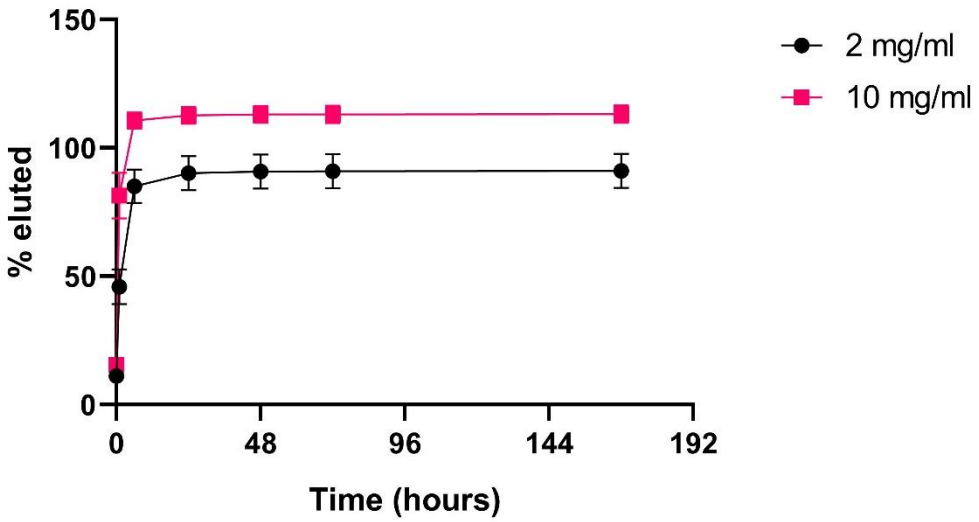

Figure 3.5. Elution of silver nitrate into 0.1M ammonium acetate (pH 7.2) from sol-gel coated cover slips for up to 1 week. Eluate was quantified by ICP-MS detection of silver ions, n = 3 and error bars represent ± standard deviation. Percentage eluted based upon the estimated amount of silver in the silver nitrate in the coating, available silver in 2mg/ml coating ~ 12.7 µg/ coverslip, 10mg/ml coating ~63.5 µg/coverslip.

3.4.1.4. Elution of triclosan

Detection and quantitation of triclosan was based upon the LC-MS detection of ions *m/z* = 287, 289 and 291 identified following direct injection of triclosan for MS detection. An effective standard curve with an $r^2 > 0.9$ was formed between concentrations of 0.1 and 12.5 µg/ml (Figure 3.7). The total amount of the available triclosan which eluted from the coating differed dependent upon the concentration within the sol-gel. At both concentrations, all the available triclosan eluted from the coating within a week (Figure 3.6).

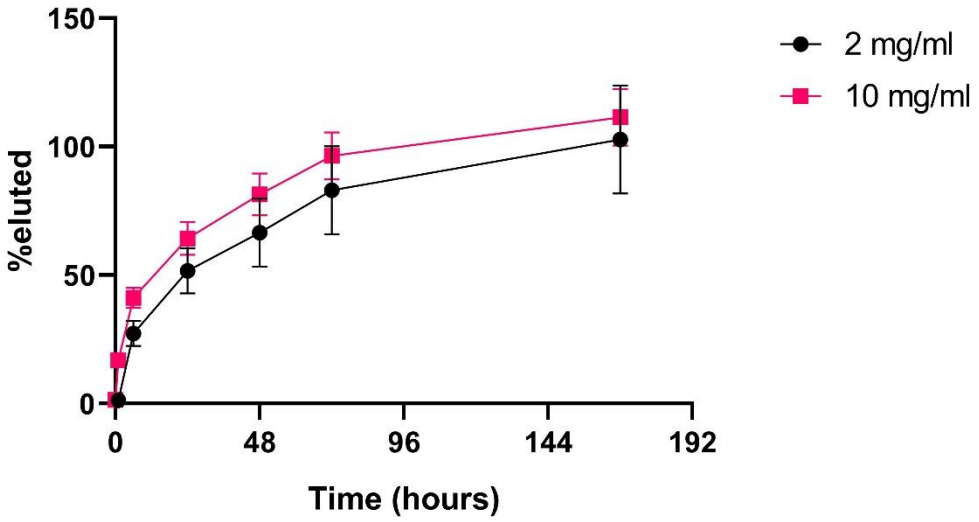

Figure 3.6. Percentage of available triclosan eluted from sol-gel coated coverslips into 0.1 M ammonium acetate (pH 7.2) for up to one week. Eluate was quantified by LC-MS detection of *m/z* = 287, 289 and 291 from sol-gel coatings containing 2 mg/ml or 10 mg/ml triclosan. N = 3 and error bars represent ± standard deviation.

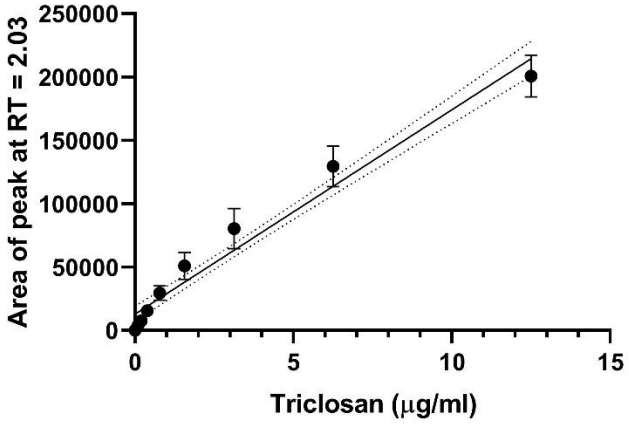

Figure 3.7. Representative standard curve of triclosan. (n = 4) error bars represent ± standard deviation and dotted line represents the 95% confidence intervals, y = 16116x +12966, r^2 = 0.948.

3.4.1.5. Elution of cinnamaldehyde

The concentration of cinnamaldehyde released from the sol-gel coating was quantified by LC-MS detection of the ion *m/z* = 133 representative of the *trans*-cinnamaldehyde molecule. Initial elution from the coating is rapid within the first 24 hours, before slowing. Unlike the profiles observed for the other antimicrobials, when incorporated into the sol-gel at 2 mg/ml there was a higher overall percentage of the available cinnamaldehyde which was eluted from the coating than the overall amount released from the 10 mg/ml coating (Figure 3.8, Figure 3.9)

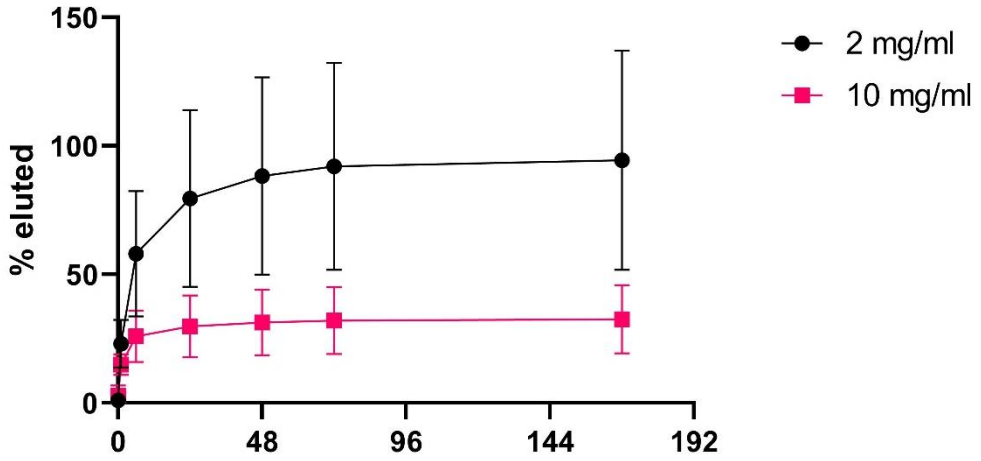

Figure 3.8. Percentage of available cinnamaldehyde released from sol-gel coatings into 0.1 M ammonium acetate (pH 7.2) over a period of one week. Eluate was quantified by measurement of the ion *m/z* = 133, representing the cinnamaldehyde molecule. Results are n = 3, error bars represent ± standard deviation.

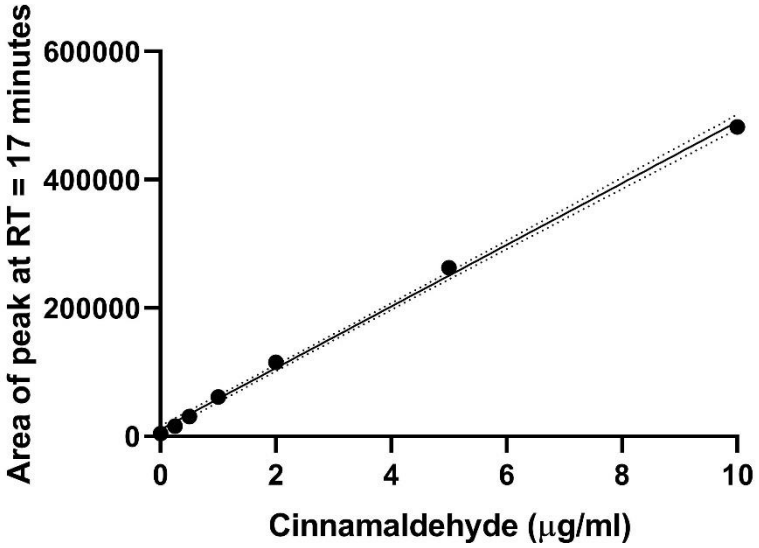

Figure 3.9. Representative standard curve of cinnamaldehyde. (n = 2) error bars represent ± standard deviation and dotted line represents the 95% confidence intervals, y = 47982 x + 10426, r^2 = 0.9978.

3.4.1.6. Elution of furanone-C30

Detection of furanone-C30 was attempted by ICP-MS detection of the bromine atoms on the molecule and through GC-MS for detection of the whole molecule. A standard curve of a bromine standard was created (Figure 3.10) and known standards of furanone-C30 were compared to this. The proportion of furanone-C30 ($C_5O_2Br_2H_2$) of which bromine is 63%, does not correlate with the estimated quantities of bromine within the sample when measured by either ^{79}Br or ^{81}Br (Table 3.1).

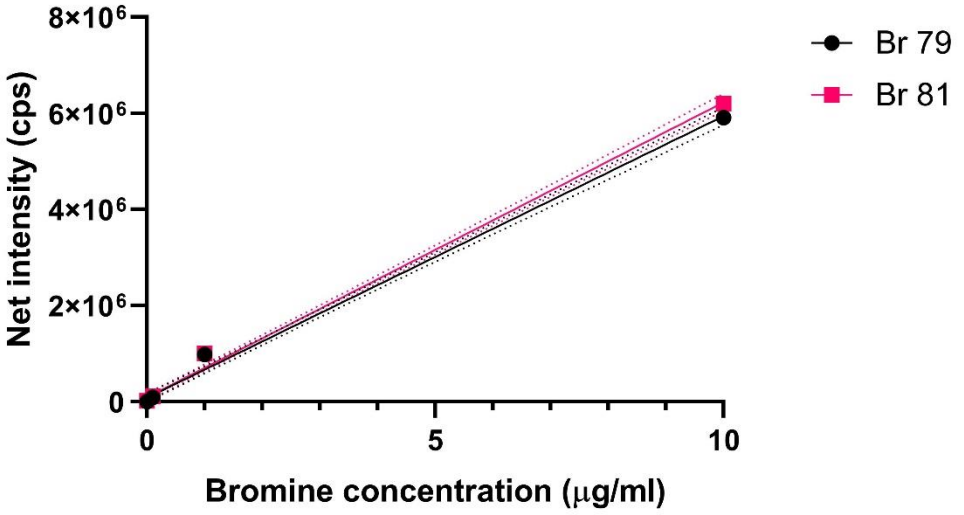

Figure 3.10. Standard curve of bromine standard for detection of both bromine isotopes (^{79}Br and ^{81}Br). N=3 with 3 readings per replicate ^{79}Br: y = 586061 x +82434, r^2 = 0.996, ^{81}Br: y = 613710 x +92082, r^2 = 0.996. Dotted lines represent the 95% confidence interval of the line.

Table 3.1. Comparison of known standards of furanone-C30 and the concentration estimated based upon the curves presented above.

Known standard of furanone-C30 (μg/ml)	^{79}Br concentration (μg/ml)	^{81}Br concentration (μg/ml)
0.001	N/A	N/A
0.01	N/A	N/A
0.1	0.00006	0.00783
1	1.35	1.34
10	12.27	12.16

Detection of furanone-C30 by GC-MS was initially investigated by a mass spec scan in the mass range of *m/z* = 50 to 500. In comparison to the blank there are substantial peaks at *m/z* = 253.8 (Figure 3.11). However, upon isolation of this ion and SIM detection, it was only measurable in concentrations above 1 mg/ml (Figure 3.12).

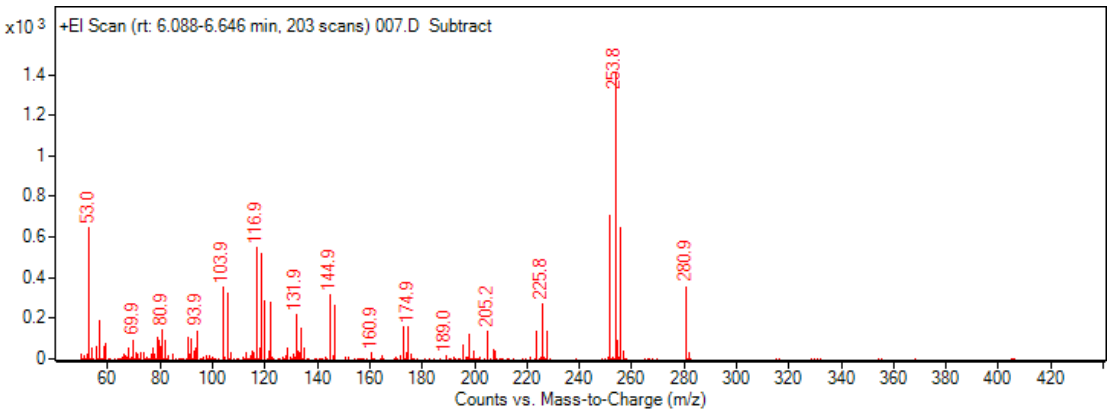

Figure 3.11. Spectra of ions at retention time 6.2 minutes.

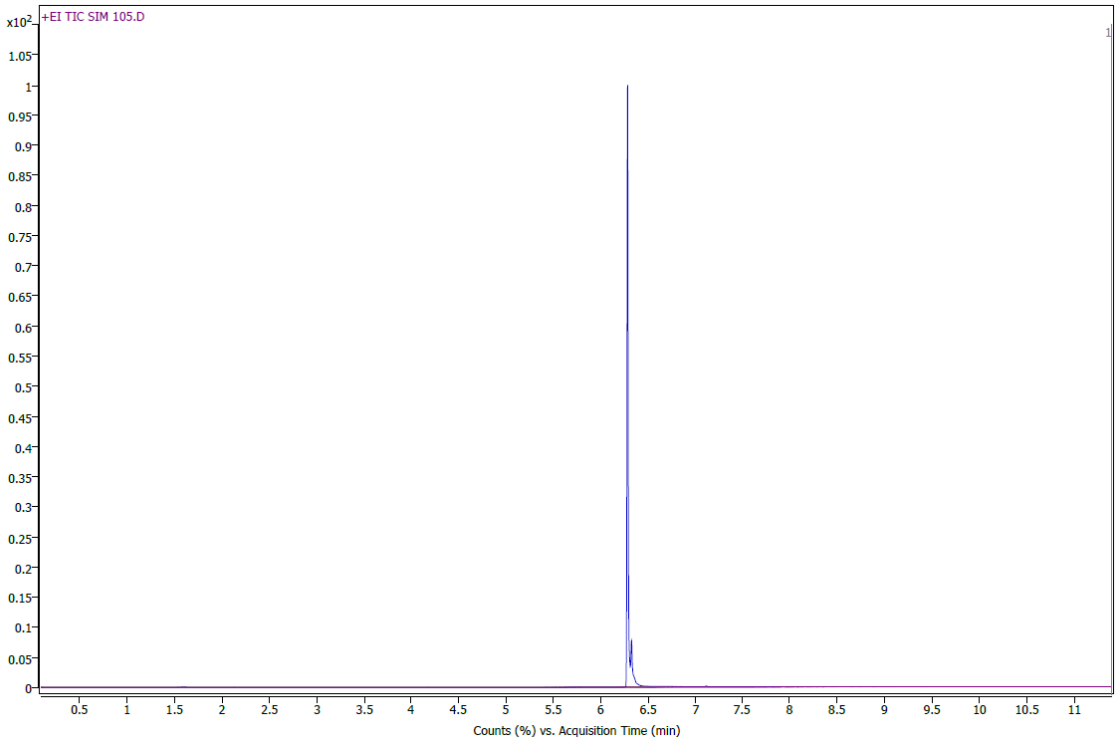

Figure 3.12. Overlayed chromatograms of SIM detection of *m/z* = 253.8. Purple – blank, red – 250 µg/ml, green 500 µg/ml, blue – 1 mg/ml.

3.4.2. Sol-gel disc diffusions

UPEC strains were exposed to the test biocides and QSIs over 12 passages using a previously validated antimicrobial gradient plating system (Henly, 2019; Henly *et al.*, 2019, 2021). Antimicrobial passaged (exposed) or un-passaged (unexposed) strains were challenged with the antimicrobial containing sol-gel coated discs at containing either 20 µg or 100 ug of antimicrobial (2mg/ml or 10 mg/ml concentration respectively) and the resulting zone of inhibition was measured. There was no statistical difference observed between passaged and un-passaged strains when exposed to PHMB (Figure 3.13), BAC (Figure 3.14) or cinnamaldehyde (Figure 3.17) at either 2mg/ml or 10 mg/ml, or silver nitrate at 2 mg/ml. At 10 mg/ml silver nitrate within the sol-gel, un-passaged EC28 and EC958 were more sensitive than the passaged isolate ($p = 0.0059$ and $p = 0.0198$ respectively, t-test, Figure 3.15). Triclosan incorporated sol-gel, at a concentration of 2mg/ml demonstrated a significantly larger zone of inhibition around un-passaged EC11 than the passaged isolate ($p = 0.0198$); at 10 mg/ml concentration within the sol-gel, the zones of inhibition were much larger than those observed at 2 mg/ml and un-passaged EC34 ($p = 0.136$) and CFT073 ($p = 0.0021$) were more sensitive than the passaged isolates (Figure 3.16). Un-passaged EC1 was more sensitive to 2 mg/ml furanone-C30 containing sol-gel than the passaged isolate ($p = 0.0121$), however at 10 mg/ml concentration passaged strains of EC1 and EC28 were more sensitive than the corresponding un-passaged strain ($p = 0.0496$ and $p = 0.0430$, respectively, Figure 3.18).

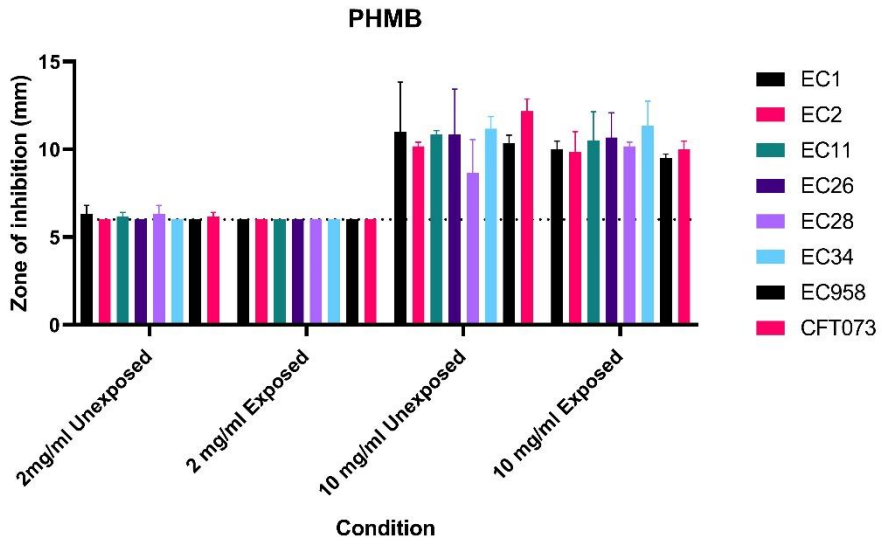

Figure 3.13. Zone of inhibition of PHMB incorporated sol-gel of UPEC strains previously unexposed to PHMB, or passaged in the presence of PHMB twelve times (Exposed). Results are an average of two biological repeats, each with three technical replicates. Error bars represent + 1 standard deviation, dotted line represents the disc diameter. No significant differences between unexposed or exposed strains, student two-tailed t-test. Dotted line represents the diameter of the test disc.

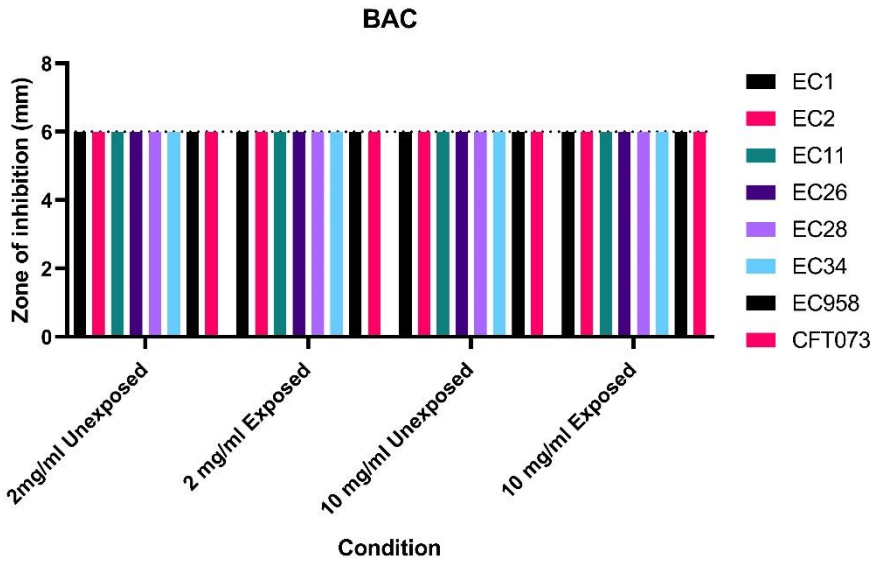

Figure 3.14. Zone of inhibition of BAC incorporated sol-gel of UPEC strains previously unexposed or passaged in the presence of BAC twelve times. Results are an average of two biological repeats, each with three technical replicates. Error bars represent + 1 standard deviation, dotted line represents the disc diameter. No significant differences between unexposed or exposed strains, student two-tailed t-test. Dotted line represents the diameter of the test disc.

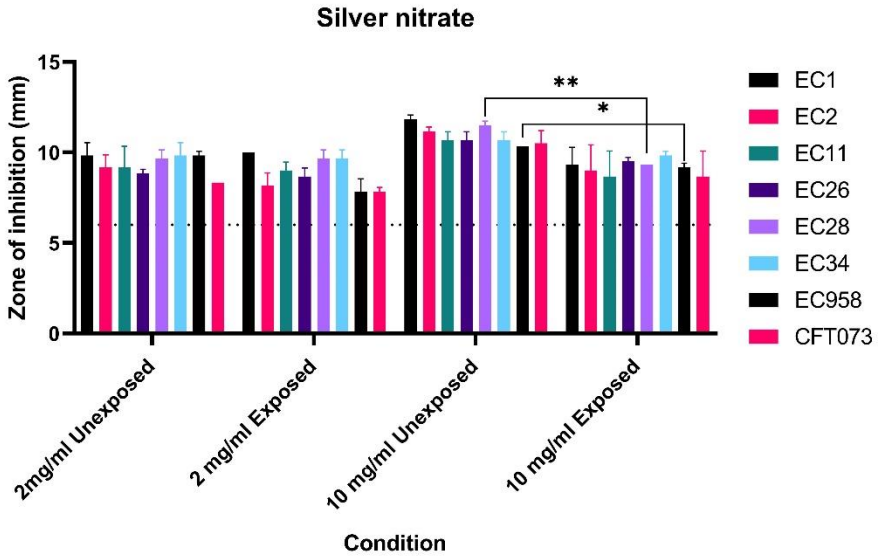

Figure 3.15 Zone of inhibition of silver nitrate incorporated sol-gel of UPEC strains previously unexposed or passaged in the presence of silver nitrate twelve times. Results are an average of two biological repeats, each with three technical replicates. Error bars represent + 1 standard deviation, dotted line represents the disc diameter. Significant differences between unexposed and exposed EC28 p = 0.0059 and EC958 p = 0.0198, student two-tailed t-test. Dotted line represents the diameter of the test disc.

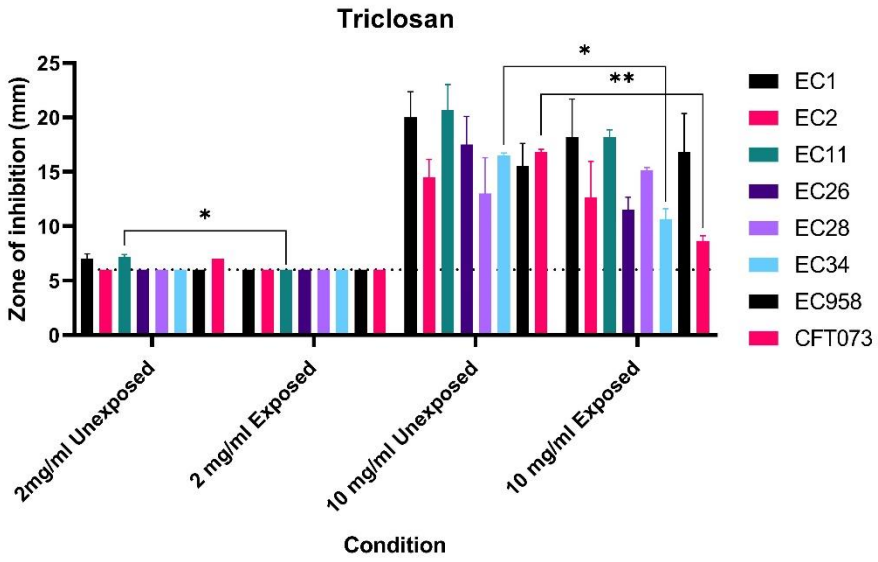

Figure 3.16. Zone of inhibition of triclosan incorporated sol-gel of UPEC strains previously unexposed or passaged in the presence of triclosan twelve times. Results are an average of two biological repeats, each with three technical replicates, dotted line represents the disc diameter. Error bars represent + 1 standard deviation. T-test analysis between unexposed and exposed strains at each concentration, * $p \leq 0.05$, ** $p \leq 0.01$. Dotted line represents the diameter of the test disc.

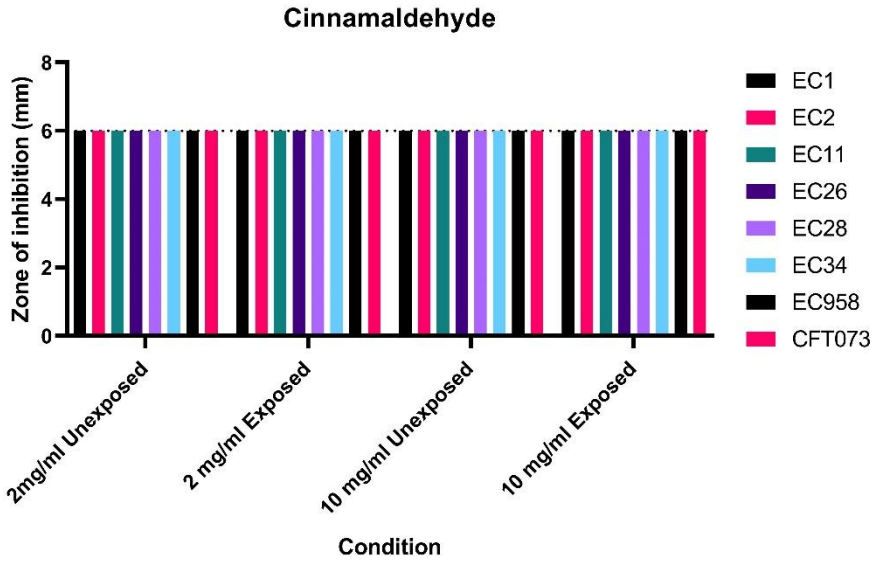

Figure 3.17. Zone of inhibition of cinnamaldehyde incorporated sol-gel of UPEC strains previously unexposed or passaged in the presence of cinnamaldehyde twelve times. Results are an average of two biological repeats, each with three technical replicates. Error bars represent + 1 standard deviation, dotted line represents the disc diameter. No significant differences between unexposed or exposed strains, student two-tailed t-test. Dotted line represents the diameter of the test disc.

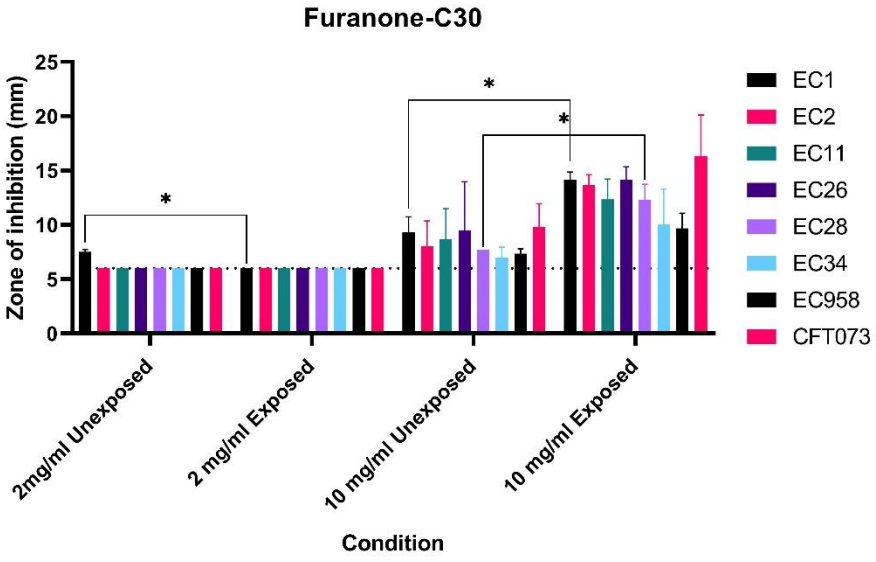

Figure 3.18. Zone of inhibition of furanone-C30 incorporated sol-gel of UPEC strains previously unexposed or passaged in the presence of furanone-C30 twelve times. Results are an average of two biological repeats, each with three technical replicates. Error bars represent + 1 standard deviation, dotted line represents the disc diameter. T-test analysis between unexposed and exposed strains at each concentration, * $p \leq 0.05$. Dotted line represents the diameter of the test disc.

3.5. Discussion

All the biocides and QSIs assessed in this research showed unique elution profiles when released from the sol-gel into ammonium acetate. Silver ions released from silver nitrate impregnated sol-gel elute rapidly and completely at both concentrations tested within as little as 6 hours, this correlates with the disc diffusion data where clear zones of bacterial growth inhibition > 8 mm were observed for each strain at both 2mg/ml and 10 mg/ml concentrations. BAC, in contrast, does not elute readily from the sol-gel coating and this is shown in the elution data where <2% of the available BAC was eluted from the coating over the course of the week. Subsequently no zone of inhibition was observed in disc diffusion assays.

At a concentration of 2 mg/ml, the time taken for the available antimicrobial to be released was ranked from fastest to slowest as: silver nitrate > PHMB = triclosan = cinnamaldehyde > BAC and unknown for furanone-C30, based on the time taken until 100% elution. Regarding the disc diffusion results, ordered by most effective to least based upon average zone of inhibition across strains: silver nitrate > triclosan > furanone-C30 > PHMB > cinnamaldehyde = BAC.

When the antimicrobials were incorporated at 10 mg/ml concentration, the rate of release was most rapid from silver nitrate > PHMB = triclosan > cinnamaldehyde > BAC. In order of the most effective disc diffusions at 10 mg/ml: triclosan > silver nitrate >PHMB > furanone-C30 >cinnamaldehyde = BAC.

In disc diffusion assays, both cinnamaldehyde and BAC were ineffective. Although cinnamaldehyde was shown to be released from the coatings by the elution data, the available concentrations would likely be too low to inhibit bacterial growth, with MIC concentrations of at least 250 µg/ml required (Henly *et al.*, 2021). Both triclosan and silver nitrate were effective in the disc diffusion assays. Although triclosan release was slower than silver nitrate, the effective concentrations required to inhibit bacterial growth would be lower as seen in previous MIC experiments with an MIC of triclosan at 0.00001 – 0.2 µg/ml and MIC of silver nitrate at 31.3 µg/ml (Henly *et al.*, 2019).

The release rate of the antimicrobials will impact the antimicrobial efficacy of the sol-gel coatings. A release rate that is too rapid would lead to depletion of the antimicrobial within the coating, providing only a short window of efficacy, it may also lead to initial

concentrations which are cytotoxic to the host. A release rate that is too low may lead to antimicrobial concentrations which are unable to inhibit bacterial colonisation of the catheter surface or may even provide a selective pressure leading to selection of resistant populations. Therefore, optimum release profiles must be determined when developing a coating strategy.

3.5.1. PHMB

PHMB is a heterogeneous polymeric molecule, composed of repeating units of a hexamethylene biguanide $(C_8H_{17}N_5)_n$, where n can range from 1-40 (Gilbert and Moore, 2005; Allen, White and Morby, 2006) and a range of end groups which may include an amine, a cyanoamine, a guanidine or a cyanoguanidine group in any combination (O'Malley *et al.*, 2006).

Detection of PHMB was based upon the ion of *m/z* = 184 which relates to a single repeating unit of the hexamethylene biguanide (O'Malley *et al.*, 2006). PHMB eluted completely within 1 week when incorporated into the sol-gel at a concentration of 2 mg/ml, and within approximately 24 hours when incorporated into the sol-gel at a concentration of 10 mg/ml. Higher concentrations of PHMB have been shown to aggregate especially with higher degrees of polymerisation (Sowlati-Hashjin, Carbone and Karttunen, 2020), this could affect the incorporation into the sol-gel potentially leading to less even distribution through the coating.

The limitation of this protocol for quantitation of PHMB released from the sol-gel coating is that it provides no information on the structures of PHMB released from the sol-gel coating. It cannot confirm the number of the repeating units, whether those released are the small oligomers of the molecule, or whether large units are released and are effectively measured via the quantitation of the hexamethylene biguanide unit. Further studies using time of flight (TOF) based mass spectrometry could provide a method to identify the specific structures of PHMB released from the coating (O'Malley *et al.*, 2006; Rembe *et al.*, 2016). but even this has a limit as to the number of repeating units which are measurable, due to the potential long lengths of the molecule with high numbers of repeating units (O'Malley *et al.*, 2006).

PHMB incorporated into sol-gel at 10 mg/ml led to zones of inhibition ranging from 8.7 mm to 12.2 mm. This demonstrates that the incorporation of the antimicrobial into the sol-gel coating does not prevent the functionality of PHMB to inhibit the bacterial growth.

PHMB Is commonly used in contact lens solutions, it has been shown that the properties of the hydrogel of the contact lens can affect the uptake and release of PHMB from the lenses. The available charges of the hydrogel, when negative, increased the uptake of positively charged PHMB, and lenses with hydrophilic surfaces had faster release of PHMB from the surface. PHMB is hydrophilic, therefore easily elute from the lens the water content of the lens was important (Yee, Phan and Jones, 2022). Elution into urine could lead to a different elution profile. PHMB eluted into different solutions, Tris-HCL and PBS, both at pH 7.4 led to different elution profiles from a bacterial cellulose and alginate-based hydrogel, due to the interactions between PHMB and the different ions in the two buffers (Chanabodeechalermrung *et al.*, 2022).

3.5.2. BAC

Discs coated with BAC incorporated sol-gel did not have a zone of inhibition, this correlates with the elution data which shows that BAC was not eluted from the sol-gel coating. The lack of BAC detected within the eluate was first hypothesised that it is degrading, however it was shown to be robust, and standards stored at room temperature, refrigerated or fresh did not affect the reproducibility of the standard curve created. The BAC used in this work was composed of 70% benzyldimethyldodecylammonium chloride (C_{12}-BAC) and 30% benzyldimethyltetradecylammonium chloride (C_{14}-BAC), this was confirmed by initial direct injection (data not shown). The fragmentation of both C_{12}-BAC and C_{14}-BAC was by breaking of the carbon and nitrogen, releasing toluene, which then stabilises to tropylium and is detected as an ion with a m/z = 91 (Takeoka *et al.*, 2005).

Although no BAC eluted from the coating into the ammonium acetate it could function as a surface upon which bacteria cannot attach, however this may be of limited use as a conditioning film deposited onto the surface could prevent any potential contact killing efficacy of the coating (Buhmann *et al.*, 2016). BAC is an amphoteric surfactant, the impact of the positive head group and negative tail could be impacting upon the gel

formation of the sol-gel and resulting in steric hinderance of the release of BAC from the sol-gel.

3.5.3. Silver nitrate

Silver nitrate incorporated into the sol-gel led to effective antimicrobial activity with zones of inhibition larger than 8 mm at both 2 mg/ml and 10 mg/ml incorporated concentrations. This correlated with the sudden release of silver ions, measured by ICP-MS which was observed at both concentrations, where full elution was achieved within 24 hours.

Although silver hydrogel catheters (Lubri-Sil® I.C. and Bardex ® I.C.) are commercially available, there has been shown to be no overall advantage to their use in a clinical setting to prevent the incidence of bacteriuria and CAUTI (Lam *et al.*, 2014). In *in vitro* studies, silver containing catheters have been shown to be no more effective than uncoated, or hydrogel only catheters against *E. coli* (Desai *et al.*, 2010; Johnson, Johnston and Kuskowski, 2012).

Silver nitrate has been incorporated into sol-gel systems previously, the release from an methyltriethoxysilane based sol-gel demonstrated a similar sudden release of silver, which slowed over a 24 hour period (Jaiswal, McHale and Duffy, 2012). The matrix into which the silver ions are eluted may affect the release rate from sol-gel coatings. Phenyl-TEOS based sol-gel coating showed a sustained release of silver into PBS, whereas a sudden burst, followed by trace amounts released into deionised water. (Stobie *et al.*, 2008). There is potential for the silver released from the coating to interact with the matrix into which it is eluted, this could lead to issues with crystallisation with the available ions within urine which could lead to insoluble salt deposition on the surface (Stobie *et al.*, 2008). As commented on within discussion of BAC, this could lead to a blocking of the surface, leading to prevention of any contact killing efficacy and potentially deposition of insoluble salts which could block the lumen of the catheter.

3.5.4. Triclosan

Triclosan incorporated into sol-gel at a concentration of 10 mg/ml led to effective zones of inhibition from 8.7 – 20.7 mm in diameter. When incorporated into the sol-gel at 2

mg/ml and 10 mg/ml the elution profiles were similar, both with more rapid initial elution, slowing until complete release within a week.

Triclosan has been investigated as a solution in polyethylene glycol with which to inflate the balloon of a Foley catheter, at a concentration of 10 mg/ml this was shown to prevent formation of biofilms within a glass bladder model. Triclosan was shown to elute at a high concentration of up to 20 - 160 µg/ml (Jones *et al.*, 2006). Combinations of triclosan with EDTA or cranberry extracts have also been investigated as potential solutions to inflate the balloon of the catheter, again triclosan was seen to diffuse readily through the silicone of the balloon but elution was not quantified in this study (Ayyash *et al.*, 2019).

Triclosan has been viewed as a contaminant which is potentially bio accumulative, it has been detected in the urine of American (Calafat *et al.*, 2008) and Korean populations (Kim *et al.*, 2011) and in the environment, largely due to its widespread use in cleaning or cosmetic products (Bedoux *et al.*, 2011). Detection methods for triclosan have included HPLC, quantitation at wavelengths in the range of 200 – 282 nm (Piccoli *et al.*, 2002; Liu and Wu, 2012; Bai and Acharya, 2016; Wang, Yin and Wang, 2017; Aminu *et al.*, 2018) and mass spectrometry detection of the whole molecule (Wang, Yin and Wang, 2017), or its by-products (Chen *et al.*, 2020; Jia *et al.*, 2020).

Triclosan has been incorporated into sol-gel based materials previously, including in a TEOS based sol-gel for use on textiles. It was shown to provide antifungal properties but activity was not sustained after washing. Triclosan eluted readily from the sol-gel, leading to a zone of fungal inhibition around the fabric but the amount of triclosan eluted was not quantified in this application (Foksowicz-Flaczyk *et al.*, 2016).

3.5.5. Cinnamaldehyde

Cinnamaldehyde incorporated into the sol-gel at 2 mg/ml led to a higher total percentage release into ammonium acetate than when incorporated into the sol-gel at 10 mg/ml. Cinnamaldehyde is a hydrophobic molecule, which has a low solubility in water at only 1.35 mg/ml (Yildiz *et al.*, 2019). At the higher concentration of 10 mg/ml it may not be as soluble as at the 2 mg/ml concentration and therefore the elution from the sol-gel coating would be limited.

The lack of a zone of microbial inhibition, despite the demonstrated release, is likely due to the low level of antimicrobial activity of cinnamaldehyde. The maximum concentration in the 10 mg/ml sol-gel disc was only 100 µg cinnamaldehyde per disc whereas effective inhibitory concentration may be as high as 250 µg/ml (Henly *et al.*, 2021).

Cinnamaldehyde had been previously included in TEOS based sol-gel based microcapsules within a poly (butyleneadipate-*co*-terephthalate) film. It was shown that the temperature and the humidity affected the elution of cinnamaldehyde from the microcapsules, which was quantified by UV-vis spectroscopy. Higher temperature and higher humidity increased the rate of elution (Xu *et al.*, 2020). This is something to consider, that along the length of the catheter there is going to be temperature changes, from 37^{o}C within the body to lower along the length of the catheter to the drainage bag, meaning the rate of elution may change across the device surface.

Research into the use of cinnamaldehyde within antimicrobial coatings has been focussed on packaging of food materials. Cinnamaldehyde released from a chitosan film into 10% or 50% v/v ethanol solutions showed faster release into higher alcohol content solutions than into lower (Chen *et al.*, 2016) further highlighting the impact of the surrounding solution of the elution profile.

3.5.6. Furanone-C30

From the ICP-MS analysis which aims to detect the bromine of the furanone-C30 molecule, there appeared to be a higher concentration of bromine than expected within the test concentration of Furanone-C30. Further analysis would be required to address this, it could be that there was free bromine available alongside the furnaone-C30. It may also have degraded over time since the initial in-house production of the antimicrobial.

Detection of furanone-C30 by GC-MS does not appear to have a known spectra within the available chemical databases. The ion at *m/z* = 253.8 was detected only in the furanone-C30 sample, not in the blank, and only at concentrations above 1 mg/ml. As the total available concentration in the 10 mg/ml sol-gel is only 100 µg this method would therefore not be suitable for use. Future work could optimise the sample

preparation process for this to be used effectively. There are zones of inhibition at 10 mg/ml (7 – 16.3 mm). Prior exposure to furanone-C30 appears to increase the susceptibility of UPEC to the QSI therefore increased zones of inhibition were observed at 10 mg/ml in EC1 and EC28 after long-term furanone-C30 exposure.

Previous research into the use of furanones as antimicrobial coatings has used technology including x-ray photoelectron spectroscopy of bromine from deposited 3-(1-bromohexyl)-5-dibromomethylene-2(5H)-furanone on a range of materials to determine the concentration within the coating (Baveja *et al.*, 2004).

3.5.7. Future work

Optimisation of the sol-gel formulation to control the antimicrobial release rates would be the next step in this investigation and there are a wide range of modifications that could be made to the sol-gel itself which could impact the final coating properties. Changes to the precursor solution could include additional functional groups which could change the polymerisation of the sol-gel or could bond to the antimicrobials. The catalyst solution could be modified, lower pH concentrations lead to more linear polymerisation whereas higher pH concentrations lead to higher branching of the gel as it polymerises. The water and solvent concentration within the sol-gel has an impact on the rate of condensation and hydrolysis reactions, as well as the rate at which the gel dries (Jones, 1989; Brinker, C and Scherer, George, 1990; Brinker *et al.*, 1992). All these modifications would have profound effects on the elution of each antimicrobial, however coating adjustments fell outside the scope of this PhD.

Where these antimicrobials have been previously assessed for their elution from sol-gels, hydrogels and other coatings, it has been noted that the medium into which they are released impacts the rate of release (Stobie *et al.*, 2008; Chanabodeechalermrung *et al.*, 2022). The release of these agents from a sol-gel coating into urine should be assessed as a next step, this however comes with significant complications, including the fact that urine is a highly heterogeneous solution, with a significant salt and ion content which varies within a single person throughout the day (Sarigul, Korkmaz and Kurultak, 2019).

3.6.Conclusions

A silica-based hybrid sol-gel formulation was assessed for the release of PHMB, BAC, silver nitrate, triclosan, cinnamaldehyde and furanone-C30 into ammonium acetate. The amount of antimicrobial released was quantified by mass spectrometry methods and the antimicrobial efficacy of the coatings at 2 mg/ml and 10 mg/ml concentrations was assessed by disc diffusion assay. The elution profiles varied dependent upon the antimicrobial incorporated; silver nitrate demonstrated rapid elution from the coating, whereas BAC did not appear to elute from the coating over the course of one week. This was mirrored by the effective zones of microbial inhibition, at 10 mg/ml of silver nitrate and absence of a zone of inhibition of BAC. Further work would be required to profile the release of these antimicrobials into the complex matrix that urine would provide, as it potentially could impact the elution rates of these antimicrobials as has been shown in other studies where salts within and the polarity of the matrix impacts the release rate. Future work could also encompass the optimisation of the sol-gel coating itself to control elution profiles and subsequent antimicrobial efficacy.

4.
Combined efficacy of biocides and quorum sensing inhibitors against clinically relevant uropathogenic *Escherichia coli* strains

Parts of this work have been published in Capper-Parkin, K. L., Nichol, T., Smith, T. J., Lacey, M. M., & Forbes, S. (2023). Antimicrobial and cytotoxic synergism of biocides and quorum-sensing inhibitors against uropathogenic Escherichia coli. *Journal of Hospital Infection*, *134*, 138–146. https://doi.org/10.1016/j.jhin.2023.02.004

4.1.Abstract

Background: Uropathogenic *Escherichia coli* (UPEC) are a primary cause of catheter associated urinary tract infections (CAUTI) often forming mature recalcitrant biofilms on the catheter surface. Anti-infective catheter coatings containing single biocides have been developed but display limited antimicrobial activity due to the selection of biocide resistant bacterial populations. Furthermore, biocides often display cytotoxicity at concentrations required to eradicate biofilms limiting their antiseptic potential. Quorum sensing inhibitors (QSIs) provide a novel anti-infective approach to disrupt biofilm formation on the catheter surface and help prevent CAUTI.

This chapter aims to evaluate the combinatorial impact of biocides and QSIs at bacteriostatic, bactericidal and biofilm eradication concentrations in parallel to assessing cytotoxicity in L929 murine fibroblast cells and human bladder smooth muscle (BSM) cells.

Methods: Checkerboard assays were performed to determine fractional inhibitory, bactericidal and biofilm eradication concentrations of biocides in combination with QSIs in eight UPEC strains. Combined cytotoxic effects in L929 mouse fibroblast cells and human bladder smooth muscle cells was assessed by MTT assay.

Results: Synergistic antimicrobial activity was observed between polyhexamethylene biguanide (PHMB), benzalkonium chloride (BAC) or silver nitrate in combination with either cinnamaldehyde or furanone-C30 against UPEC biofilms. However, furanone-C30 was cytotoxic in both cell lines at concentrations below those required for even bacteriostatic activity. For both cell lines assayed, a dose-dependent cytotoxicity profile was observed for cinnamaldehyde when in combination with BAC, PHMB or silver nitrate. Both PHMB and silver nitrate displayed combined bacteriostatic and bactericidal activity below IC_{50} in BSM cells. Triclosan in combination with both QSIs displayed antagonistic activity in UPEC and BSM cells.

Conclusions: PHMB and silver nitrate in combination with cinnamaldehyde display synergistic antimicrobial activity in UPEC at non cytotoxic concentrations in human BSM cells, suggesting potential as anti-infective catheter coating agents.

4.2.Introduction

Catheter associated urinary tract infections (CAUTI) pose a significant burden to healthcare; with an incidence rate of 1.64 cases per 1000 catheter-days and a rise in infection rates for each day that the catheter is left in place (Letica-Kriegel *et al.*, 2019; Li *et al.*, 2019). Uropathogenic *Escherichia coli* (UPEC) are a primary cause of CAUTI and display an array of virulence factors that facilitate the formation of biofilms on the catheter surface and promote colonisation of the urinary tract (Tartof *et al.*, 2005; Terlizzi, Gribaudo and Maffei, 2017). With an aging global population, the incidence of CAUTI is predicted to rise, posing an escalating risk to the populous and a heightening financial pressure on healthcare service providers (Mandakhalikar, Chua and Tambyah, 2016).

In order to reduce the incidence of CAUTI, approaches into the production of anti-infective catheter surface coatings are being widely considered. Commercially available nitrofurazone impregnated (ReleaseNF, Rochester Medical) and silver coated (Lubri-Sil and Bardex IC, Bard Care) catheters have been used in clinical settings with mixed outcomes (Johnson, Kuskowski and Wilt, 2006; Menezes *et al.*, 2019). Biocides are promising antimicrobial agents for use as catheter surface coatings due to their non-specific mechanism of action, working on multiple target sites meaning the selection of resistant bacterial populations is comparatively rare when compared to site specific therapeutics such as antibiotics (Singha, Locklin and Handa, 2017). Whilst biocide impregnated catheter coatings have shown promising antimicrobial activity *in vitro*, growing concerns over biocide cytotoxicity, in addition to reports of inducible biocide resistance and antibiotic cross resistance, have fuelled the search for further compounds that maintain long-term antimicrobial potency whilst exhibiting low cytotoxicity (Curiao *et al.*, 2015; Forbes *et al.*, 2015; Henly *et al.*, 2019). One such approach is to use quorum sensing inhibitors (QSIs) as anti-infective coatings agents (Roy, Adams and Bentley, 2011). Quorum sensing (QS) is a bacterial mechanism of gene regulation in a cell density dependent manner. Bacteria release small autoinducer molecules into the surrounding environment, allowing neighbouring bacteria to determine cell density and mediate a group response via synchronised changes in gene expression (Papenfort and Bassler, 2016). Autoinducer-2 (AI-2) is the main QS system used by *E. coli* and has been shown to induce biofilm formation through modulation of a number of motility related genes,

controlled by motility quorum-sensing regulator MqsR (González Barrios *et al.*, 2006). Acyl-homoserine lactones (AHL) are another class of autoinducers, however, *E. coli* possess only a homologue of the LuxR receptor and not the gene for AHL synthesis (Houdt *et al.*, 2006).

QS has also been linked to expression of virulence factors across multiple species of bacteria, therefore identification of QSIs has been noted as a potential anti-virulence strategy in antimicrobial chemotherapy (González Barrios *et al.*, 2006; Roy, Adams and Bentley, 2011). *Trans*-cinnamaldehyde has been shown to reduce LuxR based activation of virulence factor expression in *Vibrio* species (Brackman *et al.*, 2008, 2011). Although the exact mechanism of action remains unknown in *E. coli, trans*-cinnamaldehyde has been shown to inhibit the expression of QS related genes (Niu, Afre and Gilbert, 2006) and reduce biofilm formation in UPEC (Amalaradjou *et al.*, 2010; Amalaradjou, Narayanan and Venkitanarayanan, 2011; Kot *et al.*, 2015). Brominated furanones have also demonstrated an ability to interrupt AI-2 based QS in bacteria (Brackman and Coenye, 2015) and have shown inhibitory effects on *E. coli* biofilms (Ren, Sims and Wood, 2001).

Combinatorial use of antibiotics, drugs and chemical agents have been assayed though numerous methods and models, dependent upon their function and use. Antimicrobial assays have commonly used a checkerboard assay with interpretation of the fractional inhibitory concentration index (Hall, Middleton and Westmacott, 1983; Rand et al., 1993; White et al., bliss1996; Orhan et al., 2005; Sopirala et al., 2010; Fratini et al., 2017). Whereas in cell culture based research, many different models to interpret the combinations of chemical agents have been developed from the Bliss Independence model, Loewe theory of additivity, highest single agent combinations and further more unique models (Chou and Talalay, 1984; Zhao *et al.*, 2014; van der Borght *et al.*, 2017).

When considering the antibacterial assessment, synergistic activity between the biocides and QSIs would be the optimum outcome, indicating that when used in combination we require a lower concentration of the antimicrobial agents to exert the same effect as when used independently. In contrast, when considering cytotoxicity, the optimum situation is one of antagonism, where a higher concentration of each agent is required to kill the same percentage of cells when used in combination when compared to when used independently.

4.2.1. Aims of this chapter

This work aimed to evaluate the pairwise combinatorial effects of the biocides polyhexamethylene biguanide (PHMB), benzalkonium chloride (BAC), silver nitrate and triclosan in combination with the QSIs *trans*-cinnamaldehyde and [z]-4-bromo-5[bromomethylene]-2[5H]-furanone (furanone-C30) in UPEC, through determining combined bacteriostatic, bactericidal and biofilm eradication activities. In parallel, combined cytotoxicity against an L929 mouse fibroblast cell line and primary human bladder smooth muscle (BSM) cell line was measured. These data enable evaluation of the biocompatibility of these agents for potential use in catheter coatings.

4.3.Methods

4.3.1. Bacteria, cell lines and chemical reagents

Six UPEC clinical strains (EC1, EC2, EC11, EC26, EC28 and EC34) previously isolated from urinary tract infections (UTIs) (Stepping Hill Hospital, Stockport, UK) and two laboratory characterised UPEC stains (EC958 and CFT073) were used in this work (Henly *et al.*, 2019, 2021). Bacteria were cultured in Mueller Hinton broth (MHB) or on Mueller Hinton agar (MHA) (Sigma Aldrich, UK) and incubated under aerobic conditions at 37^{o}C overnight before use unless otherwise stated.

BAC (Sigma Aldrich, UK), PHMB (Lonza, UK), silver nitrate (Alfa Aesar, UK) and *trans*-cinnamaldehyde (Sigma Aldrich, UK), were diluted to working concentrations in water. Triclosan (Sigma Aldrich, UK) and (z)-4-bromo-5(bromomethylene)-2(5H)-furanone) (furanone-C30; synthesised in house as described in Guo, *et al* (2009)) were diluted to working concentrations in 5% v/v ethanol.

L929 mouse fibroblast cells (ATCC) were cultured in Eagles Minimum Essential Medium (EMEM; Gibco), supplemented with 10% foetal bovine serum (FBS; Gibco) and 1% L-glutamine (Gibco). Human primary bladder smooth muscle (BSM) cells were cultured in Vascular Cell Basal Medium (ATCC) supplemented with a Vascular Smooth Muscle Cell Growth Kit (ATCC). Both cell lines were incubated at 37^{o}C with 5% CO_2. 3-(4,5-dimethylthiazol-2-yl)-2, 5-diphenyltetra-zolium bromide (MTT, Sigma Aldrich) was prepared as a stock solution of 50 mg/ml in phosphate buffered saline (PBS) and filter sterilised before use.

4.3.2. Fractional inhibitory concentrations

Fractional inhibitory concentrations were determined in a checkerboard assay modified from Orhan *et al* (Orhan *et al.*, 2005). In brief, two-fold dilutions of QSIs were performed vertically down a 96-well microtiter plate and two-fold dilutions of biocide were performed horizontally in a total volume of 150 µl per well. Overnight UPEC cultures were diluted with MHB to an OD_{600} of 0.008 and 150 µl was then added to each test well. Plates were incubated overnight at 37^{o}C, 100 RPM. The lowest concentration where growth was completely inhibited was deemed the minimum inhibitory concentration (MIC).

The fractional inhibitory concentration (FIC) is the ratio of the effective concentration of the biocide or QSI in combination and alone, Equation 1. The sum of the $FIC_{biocide}$ and FIC_{QSI} is the fractional inhibitory concentration index (FICI), Equation 2. The FICI is defined as synergistic where FICI ≤ 0.5, additive where 0.5 < FICI ≤ 1, indifferent where 1 < FICI < 2 and antagonistic where FICI ≥ 2 (Hall, Middleton and Westmacott, 1983; European Committee for Antimicrobial Susceptibility Testing (EUCAST) of the European Society of Clinical Microbiology and Infectious Diseases (ESCMID), 2000).

Equation 1. Fractional inhibitory concentration (a) of the biocide and (b) of the QSI.

$$\text{(a) } FIC_{biocide} = \frac{MIC_{biocide\ in\ combination}}{MIC_{biocide\ on\ its\ own}}$$

$$\text{(b) } FIC_{QSI} = \frac{MIC_{QSI\ in\ combination}}{MIC_{QSI\ on\ its\ own}}$$

Equation 2. Fractional inhibitory concentration index.

$$FICI = FIC_{biocide} + FIC_{QSI}$$

4.3.3. Fractional bactericidal concentrations:

Following determination of the MIC, 10 µl aliquots were taken from each well of the MIC plate, spot plated in triplicate onto MHA and incubated overnight at 37°C to determine the minimum bactericidal concentration (MBC). Using the MBC values rather than MIC, fractional bactericidal concentration index values (FBCI) were calculated and defined as for FICI.

4.3.4. Fractional biofilm eradication concentrations

Overnight UPEC cultures were diluted to an OD_{600} of 0.008 and 100 µl of culture was added per well to a 96 well plate prior to addition of a peg lid and incubation for 48 hours at 37°C and 30 RPM to allow biofilm formation. Peg lids were then placed into an antimicrobial challenge plate, set out in the same checkerboard format as MIC assays described above. The challenge plate was incubated overnight at 37°C and 100 RPM. Peg lids were then rinsed twice in 200 µl PBS per peg, placed into a recovery plate containing 200 µl MHB per well and incubated for 72 hours at 37°C and 100 RPM. The

MBEC was deemed the lowest concentration that completely inhibited regrowth. The fractional biofilm eradication concentration index (FBECI) was calculated as for the FICI.

4.3.5. Checkerboard cytotoxicity assays

Cytotoxicity of biocides in combination with QSIs was determined in a checkerboard format. L929 cells were seeded at 0.5 x 10^5 cells per well and BSM cells were seeded at 2.5 x 10^4 cells per well in a 96 well plate and grown to > 80% confluency in 24 hours. Antimicrobials were diluted in culture medium and added to the plate, resulting in two-fold dilutions of QSI vertically and two-fold dilutions of biocide horizontally, with a total volume of 200 µl per well. Plates were incubated for 24 hours, washed twice in 200 µl PBS and 100 µl of 0.5 mg/ml MTT was added to each well before incubation at 37^{o}C for 4 hours. The MTT containing medium was removed, the precipitated formazan product was solubilised in 200 µl isopropyl alcohol containing 0.04 M HCl and incubated at room temperature on an orbital shaker for 1 hour. Plates were centrifuged for 5 minutes at 1000 RPM, 100 µl of supernatant was then decanted and absorbance was measured at 570 nm. All assays were performed in 6 biological replicates.

Survival curves of cytotoxicity data were plotted using a sigmoidal curve of log(inhibitor) vs. response with 4 parameters (variable slope, least squares fit) fit to each single agent allowing determination of the IC_{50} value, defined as the concentration at which 50% of the cells are viable (GraphPad, Prism, 8.1). Identification of synergism or antagonism between biocides and QSIs was analysed by SynergyFinderPlus (synergyfinder.org) using the % viability data, baseline correction of the whole matrix was selected for each antimicrobial combination and the Bliss Independence model of synergism was calculated across all test concentrations (Zheng *et al.*, 2022).

4.4. Results

4.4.1. Antimicrobial assays:

Fractional inhibitory, bactericidal and biofilm eradication concentration indices were determined by checkerboard assay against eight UPEC strains.

4.4.1.1. Inhibitory concentrations

At inhibitory concentrations cinnamaldehyde and silver nitrate were synergistic against 2/8 strains (EC2 and EC11, Figure 4.1, Appendix Table 8.8)) and PHMB in combination with furanone-C30 showed synergism against one strain, CFT073 (Figure 4.2 & Appendix Table 8.9). Antagonism was observed against 6/8 strains when triclosan was combined with either QSI; in combination with cinnamaldehyde this included EC1, EC11, EC26, EC28, EC34 and EC958 and in combination with furanone-C30 EC1, EC2, EC26, EC34, EC958 and CFT073.

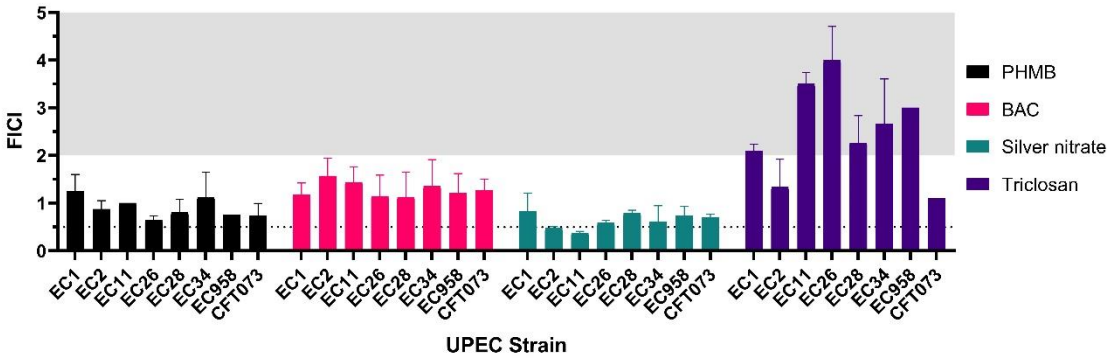

Figure 4.1. Fractional inhibitory index values of biocides (PHMB, BAC, silver nitrate and triclosan) in combination with cinnamaldehyde. All results are an average of 2 biological replicates, each with 3 technical repeats. Error bars represent ± 1 standard deviation. The FICI is defined as synergistic where FICI ≤ 0.5, additive where 0.5 < FICI ≤ 1, indifferent where 1 < FICI < 2 and antagonistic where FICI ≥ 2. Dotted line represents FICI = 0.5 and grey area represents antagonistic combinations where FICI ≥ 2.

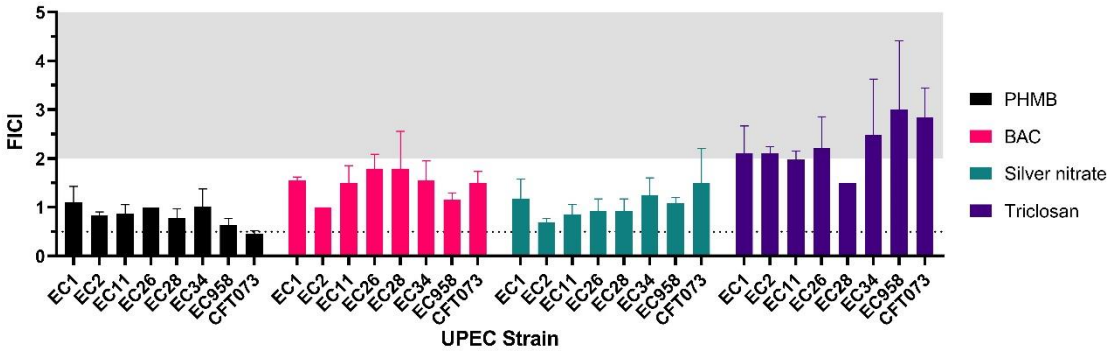

Figure 4.2. Fractional inhibitory index values of biocides (PHMB, BAC, silver nitrate and triclosan) in combination with furanone-C30. All results are an average of 2 biological replicates, each with 3 technical repeats. Error bars represent ± 1 standard deviation. The FICI is defined as synergistic where FICI ≤ 0.5, additive where 0.5 < FICI ≤ 1, indifferent where 1 < FICI < 2 and antagonistic where FICI ≥ 2. Dotted line represents FICI = 0.5 and grey area represents antagonistic combinations where FICI ≥ 2.

4.4.1.2. Bactericidal concentrations

At bactericidal concentrations cinnamaldehyde in combination with PHMB was synergistic against 6/8 strains; EC1, EC2, EC11, EC26, EC958 and CFT073 and was synergistic against 4/8 strains when combined with silver nitrate; EC11, EC28, EC3 and EC958 (Figure 4.3, Appendix Table 8.10). Synergism was also observed between furanone-C30 and PHMB against 3/8 strains: EC2, EC11 and EC34 (Figure 4.4, Appendix Table 8.11).

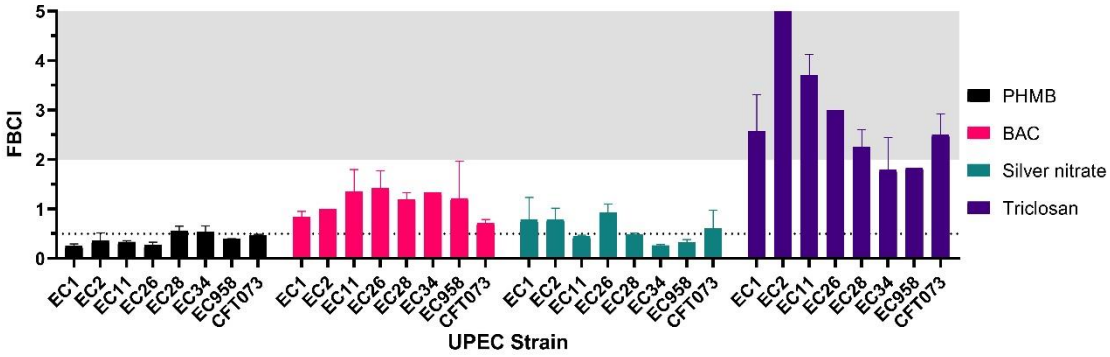

Figure 4.3. Fractional bactericidal concentration index (FBCI) values of biocides (PHMB, BAC, silver nitrate and triclosan) in combination with cinnamaldehyde. All results are an average of 2 biological replicates, each with 3 technical repeats. Error bars represent ± 1 standard deviation. FBCI value of EC2 triclosan/cinnamaldehyde combination = 16.37 (12.21). The FBCI is defined as synergistic where FBCI ≤ 0.5, additive where 0.5 < FBCI ≤ 1, indifferent where 1 < FBCI < 2 and antagonistic where FBCI ≥ 2. Dotted line represents FBCI = 0.5 and grey area represents antagonistic combinations where FBCI ≥ 2.

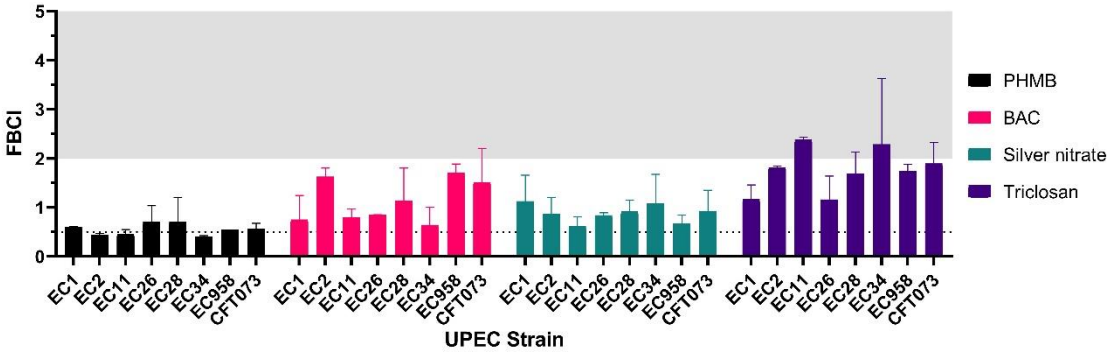

Figure 4.4. Fractional bactericidal concentration index (FBCI) values of biocides (PHMB, BAC, silver nitrate and triclosan) in combination with furanone-C30. All results are an average of 2 biological replicates, each with 3 technical repeats. Error bars represent ± 1 standard deviation. The FBCI is defined as synergistic where FBCI ≤ 0.5, additive where 0.5 < FBCI ≤ 1, indifferent where 1 < FBCI < 2 and

antagonistic where FBCI ≥ 2. Dotted line represents FICI = 0.5 and grey area represents antagonistic combinations where FICI ≥ 2.

4.4.1.3. Biofilm eradication concentrations

At biofilm eradication concentrations, PHMB and cinnamaldehyde showed synergism with 6/8 strains: EC1, EC2, EC11, EC26, EC28, EC958. Synergism was also observed for 5/8 strains for BAC in combination with cinnamaldehyde: EC1, EC11, EC34, EC958 and CFT073 and all eight strains for silver nitrate in combination with cinnamaldehyde Figure 4.5, Appendix Table 8.12). When combined with furanone-C30 synergism was observed against 3/8 strains for PHMB; EC1, EC28 and EC958, 4/8 strains for BAC; EC1, EC28, EC958, CFT073 and 6/8 strains for silver nitrate; EC1, EC11, EC26, EC28, EC958 and CFT073 (Figure 4.6, Appendix Table 8.13).

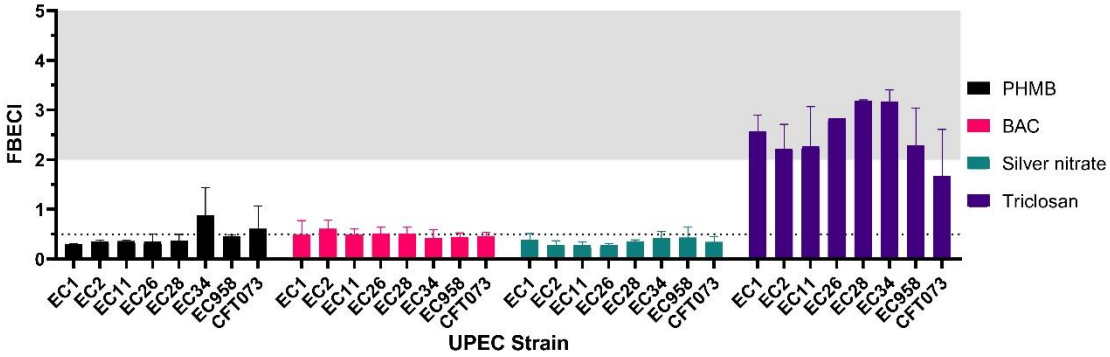

Figure 4.5. Fractional biofilm eradication concentration index (FBECI) values of biocides (PHMB, BAC, silver nitrate and triclosan) in combination with cinnamaldehyde. All results are an average of 2 biological replicates, each with 3 technical repeats. Error bars represent ± 1 standard deviation. The FBECI is defined as synergistic where FBECI ≤ 0.5, additive where 0.5 < FBECI ≤ 1, indifferent where 1 < FBECI < 2 and antagonistic where FBECI ≥ 2. Dotted line represents FBECI = 0.5 and grey area represents antagonistic combinations where FBECI ≥ 2.

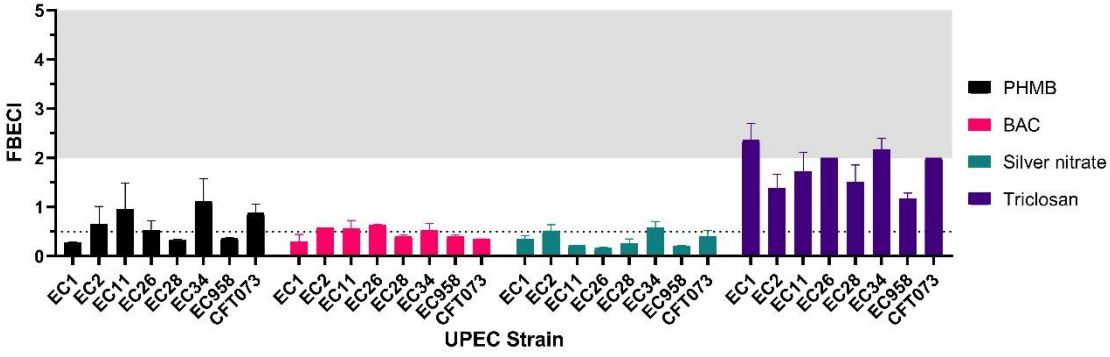

Figure 4.6. Fractional biofilm eradication concentration index (FBECI) values of biocides (PHMB, BAC, silver nitrate and triclosan) in combination with furanone-C30. All results are an average of 2 biological replicates, each with 3 technical repeats. Error bars represent ± 1 standard deviation. The FBECI is defined as synergistic where FBECI ≤ 0.5, additive where 0.5 < FBECI ≤ 1, indifferent where 1

< FBECI < 2 and antagonistic where FBECI ≥ 2. Dotted line represents FBECI = 0.5 and grey area represents antagonistic combinations where FBECI ≥ 2.

4.4.2. Cytotoxicity

Cytotoxicity of biocides and QSIs was determined via MTT assay of L929 mouse fibroblast cells and BSM cells, the concentrations at which 50% of cells survived (IC_{50}) were determined.

4.4.2.1. L929 cytotoxicity

In L929 cells, the IC_{50} of cinnamaldehyde independently was in the range of 116 – 286 µg/ml. Furanone-C30 was more potent than cinnamaldehyde, with a range of 16.9 – 34 µg/ml required to kill 50% of cells. Of the biocides, silver nitrate was the most cytotoxic requiring as little as 0.41 µg/ml to kill 50% of the cells whilst PHMB was the least cytotoxic biocide requiring up to 46.5 µg/ml. (Figure 4.7, Figure 4.8 and Table 4.1).

When combined there were small changes in the effective concentrations, however, these dell within an overlap of confidence intervals for most combinations tested, with the exception of silver nitrate with furanone-C30 where decreases in the IC_{50} when combined were observed (Table 4.1). Following SynergyFinder analysis and identification of regions of synergism and antagonism based upon the Bliss Independence model, regions of antagonism were observed below the independent IC_{50} for cinnamaldehyde in combination with PHMB, BAC and triclosan, however where the IC_{50} of each agent meets there are areas of strong synergism for cinnamaldehyde combined with silver nitrate or with triclosan (Figure 4.9). Furanone-C30 in combination with silver nitrate or triclosan led to strong synergism at IC_{50} concentrations (Figure 4.10).

Comparison of effective antimicrobial activity of the biocides and QSIs were compared with the cytotoxicity of L929 cells, only PHMB in combination with cinnamaldehyde at inhibitory concentrations fell below the IC_{50} of EC11, EC958 and CFT073, all other antimicrobial assays were above the IC_{50} of either the biocide or QSI (Figure 4.9 and Figure 4.11). The IC_{50} concentrations of furanone-C30 were lower than the inhibitory, bactericidal and biofilm eradication concentrations for all combinations tested (Figure 4.10 and Figure 4.12).

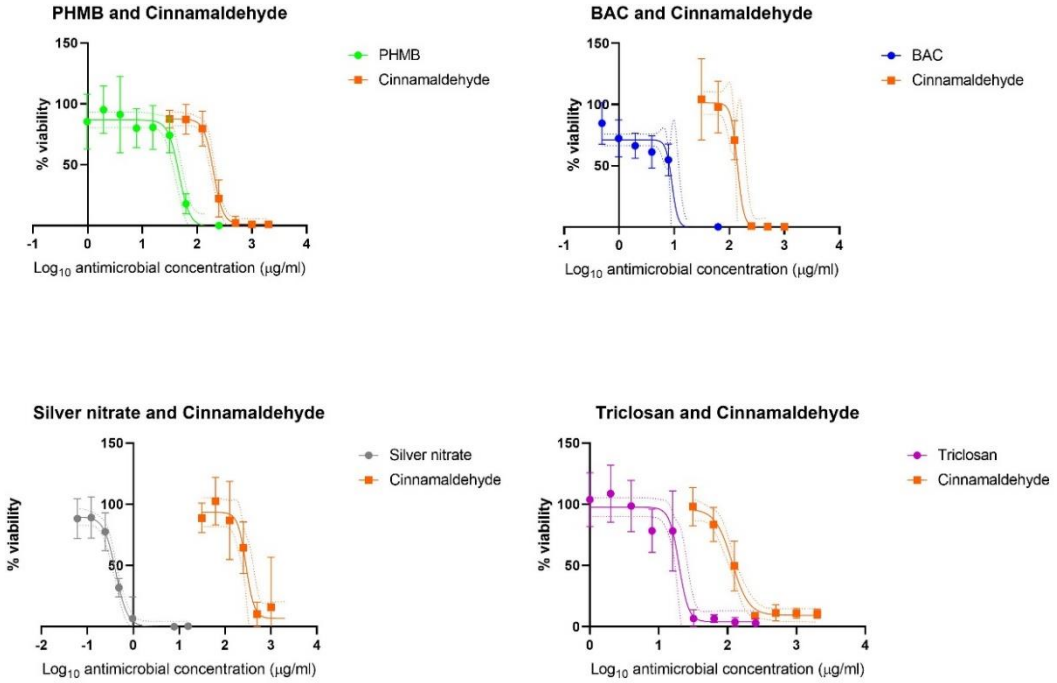

Figure 4.7. Survival curves of L929 cells when challenged with a single biocide or cinnamaldehyde. Both biocide and cinnamaldehyde assays were completed in the same plate. Curve determined in prism and dotted line represents 95% confidence intervals, error bars represent ± standard deviation, n = 6.

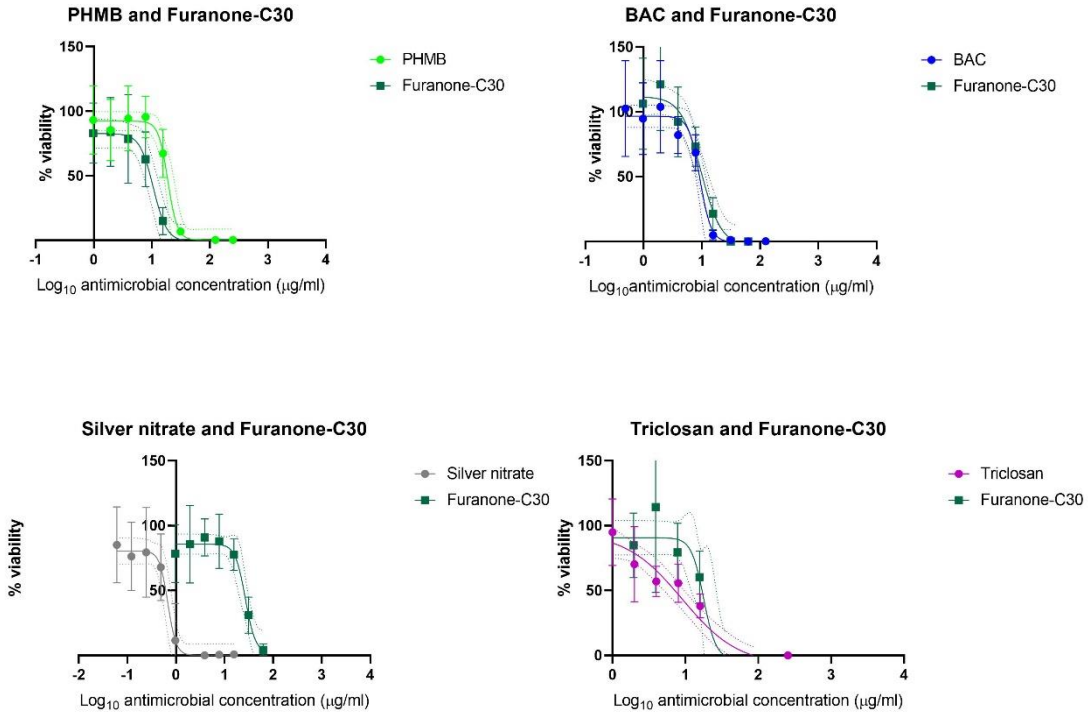

Figure 4.8. Survival curves of L929 cells when challenged with a single biocide or Furanone-C30. Both biocide and QSI assays were completed in the same plate. Curve determined in prism and dotted line represents 95% confidence intervals, error bars represent ± standard deviation, n = 6.

Table 4.1. IC_{50} concentrations of biocides and QSIs against an L929 fibroblast cell line and effective concentrations of combinations (µg/ml).

	Independent		Combined	
Combination	Biocide	QSI	Biocide	QSI
PHMB / Cinnamaldehyde	46.45 (37.77 – 57.12)	199.1 (176.7 – 224.5)	57.29 (18.95 - 95.63)	145.8 (92.28 - 199.4)
BAC / Cinnamaldehyde	9.08 (6.49 – 12.7)	140.1 (109.1 – 180.0)	5.046 (-1.08 - 11.17)	145.8 (92.28 - 199.4)
Silver nitrate / Cinnamaldehyde	0.41 (0.36 – 0.48)	286.0 (218.7 – 374.1)	0.3906 (0.22 - 0.56)	400 (230 - 570)
Triclosan / Cinnamaldehyde	19.7 (15.46 – 25.09)	116.1 (99.22 – 135.8)	12.67 (7.09 - 18.25)	72.92 (46.14 - 99.69)
PHMB / Furanone-C30	18.87 (15.47 – 23.03)	10.60 (7.84 – 14.34)	18.23 (11.53 - 24.92)	10.42 (6.18 - 14.65)
BAC / Furanone-C30	9.29 (7.56 – 11.42)	9.68 (7.20 – 13.01)	8.14 (1.73 - 14.54)	7.16 (2.37 - 11.95)
Silver nitrate / Furanone-C30	0.68 (0.52 – 0.89)	26.84 (21.17 – 34.03)	0.24 (0.10 - 0.38)	12.37 (6.92 - 17.82)
Triclosan / Furanone-C30	9.03 (4.93 – 16.53)	17.81 (12.14 – 26.12)	6.67 (1.58 - 11.75)	14.32 (10.98 - 17.67)

N = 6, 95% confidence intervals in brackets.

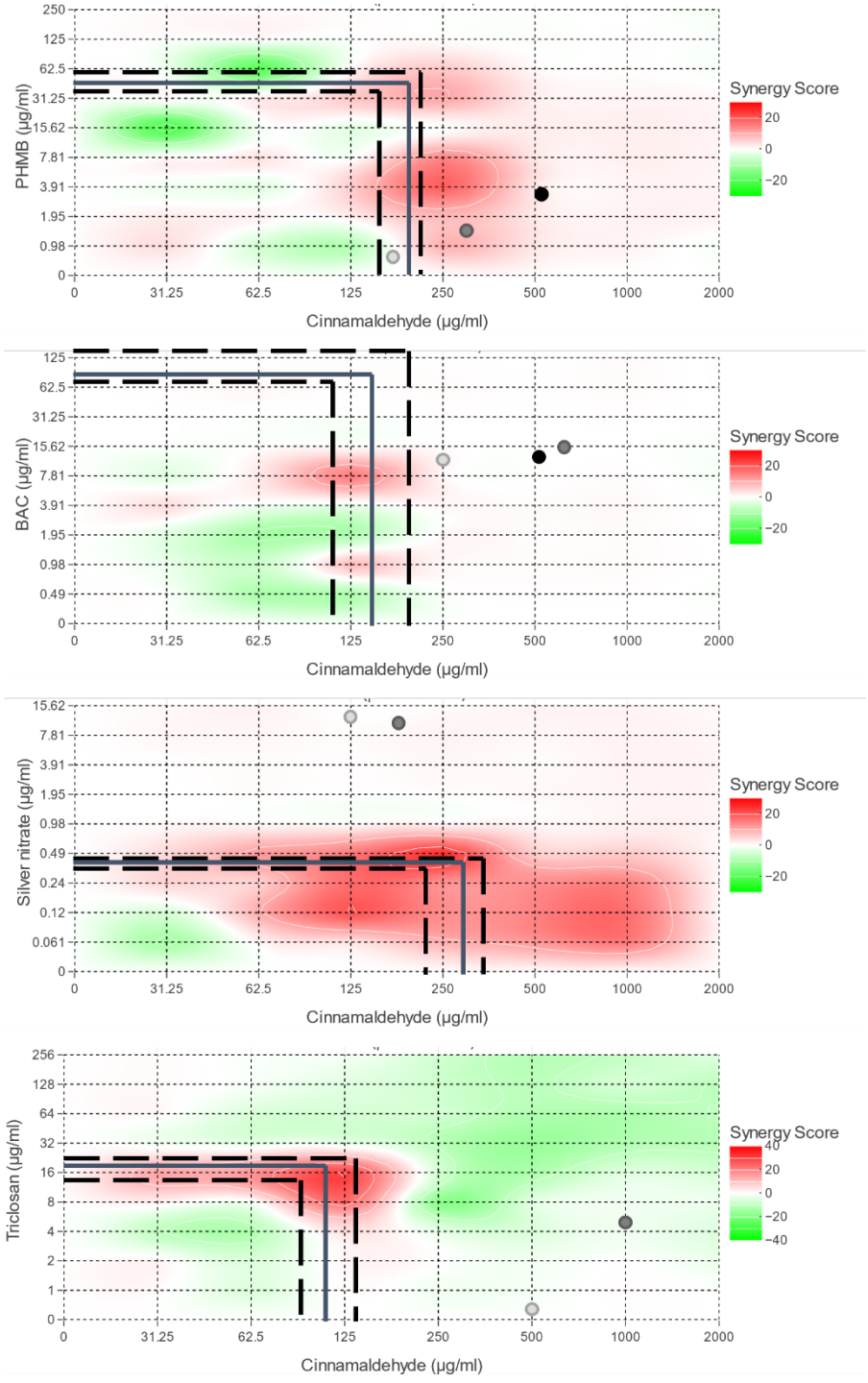

Figure 4.9. Plots of synergy scores assessed by the Bliss independence model and with the minimum inhibitory, bactericidal and biofilm eradication concentrations against EC958. Synergy scores and plots produced in synergy finder plus **(Zheng *et al.*, 2022)**. Green indicates antagonism of the combination against bladder smooth muscle cells, red indicates synergism. Points indicate the minimum inhibitory (light grey), minimum bactericidal (dark grey) and minimum biofilm eradication (black) concentrations of the combinations against UPEC strain EC958. Where the combinations exceed the cytotoxicity range, these points are

not identified. Solid line represents the IC_{50} concentration and dashed lines are the 95% confidence intervals.

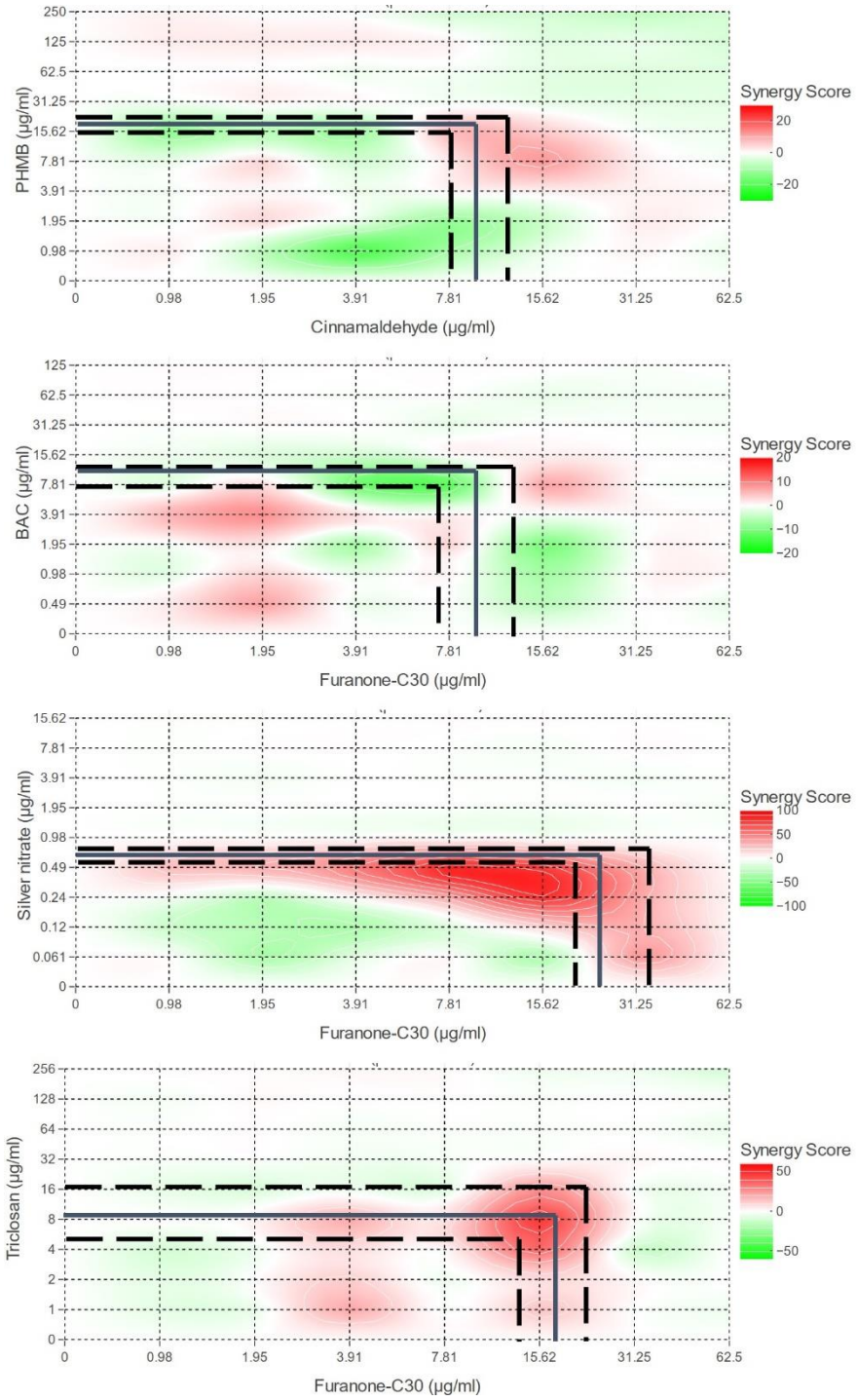

Figure 4.10. Plots of synergy scores of biocides in combination with furanone-C30 against L929 cell line, assessed by the Bliss Independence model. Synergy scores and plots produced in Synergy Finder Plus **(Zheng *et al.*, 2022)**. Green indicates antagonism of the combination against bladder smooth muscle cells, red indicates synergism. Solid line represents the IC_{50} concentration and dashed lines are the 95% confidence intervals. MIC, MBC and MBEC values not presented as all concentrations exceeded the range tested for L929 cytotoxicity.

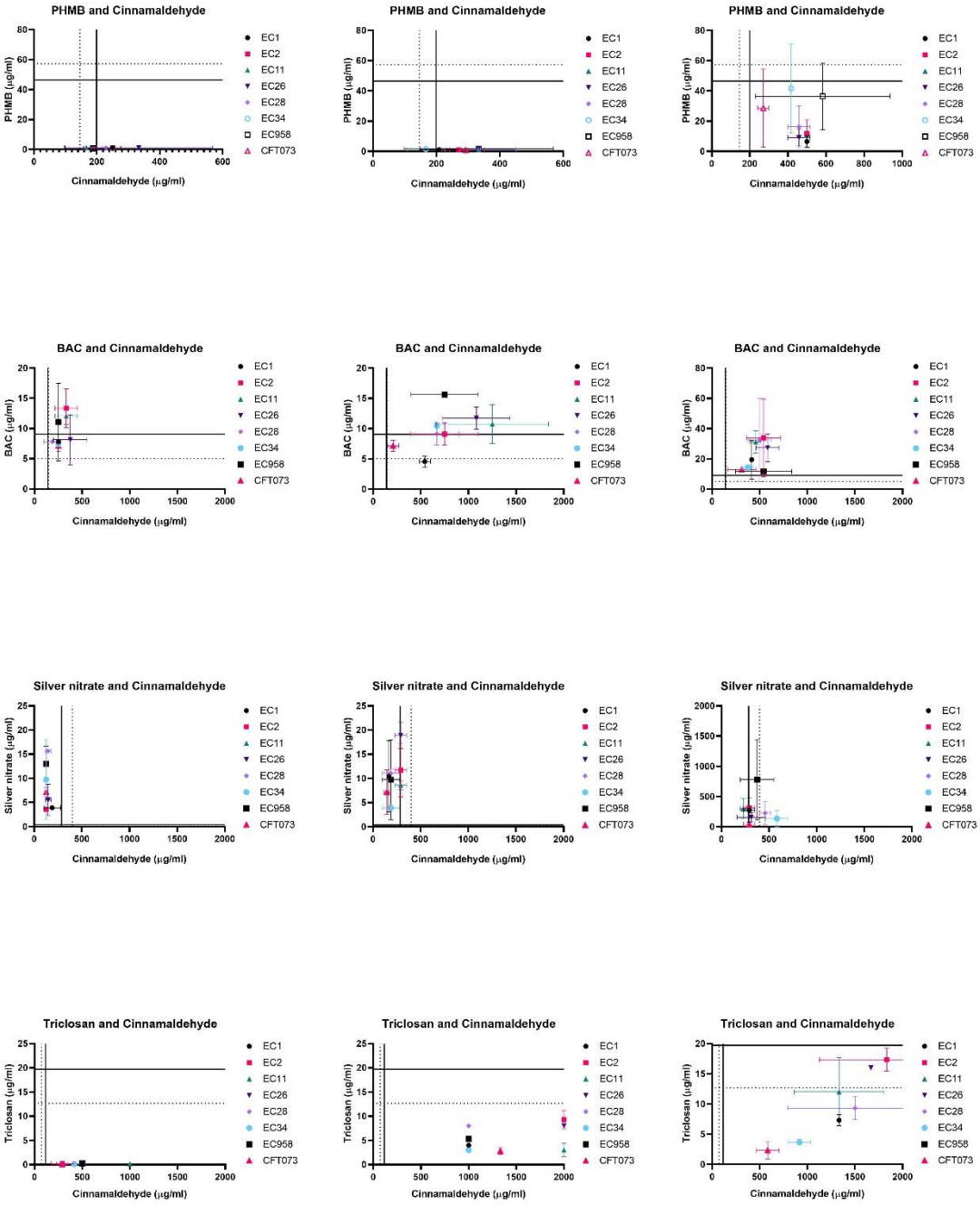

Figure 4.11. Summary plots presenting the fractional inhibitory, bactericidal, and biofilm eradication concentrations with the cytotoxic concentrations. All strains of UPEC data presented in Table 8.8 – 8.14, mean with standard deviation . IC_{50} of biocide and or cinnamaldehyde alone (solid line) and in combination (dotted line) against L929 presented.

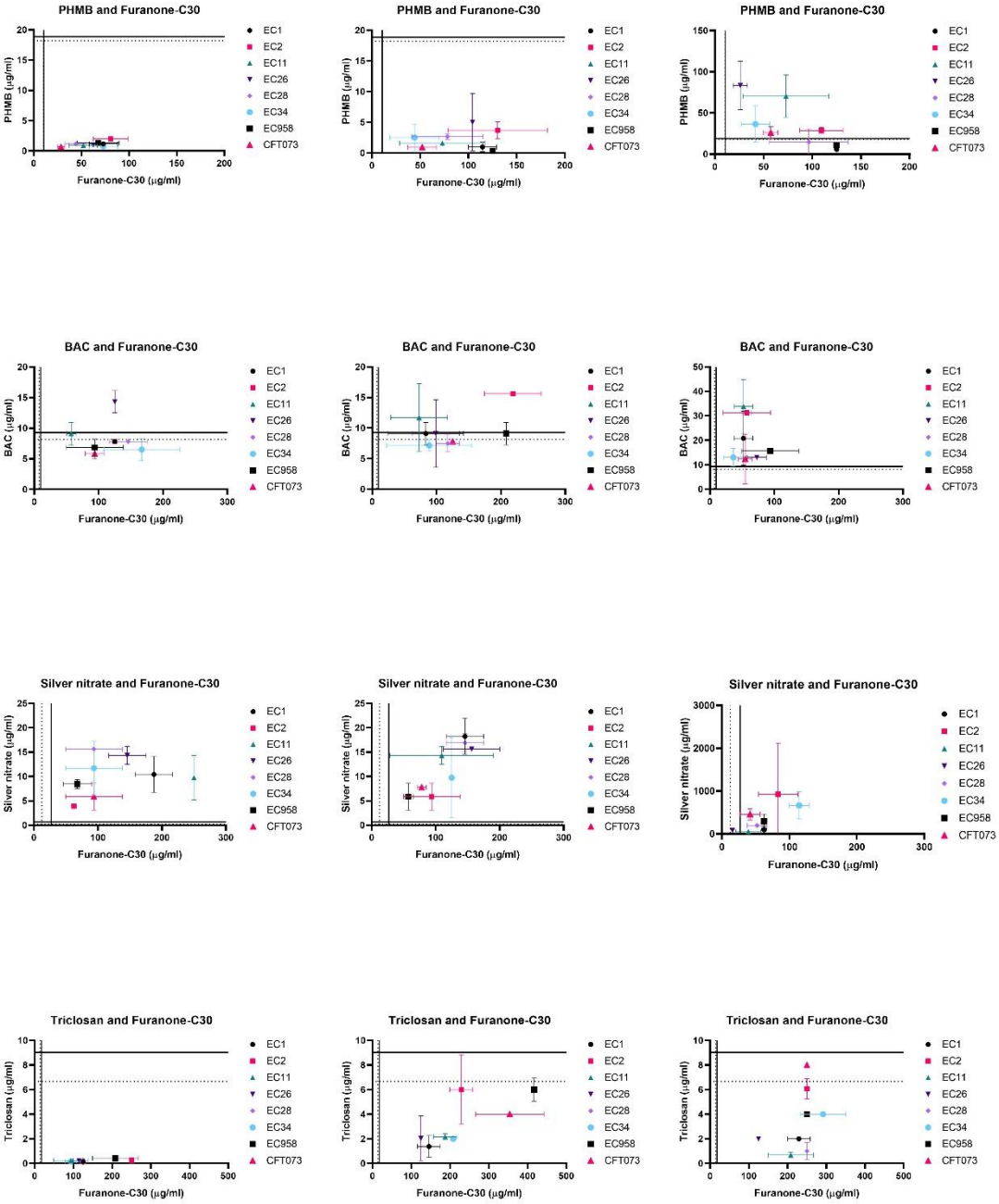

Figure 4.12. Summary plots presenting the fractional inhibitory, bactericidal, and biofilm eradication concentrations with the cytotoxic concentrations. All strains of UPEC data presented in Table 8.8 – 8.14. IC_{50} of biocide and or furanone-C30 alone (solid line) and in combination (dotted line) against L929 presented.

4.4.2.2. BSMC cytotoxicity

Cytotoxicity of biocides and QSIs in primary human bladder smooth muscle cells demonstrated IC_{50} concentrations for PHMB, BAC and furanone-C30 which were lower than in L929 cells. Whereas the effective concentrations were higher for cinnamaldehyde and silver nitrate(Figure 4.13, Figure 4.14 and Table 4.2) .

Identification of regions of antagonism or synergism were compared to Bliss Independence model data and a synergy score was determined across the concentration range tested (Figure 4.15 and Figure 4.16). PHMB or BAC combined with cinnamaldehyde showed antagonism at low combined concentrations and synergism at high combined concentrations. Silver nitrate with both cinnamaldehyde and furanone-C30 was predominantly synergistic when in combination whereas triclosan in combination with both QSIs was predominantly antagonistic across all concentration combinations.

4.4.2.3. Comparison of antimicrobial and cytotoxic concentrations

Combined concentrations of biocides and QSIs that elicited inhibitory, bactericidal and biofilm eradication effects against UPEC strain EC958 were compared to concentrations that cause BSM cell cytotoxicity alone and combined (Figure 4.17, Figure 4.18, Figure 4.19, Figure 4.20, Figure 4.21, Figure 4.22). PHMB in combination with cinnamaldehyde resulted in FIC and FBC values below the independent IC_{50}, however concentrations required for biofilm eradication (FBEC) were above IC_{50}. BAC and cinnamaldehyde were above IC50 at all antimicrobial concentrations, silver nitrate in combination with cinnamaldehyde showed inhibitory (FIC) and bactericidal (FBC) concentrations below those deemed to be cytotoxic (IC_{50}) with the exception of EC26, the biofilm eradication concentrations of these agents were above the concentration range used for cytotoxicity testing. Triclosan in combination with cinnamaldehyde demonstrated antimicrobial activity (FIC, FBC and FBEC) at concentrations which exceeded cytotoxicity (IC_{50}) of cinnamaldehyde yet below the cytotoxic concentrations of triclosan.

For all antimicrobial assays, the effective concentration of furanone-C30 when combined with any of the biocides far exceeded the IC50 cytotoxic concentration of Furanone-C30 against BSMCs against all strains tested (Figure 4.20). The antimicrobial concentration of furanone-C30 required for inhibitory activity exceeded the range

tested for cytotoxicity in the majority of cases. PHMB and furanone-C30 showed FIC, FBC and FBEC that were above the IC_{50}. This was also observed for BAC, silver nitrate and triclosan in combination with furanone-C30 (Figure 4.16).

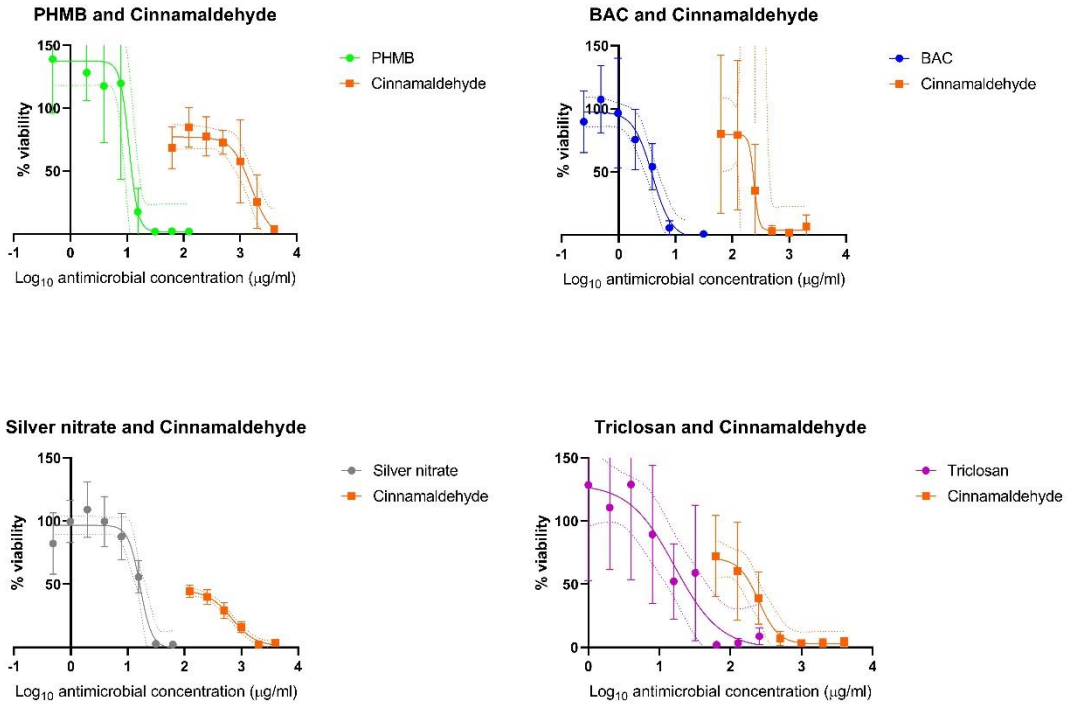

Figure 4.13. Survival curves of BSM cells when challenged with a single biocide or cinnamaldehyde. Both biocide and QSI assays were completed in the same plate. Different cinnamaldehyde along on different days. Curve determined in prism and dotted line represents 95% confidence intervals, error bars represent ± standard deviation, n = 6.

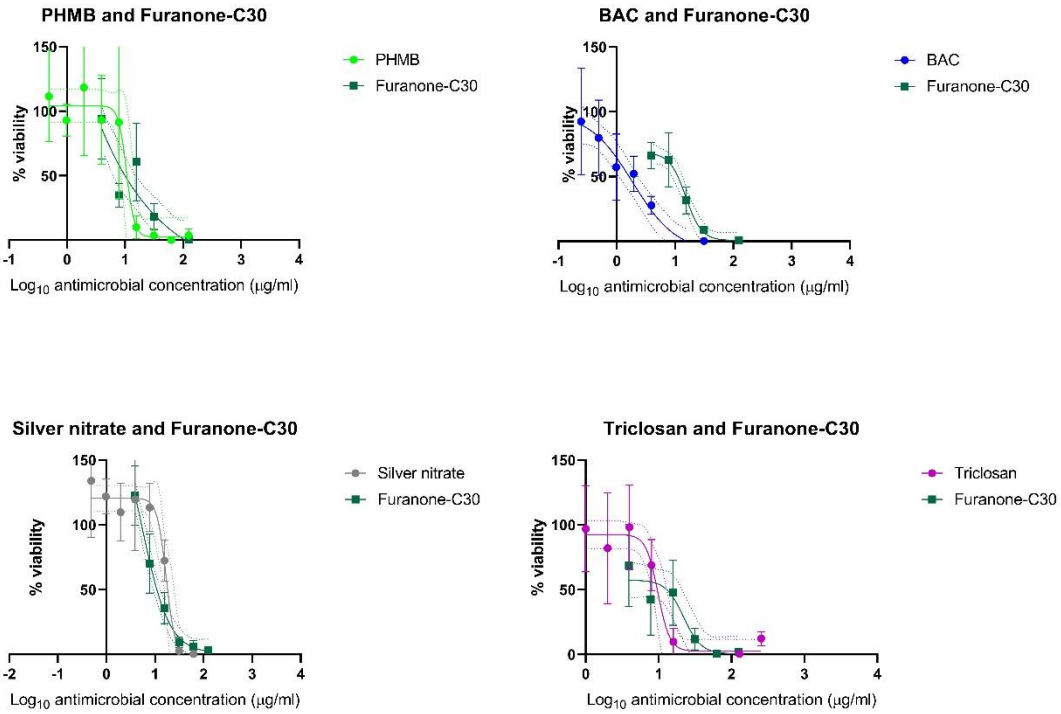

Figure 4.14. Survival curves of BSM cells when challenged with a single biocide or furanone-C30. Both biocide and QSI assays were completed in the same plate. Different cinnamaldehyde along on different days. Curve determined in prism and dotted line represents 95% confidence intervals, error bars represent ± standard deviation, n = 6.

Table 4.2. IC_{50} concentrations of biocides and QSIs against bladder smooth muscle cells.

Combination	Independent		Combined	
	Biocide	QSI	Biocide	QSI
PHMB / Cinnamaldehyde	10.9 (7.56 - 15.71)	1574 (906.4 - 2735)	1.76 (0.01- 3.50)	150 (-92.94 - 392.9)
BAC / Cinnamaldehyde	3.31 (2.73 - 4.02)	7.61 (0.01 - 4504)	0.49 (0.49 - 0.49)	62.5 (62.5 - 62.5)
Silver nitrate / Cinnamaldehyde	17.25 (14.29 - 20.84)	675.2 (546.8 - 833.7)	2.93 (-1.04 - 6.90)	145.8 (92.28 - 199.4)
Triclosan / Cinnamaldehyde	16.68 (8.44 - 32.95)	234.4 (188.2 - 292.1)	3.17 (0.24 - 6.09)	312.5 (85.29 - 539.7)
PHMB / Furanone-C30	5.29 (4.693 - 5.95)	6.69 (4.09 - 10.94)	1.95 (0.37 - 3.54)	6.51 (4.39 - 8.63)
BAC / Furanone-C30	1.88 (0.89 - 3.96)	15.19 (12.49 - 18.47)	1.06 (0.55 - 1.56)	5.21 (3.09 - 7.33)
Silver nitrate / Furanone-C30	5.41 (1.48 - 19.76)	17.07 (13.53 - 21.53)	0.49 (0.49 - 0.49)	9.12 (5.77 - 12.46)
Triclosan / Furanone-C30	9.79 (7.6 - 12.6)	21.55 (12.86 - 36.1)	10 (4.86 - 15.14)	15.63 (2.92 - 28.33)

N= 6, 95% confidence intervals in brackets. Calculated based upon sigmoidal curve analysis in GraphPad Prism v8.

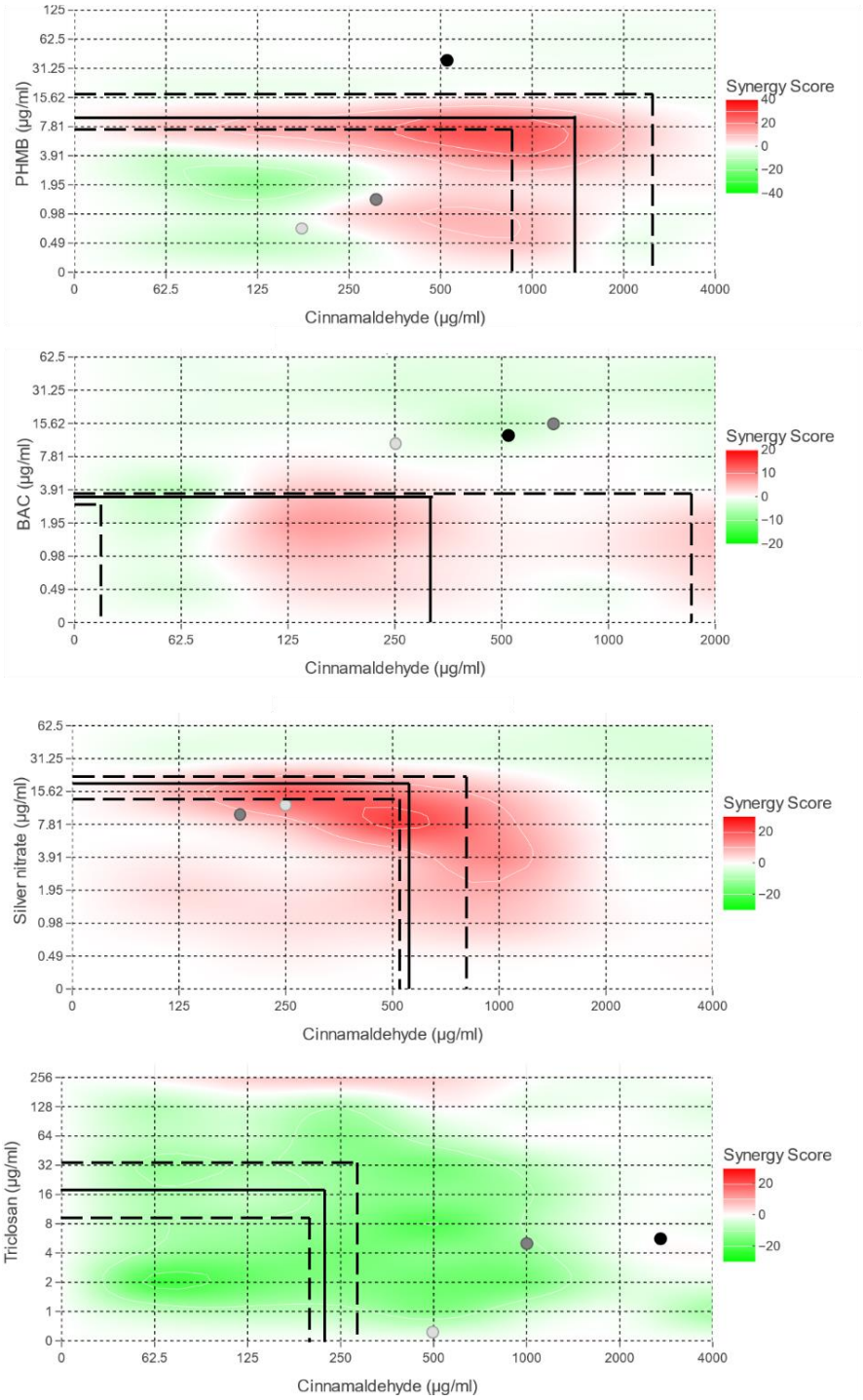

Figure 4.15. Plots of synergy scores assessed by the Bliss independence model and with the minimum inhibitory, bactericidal and biofilm eradication concentrations against EC958. Synergy scores and plots produced in synergy finder plus **(Zheng *et al.*, 2022)**. Green indicates antagonism of the combination against bladder smooth muscle cells, red indicates synergism. Points indicate the minimum inhibitory (light grey), minimum bactericidal (dark grey) and minimum biofilm eradication (black) concentrations of the combinations against UPEC strain EC958. Where the combinations exceed the cytotoxicity range, these points are

not identified. Solid line represents the IC_{50} concentration and dashed lines are the 95% confidence intervals.

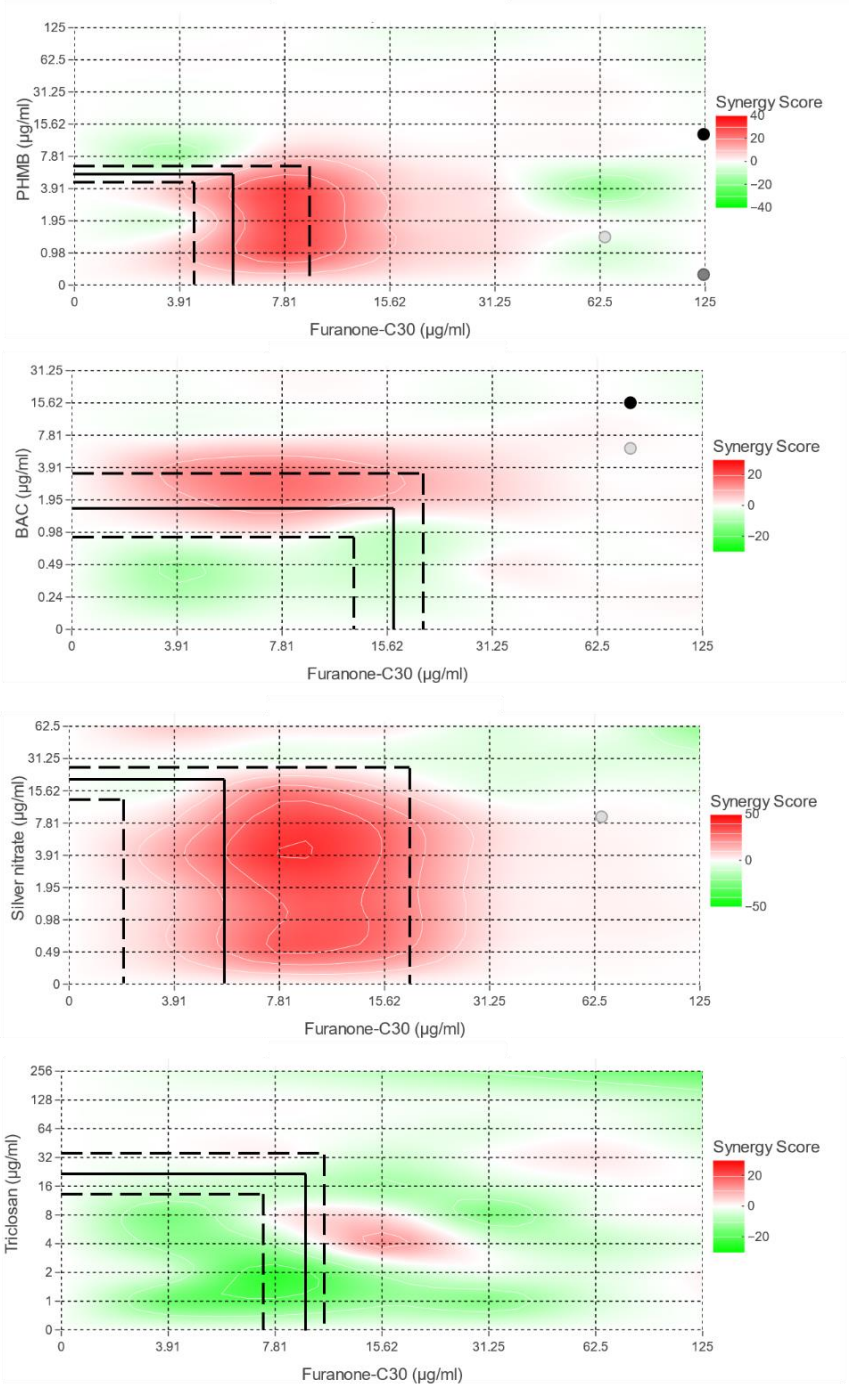

Figure 4.16. Plots of synergy scores assessed by the Bliss independence model and with the minimum inhibitory, bactericidal and biofilm eradication concentrations against EC958. Synergy scores and plots produced in synergy finder plus **(Zheng *et al.*, 2022)**. Green indicates antagonism of the combination against bladder smooth muscle cells, red indicates synergism. Points indicate the minimum inhibitory (light grey), minimum bactericidal (dark grey) and minimum biofilm eradication (black) concentrations of the combinations against UPEC strain

EC958. Where the combinations exceed the cytotoxicity range, these points are not identified. Solid line represents the IC_{50} concentration and dashed lines are the 95% confidence intervals.

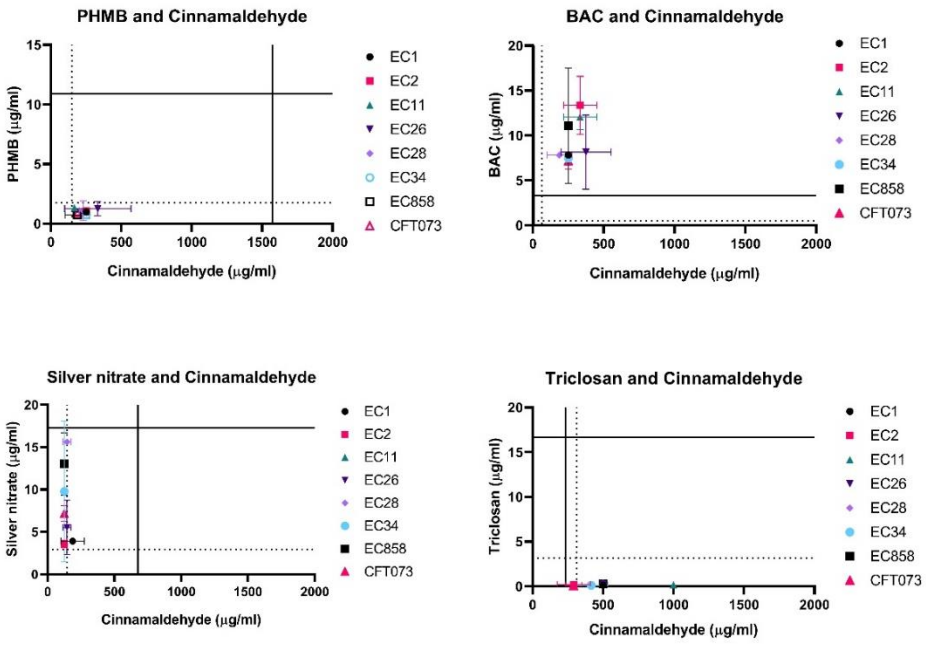

Figure 4.17. All minimum inhibitory concentrations of biocides in combination with cinnamaldehyde plotted against the IC_{50} of the biocide or cinnamaldehyde independently (solid line) or in combination (dotted line) against BSMCs. Mean with standard deviation of antimicrobial concentrations.

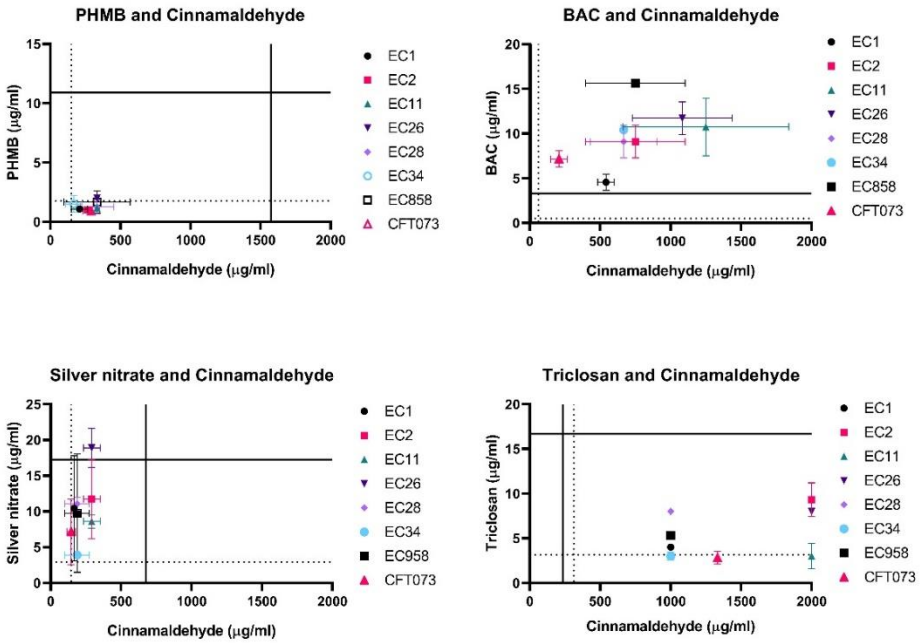

Figure 4.18 All minimum bactericidal concentrations of biocides in combination with cinnamaldehyde plotted against the IC_{50} of the biocide or cinnamaldehyde independently (solid line) or in combination (dotted line) against BSMCs. Mean with standard deviation of antimicrobial concentrations.

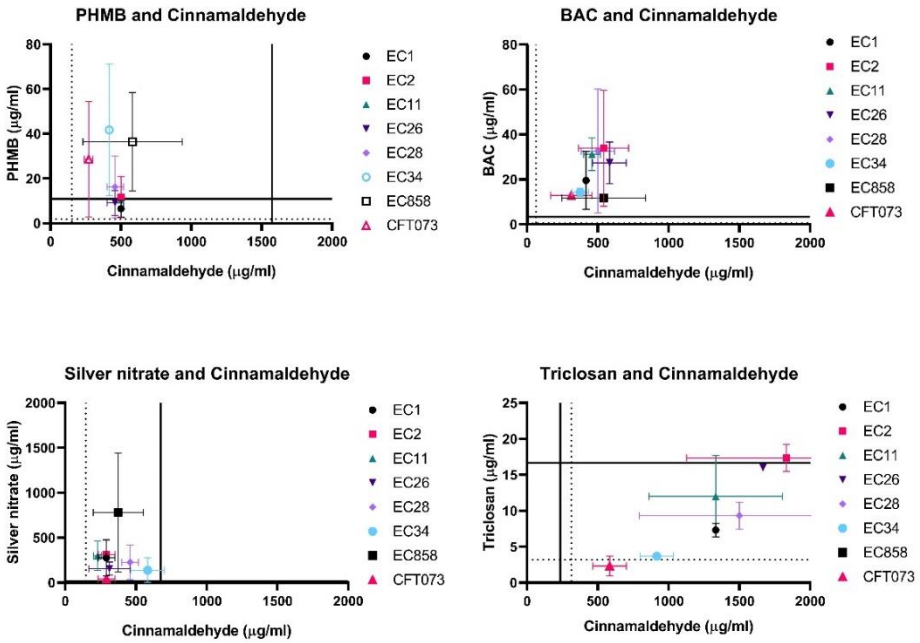

Figure 4.19. All minimum biofilm eradication concentrations of biocides in combination with cinnamaldehyde plotted against the IC_{50} of the biocide or cinnamaldehyde independently (solid line) or in combination (dotted line) against BSMCs. Mean with standard deviation of antimicrobial concentrations.

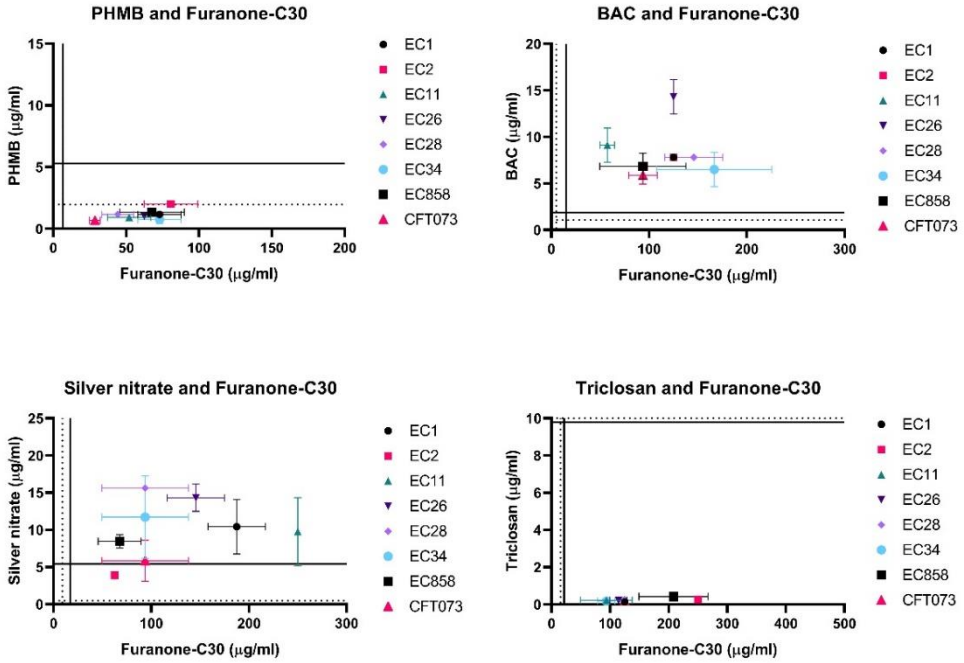

Figure 4.20. All minimum inhibitory concentrations of biocides in combination with furanone-C30 plotted against the IC_{50} of the biocide or cinnamaldehyde independently (solid line) or in combination (dotted line) against BSMCs. Mean with standard deviation of antimicrobial concentrations.

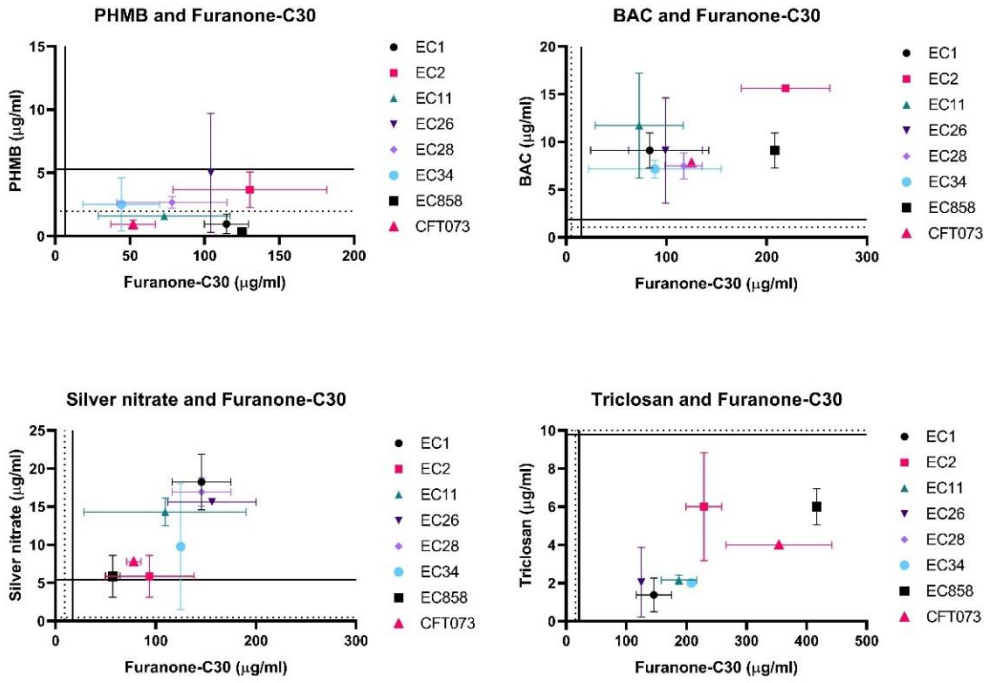

Figure 4.21. All minimum bactericidal concentrations of biocides in combination with furanone-C30 plotted against the IC_{50} of the biocide or cinnamaldehyde

independently (solid line) or in combination (dotted line) against BSMCs. Mean with standard deviation of antimicrobial concentrations.

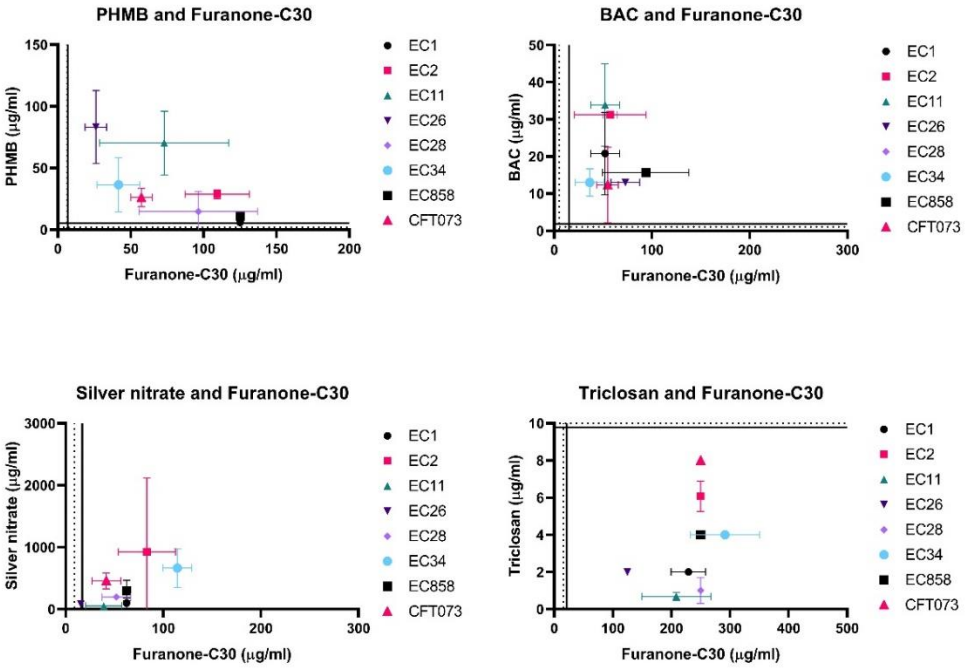

Figure 4.22. All minimum biofilm eradication concentrations of biocides in combination with furanone-C30 plotted against the IC_{50} of the biocide or cinnamaldehyde independently (solid line) or in combination (dotted line) against BSMCs. Mean with standard deviation of antimicrobial concentrations.

4.5. Discussion

Biocides and quorum sensing inhibitors demonstrated synergistic, additive and antagonistic interactions at bacteriostatic, bactericidal and biofilm eradication concentrations against UPEC dependent on the test agents combined and strain assayed. Cinnamaldehyde in combination with silver nitrate and furanone-C30 in combination with PHMB, demonstrated synergism against 2/8 UPEC strains at inhibitory concentrations. At bactericidal concentrations synergistic interactions were observed between PHMB with cinnamaldehyde or furanone-C30 and silver nitrate with cinnamaldehyde against 6/8, 3/8 and 4/8 strains respectively. Synergistic activity was observed at biofilm eradication concentrations where cinnamaldehyde was combined with PHMB, BAC or silver nitrate against 6/8, 5/8 and 8/8 strains respectively. Similarly, furanone-C30 in combinations demonstrated synergism at biofilm eradication concentrations with PHMB against 3/8 strains, with BAC against 4/8 strains and 6/8 strains when combined with silver nitrate. This highlights the strong synergistic potential of biocides and QSIs against UPEC biofilms.

With regards to cytotoxicity, against mammalian cells the ideal situation is for an antagonistic interaction – increasing the concentrations of each agent needed when in combination to achieve IC_{50}. In BSM cells, both cinnamaldehyde and furanone-C30 in combination with PHMB, BAC or silver nitrate led to a predominantly synergistic interaction whilst both QSIs with triclosan led to an antagonistic interaction across the concentration ranges tested.

4.5.1. The bacteriostatic and bactericidal effects of combined biocides and QSIs against UPEC

The test biocides and QSIs have a number of inhibitory and bactericidal modes of action which may account for the synergism observed at bacteriostatic and bactericidal concentrations. PHMB in combination with cinnamaldehyde was synergistic at bactericidal concentrations against 6/8 UPEC strains. PHMB has been shown to reduce the fluidity of the bacterial membrane due to the bridging of adjacent phospholipids by the biguanide causing fissure ultimately leading to leakage of cytoplasmic components. At bactericidal concentrations, PHMB has been shown to condense DNA halting cell

division (Gilbert and Moore, 2005; Chindera *et al.*, 2016; Sowlati-Hashjin, Carbone and Karttunen, 2020). Cinnamaldehyde has also been shown to permeabilise the cell membrane, inhibit FtsZ polymerisation thus impairing cell division, and reduce ATP and ATPase activity (Domadia *et al.*, 2007; Doyle and Stephens, 2019). The combination of two membrane active agents may exert a cumulative disruptive effect of the bacterial cytoplasmic membrane explaining the synergistic bactericidal activity. Furthermore, by causing increased cellular permeability this would facilitate entry of the agents into the cytoplasm more readily enabling them to reach intracellular targets. The combined targeting of cellular replication through condensation of DNA and inhibition of FtsZ polymerisations could also contribute towards the bacteriostatic synergism observed.

Silver nitrate has been shown to inactivate microbial enzymes through interaction with thiol groups leading to dysregulation of membrane potential and impaired respiratory capacity impacting growth and replication. It is also suggested to cause cell envelope damage due to membrane shrinkage and condensation of DNA (Furr *et al.*, 1994; Feng *et al.*, 2000; Woo *et al.*, 2008; Majeed *et al.*, 2019). The combination of inhibited ATPase activity by cinnamaldehyde (Doyle and Stephens, 2019) and further inhibited enzymic activity by silver nitrate could contribute towards the synergistic inhibitory activity whilst synergistic bactericidal effects may be attributed to combined disruption of the cell envelope and underlying cytoplasmic membrane.

PHMB and furanone-C30 in combination were synergistic against CFT073 and bactericidal against 3/8 strains. Furanones have been shown to increase the membrane permeability and affect the membrane potential of *Pseudomonas aeruginosa,* however its membrane disrupting effects in *E. coli* have not been previously documented (Zhang *et al.*, 2021). Any increase in membrane permeability due to the actions of furanone-C30 may increase the intracellular accessibility of PHMB facilitating contact with intracellular targets. Furthermore, as PHMB is a known decoupling agent, this paired with further disruption to membrane potential could impair respiration and cell growth.

Triclosan was antagonistic in most bacteriostatic and bactericidal assays when combined with both cinnamaldehyde and furanone-C30. Within *E. coli*, triclosan inhibits enoyl acyl carrier protein reductase enzyme FabI, inhibiting fatty acid synthesis at inhibitory concentrations and causing membrane damage at bactericidal concentrations(Levy, McMurry and Oethinger, 1998; Stewart *et al.*, 1999; Russell, 2004). At subinhibitory

concentrations triclosan has been shown to induce oxidative stress, cause damage to the membrane and induce expression of *umuC*, *dinB* and *dinD* genes which are involved in the regulation of the SOS response (Lu *et al.*, 2018). Exposure of *E. coli* to triclosan prior to antibiotic treatment has been shown to induce tolerance to antibiotics through induction of ppGpp synthesis(Westfall *et al.*, 2019). Studies have indicated that elevated intracellular levels of ppGpp activates the bacterial toxin-antitoxin molecule TA resulting in the bacterial cell entering a persister like state with decreased antimicrobial susceptibility (Kanjee, Ogata and Houry, 2012; Kester and Fortune, 2014).

4.5.2. Anti-biofilm effects of combined biocides and QSIs against UPEC

At biofilm eradication concentrations, combinations of PHMB, BAC or silver nitrate with cinnamaldehyde demonstrated synergism against 6/8, 5/8 and 8/8 UPEC strains respectively, and combined with furanone-C30 against 3/8, 4/8 and 6/8 strains respectively. Both cinnamaldehyde and furanone-C30 have been previously shown to inhibit quorum sensing activity and biofilm formation of *E. coli*. Cinnamaldehyde has been shown to inhibit biofilm formation in UPEC strains (Amalaradjou *et al.*, 2010; Kot *et al.*, 2015) which has been attributed to a reduction in the expression of attachment associated genes, including *fimA*, *fimH*, *focA*, *sfaA*, *sfaS* and *papG.* This suggests that there may be a mechanism to interfere with adhesin expression, thus attachment and initiation of biofilm formation by cinnamaldehyde (Amalaradjou, Narayanan and Venkitanarayanan, 2011). Furthermore, reduced expression of AI-2 associated promoters in *Vibrio harveyii* have been observed following exposure to cinnamaldehyde (Niu, Afre and Gilbert, 2006) and AI-2 signalling has been associated with biofilm formation of *E. coli* through AI-2 control of the *mqsR* regulator gene (González Barrios *et al.*, 2006).

Furanone-C30 has also been shown to interrupt the AI-2 signalling of *E. coli*, reducing the expression of genes associated with chemotaxis, motility and flagellar synthesis (Ren *et al.*, 2004) and inhibit biofilm formation (Ren, Sims and Wood, 2001). Both cinnamaldehyde and furanone-C30 could be interrupting the initiation of biofilm formation and subsequent biofilm development. The resulting residual bacteria may therefore be eliminated more readily by lower concentrations of biocide than would be required to eradicate a mature biofilm.

4.5.3. Cytotoxicity of biocides and QSIs against L929 cells at effective concentrations

To produce an effective anti-infective catheter coating with a high level of biocompatibility we ideally require synergistic antimicrobial activity whilst avoiding synergistic cytotoxic activity. Effective antimicrobial concentrations against eight UPEC strains were compared to the cytotoxicity of the agents against L929 cell line and BSM cells (discussed below). At effective inhibitory antimicrobial concentrations, only triclosan with cinnamaldehyde against EC2 and CFT073 was below the combined cytotoxic concentration, all other combinations led to a higher cytotoxic concentration of at least one of the agents.

L929 cells are commonly used in initial cytotoxicity assessment of medical devices and are specifically listed in the international standard: ISO 10993-5 Biological evaluation of medical devices – Part 5: Test for *in vitro* cytotoxicity ('Biological evaluation of medical devices-16:45:28, 2009). L929 have been used in initial assessment of many experimental catheter coatings (Shalom *et al.*, 2017; Zhang *et al.*, 2020; Koc *et al.*, 2021). However, the use of mouse fibroblast cells is not representative of the urinary tract of humans therefore the cytotoxicity biocides and QSIs was determined in a primary cell line of human bladder smooth muscle cells. The specific mechanisms of the biocides and QSIs against mammalian cells are discussed below.

4.5.4. Cytotoxicity of biocides and QSIs against BSM cells at effective concentrations

PHMB combined with cinnamaldehyde showed synergistic activity against the BSM cell line at 3.9 – 15.6 µg/ml PHMB and 250 – 2000 µg/ml cinnamaldehyde, which includes effective FBC of most strains, including EC958. Antagonistic activity was observed at concentrations below 3.9 µg/ml PHMB and 250 µg/ml cinnamaldehyde which includes the FIC of all strains tested. The FBEC fell above the IC_{50} concentration of PHMB in an indifferent zone. Both PHMB and cinnamaldehyde have membrane permeabilising activity against both bacterial and eukaryotic cells (Doyle and Stephens, 2019; Sowlati-Hashjin, Carbone and Karttunen, 2020), which may increase the intracellular cytotoxic effects of these agents. However, PHMB is less readily attracted to the relatively neutrally charged mammalian cell membrane when compared to the electronegative

bacterial cell (Gilbert and Moore, 2005), and whilst PHMB can enter both eukaryotic and bacterial cells, the condensation of DNA has been shown to impact only bacteria as it does not enter the eukaryotic nucleus (Chindera *et al.*, 2016). Cinnamaldehyde has demonstrated cytotoxic effects which include induction of apoptosis and decreases in mitochondrial membrane potential (Zhang *et al.*, 2010). The combination of PHMB and cinnamaldehyde could increase the permeability of the membrane and allow more PHMB into the bacterial cell, causing DNA condensation and increased antimicrobial activity. There would be no cytotoxic synergism against human cells at the same concentrations because the eukaryotic nucleus is protected.

BAC and cinnamaldehyde combinations led to cytotoxic synergistic activity at IC_{50} concentrations, all antimicrobial activity fell within a concentration which would be considered antagonistic or indifferent, however, these all fell above the IC_{50} concentrations of BAC. BAC and cinnamaldehyde both have membrane permeabilising activity (Gilbert and Moore, 2005), however, BAC, like PHMB, is cationic and is more readily attracted to the bacterial membrane through electrostatic attraction (Gilbert and Moore, 2005). In addition to membrane permeabilsation, BAC has been shown to induce apoptosis and cell necrosis in human cells (Debbasch *et al.*, 2000; Deutschle *et al.*, 2006; Chang *et al.*, 2015). The complementation of mechanisms between cinnamaldehyde and BAC against mammalian cells may account for the lower concentrations required for cytotoxic activity in comparison to antimicrobial activity.

Silver nitrate in combination with cinnamaldehyde at IC_{50} concentrations and below demonstrated synergistic cytotoxic activity. FIC of all strains and FBC of all strains with the exception of EC26 fell within this range whereas the FBEC exceeded the range tested. Silver nitrate has multiple targets against bacterial and mammalian cells in addition to membrane permeabilization. The permeabilization of the cell membrane by cinnamaldehyde may lead to inhibition of additional intracellular enzymes in both eukaryotic and prokaryotic cells (Feng *et al.*, 2000; Woo *et al.*, 2008). It has been observed previously that silver has a similar effective range of bacterial inhibition and bactericidal activity as cytotoxicity against mammalian cells (Greulich *et al.*, 2012).

The combination of triclosan and cinnamaldehyde had an antagonistic relationship against BSM cells at all concentrations. The effective antimicrobial concentrations all fell above the IC_{50} values of cinnamaldehyde. Triclosan has been shown to be cytotoxic to

zebrafish cells through impairment of mitochondrial activity, loss of membrane stability and leading to apoptosis of cells (Guidony *et al.*, 2021). Triclosan has been shown to affect membrane ion transporters in human erythrocytes and increase the expression of stress cytokines (Alfhili and Lee, 2019). Both triclosan and cinnamaldehyde have poor solubility, the combination of both agents may antagonise this and lead to poorer solubility of the agents, hence the antagonistic effects observed in both cytotoxicity and antimicrobial assays.

All cytotoxic concentrations of furanone-C30 whether alone or combined were below those required for antimicrobial activity. Furanones have been shown to be cytotoxic and as such they are often a focus of anti-cancer drug discovery (Kim *et al.*, 2002). Efforts have been made to reduce the toxicity of the naturally occurring furanones, and derivatives including furanone-C30 (Yang *et al.*, 2014). However, the exact mechanism of furanone-C30 toxicity against mammalian cells is currently unknown. Cytotoxic synergistic activity was observed at IC_{50} concentrations for furanone-C30 in combination with PHMB, BAC and silver nitrate, however when combined with triclosan antagonism was observed. This may be due to low solubility of both agents, as hypothesised for antagonism observed between triclosan and cinnamaldehyde.

Although the use of human BSM primary cells is advantageous over mouse fibroblasts in the assessment of cytotoxicity of agents to be used in a urinary catheter for human use, there are limitations to the use of 2D cell culture to represent the complexity of *in vivo* systems. The development of 3D models has advanced in recent years and models of the urinary tract have been developed to mimic UPEC infection (Smith *et al.*, 2006; Zalewska-Piątek *et al.*, 2020), for assessment of toxicity of antibiotics against cancer cell organoids (Kloskowski *et al.*, 2021)and models of biofilm clearance (Wang *et al.*, 2021). The benefits of 3D models are that the cellular morphology and gene expression are more similar to *in vivo* than 2D cultures and resistance to drugs is modified in comparison to 2D cell cultures (Fontoura *et al.*, 2020). To measure the cytotoxicity of the biocides and QSIs in a way which is more representative of *in vivo* would be to use a 3D culture model of the urinary tract. Further work to determine the cytotoxic combinations of biocides and QSIs in an organoid or 3D culture system could provide a better prediction of the *in vivo* cytotoxicity.

4.6.Conclusions:

Existing anti-infective catheter coatings often use a single biocidal agent in an attempt to prevent bacterial colonisation of the catheter surface. This study investigated the combinatorial potential of biocides and QSIs in impairing UPEC growth and biofilm clearance in parallel to evaluating combined cytotoxicity in mouse fibroblasts and human bladder smooth muscle cells. Promising combinations of PHMB with cinnamaldehyde and BAC with cinnamaldehyde show active synergism against UPEC in both planktonic and biofilm states whilst displaying indifferent or antagonistic cytotoxicity at active antimicrobial concentrations.

To develop an effective antimicrobial catheter coating using a combination of biocides shown to be effective here the concentrations of the biocides and QSIs within the coating need to be at concentrations high enough for antimicrobial activity.

5.
Validation of combined biocide and quorum sensing inhibitor sol-gel coated catheters in prevention of biofilm formation by uropathogenic *Escherichia coli*

5.1.Abstract

Background: Catheter associated urinary tract infections (CAUTI) are frequently associated with uropathogenic *E. coli* (UPEC) contamination and the subsequent formation of biofilms on the catheter surface. These biofilms can lead to reservoirs of bacteria, harbouring persister cells which are often recalcitrant to antibiotic therapies. To be truly effective at reducing the incidence of CAUTI, an anti-infective urinary catheter will need to prevent bacterial contamination and resulting biofilm formation.

Methods: In previous chapters, the release profiles of biocides and QSIs from a silica-based hybrid sol-gel coating and the effective combinations were assessed. Within this chapter, each biocide with each QSI were combined within the sol-gel coating and evaluated for their capability to prevent bacterial growth and biofilm formation on disc-based and well based high throughput biofilm systems in addition to a drip flow reactor continuous culture model. Biofilm viability was determined both through culture-based analysis and through the use of confocal microscopy.

Results: Combinations of PHMB or silver nitrate with either QSI in sol-gel were effective at preventing the growth of bacteria in disc diffusion assays and reduced biofilm formation on coated peg lids. However, in the drip flow biofilm reactor, only coatings containing silver nitrate with cinnamaldehyde, silver nitrate with furanone-C30 and triclosan with furanone-C30 significantly reduced the number of bacteria within a biofilm on coated silicon square.

In the process of optimisation for imaging of biofilms on coated surfaces, GFP was inserted into UPEC strain EC958 and the resultant growth was imaged via confocal microscopy. Whilst the bacteria can be imaged on an untreated surface; the sol-gel auto-fluoresces and therefore quantitation of the viable bacteria could not be determined.

Conclusions: This work suggests that at the highest concentrations tested combinations of silver nitrate and QSIs have the best potential as anti-infective coatings, as shown through reduction in biofilm formation across all assays performed so far.

5.2. Introduction

Many nosocomial infections are associated with the formation of a bacterial biofilms, including catheter associated urinary tract infections (CAUTI) (Bjarnsholt, 2013). Studies have suggested that a range of 36 – 70% of CAUTI are related to biofilm formation (Sabir *et al.*, 2017; Almalki and Varghese, 2020). The catheter acts as a bridge between the external environment to the urinary tract, providing a surface upon which bacteria may attach and gain access to the host that helps to facilitate further infection (Trautner and Darouiche, 2004).

Bacterial biofilms harbour many advantages over planktonic life including recalcitrance to antimicrobials (Orazi and O'Toole, 2019) and protection from the host immune clearance mechanisms (Roilides *et al.*, 2015; Arciola, Campoccia and Montanaro, 2018). This is in part achieved through a reservoir of intrinsically resistant persister cells (Keren *et al.*, 2004; Roberts and Stewart, 2005), due to activated stress responses within bacterial biofilm members increasing efflux activity and reducing cell permeability and due to an escalated level of horizontal gene transfer of resistance genes within a biofilm community (Stewart and Costerton, 2001; Trautner and Darouiche, 2004; Høiby *et al.*, 2010; Bjarnsholt, 2013).

Multiple studies have identified uropathogenic *E. coli* (UPEC) to be the most common uropathogen associated with CAUTI due to the formation of mature biofilms on the catheter surfaces. (Sabir *et al.*, 2017; Almalki and Varghese, 2020; El-Mahdy, Mahmoud and Shrief, 2021; Zou *et al.*, 2023). UPEC strains have a high number of associated virulence factors including adhesins and flagella, iron-acquisition systems, polysaccharides and toxins (Terlizzi, Gribaudo and Maffei, 2017). Particular virulence genes which have been identified in clinical isolates of UPEC and correlated with high biofilm formation included antigen 43 (*flu*), ferric citrate transport system (*fecABCDIR*) and the aerobactin siderophore system (*iuc*) (Zou *et al.*, 2023). Antigen 43 has been known to be involved in biofilm formation through cell-cell attachment (Danese *et al.*, 2000). The function of the ferric citrate transport and aerobactin siderophore systems is not confirmed, however it is hypothesised that the ability of UPEC to use the available urinary citrate provides an advantage or that it may have a yet unknown biofilm-specific function (Zou *et al.*, 2023). The most common virulence factors associated with UPEC include type 1 fimbriae D-mannose specific adhesin (*fimH*), siderophore iron transporter

proteins (*sitA*), S fimbriae (*sfa*), and aerobactin (*aer*), which were identified in more than 70% of clinically isolated UPEC strains from Poland (Karczewska *et al.*, 2023).

Biofilm formation is aided by the deposition of a conditioning film on the catheter surface composed of proteins and salts from the urine, reducing the hydrophobic and electrostatic charges of the surface, lessening any potentially repulsive forces between the surface and bacterial cell (Santin *et al.*, 1999; Trautner and Darouiche, 2004). The exposure of the catheter to urine and to host cell lysates provides a source of glycoproteins that help to build the conditioning film and provides the ideal conditions for bacterial attachment (Ferrières, Hancock and Klemm, 2007).

Current commercially available catheters have been underwhelming in addressing the challenge posed by CAUTI. Bardex silver alloy catheters have been shown to be no better than uncoated catheters and Nitrofurazone catheters have been shown to increase patient discomfort in clinical trials (Karchmer *et al.*, 2000; Johnson, Kuskowski and Wilt, 2006; Beattie and Taylor, 2011; Lam *et al.*, 2014; Loveday *et al.*, 2014). There have been significant advances into the development of anti-infective catheter coatings *in vitro* which has been discussed in many review articles (Singha, Locklin and Handa, 2017; Cortese *et al.*, 2018; Ramstedt *et al.*, 2019; Andersen and Flores-Mireles, 2020; Bhattacharjee *et al.*, 2022; Dai, Gao and Duan, 2023). The main areas of research include antimicrobial coated/impregnated coatings including those containing biocides, AMPs, metals, bacteriophages and enzymes (Mandakhalikar, Chua and Tambyah, 2016; Singha, Locklin and Handa, 2017; Cortese *et al.*, 2018; Ramstedt *et al.*, 2019; Andersen and Flores-Mireles, 2020), those containing surface structure modifications (Mandakhalikar, Chua and Tambyah, 2016; Cortese *et al.*, 2018; Ramstedt *et al.*, 2019; Andersen and Flores-Mireles, 2020) and others incorporating competitive non-pathogenic strains (Mandakhalikar, Chua and Tambyah, 2016; Andersen and Flores-Mireles, 2020).

5.2.1. Aims of this chapter

The aim of this chapter was to evaluate the antimicrobial and anti-biofilm activity of combinations of biocides (PHMB, BAC, silver nitrate and triclosan) with QSIs (cinnamaldehyde and furanone-C30) in a sol-gel coating. This was assessed by disc based assay, peg-lid based systems and within a drip flow reactor model.

5.3.Methods:

Unless stated otherwise, all chemicals were purchased from Sigma Aldrich.

5.3.1. Bacteria, antimicrobials, and chemical reagents:

UPEC strains EC958 and CFT073 were cultured in Mueller Hinton broth (MHB), Mueller Hinton agar (MHA) or Luria broth (LB) and incubated under aerobic conditions at 37^{o}C overnight before use at an OD_{600} of 0.008 unless otherwise stated. PHMB (P; Lonza, UK), BAC (B), silver nitrate (S; Alfa Aesar, UK) and *trans*-cinnamaldehyde (C), were diluted to working concentrations in water. Triclosan (T) and (z)-4-bromo-5(bromomethylene)-2(5H)-furanone) (furanone-C30; F; synthesised in house as described in Guo, *et al* (2009)) were diluted to working concentrations in 5% v/v ethanol.

5.3.2. Sol-gel coating preparation and antimicrobial incorporation

The silica-based hybrid sol-gel was prepared by mixing 0.5 ml of tetraethyl orthosilicate (TEOS), 1 ml tetramethyl orthosilicate (TMOS) and 2.18 ml anhydrous isopropanol for 5 minutes at room temperature. To this, 1 ml Trimethoxymethylsilane (MTMS) was added slowly, followed by dropwise addition of 2.35 ml of acid/solvent mix (total acid/solvent catalyst was composed of 2.18 ml anhydrous isopropyl alcohol and 2.5 ml 0.07 M nitric acid). Polydimethylsiloxane (0.65ct, molecular weight 162, PDMS) was added slowly (4 additions of 50 µl before the remaining acid/solvent mix was added dropwise and stirred for 10 minutes followed by dropwise addition of 2.4 ml 0.07 M nitric acid. The solution was stirred for 72 hours prior to use as in Nichol et al., (2021).

Stock solutions of antimicrobials were added to the sol-gel just prior to coating at a ratio of 1:10 to the provide the final required concentration. Control sol-gel was prepared with the addition of H_2O at 1:10 ratio.

5.3.3. Combined biocide and QSI disc diffusion assays

Antimicrobial sol-gel discs were created by coating one side of a 6mm round coverslip with 10 µl of biocide, QSI or combined antimicrobial sol-gel at either 2 mg/ml or 10 mg/ml concentration. Discs were left to dry overnight and stored in the fridge prior to use. Overnight cultures of EC958 or CFT073 were diluted to an OD_{600} of 0.008 and spread onto MHA plates. Three antimicrobial discs were placed, face down, on the bacterial

lawn and incubated for 24 hours. The zone of inhibition around the disc was measured in mm. Statistically significant differences between discs were identified by one-way ANOVA followed by Sidak's multiple comparisons test within GraphPad Prism v8.1.1.

5.3.4. Evaluation of biofilms on sol-gel coated peg lids

Antimicrobial sol-gel coated peg lids were prepared by immersion of a peg lid (Ceri *et al.*, 1999) into 200 µl of antimicrobial sol-gel (prepared as described in section 5.3.2.) for 2 seconds before being slowly removed. Peg lids were then left to dry overnight and stored in the fridge until use. Overnight cultures of EC958 were diluted to an OD_{600} of 0.008 and 100 µl added to the wells of 96 well plate. The sol-gel coated peg lid was added to the plate and incubated for 48 hours at 37^{o}C and 30 RPM. Peg lids were removed from the plate and rinsed twice in 200 µl PBS before being processed for counts of colony forming units or a luminescence-based viability assay.

For colony counts, the rinsed peg lid was placed in a plate of 100 µl MHB and sonicated for 10 minutes. Samples were serially diluted to 10^{-4} and 10 µl spots were plated in triplicate onto MHA. Plates were incubated overnight, and the CFU/peg was calculated based upon the counts.

For determination of the viability of the biofilm, the rinsed peg lids were placed into 100 µl fresh MHB per well of an opaque walled 96 well plate before sonication for 10 minutes. BacTitre-Glo™ (Promega, UK) was used as per manufacturer's instructions, briefly, 100 µl of reconstituted solution was added to each test well and mixed by orbital shaker for 5 minutes at room temperature before luminescence was measured of the CLARIOstar (BMG Labtech, Germany).

5.3.5. Drip flow biofilm reactor modelling

Antimicrobial sol-gel coated silicon squares were prepared by dip coating sterilised silicon into 10 ml of combined antimicrobial sol-gel in a universal through use of a Precision Dip Coater (Qualtech Products Industry, UK) with a withdrawal rate of 400 mm/min. Antimicrobial sol-gel coated silicon sections were dried overnight and stored in the fridge until use. Using a sterile scalpel, antimicrobial sol-gel silicon squares were cut to 1.5 x 1.5 cm before use.

Artificial urine (AU) was prepared as described in (Brooks and Keevil, 1997): 1 g peptone, 0.005 g yeast extract (Alfa Aesar), 0.1 g lactic acid, 0.4 g citric acid (Melford), 2.1 g sodium bicarbonate (ACROS organics), 10 g urea (EMD Millipore), 0.07 g uric acid (Alfa Aesar), 0.8 g creatine (Millipore), 0.37 g calcium chloride dihydrate (VWR), 5.2 g sodium chloride (Fischer Chemical), 0.0012 g iron II sulphate heptahydrate (VWR), 0.49 g magnesium sulphate heptahydrate, 3.2 g sodium sulphate decahydrate (VWR), 0.95 g potassium di-hydrogen phosphate (Alfa Aesar), 1.2g di-potassium hydrogen phosphate (Lancaster) and 1.3 g ammonium chloride (Alfa Aesar) were dissolved per 1 L distilled H_2O and adjusted to pH 6.5 with hydrochloric acid. AU was filter sterilised before use.

EC958 was cultured overnight in AU and diluted to OD_{600} of 0.008 before use. Three sol-gel coated silicon squares were placed into each channel of the Drip Flow Biofilm Reactor (DFR 110-6, Biosurface Technologies Corporation, USA). The DFR was inoculated with 15 ml EC958 per channel and incubated flat for 4 hours at 37^{o}C. Continuous phase incubation was performed by setting the DFR at a 10^{o} angle, and with a flow rate of AU at 0.83 ml/min for 44 hours (total incubation time 48 hours).

Colony forming units per silicon square were calculated by removal of the silicon squares from the DFR with sterile forceps, adding to 10 ml PBS and vortexing for 30 seconds before serial dilution and 10 µl spot plating in triplicate on MHA.

5.3.6. Chromosomal insertion of *gfp-mut3* into EC958

Tn7 transposon mediated insertion was used to insert *gfp-mut3* into the chromosome of EC958 as described in Choi and Schweizer, (2006). Plasmids of pUC18T-mini-Tn7T-Zeo-gfpmut3 and pTNS2 (gift from Herbert Schweizer, pUC18T- mini-Tn7T-Zeo-gfpmut3 - Addgene plasmid #65037; pTNS2 - Addgene plasmid #64968). Plasmids were recovered from *E. coli* by plasmid miniprep kit (GeneJet) quantified by Nanodrop (ND 1000 v3.8), plasmid size was confirmed by digestion by XbaI and run on a 1.5% agarose gel.

To prepare electrocompetent cells, overnight cultures of EC958 in LB were centrifuged, washed twice in 300 mM sucrose, and suspended in 200 µl 300 mM sucrose before transfer to an electroporation cuvette with 50 ng of each plasmid. Cells were electroporated at 25 µF, 200 Ω, 2.5 kV for < 5 ms (EC1 settings, Micropulser, BioRad), and 1 ml LB was then immediately added and incubated for 1 hour at 200 RPM, 37^{o}C.

100 µl of cells were plated onto LB agar plate containing 100 µg/ml ampicillin, remaining cells were concentrated in 200 µl LB and plated and incubated over night at 37^{o}C.

Colonies were streaked from the overnight plates to obtain single colonies on LB agar plates with 100 µg/ml ampicillin and 50 µg/ml zeocin. Colony PCR was performed to confirm insertion. EC958$^{+gfpmut3}$ was then used as EC958 was used previously.

Table 5.1. Strains, plasmids, and primers used in this chapter.

Strain / Plasmid / Primer	Characteristics	Source / Reference
Strains		
EC958	Globally disseminated ST131 strain.	(Totsika *et al.*, 2011)
CFT073	Patient isolate, P-fimbriated pyelonephritic, haemolysin-positive strain.	(Mobley *et al.*, 1990)
E. coli 25922GFP	Derivative of ATCC 25922 containing pUCP15-MCSgfpmut3 plasmid	ATCC
EC958$^{+gfpmut3}$	EC958 strain with Tn7 transposon mediated chromosomal insertion of *gfpmut3*	This chapter
Plasmids		
pUC18T-mini-Tn7T-Zeo-gfpmut3	DQ493885	(Choi and Schweizer, 2006) Addgene
pTNS2	AY884833	(Choi and Schweizer, 2006) Addgene
Primers		
Tn7R	CACAGCATAACTGGACTGATTTC	ThermoFisher Scientific
Tn7L	ATTAGCTTACGACGCTACACCC	ThermoFisher Scientific
Bleo-Fwd	GATGAACAGGGTCACGTCGT	ThermoFisher Scientific
Bleo-Rev	CAAGTTGACCAGTGCCGTTC	ThermoFisher Scientific
glmS	TATCGTCGTTGCACCGAACA	ThermoFisher Scientific
pstS	ACCAGTTCGCCAGACTTCAG	ThermoFisher Scientific
GFP-Fwd	GCGATGGCCCTGTCCTTTTA	ThermoFisher Scientific
GFP-rev	TGCCATGTGTAATCCCAGCA	ThermoFisher Scientific

5.3.7. Confocal microscopy of EC958$^{+gfpmut3}$

Overnight cultures of EC958$^{+gfpmut3}$ or *E. coli* 25922 + GFP were diluted to an OD_{600} of 0.008 in either MHB or AU. 22 x 22 mm glass coverslips coated with sol-gel or uncoated were placed within a 6 well plate and inoculated with the diluted bacteria, then incubated for 48 hours at 37^{o}C. Coverslips were removed from the wells with sterile forceps, rinsed twice by submersion in PBS and imaged by confocal laser scanning microscopy (LSM 800, Zeiss). Images were captured with an excitation wavelength of 482 nm and emission wavelength of 503 nm. Images were captured as z-stacks of with a step of 16 µm per slice and images were exported as orthogonal projections. Images were analysed within ImageJ (Fiji, v1.53) by splitting of the RGB channels and quantification of the percentage of green pixels. The mean percentage coverage of the field of view was compared by t-test (GraphPad, Prism, v8.1.).

5.4.Results

Combinations of biocide and QSI within sol-gel discs demonstrated that silver nitrate with cinnamaldehyde was more effective at inhibiting bacterial growth than cinnamaldehyde alone against both EC958 and CFT073 in a disc diffusion assay. At 10 mg/ml PHMB with cinnamaldehyde was more effective than cinnamaldehyde alone against both strains and PHMB with furanone-C30 was more effective than furnaone-C30 alone. Biofilm formation on coated peg lids was significantly impeded by PHMB, silver nitrate or triclosan in combination with cinnamaldehyde. In the drip flow reactor model biofilm formation was significantly reduced on silicon coated with silver nitrate in combination with either cinnamaldehyde or furanone-C30, or triclosan in combination with furanone-C30.

5.4.1. Disc diffusions

Combined biocide and QSI containing sol-gel discs were compared with those containing the biocide or QSI alone in terms of the zone of inhibition generated against UPEC strains EC958 and CFT073. At a concentration of 2 mg/ml (containing 20 µg of antimicrobial), only the combination of silver nitrate with cinnamaldehyde, or silver nitrate with furanone demonstrated significant differences (one-way ANOVA $p < 0.0001$) between the combined and single agents for both EC958 (Figure 5.1) and CFT073 (Figure 5.2). Against EC958, silver nitrate in combination with cinnamaldehyde was more effective than cinnamaldehyde alone ($p = 0.0018$, Dunnett's multiple comparisons post-test) however, silver nitrate alone was more effective than when combined ($p < 0.0001$). Against CFT073, silver nitrate combined with each QSI was more effective than the QSI alone ($p < 0.0001$ for both cinnamaldehyde and furanone-C30) but not significantly different from silver nitrate alone (with cinnamaldehyde: $p = 0.3156$, with furanone-C30: $p = 0.0677$).

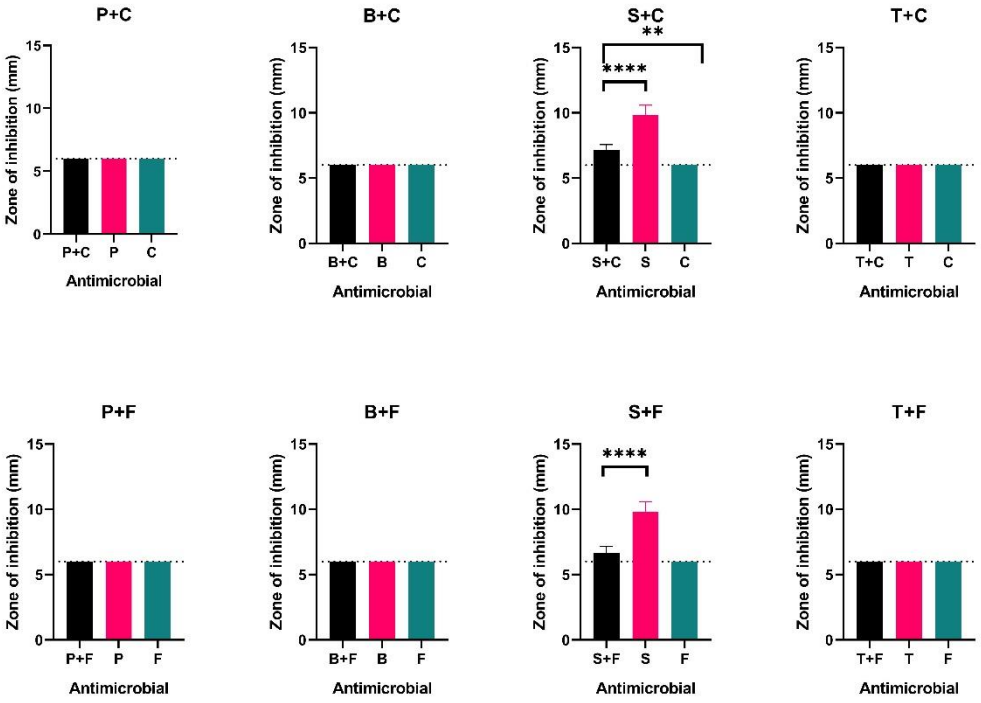

Figure 5.1. Zone of inhibition of combined and single agent sol-gel discs against EC958. Total concentration of antimicrobial is 2 mg/ml, results are an average of 2 biological repeats, each with 3 technical replicates, mean +/- SD. One-way ANOVA analysis of each group demonstrated $p < 0.0001$ for silver nitrate with cinnamaldehyde and silver nitrate with furanone-C30 only. Dunnett's multiple comparisons test represented on graphs, ** $p \leq 0.01$, **** $p \leq 0.0001$. Dotted line represents diameter of the test disc.

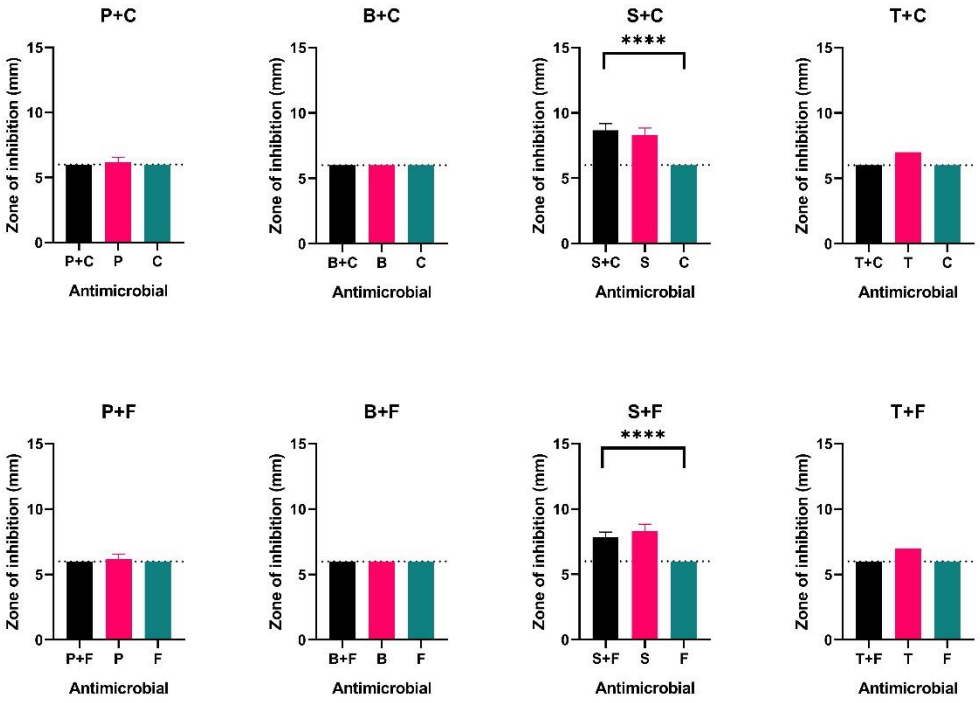

Figure 5.2. Zone of inhibition of combined and single agent sol-gel discs against CFT073. Total concentration of antimicrobial is 2 mg/ml, results are an average of 2 biological repeats, each with 3 technical replicates, mean +/- SD. One-way ANOVA analysis of each group demonstrated $p < 0.0001$ for silver nitrate with cinnamaldehyde and silver nitrate with furanone-C30 only. Dunnett's multiple comparisons test represented on graphs, **** $p \leq 0.0001$. Dotted line represents diameter of the test disc.

At 10 mg/ml concentrations, increased antimicrobial efficacy against EC958 was observed in the combined biocide and QSI formulations when compared to the QSI alone in the case of PHMB with cinnamaldehyde (Dunnett's multiple comparisons test, $p = 0.0005$), silver nitrate with cinnamaldehyde ($p = 0.0050$) and PHMB with furanone-C30 ($p = 0.0065$). Silver nitrate alone was more potent than when combined with cinnamaldehyde ($p = 0.0006$) or furanone-C30 ($p = 0.0345$) and triclosan alone was more potent than when combined with cinnamaldehyde ($p < 0.0001$) or furanone-C30 ($p < 0.0001$) (Figure 5.3).

Similarly, with regards to CFT073, significant increases in efficacy for the combined QSI/biocide compared to the QSI alone was observed for PHMB with cinnamaldehyde ($p < 0.0001$), and silver nitrate with cinnamaldehyde ($p < 0.0001$). Reduced efficacy of

combinations compared to the QSI alone was observed for BAC with furanone-C30 (p = 0.0149) and triclosan with furanone-C30 (p = 0.0385, Figure 5.4).

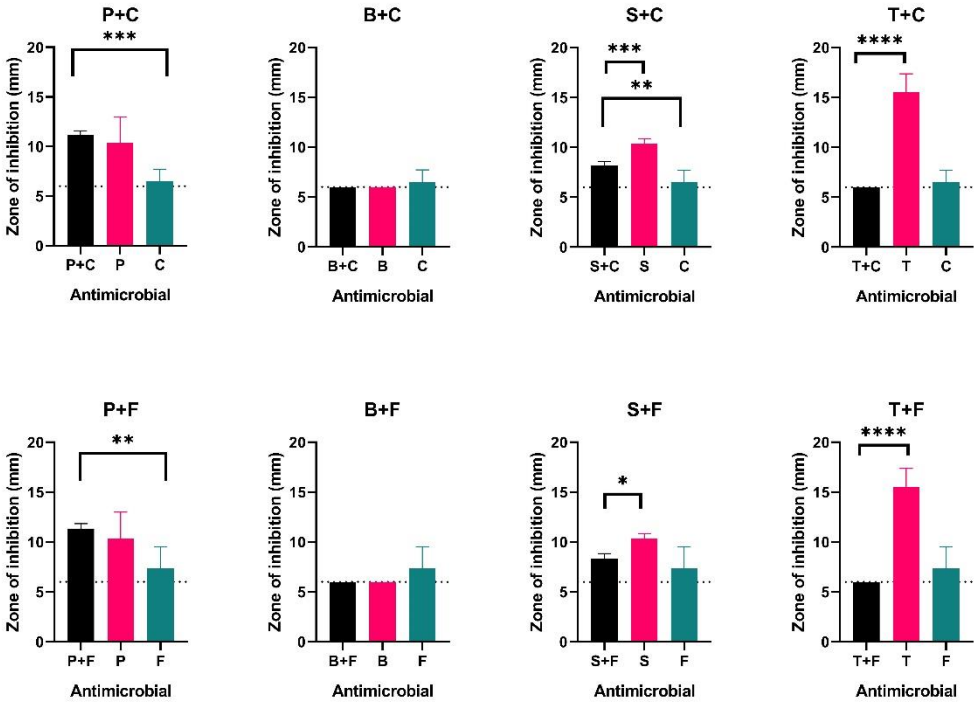

Figure 5.3. Zone of inhibition of combined and single agent sol-gel discs against EC958. Total concentration of antimicrobial is 10 mg/ml, results are an average of 2 biological repeats, each with 3 technical replicates, mean +/- SD. Dunnett's multiple comparisons test represented on graphs, * $p \leq 0.05$ ** $p \leq 0.01$, *** $p \leq 0.001$, **** $p \leq 0.0001$. Dotted line represents diameter of the test disc.

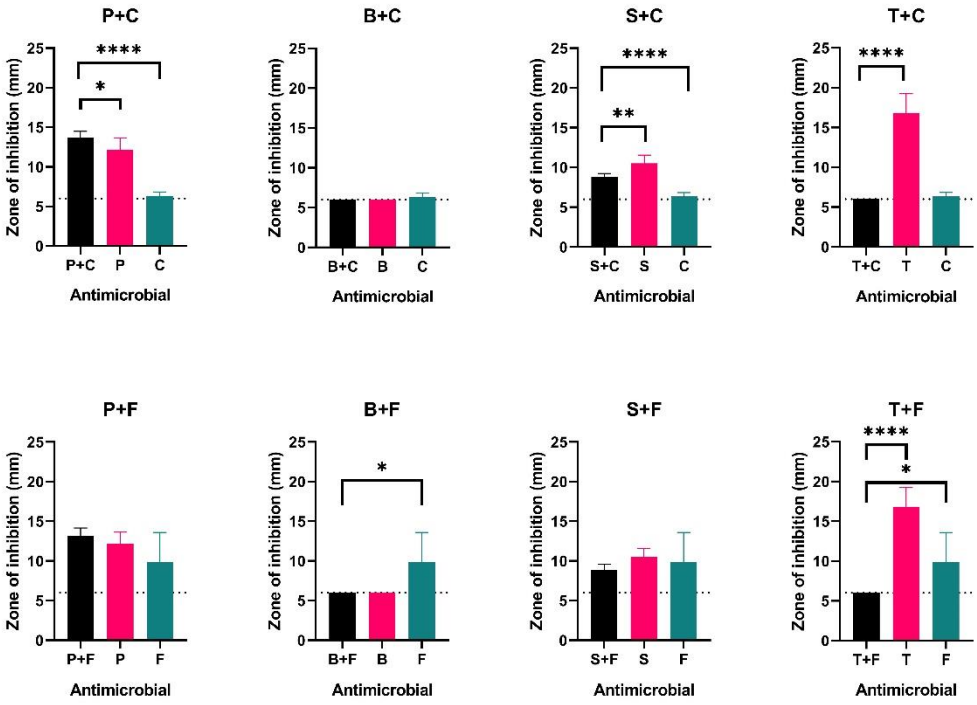

Figure 5.4. Zone of inhibition of combined and single agent sol-gel discs against CFT073. Total concentration of antimicrobial is 10 mg/ml, results are an average of 2 biological repeats, each with 3 technical replicates, mean +/- SD. Dunnett's multiple comparisons test represented on graphs, * $p \leq 0.05$, ** $p \leq 0.01$, **** $p \leq 0.0001$. Dotted line represents diameter of the test disc.

5.4.2. Biofilm formation on peg lids

The impact of biocide/QSI combinations on preventing biofilm growth on a sol-gel coated pegged lid system was assessed. Colony counts were performed and compared to the sol-gel only coatings. Significant decreases in biofilm was observed for PHMB, silver nitrate, triclosan, PHMB with cinnamaldehyde, silver nitrate with cinnamaldehyde and triclosan with cinnamaldehyde. A significant increase in CFU was observed on the pegs coated with BAC combined with cinnamaldehyde compared to the sol-gel only condition ($p = 0.0002$; Figure 5.5).

A BacTiter-Glo luminescence assay was used to determine the metabolic activity of the biofilms formed on the pegged lids. Sol-gel only coated pegs showed a significant increase in detectable metabolic activity of the biofilm compared to uncoated pegs (Figure 5.6). Comparisons of biocide and furanone-C30 containing sol-gel demonstrated no significant differences in CFU/ml (Figure 5.7) when used independently or in

combination relative to the control. However, there were significant reductions observed between the viability of PHMB, silver nitrate, P+F, S+F and T+F coated pegs when compared to those coated with sol-gel alone (Figure 5.8).

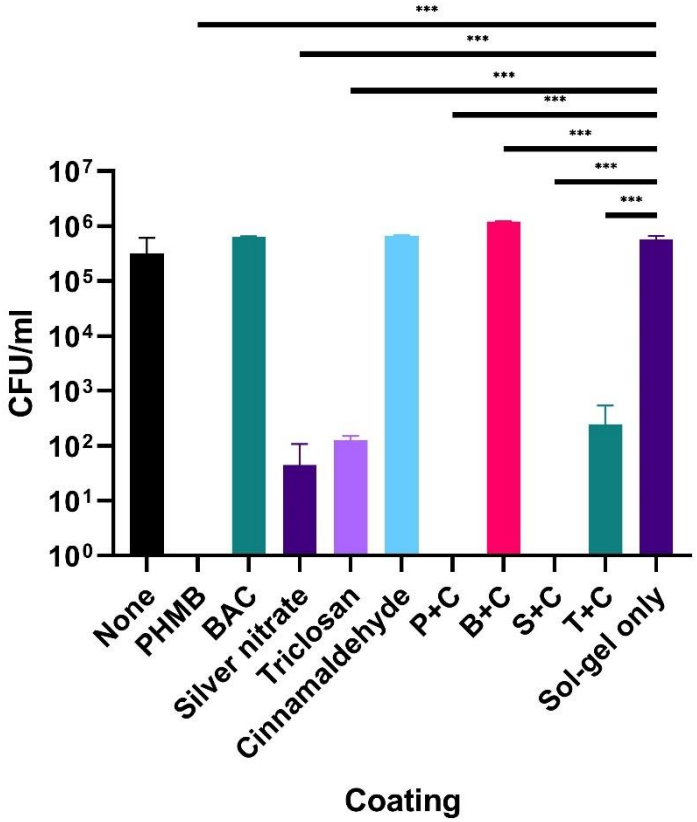

Figure 5.5. Colony forming units per ml of EC958 biofilms formed on sol-gel coatings. Results are the mean of two biological repeats, each with 3 technical replicates, + 1SD. Dunnett's multiple comparisons test shown, *** $p \leq 0.001$.

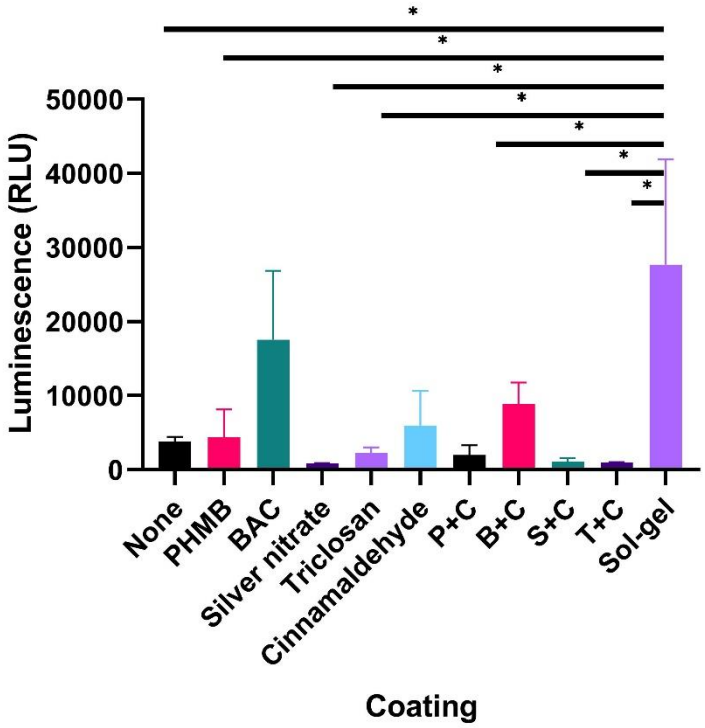

Figure 5.6. Luminescence of EC958 biofilms formed on peg lids coated with or without antimicrobial sol-gel. Results are the mean of two biological repeats, each with 3 technical replicates, + 1SD. Dunnett's multiple comparisons test shown, * $p \leq 0.05$. RLU – relative light units.

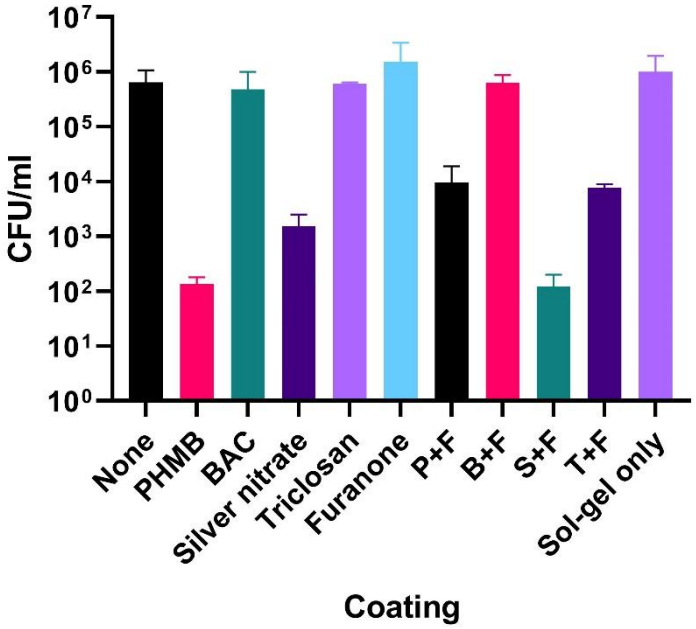

Figure 5.7. Colony forming units per ml of EC958 biofilms formed on sol-gel coatings. Results are the mean of two biological repeats, each with 3 technical replicates, + 1SD. No statistically significant differences between any condition tested.

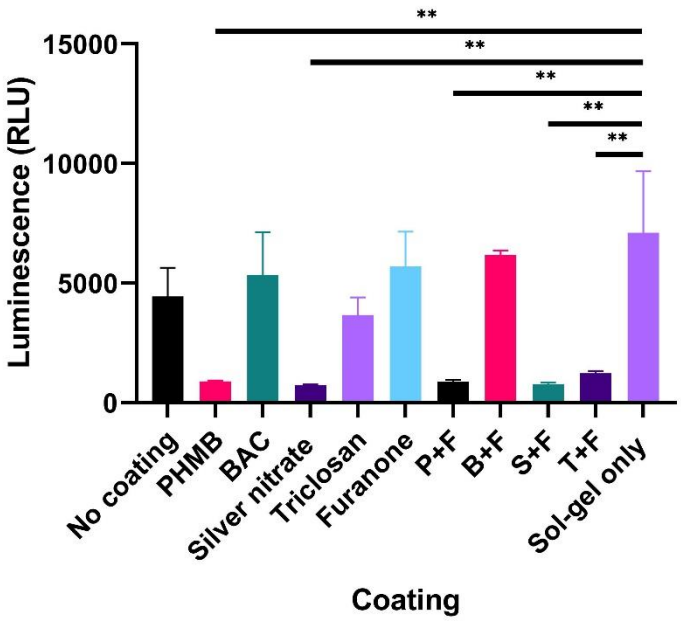

Figure 5.8. Luminescence of EC958 biofilms formed on peg lids coated with or without antimicrobial sol-gel. Results are the mean of two biological repeats, each with 3 technical replicates, + 1SD. Dunnett's multiple comparisons test shown, ** $p \leq 0.01$. RLU – relative light units.

5.4.3. Biofilm formation within a drip flow reactor

Biofilms of EC958 were grown within a drip flow reactor containing silicon squares coated with antimicrobial containing sol-gel under a continuous flow of artificial urine over two days. There was significantly less biofilm formation upon silver nitrate with cinnamaldehyde, silver nitrate with furanone-C30 and triclosan with furanone-C30 containing sol-gel coated samples compared to the sol-gel only coating ($p = 0.0014$, $p = 0.0019$ and $p = 0.0034$ post hoc Dunnett's multiple comparisons, respectively), see Figure 5.9.

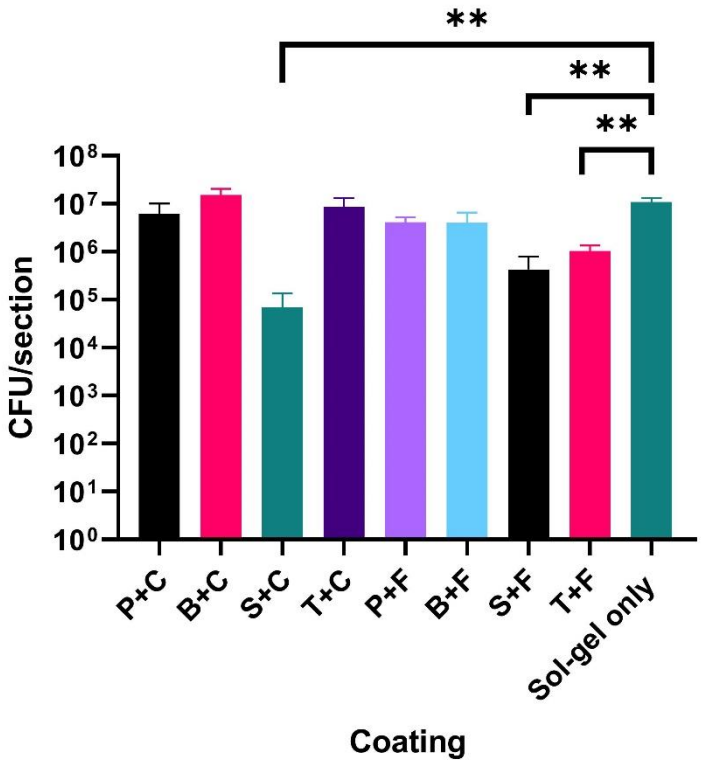

Figure 5.9. Colony forming units per silicon square coated in 10 mg/ml antimicrobial sol-gel. Three silicon squares per condition, average CFU + SD represented. Dunnett's multiple comparisons post hoc test comparisons of all conditions vs sol-gel only. ** ≤ 0.01.

5.4.4. GFP insertion into EC958

To visualise biofilms formed on sol-gel coatings, the *gfpmut3* gene was inserted into the chromosome of EC958 by Tn7 mediated insertion. Chromosomal insertion was chosen as it would not require additional antimicrobials to be required to maintain a plasmid within the bacterium, which may lead to additional potential synergistic or antagonistic interactions with the test antimicrobial combinations.

Average coverage of a coverslip by biofilm varied dependent upon the broth used and the bacterial strain, 25922-GFP covered 1.66 % (± 0.34) of the field of view in MHB and 5.89 % (± 2.05) in AU. There was higher coverage by EC958$^{+gfpmut3}$ with 5.88% (± 5.06) in MHB and 15.82% (± 8.13) in AU.

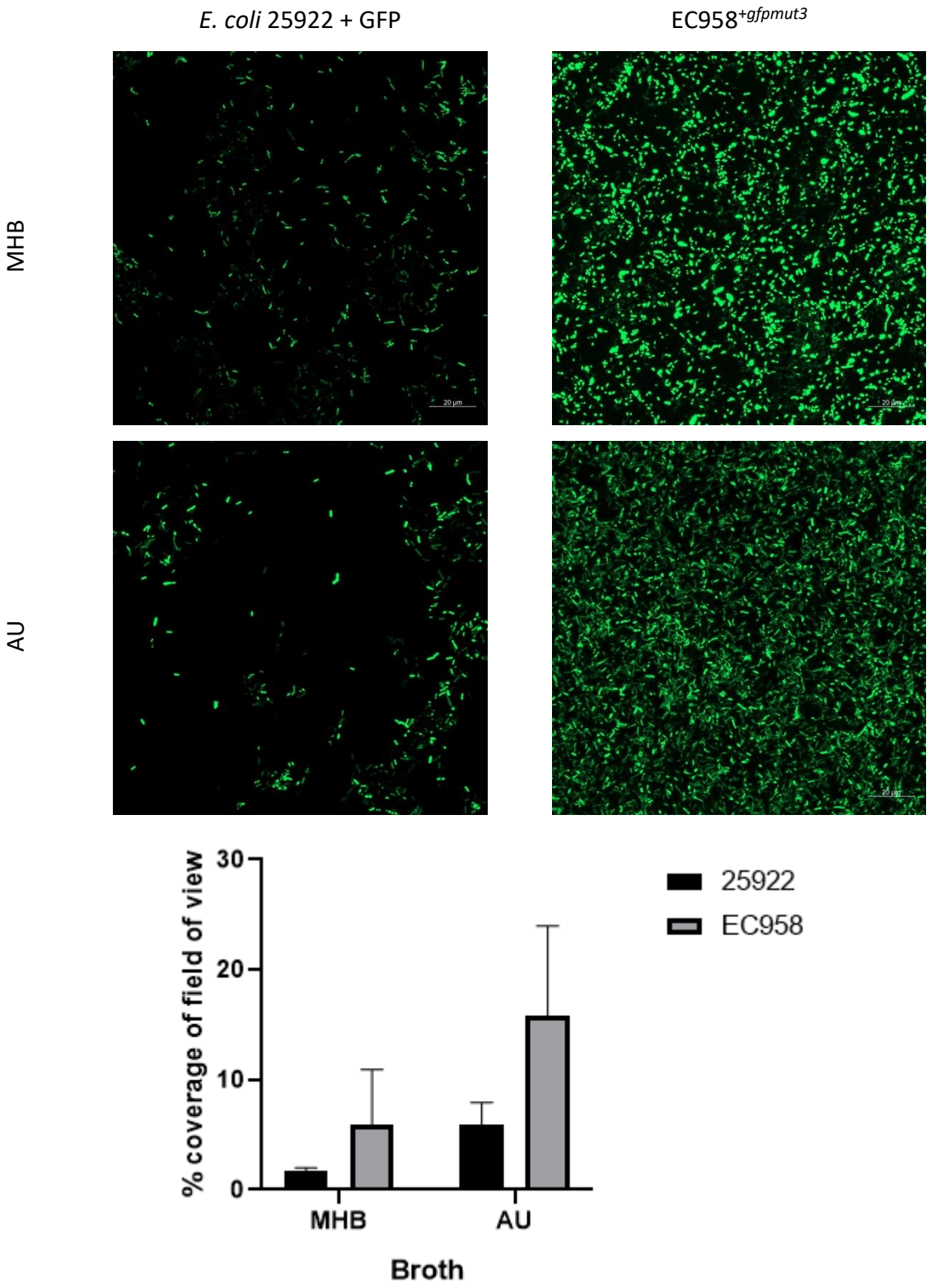

Figure 5.10. Representative images of GFP expressing *E. coli*. Commercial strain 25922+GFP (ATCC) or EC958$^{+gfpmut3}$ grown in either MHB or AU. Percentage of green pixels per field of view. Cells were grown on cover slips over 48 hours, imaged by confocal microscopy, images are orthogonal projections of z-stack images.

When grown upon sol-gel, we observed fluorescence of the sol-gel itself as well as the bacterial cells. Which led to a significant amount of variation in the image analysis results (un-paired, two-tailed t-test, p = 0.133).

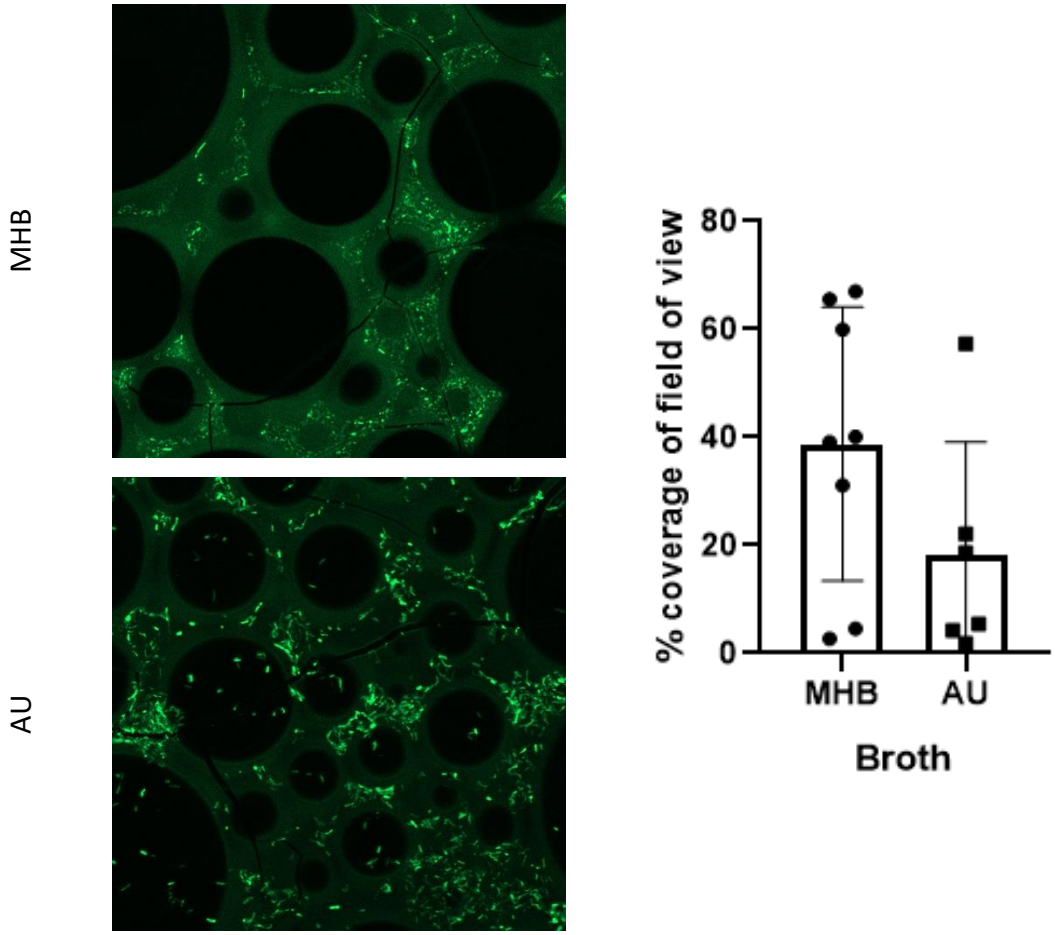

Figure 5.11. Representative images of EC958$^{+gfpmut3}$ on sol-gel coated coverslips and quantitation of the percentage of field of view covered by bacteria, as calculated above.

5.5. Discussion

Catheter associated urinary tract infections are predominantly caused by uropathogenic *E. coli* which form recalcitrant biofilms upon the catheter surfaces (Flores-Mireles *et al.*, 2015). Development of a catheter coating which prevents biofilm formation is therefore key to minimising the chance of infection (Almalki and Varghese, 2020). Existing commercially available catheters are limited to the Release NF (Rochester Medical) nitrofurazone impregnated and silver coated catheters (Lubri-Sil and Bardex IC, Bard Care), however these have limitations including limited temporal efficacy and increases in patient discomfort (Lam *et al.*, 2014). Initial validation of a potential novel coating, combining biocides and QSIs in a silica-based hybrid sol-gel for use on urinary catheters is presented here.

Each biocide (PHMB, BAC, silver nitrate and triclosan) was combined with the QSIs (cinnamaldehyde or furanone-C30) at a total antimicrobial concentration of either 2 mg/ml or 10 mg/ml within a sol-gel coating which was then applied to various substrate surfaces. Within disc diffusion assays silver nitrate in combination with either of our test QSIs led to significant increases in the zone of inhibition compared to the QSI alone within the sol-gel. Biofilm formation upon silver nitrate and cinnamaldehyde containing coatings was also significantly decreased on both the peg lid based assay and within the drip flow reactor. Within the DFR there was also a significant reduction in the number of bacteria within the biofilm formed on silicon coated with either silver nitrate with cinnamaldehyde, silver nitrate with furanone-C30 or triclosan with furanone-C30 sol-gel.

Imaging of the biofilms formed by UPEC on the sol-gel coating had been previously challenging, the sol-gel was able to uptake fluorescent stains and therefore the use of GFP expressing bacteria was proposed. EC958 was modified to express GFP through Tn7 insertion into the chromosome and expressed GFP to a level which was high enough to allow imaging by confocal microscopy. Growth in AU led to an increase in biomass, however quantitation by image analysis software of the biofilm formed on sol-gel coatings was still challenging due to the background fluorescence of the sol-gel.

5.5.1. Disc diffusions

The combination of biocides with QSIs within sol-gel led to an increase in the zone of inhibition compared to the QSI alone in the cases of silver nitrate with cinnamaldehyde for both strains and concentrations tested. At a concentration of 10 mg/ml, PHMB with cinnamaldehyde led to a larger zone of inhibition than either antimicrobial alone against CFT073 and was larger than cinnamaldehyde alone against EC958. Comparisons of the combinations to the biocide alone showed a reduction in the zone of inhibition in the case of silver nitrate with cinnamaldehyde for both strains, silver nitrate with furanone-C30 for EC958, and triclosan with either QSI for both strains. This could be due to differences in the concentration of each agent within the coating, the total antimicrobial concentration of each disc was 10 mg/ml, i.e., containing 50 μg of biocide and 50 μg of QSI. Regarding the effective concentrations of biocides this should provide an inhibitory concentration, however, with regards to the QSIs this may fall below active inhibitory concentrations when in combination (Chapter 4). A limitation of the disc diffusion assay is the elution of the antimicrobials from the disc could be affected as the elution onto agar would differ from that of the quantified elution in Chapter 3. From the disc diffusion data, combinations of PHMB with either QSI or silver nitrate with cinnamaldehyde were more effective than each antimicrobial alone against EC958, similarly the combinations of either PHMB or silver nitrate with cinnamaldehyde against CFT073 were most effective. However, this assay does not assess the impact of these combinations within the sol-gel on the formation of biofilms, which is a key consideration due to the fact that the impact from the QSIs could be more effective in this role. Both cinnamaldehyde and furanone-C30 have been shown to impact *E. coli* biofilms (Ren, Sims and Wood, 2001; Kot *et al.*, 2015).

5.5.2. Biofilm formation in static assays

Combined biocides and QSI sol-gel was used to coat a peg lid for use with 96-well microtiter plates. Biofilm formation on the sol-gel coated peg lids was assessed by performing colony counts and through use of an ATP based luminescence viability assay. There was complete eradication as measured through CFU counts of the bacteria on the PHMB or silver nitrate combined with cinnamaldehyde coated pegs, this is likely to be due to the rapid release of both PHMB and silver nitrate into the surrounding

environment as seen in chapter 4, and due to the synergism between these agents, as seen in chapter 3. The combination of the membrane active effects of cinnamaldehyde and PHMB or silver nitrate was proposed to lead to a cumulative disruption of the membrane, leading to an increase in the permeability of the bacterial cell, thus facilitating entry into the cytoplasm and increasing the availability of intracellular targets (Woo *et al.*, 2008; Doyle and Stephens, 2019; Sowlati-Hashjin, Carbone and Karttunen, 2020). Significant reductions were also observed in the CFU on triclosan and cinnamaldehyde coated peg lids, this may be due to the low concentration of triclosan required to inhibit growth (MIC < 0.4 μg/ml, chapter 4). All conditions other than BAC alone led to a reduction in the viability of the biofilms as measured by an ATP based luminescence assay. The lack of inhibition of biofilm formation by BAC impregnated sol-gel both independently and in combination with QSIs could be due to the complete lack of release from the sol-gel, as shown in chapter 4, preventing interaction with the surrounding bacteria and the concentrations of the QSIs may not be high enough to exhibit direct antimicrobial activity alone.

Discrepancies between count results and the ATP assay have been observed previously, this was proposed as the possibility of missing the peak point of metabolic activity during the growth phase of the biofilm or that the ATP levels per cell could vary (Farhat *et al.*, 2018). This could be the case within the biofilms that there are different phenotypes within a single biofilm (Kester and Fortune, 2014) including persister cells and slow growing cells (Stewart, 2002) that could lead to a high CFU whilst maintaining low levels in the ATP-based assessment.

5.5.3. Biofilm formation within a drip flow reactor

Formation of biofilms on antimicrobial sol-gel coated silicon was performed within a DFR, in the presence of artificial urine to represent a more realistic environment for the establishment of a uropathogenic biofilm on a catheter surface.

An important aspect of using the drip flow reactor is the provision of a flow over the silicon samples. Flow over a surface has been seen to affect the initial attachment and formation of biofilms of many bacterial species, (Conrad and Poling-Skutvik, 2018). Lower flow rates have been associated with higher *E. coli* biofilm thickness and weight

than biofilms formed under high flow conditions, due to the higher availability of nutrients and lower shear stress (Moreira *et al.*, 2013). This highlights the importance of mimicking the conditions of catheter use to accurately assess the impact of the anti-infective coating on biofilm formation.

Observed here was a significant reduction in biofilm formation on coatings containing silver nitrate with cinnamaldehyde, silver nitrate with furanone-C30 and triclosan with furanone-C30. In contrast, during the coated peg lid analysis there was also a reduction in biofilm on PHMB and QSI coatings. The impact of continuous flow on biofilm formation could impact the coatings perceived efficacy. As seen in chapter 3, there were different release profiles of each antimicrobial which would affect the available concentrations to prevent biofilm formation. The initial static stage of incubation would have allowed accumulation of the antimicrobial within the channel, this may be why the silver nitrate combinations were so effective, as the majority of the available silver elutes from the coating within the first few hours. The anti-biofilm effects of cinnamaldehyde and furanone-C30 may then impair the formation of biofilm by the remaining bacteria (Ren, Sims and Wood, 2001; Kot *et al.*, 2015). Although triclosan had a slower rate of elution (chapter 3) the low effective concentrations of this may have inhibited bacterial growth for a prolonged period preventing biofilm formation initially before the antimicrobial was lost from the system.

For silver nitrate coatings there was a rapid initial release of antimicrobial and for triclosan coatings this release was more sustained over the course of the week. The amount of antimicrobial available initially during the attachment phase and the release and continuous removal of the antimicrobial from the environment by the continuous flow of the media is likely to impact biofilm development.

Whilst providing a more realistic assessment of coating efficacy than batch culture systems, the DFR still has limitations including potentially provision of excessive nutrients and the use of a single strain when multiple are likely to be encountered *in vivo* (Buhmann *et al.*, 2016). The potential limitations to using the silicone squares over the use of the catheter segments is the different topography of the surfaces which could impact the flow forces and therefore impact the biofilm formation further (Conrad and Poling-Skutvik, 2018).

5.5.4. GFP UPEC

Imaging of biofilms formed on the sol-gel is challenging as the sol-gel absorbs and retains the fluorescent dyes that are commonly used, previous work staining biofilms formed upon sol-gel led to a large amount of background fluorescence. Therefore, in an attempt to overcome this issue, the GFP gene (*gfpmut3*) was inserted into the chromosome of EC958 to aid imaging of biofilms formed on the surface of the sol-gel. The Tn7 chromosomal insertion was used over the use of a plasmid to prevent the requirement of additional antibiotics to maintain the plasmid which may lead to additional synergistic or antagonistic interactions to those identified in chapter 4. In comparisons of the commercially available *E. coli* 25922GFP strains, there appeared to be higher biofilm formation by the EC958$^{+gfpmut3}$.

There was a higher level of biofilm formation on the coated surface following growth in artificial urine compared to Mueller Hinton broth. The artificial urine recipe used in this work was first proposed by Brooks & Keevil (1997). It has been cited more than 100 times, most recently used as an AU in Dubern et al. (2023); Yazdani-Ahmadabadi et al. (2022); and Zou et al. (2023) and is shown to be relatively comparable to human urine (Sarigul, Korkmaz and Kurultak, 2019).

EC958$^{+gfpmut3}$ growth was evident on sol-gel coated silicon visually, however, software-based quantitation of this was challenging due to background fluorescence of the sol-gel. Further optimisation of imaging would be required, potential future experiments include counterstaining the sol-gel could be a method which may allow quantitation of the biofilm formed upon the coating.

5.6. Conclusions

Overall, further optimisation of the sol-gel coating would be required before moving into *in vivo* studies as a potential catheter coating. Namely, coating consistency would need to be further optimised and validated. There was demonstratable potential of silver nitrate with cinnamaldehyde, silver nitrate with furanone-C30 and triclosan with furanone-C30 coatings to effectively reduce the number of bacteria which may grow upon silicon as demonstrated through the assays within the drip flow reactor. However, cytotoxicity of furanone-C30 was high (chapter 4) therefore further analysis of the

coating cytotoxicity within a continuous flow environment could provide a more accurate prediction of the overall efficacy

6.
General Discussion

6.1. A sol-gel based urinary catheter coating containing a combination of biocides and quorum sensing inhibitors has potential to inhibit uropathogenic *E. coli* biofilm formation.

Catheter associated urinary tract infections (CAUTI) pose a substantial burden to healthcare systems across the globe. For the NHS, CAUTI is estimated to account for 43% - 56% of all healthcare associated urinary trat infections totalling an expense of £1 – 2.5 billion per annum (Jacobsen *et al.*, 2008; Loveday *et al.*, 2014). Uropathogenic *Escherichia coli* (UPEC) are the most common causative pathogen of UTIs, responsible for approximately 65% of complicated UTIs of which CAUTI are the most frequent type (Flores-Mireles *et al.*, 2015).

There are many strains of UPEC, all of which are adapted to effectively colonise the urinary tract. They harbour many virulence factors including toxins, adhesins, flagella and iron acquisition systems as well as often containing multiple antimicrobial resistance mechanisms (Terlizzi, Gribaudo and Maffei, 2017). UPEC strains EC958 and CFT073, used throughout this research, are well characterised strains harbouring many of these virulence factors in addition to displaying resistance to a number of clinically relevant antibiotics (Welch *et al.*, 2002; Totsika *et al.*, 2011).

Current anti-infective urinary catheters which are commercially available include the Nitrofurazone impregnated ReleaseNF (Rochester Medical) and silver coated Lubri-Sil and Bardex IC (BardCare). However, these have been shown to have no overall advantage with regards to infection prevention and reportedly may even increase patient discomfort compared to standard catheters (Lam *et al.*, 2014).

The aim of this thesis was to develop an antimicrobial impregnated catheter coating to prevent UPEC colonisation and biofilm formation thus posing a suitable strategy against CAUTI. Previous work had investigated the impacts of four biocides (polyhexamethylene biguanide [PHMB], benzalkonium chloride [BAC], silver nitrate and triclosan) and three quorum sensing inhibitors (QSIs) (*trans*-cinnamaldehyde, (z)-4-bromo-5(bromomethylene)-2(5H)-furanone [furanone-C30] and 4-fluoro-5-hydroxypentane-2,3-dione [F-DPD]) on a panel of 8 UPEC strains (EC1, EC2, EC11, EC26, EC28, EC35, EC958 and CFT073) (Henly, 2019; Henly *et al.*, 2019, 2021). Whilst all test agents showed bacteriostatic, bactericidal and anti-biofilm capability in UPEC, long-term exposure was

seen to lead to changes in the phenotype in a strain dependent and antimicrobial dependent manner. These changes impacted antimicrobial resistance profiles, growth, biofilm formation and pathogenicity. Genomic and transcriptomic analysis of EC958 was also undertaken to elucidate the mechanisms behind the observed phenotypic changes.

Throughout this thesis was an interrogation of the transcriptome and proteome in response to long-term exposure to these biocides and QSIs (Chapter 2). All antimicrobials evaluated (with the exception of F-DPD due to availability) were incorporated into a silica-based hybrid sol-gel coating and the profile of antimicrobial release was measured over a period of a week (Chapter 3). Effective antimicrobial combinations of the biocides and QSIs were identified, and the cytotoxicity of the combinations was assessed (Chapter 4). Synergistic potential of antimicrobial combinations was determined, and this was followed by an evaluation of biofilm formation on the coatings which incorporated both biocide and QSI within a continuous culture drip flow reactor model (Chapter 5).

6.2. Long-term exposure to biocides and QSIs leads to a high number of significant transcriptomic changes but a low number of significant proteomic changes.

UPEC strain EC958 was passaged repeatedly at sub-lethal biocide/QSI concentrations prior to determination of phenotypic, transcriptomic and proteomic change. Previous work had indicated that PHMB led to significant elevation of MBEC yet induced reduction in total biofilm formation on a catheter surface in addition to reduced relative pathogenicity in a *Galleria mellonella* model. BAC exposure led to an increase in MIC and MBEC, an increase in invasive capability in bladder smooth muscle cells, and a reduction in relative pathogenicity. Silver nitrate exposure led to increases in MIC, MBC and MBEC but caused no further adaptation. Triclosan led to increases in MIC, MBC, MBEC, and cross resistance to nitrofurantoin. Reductions in biofilm formation and pathogenicity were also observed after triclosan exposure (Henly, 2019; Henly *et al.*, 2019).

Regarding long-term exposure to QSIs, reductions in the MIC, MBC and MBEC were observed after exposure to cinnamaldehyde and furanone-C30, decreases in biofilm formation on a catheter surface were observed in furanone-C30 and F-DPD exposed

strains and a decrease in pathogenicity was reported in furananone-C30 exposed strains (Henly, 2019; Henly *et al.*, 2021). Understanding the pathways that govern bacterial adaptation to biocides and QSIs is of significant importance when determining the long-term efficacy, thus clinical value, of an antimicrobial coated medical device. In addition, it evaluates the potential risk that a coating poses on the bacterial populations it encounters with regards to increased resistance or virulence.

For all biocides and QSIs there were significant changes in differentially regulated genes when compared to a control strain passaged in an antimicrobial free environment. However, the changes observed in the proteome were far fewer with only a total of 96 proteins significantly differentially expressed across all the exposed conditions, and both triclosan and F-DPD led to no significantly differentially expressed proteins. There was a high amount of variation within the proteomic profiles of each biologic repeats, including within the control condition. This would have an impact on the statistical significance of the observed proteomic changes. Additional repeats may be required to identify the differences between these groups, or a more targeted top-down proteomic approach could increase the power of the analysis by looking at the change in specific proteins across the conditions.

Change in the regulation of genes associated with motility (e.g., flagellar associated *fli* genes and chemotaxis related *che* genes) were observed following exposure to PHMB, BAC, cinnamaldehyde and F-DPD exposed conditions. Motility has been associated with initial contact and attachment of a biofilm (Pratt and Kolter, 1998). Genes associated with motility were predominantly down regulated in PHMB and F-DPD where biofilm formation was reduced on catheter segments. However, motility genes were also down regulated following long-term BAC and cinnamaldehyde exposure, whereas biofilm formation was increased in a multi-well plate. Following exposure to cinnamaldehyde, the highest number of proteins were differentially expressed, including increased expression of many associated with motility (i.e., flagellar associated proteins FliC and FliD and chemotaxis proteins Tsr and CheY). These specific changes in the protein expression could be evaluated further within the other UPEC strains for which phenotypic data is available by qPCR or western blotting analysis of these specific genes and proteins.

Investigation into other UPEC strains should be performed, including the clinical isolates used within this thesis. CFT073 has been previously shown to have an altered transcriptome in response to exposure to a range of biocides including BAC and triclosan including changes in the regulation of transport related and cell adhesion associated genes (Ligowska-Marzęta *et al.*, 2019). The phenotypic changes in response to long-term exposure to the biocides and QSIs was unique for each of the 8 strains of UPEC challenged by Henly, *et al* (2019, 2021). Therefore, further analysis of the transcriptomic and proteomic changes could provide additional clues as to the mechanisms of the changes which led to the phenotypes observed. A comprehensive understanding of the mechanisms which the long-term exposure to these biocides and QSIs elicit can aid in the development of the catheter coating. In order to minimise the chance of detrimental traits within the pathogens developing, the release of the antimicrobials from the catheter coating should be assessed and optimised to minimise the release of sub-inhibitory concentrations.

6.3. Variable release profiles are observed between antimicrobials when eluted from a silica-based hybrid sol-gel coating.

An effective coating would release the antimicrobials at a concentration which is balanced to prevent microbial colonisation whilst limiting cytotoxicity. A release rate which is too rapid, whilst useful in preventing microbial contamination during catheter insertion, could potentially lead to cytotoxic concentrations and may also lead to a limited window of efficacy as the reserve of antimicrobial within the coating is depleted rapidly. If antimicrobials are released at a rate which is too slow, the available antimicrobial could provide a subinhibitory concentration, therefore not only proving ineffective at preventing infection, but also promoting the selection of resistance or changes to virulence (Henly *et al.*, 2019, 2021).

The release of antimicrobial from the sol-gel coating was observed to be most rapid for silver nitrate, followed by PHMB, cinnamaldehyde, then triclosan. BAC did not appear to elute from the coating and the release of furanone-C30 could not be quantified within the timeframe of this PhD (Chapter 3).

The use of a silica-based hybrid sol-gel as the coating technology of a medical device is ideal as the resultant properties of the coating are fully controllable through modification of the formulation, this would allow the release profiles to be fine-tuned for optimal release of each antimicrobial. This particular formulation has also been shown to be biocompatible *in vivo* (Nichol *et al.*, 2021). The components of the precursor solution can be revised to include different functional groups which would modify the polymerisation steps within the gel formation. The pH of the catalyst solution can affect the final structure of the gel as well, with low pH concentrations leading to more linear structures and higher pH leading to more branching and polymerisation. The drying process can also impact the final coating conditions, as it dries it shrinks in volume. Dependent upon the catalyst used and the ratio of solvent to water, there can be higher or lower levels of porosity in the final coating due to changes in the reaction rate of hydrolysis and condensation and the rate of evaporation (Jones, 1989; Brinker, C and Scherer, George, 1990; Brinker *et al.*, 1992).

There was heterogeneity in the release profiles of the antimicrobials: silver nitrate was fully released from the coating within 6 hours, whereas BAC did not elute from the coating over a period of one week. Differences in the molecular structures of the antimicrobials could explain the differences in the elution rates. Silver nitrate within solution dissociates and releases silver ions (Ag^{+}), which may not interact with the sol-gel and therefore are released easily. Whereas BAC, which contains a long hydrocarbon chain could remain trapped within the gel matrix by steric hinderance. PHMB is a heterologous mixture of polymer lengths, can be much larger than BAC, with up to 40 repeating units which may not be fully incorporated into the sol-gel as it is added after 72 hours of mixing when the gel structure has started to form, hence the faster release from the sol-gel observed.

With regards to cinnamaldehyde, the active concentrations which were released from the coating were below the concentrations which were required to inhibit bacterial growth. The maximum concentration of cinnamaldehyde was 10 mg/ml and into ammonium acetate a maximum quantity of 32.5 µg was released over 1 week, whereas the MIC range of cinnamaldehyde was 125 µg/ml (when combined with silver nitrate for EC2, EC11, EC34, EC958 and CFT073) to 1000 µg/ml (alone against EC26 or combine with triclosan against EC11). As discussed in chapter 1, there could be adaptation by the

bacteria and changes to the susceptibility from long-term exposure to low concentrations which remain within the coating (Henly *et al.*, 2019, 2021).

Further work would be required to optimise the sol-gel formulation used here. The proposed next step would be to reduce the water content of the sol-gel, this may also allow better incorporation of cinnamaldehyde in particular. The incorporation of essential oils in to a TEOS based sol-gel was more successful at water concentrations below 2% (Haufe *et al.*, 2008), whereas 10% was used here. Treatment post coating has also been shown to impact the efficacy of antimicrobial coatings. Temperature increases to the heat treatment of silver nitrate incorporated TEOS based sol-gel films showed differences in the resultant properties of the coatings and led to the formation of silver nanoparticles (Li *et al.*, 2003). Alternatively, a simple method of layering the sol-gel coatings could provide a longer release profile or could create waves of release of different antimicrobials, prolonging the efficacy of the coating.

The use of a single antimicrobial has an inherent risk of selection for resistance, especially at this stage of development where the elution of the antimicrobial has not been fine tuned. It was hypothesised that the combination of a biocide with a QSI could result in a synergistic effect on the efficacy of the coating.

6.4. PHMB, BAC or silver nitrate in combination with either cinnamaldehyde or furanone-C30 are synergistic against UPEC biofilms.

Against the panel of 8 UPEC strains synergistic anti biofilm activity was observed following combination of PHMB with cinnamaldehyde (6/8 strains), BAC with cinnamaldehyde (5/8 strains), silver nitrate with cinnamaldehyde (8/8 strains), PHMB with furanone-C30 (3/8 strains) BAC with furanone-C30 (4/8 strains) and silver nitrate with furanone-C30 (6/8 strains). Triclosan in combination with either cinnamaldehyde or furanone-C30 was antagonistic (7/8 and 4/8 strains respectively) or indifferent at biofilm eradication concentrations. Combinations of PHMB with cinnamaldehyde or BAC with cinnamaldehyde demonstrated indifferent or antagonistic cytotoxicity at active antimicrobial concentrations. However, furanone-C30 was highly cytotoxic to L929

mouse fibroblast cells and primary human bladder smooth muscle cells (Chapter 4, Capper-Parkin et al., 2023).

The commercially available antimicrobial catheters, and many others in development incorporate the use of a single antimicrobial agent (Singha, Locklin and Handa, 2017; Cortese *et al.*, 2018; Ramstedt *et al.*, 2019; Andersen and Flores-Mireles, 2020; Bhattacharjee *et al.*, 2022; Dai, Gao and Duan, 2023). The combination of QSIs, with biocides is theorised to be more effective and less likely to lead to resistance due to the use of a multitargeted approach. The use of QSI within the coating were expected to prevent biofilm initiation hence requiring lower overall concentrations of biocide to kill the residual non-biofilm associated planktonic cells. Whether the exposure to the combined biocides and QSIs could reduce the selection pressure on the UPEC and reduce the selection of antimicrobial resistant populations is a key area for future investigation.

The use of triclosan led to predominantly antagonistic interactions and this was hypothesised to be due to the insolubility of the molecule in the combinatorial experiments. The release of triclosan from the sol-gel coating also differed to other molecules, it was slower to elute at all concentrations tested. The insolubility of the molecule in aqueous solutions could result in retention within the coating.

From the elution data (Chapter 3) the concentrations of the antimicrobials within the sol-gel would need to be further optimised to fall within the effective ranges identified when used in combination (Chapter 4). The maximum amount which was available within the sol-gel coated samples was 100 µg of antimicrobial. This would need to be significantly higher, particularly regarding cinnamaldehyde, where over the course of a week a maximum of 32.5 µg was released from the sol-gel whereas the effective bactericidal concentrations of cinnamaldehyde was as high as 1083.3 µg/ml in combination with BAC against EC26, or as low as 125 µg/ml in combination with BAC against EC11.

6.5. Sol-gel coatings containing silver nitrate with cinnamaldehyde or furanone-C30 and triclosan with furanone-C30 reduced biofilm formation in a continuous culture drip flow reactor model.

When evaluating reduction in biofilm formation using the Calgary biofilm device, we observed significantly lower levels of biofilm on pegs coated with sol-gel containing PHMB, silver nitrate or triclosan in combination with cinnamaldehyde. When evaluated by the BACtitre Glo viability assay alone, biofilm formation was also inhibited by PHMB, silver nitrate or triclosan in combination with furanone-C30, however there was no significant difference in the number of recovered CFU. When challenged within a drip flow reactor, there was only significant reduction in biofilm formation on silicon coated with combinations of silver nitrate with cinnamaldehyde, silver nitrate with furanone-C30 or triclosan with furanone-C30 (Chapter 5).

As shown in Chapter 3, the elution rates of each antimicrobial from the sol-gel coating vary. Within the drip flow reactor, we can predict that the released antimicrobial flows out of the system, whereas in the peg lid assay the antimicrobial released from the coating remained contained within the well. Therefore, the concentration of available antimicrobial reduces over time within the drip flow reactor. This may result in regrowth of microbial communities if they are not completely eradicated during the initial antimicrobial release, or if the effective concentrations required to inhibit or kill the bacteria are not available.

Future analysis should aim to determine the amount of available antimicrobial within the drip-flow model at different time points to determine the potential for community regrowth and further the relevant concentrations which would be achieved in a realistic setting. Furthermore, the release of the antimicrobials from the sol-gel into urine could differ significantly than what was determined through the mass spectrometry analysis when elution was performed into ammonium acetate due to variations in pH and salt concentration within the formulations (Chanabodeechalermrung *et al.*, 2022). The impact of urine on the stability of the sol-gel coating should also be assessed.

Not only the elution into artificial, or pooled, urine should be assessed, but also the effects of urine on the activity and efficacy of the antimicrobials. It has been shown previously that the efficacy of gentamicin is dependent upon the pH and the

concentration of urine with increased MIC and MBC at lower pH and higher concentrations (Minuth, Musher and Thorsteinsson, 1976). Ciprofloxacin MIC is increased in artificial urine compared to MHB and change in susceptibility is strain dependent at different pH (Dalhoff, Stubbings and Schubert, 2011). To assess the potential impact of urine on the efficacy of the antimicrobials, screening of the antimicrobials in artificial urine to determine the effects on MIC and MBC would provide an indication of this.

6.6. Further development of an antimicrobial impregnated catheter coating to prevent uropathogenic *E. coli* infections.

Further optimisation is required to develop a fully functional and long-lasting urinary catheter coating to prevent UPEC infections. Initially, further optimisation of the sol-gel formulation is required to allow prolonged release at effective concentrations. This could be achieved through initial increases in the concentration of antimicrobial incorporated into the sol-gel and by simple changes to the sol-gel formulation, such as, a reduction in the water content or changes to the precursor chemicals used. In tandem with this, the release of the antimicrobials into a urine mimic matrix would be required, as this could lead to differences in the release profiles.

The impact of these combinations was tested here only on UPEC, and predominantly only the EC958 strain. Any potential coating should be further tested against a panel of uropathogens, e.g., *Klebsiella pneumoniae*, *Enterococcus* spp., *Candida* spp. and *Proteus mirabilis*. The efficacy of the coating against *P. mirabilis* would be of particular interest due to this organism's ability to form crystalline biofilms which lead to the blockage of catheters (Flores-Mireles *et al.*, 2015). The impact on polymicrobial infections should also be considered as they account for a significant proportion of infections, 15% of all bacterial CAUTIs recorded in the UK between 1996 – 2001 (Wazait *et al.*, 2003). The impact of the coating on human cells relevant to the urinary tract needs to be further characterised, addressed here was only the effects of the antimicrobials against human bladder smooth muscle cells. Development of a urinary tract 3D model would be more

representative of *in vivo* conditions compared to the 2D cultures used thus far (Fontoura *et al.*, 2020).

Once the efficacy of the coating is quantified through antimicrobial elution into urine and optimised to provide relevant concentrations required to prevent colonisation by a range of uropathogens, the remaining challenge is to identify a mechanism to efficiently coat a urinary catheter, intra and extra-luminally.

In addition to use upon a urinary catheter, an effective anti-infective coating which can prevent bacterial colonisation and biofilm formation would be revolutionary for medical care. Bacterial colonisation and biofilm formation upon medical devices is a significant issue, leading to persistent infections and device failure (Costerton, Stewart and Greenberg, 1999; Bjarnsholt, 2013). Previous work has investigated the application of sol-gel technology for the delivery of antibiotics to prevent prosthetic joint infections (Nichol *et al.*, 2021), but the provision of a thin coating upon an implant could also be applicable to many implantable medical devices such as dental implants (Camps-Font *et al.*, 2015), or for use upon the surface of other medical devices such as ventilator tubing (Gil-Perotin *et al.*, 2012), or central lines (Gominet *et al.*, 2017), all of which are sources of healthcare associated infections.

6.7. Overall conclusions

Urinary catheters are an essential medical device, but the incidence of CAUTI is high and of significant concern to healthcare systems across the globe. Presented here is a study looking at the development of potential antimicrobial impregnated urinary catheter coatings to prevent uropathogenic *E. coli* biofilm formation providing a potential solution to combat future infections. Data indicates that long-term exposure to biocides and QSIs leads to significant changes in phenotype, impacting antimicrobial resistance profiles, biofilm formation and pathogenicity. This is associated with change in the underlying transcriptome in EC958, however our data indicates that relatively few proteins showed significant difference in their expression. Each antimicrobial tested led to a unique combination of phenotypic, genotypic, transcriptomic and proteomic

responses which highlights the varying mechanisms of antimicrobial action and resulting bacterial response to the panel of antimicrobials.

When incorporated into the silica-based hybrid sol-gel coating, each antimicrobial was eluted in a different manner. Silver ions eluted rapidly from the coating, whereas BAC was assumed to be maintained within the coating as it was detected at very low concentrations only in the eluate. Combinations of biocides with QSIs were assayed as a potential way to maximise antimicrobial activity whilst minimising cytotoxicity. PHMB combined with cinnamaldehyde, or silver nitrate combined with cinnamaldehyde displayed synergistic antimicrobial activity at non-cytotoxic concentrations. When combined within a sol-gel coating, silver nitrate combined with cinnamaldehyde reduced biofilm formation in a drip flow reactor model with a constant flow of artificial urine.

The most promising coating option from this research would therefore be a silver nitrate and cinnamaldehyde impregnated sol-gel coating. It was shown that in combination the active antimicrobial concentrations were at non-cytotoxic concentrations. There was rapid release of silver from the coating, whereas cinnamaldehyde was maintained for longer and in the drip flow reactor model, the formation of biofilm on coated silicon was significantly reduced compared to sol-gel alone.

7. References

Adams, C.S., Antoci, V., Harrison, G., Patal, P., Freeman, T.A., Shapiro, I.M., Parvizi, J., Hickok, N.J., Radin, S. and Ducheyne, P. (2009) 'Controlled release of vancomycin from thin sol-gel films on implant surfaces successfully controls osteomyelitis', *Journal of Orthopaedic Research*, 27(6), pp. 701–709. Available at: https://doi.org/10.1002/JOR.20815.

Alfhili, M.A. and Lee, M.-H.H. (2019) *Triclosan: An update on biochemical and molecular mechanisms*, *Oxidative Medicine and Cellular Longevity*. Available at: https://doi.org/10.1155/2019/1607304.

Allen, M.J., White, G.F. and Morby, A.P. (2006) 'The response of Escherichia coli to exposure to the biocide polyhexamethylene biguanide', *Microbiology*, 152(4), pp. 989–1000. Available at: https://doi.org/10.1099/mic.0.28643-0.

Almalki, M.A. and Varghese, R. (2020) 'Prevalence of catheter associated biofilm producing bacteria and their antibiotic sensitivity pattern', *Journal of King Saud University - Science*, 32(2), pp. 1427–1433. Available at: https://doi.org/10.1016/j.jksus.2019.11.037.

Amalaradjou, M.A.R., Narayanan, A., Baskaran, S.A. and Venkitanarayanan, K. (2010) 'Antibiofilm Effect of Trans-Cinnamaldehyde on Uropathogenic Escherichia coli', *Journal of Urology*, 184(1), pp. 358–363. Available at: https://doi.org/10.1016/j.juro.2010.03.006.

Amalaradjou, M.A.R., Narayanan, A. and Venkitanarayanan, K. (2011) 'Trans-cinnamaldehyde decreases attachment and invasion of uropathogenic Escherichia coli in urinary tract epithelial cells by modulating virulence gene expression', *Journal of Urology* [Preprint]. Available at: https://doi.org/10.1016/j.juro.2010.11.078.

Aminu, N., Chan, S.-Y., Khan, N.H. and Toh, S.-M. (2018) 'Concurrent determination of triclosan and flurbiprofen by high-performance liquid chromatography in simulated saliva and its application in dental nanogel formulation', *Acta Chromatographica*, 30(4), pp. 219–224. Available at: https://doi.org/10.1556/1326.2017.00286.

Andersen, M.J. and Flores-Mireles, A.L. (2020) 'Urinary catheter coating modifications: The race against catheter-associated infections', *Coatings*. Available at: https://doi.org/10.3390/coatings10010023.

Anjum, S., Singh, S., Benedicte, L., Roger, P., Panigrahi, M. and Gupta, B. (2018) 'Biomodification Strategies for the Development of Antimicrobial Urinary Catheters: Overview and Advances', *Global Challenges*, 2(1), pp. 170006-n/a. Available at: https://doi.org/10.1002/gch2.201700068.

Arciola, C.R., Campoccia, D. and Montanaro, L. (2018) 'Implant infections: adhesion, biofilm formation and immune evasion', *Nature Reviews Microbiology 2018 16:7*, 16(7), pp. 397–409. Available at: https://doi.org/10.1038/s41579-018-0019-y.

Ayyash, M., Shehabi, A.A., Mahmoud, N.N. and Al-Bakri, A.G. (2019) 'Antibiofilm properties of triclosan with EDTA or cranberry as Foley Catheter lock solutions', *Journal of Applied Microbiology*, 127(6), pp. 1876–1888. Available at: https://doi.org/10.1111/jam.14439.

Bai, X. and Acharya, K. (2016) 'Removal of trimethoprim, sulfamethoxazole, and triclosan by the green alga Nannochloris sp.', *Journal of Hazardous Materials*, 315, pp. 70–75. Available at: https://doi.org/10.1016/j.jhazmat.2016.04.067.

Barak, R. and Eisenbach, M. (2001) 'Acetylation of the response regulator, CheY, is involved in bacterial chemotaxis', *Molecular Microbiology*, 40(3). Available at: https://doi.org/10.1046/j.1365-2958.2001.02425.x.

Baveja, J.K., Willcox, M.D.P., Hume, E.B.H., Kumar, N., Odell, R. and Poole-Warren, L.A. (2004) 'Furanones as potential anti-bacterial coatings on biomaterials', *Biomaterials*, 25(20), pp. 5003–5012. Available at: https://doi.org/10.1016/J.BIOMATERIALS.2004.02.051.

Beattie, M. and Taylor, J. (2011) 'Silver alloy vs. uncoated urinary catheters: A systematic review of the literature', *Journal of Clinical Nursing*, 20(15–16), pp. 2098–2108. Available at: https://doi.org/10.1111/J.1365-2702.2010.03561.X.

Bedoux, G., Roig, B., Thomas, O., Dupont, V. and Le Bot, B. (2011) 'Occurrence and toxicity of antimicrobial triclosan and by-products in the environment', *Environmental*

Science and Pollution Research 2011 19:4, 19(4), pp. 1044–1065. Available at: https://doi.org/10.1007/S11356-011-0632-Z.

Bhattacharjee, B., Ghosh, S., Patra, D. and Haldar, J. (2022) 'Advancements in release-active antimicrobial biomaterials: A journey from release to relief', *Wiley Interdisciplinary Reviews: Nanomedicine and Nanobiotechnology*, 14(1). Available at: https://doi.org/10.1002/WNAN.1745.

Bjarnsholt, T. (2013) 'The role of bacterial biofilms in chronic infections', *APMIS*, 121(136), pp. 1–58. Available at: https://doi.org/10.1111/apm.12099.

Blair, J.M.A., Webber, M.A., Baylay, A.J., Ogbolu, D.O. and Piddock, L.J.V. (2015) 'Molecular mechanisms of antibiotic resistance', *Nature Reviews Microbiology*. Nature Publishing Group, pp. 42–51. Available at: https://doi.org/10.1038/nrmicro3380.

van der Borght, K., Tourny, A., Bagdziunas, R., Thas, O., Nazarov, M., Turner, H., Verbist, B. and Ceulemans, H. (2017) 'BIGL: Biochemically Intuitive Generalized Loewe null model for prediction of the expected combined effect compatible with partial agonism and antagonism OPEN', 7, p. 17935. Available at: https://doi.org/10.1038/s41598-017-18068-5.

Brackman, G., Celen, S., Hillaert, U., van Calenbergh, S., Cos, P., Maes, L., Nelis, H.J. and Coenye, T. (2011) 'Structure-activity relationship of cinnamaldehyde analogs as inhibitors of AI-2 based quorum sensing and their effect on virulence of Vibrio spp', *PLoS ONE*, 6(1). Available at: https://doi.org/10.1371/journal.pone.0016084.

Brackman, G. and Coenye, T. (2015) 'Quorum sensing inhibitors as anti-biofilm agents.', *Current pharmaceutical design*, 21(1), pp. 5–11. Available at: https://doi.org/10.2174/1381612820666140905114627.

Brackman, G., Defoirdt, T., Miyamoto, C., Bossier, P., van Calenbergh, S., Nelis, H. and Coenye, T. (2008) 'Cinnamaldehyde and cinnamaldehyde derivatives reduce virulence in Vibrio spp. by decreasing the DNA-binding activity of the quorum sensing response regulator LuxR', *BMC Microbiology*, 8(1), p. 149. Available at: https://doi.org/10.1186/1471-2180-8-149.

Bragg, P.D. and Rainnie, D.J. (1974) 'The effect of silver ions on the respiratory chain of Escherichia coli', *Canadian Journal of Microbiology*, 20(6), pp. 883–889. Available at: https://doi.org/10.1139/m74-135.

Brinker, C, J. and Scherer, George, W. (1990) *Sol-Gel Science: The Physics and Chemistry of Sol-Gel Processing*. 1st edn. London: Academic Press.

Brinker, C.J., Hurd, A.J., Schunk, P.R., Frye, G.C. and Ashley, C.S. (1992) 'Review of sol-gel thin film formation', *Journal of Non-Crystalline Solids*, pp. 424–436. Available at: https://doi.org/10.1016/S0022-3093(05)80653-2.

Brooks, T. and Keevil, C.W. (1997) 'A simple artificial urine for the growth of urinary pathogens', *Letters in Applied Microbiology*, 24(3), pp. 203–206. Available at: https://doi.org/10.1046/j.1472-765X.1997.00378.x.

Buhmann, M.T., Stiefel, P., Maniura-Weber, K. and Ren, Q. (2016) 'In Vitro Biofilm Models for Device-Related Infections', *Trends in Biotechnology*. Elsevier Ltd, pp. 945–948. Available at: https://doi.org/10.1016/j.tibtech.2016.05.016.

Calafat, A.M., Ye, X., Wong, L.Y., Reidy, J.A. and Needham, L.L. (2008) 'Urinary concentrations of triclosan in the U.S. population: 2003-2004', *Environmental Health Perspectives*, 116(3), pp. 303–307. Available at: https://doi.org/10.1289/ehp.10768.

Camps-Font, O., Figueiredo, R., Valmaseda-Castellón, E. and Gay-Escoda, C. (2015) "Postoperative infections after dental implant placement: Prevalence, clinical features, and treatment," *Implant Dentistry*, 24(6), pp. 713–719. Available at: https://doi.org/10.1097/ID.0000000000000325.

Capper-Parkin, K.L., Nichol, T., Smith, T.J., Lacey, M.M. and Forbes, S. (2023) 'Antimicrobial and cytotoxic synergism of biocides and quorum-sensing inhibitors against uropathogenic Escherichia coli', *Journal of Hospital Infection*, 134, pp. 138–146. Available at: https://doi.org/10.1016/j.jhin.2023.02.004.

Ceri, H., Olson, M.E., Stremick, C., Read, R.R., Morck, D. and Buret, A. (1999) 'The Calgary Biofilm Device: New Technology for Rapid Determination of Antibiotic Susceptibilities of Bacterial Biofilms', *Journal of Clinical Microbiology*, 37(6), p. 1771. Available at: https://doi.org/10.1128/jcm.37.6.1771-1776.1999.

Chanabodeechalermrung, B., Chaiwarit, T., Sommano, S.R., Rachtanapun, P., Kantrong, N., Chittasupho, C. and Jantrawut, P. (2022) 'Dual Crosslinked Ion-Based Bacterial Cellulose Composite Hydrogel Containing Polyhexamethylene Biguanide', *Membranes 2022, Vol. 12, Page 825*, 12(9), p. 825. Available at: https://doi.org/10.3390/MEMBRANES12090825.

Chang, C., Zhang, A.Q., Kagan, D.B., Liu, H. and Hutnik, C.M.L. (2015) 'Mechanisms of benzalkonium chloride toxicity in a human trabecular meshwork cell line and the protective role of preservative-free tafluprost', *Clinical & Experimental Ophthalmology*, 43(2), pp. 164–172. Available at: https://doi.org/10.1111/CEO.12390.

Chen, H., Hu, X., Chen, E., Wu, S., McClements, D.J., Liu, S., Li, B. and Li, Y. (2016) 'Preparation, characterization, and properties of chitosan films with cinnamaldehyde nanoemulsions', *Food Hydrocolloids*, 61, pp. 662–671. Available at: https://doi.org/10.1016/J.FOODHYD.2016.06.034.

Chen, X., Ma, X., Pan, Y., Ji, R., Gu, Xueyuan, Luo, S., Bao, L. and Gu, Xuanning (2020) 'Dissipation, transformation and accumulation of triclosan in soil-earthworm system and effects of biosolids application', *Science of the Total Environment*, 712, p. 136563. Available at: https://doi.org/10.1016/j.scitotenv.2020.136563.

Chindera, K., Mahato, M., Kumar Sharma, A., Horsley, H., Kloc-Muniak, K., Kamaruzzaman, N.F., Kumar, S., McFarlane, A., Stach, J., Bentin, T. and Good, L. (2016) 'The antimicrobial polymer PHMB enters cells and selectively condenses bacterial chromosomes', *Scientific Reports*, 6. Available at: https://doi.org/10.1038/srep23121.

Choi, K.H. and Schweizer, H.P. (2006) 'mini-Tn7 insertion in bacteria with single attTn7 sites: example Pseudomonas aeruginosa', *Nature protocols*, 1(1), pp. 153–161. Available at: https://doi.org/10.1038/NPROT.2006.24.

Chou, T.C. and Talalay, P. (1984) 'Quantitative analysis of dose-effect relationships: the combined effects of multiple drugs or enzyme inhibitors', *Advances in Enzyme Regulation*, 22(C), pp. 27–55. Available at: https://doi.org/10.1016/0065-2571(84)90007-4.

Conrad, J.C. and Poling-Skutvik, R. (2018) 'Confined Flow: Consequences and Implications for Bacteria and Biofilms', *Annu. Rev. Chem. Biomol. Eng*, 9, pp. 175–200. Available at: https://doi.org/10.1146/annurev-chembioeng.

Cortese, Y.J., Wagner, V.E., Tierney, M., Devine, D. and Fogarty, A. (2018) 'Review of catheter-associated urinary tract infections and in vitro urinary tract models', *Journal of Healthcare Engineering*. Available at: https://doi.org/10.1155/2018/2986742.

Costerton, J.W., Stewart, P.S. and Greenberg, E.P. (1999) "Bacterial biofilms: A common cause of persistent infections," *Science*, 284(5418), pp. 1318–1322. Available at: https://doi.org/10.1126/SCIENCE.284.5418.1318

Cowley, N.L., Forbes, S., Amézquita, A., McClure, P., Humphreys, G.J. and McBain, A.J. (2015) 'Effects of formulation on microbicide potency and mitigation of the development of bacterial insusceptibility', *Applied and Environmental Microbiology*, 81(20), pp. 7330–7338. Available at: https://doi.org/10.1128/AEM.01985-15.

Curiao, T., Marchi, E., Viti, C., Oggioni, M.R., Baquero, F., Martinez, J.L. and Coque, T.M. (2015) 'Polymorphic variation in susceptibility and metabolism of triclosan-resistant mutants of Escherichia coli and Klebsiella pneumoniae clinical strains obtained after exposure to biocides and antibiotics', *Antimicrobial Agents and Chemotherapy*, 59(6), pp. 3413–3423. Available at: https://doi.org/10.1128/AAC.00187-15.

Dai, S., Gao, Y. and Duan, L. (2023) 'Recent advances in hydrogel coatings for urinary catheters', *Journal of Applied Polymer Science*, 140(14), p. e53701. Available at: https://doi.org/10.1002/app.53701.

Dalhoff, A., Stubbings, W. and Schubert, S. (2011) 'Comparative in vitro activities of the novel antibacterial finafloxacin against selected gram-positive and gram-negative bacteria tested in Mueller-Hinton broth and synthetic urine', *Antimicrobial Agents and Chemotherapy*, 55(4), pp. 1814–1818. Available at: https://doi.org/10.1128/AAC.00886-10.

Danese, P.N., Pratt, L.A., Dove, S.L. and Kolter, R. (2000) 'The outer membrane protein, Antigen 43, mediates cell-to-cell interactions within Escherichia coli biofilms', *Molecular Microbiology*, 37(2), pp. 424–432. Available at: https://doi.org/10.1046/j.1365-2958.2000.02008.x.

Debbasch, C., Rat, P., Warnet, J.-M., De Saint Jean, M., Baudouin, C. and Pierre-Jean, P. (2000) 'Evaluation of the Toxicity of Benzalkonium Chloride on the Ocular Surface', *Journal of Toxicology: Cutaneous and Ocular Toxicology*, 19(2–3), pp. 105–115. Available at: https://doi.org/10.3109/15569520009051506.

Desai, D.G., Liao, K.S., Cevallos, M.E. and Trautner, B.W. (2010) 'Silver or nitrofurazone impregnation of urinary catheters has a minimal effect on uropathogen adherence', *Journal of Urology*, 184(6), pp. 2565–2571. Available at: https://doi.org/10.1016/j.juro.2010.07.036.

Deutschle, T., Porkert, U., Reiter, R., Keck, T. and Riechelmann, H. (2006) 'In vitro genotoxicity and cytotoxicity of benzalkonium chloride', *Toxicology in Vitro*, 20(8), pp. 1472–1477. Available at: https://doi.org/10.1016/J.TIV.2006.07.006.

Domadia, P., Swarup, S., Bhunia, A., Sivaraman, J. and Dasgupta, D. (2007) 'Inhibition of bacterial cell division protein FtsZ by cinnamaldehyde', *Biochemical Pharmacology*, 74(6), pp. 831–840. Available at: https://doi.org/10.1016/j.bcp.2007.06.029.

Doyle, A.A. and Stephens, J.C. (2019) 'A review of cinnamaldehyde and its derivatives as antibacterial agents', *Fitoterapia*. Elsevier B.V., p. 104405. Available at: https://doi.org/10.1016/j.fitote.2019.104405.

Dubern, J.-F., Hook, A.L., Carabelli, A.M., Chang, C.-Y., Lewis-Lloyd, C.A., Luckett, J.C., Burroughs, L., Dundas, A.A., Humes, D.J., Irvine, D.J., Alexander, M.R. and Williams, P. (2023) 'Discovery of a polymer resistant to bacterial biofilm, swarming, and encrustation', *Science Advances*, 9(4). Available at: https://doi.org/10.1126/SCIADV.ADD7474.

El-Mahdy, R., Mahmoud, R. and Shrief, R. (2021) 'Characterization of E. coli phylogroups causing catheter-associated urinary tract infection', *Infection and Drug Resistance*, 14, pp. 3183–3193. Available at: https://doi.org/10.2147/IDR.S325770.

European Committee for Antimicrobial Susceptibility Testing (EUCAST) of the European Society of Clinical Microbiology and Infectious Diseases (ESCMID) (2000) 'Terminology relating to methods for the determination of susceptibility of bacteria to antimicrobial agents', *Clinical Microbiology and Infection*. Blackwell Publishing Ltd., pp. 503–508. Available at: https://doi.org/10.1046/j.1469-0691.2000.00149.x.

Farhat, N., Hammes, F., Prest, E. and Vrouwenvelder, J. (2018) 'A uniform bacterial growth potential assay for different water types', *Water Research*, 142, pp. 227–235. Available at: https://doi.org/10.1016/j.watres.2018.06.010.

Feneley, R.C.L., Hopley, I.B. and Wells, P.N.T. (2015) 'Urinary catheters: History, current status, adverse events and research agenda', *Journal of Medical Engineering and Technology*, 39(8), pp. 459–470. Available at: https://doi.org/10.3109/03091902.2015.1085600.

Feng, Q.L., Wu, J., Chen, G.Q., Cui, F.Z., Kim, T.N. and Kim, J.O. (2000) 'A mechanistic study of the antibacterial effect of silver ions onEscherichia coli andStaphylococcus aureus', *Journal of Biomedical Materials Research*, 52(4), pp. 662–668. Available at: https://doi.org/10.1002/1097-4636(20001215)52:4<662::AID-JBM10>3.0.CO;2-3.

Ferrières, L., Hancock, V. and Klemm, P. (2007) 'Specific selection for virulent urinary tract infectious Escherichia coli strains during catheter-associated biofilm formation', *FEMS Immunology & Medical Microbiology*, 51(1), pp. 212–219. Available at: https://doi.org/10.1111/j.1574-695X.2007.00296.x.

Figueira, R.B. (2020) 'Hybrid Sol–gel Coatings for Corrosion Mitigation: A Critical Review', *Polymers 2020, Vol. 12, Page 689*, 12(3), p. 689. Available at: https://doi.org/10.3390/POLYM12030689.

Flores-Mireles, A.L., Walker, J.N., Caparon, M. and Hultgren, S.J. (2015) 'Urinary tract infections: Epidemiology, mechanisms of infection and treatment options', *Nature Reviews Microbiology*, 13(5), pp. 269–284. Available at: https://doi.org/10.1038/nrmicro3432.

Foksowicz-Flaczyk, J., Walentowska, J., Przybylak, M. and Maciejewski, H. (2016) 'Multifunctional durable properties of textile materials modified by biocidal agents in the sol-gel process', *Surface and Coatings Technology*, 304, pp. 160–166. Available at: https://doi.org/10.1016/J.SURFCOAT.2016.06.062.

Fontoura, J.C., Viezzer, C., dos Santos, F.G., Ligabue, R.A., Weinlich, R., Puga, R.D., Antonow, D., Severino, P. and Bonorino, C. (2020) 'Comparison of 2D and 3D cell culture models for cell growth, gene expression and drug resistance', *Materials Science and*

Engineering: C, 107, p. 110264. Available at: https://doi.org/10.1016/J.MSEC.2019.110264.

Forbes, S., Latimer, J., Bazaid, A. and McBain, A.J. (2015) 'Altered Competitive Fitness, Antimicrobial Susceptibility, and Cellular Morphology in a Triclosan-Induced Small-Colony Variant of Staphylococcus aureus', *Antimicrobial agents and chemotherapy*, 59(8), pp. 4809–4816. Available at: https://doi.org/10.1128/AAC.00352-15.

Forbes, S., Morgan, N., Humphreys, G.J., Amézquita, A., Mistry, H. and McBain, A.J. (2019) 'Loss of function in Escherichia coli exposed to environmentally relevant concentrations of benzalkonium chloride', *Applied and Environmental Microbiology*, 85(4). Available at: https://doi.org/10.1128/AEM.02417-18.

Forde, B.M., Ben Zakour, N.L., Stanton-Cook, M., Phan, M.D., Totsika, M., Peters, K.M., Chan, K.G., Schembri, M.A., Upton, M. and Beatson, S.A. (2014) 'The complete genome sequence of escherichia coli EC958: A high quality reference sequence for the globally disseminated multidrug resistant E. coli O25b:H4-ST131 clone', *PLoS ONE*. Edited by U. Dobrindt, 9(8), p. e104400. Available at: https://doi.org/10.1371/journal.pone.0104400.

Fratini, F., Mancini, S., Turchi, B., Friscia, E., Pistelli, L., Giusti, G. and Cerri, D. (2017) 'A novel interpretation of the Fractional Inhibitory Concentration Index: The case Origanum vulgare L. and Leptospermum scoparium J. R. et G. Forst essential oils against Staphylococcus aureus strains', *Microbiological Research*, 195, pp. 11–17. Available at: https://doi.org/10.1016/j.micres.2016.11.005.

Friedrich, T. (1998) *The NADH:ubiquinone oxidoreductase complex I from Escherichia coli*, *Biochimica et Biophysica Acta*.

Fuhrman, L.K., Wanken, A., Nickerson, K.W. and Conway, T. (1998) 'Rapid accumulation of intracellular 2-keto-3-deoxy-6-phosphogluconate in an Entner-Doudoroff aldolase mutant results in bacteriostasis', *FEMS Microbiology Letters*, 159(2), pp. 261–266. Available at: https://doi.org/10.1111/j.1574-6968.1998.tb12870.x.

Furr, J.R., Russell, A.D., Turner, T.D. and Andrews, A. (1994) 'Antibacterial activity of Actisorb Plus, Actisorb and silver nitrate', *Journal of Hospital Infection*, 27(3), pp. 201–208. Available at: https://doi.org/10.1016/0195-6701(94)90128-7.

Gil-Perotin, S., Ramirez, P., Marti, V., Sahuquillo, J.M., Gonzalez, E., Calleja, I., Menendez, R. and Bonastre, J. (2012) "Implications of endotracheal tube biofilm in ventilator-associated pneumonia response: A state of concept," *Critical Care*, 16(3), pp. 1–9. Available at: https://doi.org/10.1186/CC11357/FIGURES/3.

Gilbert, P. and Moore, L.E. (2005) 'Cationic antiseptics: Diversity of action under a common epithet', *Journal of Applied Microbiology*, pp. 703–715. Available at: https://doi.org/10.1111/j.1365-2672.2005.02664.x.

Gominet, M., Compain, F., Beloin, C. and Lebeaux, D. (2017) "Central venous catheters and biofilms: where do we stand in 2017?," *APMIS*, 125(4), pp. 365–375. Available at: https://doi.org/10.1111/APM.12665.

González Barrios, A.F., Zuo, R., Hashimoto, Y., Yang, L., Bentley, W.E. and Wood, T.K. (2006) 'Autoinducer 2 controls biofilm formation in Escherichia coli through a novel motility quorum-sensing regulator (MqsR, B3022)', *Journal of Bacteriology*, 188(1), pp. 305–316. Available at: https://doi.org/10.1128/JB.188.1.305-316.2006.

Greulich, C., Braun, D., Peetsch, A., Diendorf, J., Siebers, B., Epple, M. and Köller, M. (2012) 'The toxic effect of silver ions and silver nanoparticles towards bacteria and human cells occurs in the same concentration range', *RSC Advances*, 2(17), p. 6981. Available at: https://doi.org/10.1039/c2ra20684f.

Guidony, N.S., Scaini, J.L.R., Oliveira, M.W.B., Machado, K.S., Bastos, C., Escarrone, A.L. and Souza, M.M. (2021) 'ABC proteins activity and cytotoxicity in zebrafish hepatocytes exposed to triclosan', *Environmental Pollution*, 271, p. 116368. Available at: https://doi.org/10.1016/J.ENVPOL.2020.116368.

Guo, J.-L., Li, B.-Z., Chen, W.-M., Sun, P.-H. and Wang, Y. (2009) 'Synthesis of Substituted 1H-Pyrrol-2(5H)-ones and 2(5H)-Furanones as Inhibitors of P. aeruginosa Biofilm', *Letters in Drug Design & Discovery*, 6(2), pp. 107–113. Available at: https://doi.org/10.2174/157018009787582642.

Guo, M., Gamby, S., Zheng, Y. and Sintim, H. (2013) 'Small Molecule Inhibitors of AI-2 Signaling in Bacteria: State-of-the-Art and Future Perspectives for Anti-Quorum Sensing Agents', *International Journal of Molecular Sciences*, 14(9), pp. 17694–17728. Available at: https://doi.org/10.3390/ijms140917694.

Hall, M.J., Middleton, R.F. and Westmacott, D. (1983) 'The fractional inhibitory concentration (FIC) index as a measure of synergy', *Journal of Antimicrobial Chemotherapy*, 11(5), pp. 427–433. Available at: https://doi.org/10.1093/jac/11.5.427.

Haufe, H., Muschter, K., Siegert, J. and Böttcher, H. (2008) 'Bioactive textiles by sol-gel immobilised natural active agents', *Journal of Sol-Gel Science and Technology*, 45(1), pp. 97–101. Available at: https://doi.org/10.1007/S10971-007-1636-5/FIGURES/3.

Hayden, J.D. and Ades, S.E. (2008) 'The Extracytoplasmic Stress Factor, σE, Is Required to Maintain Cell Envelope Integrity in Escherichia coli', *PLoS ONE*. Edited by S. Sandler, 3(2), p. e1573. Available at: https://doi.org/10.1371/journal.pone.0001573.

Hegde, M., Englert, D.L., Schrock, S., Cohn, W.B., Vogt, C., Wood, T.K., Manson, M.D. and Jayaraman, A. (2011) 'Chemotaxis to the quorum-sensing signal AI-2 requires the Tsr chemoreceptor and the periplasmic LsrB AI-2-binding protein', *Journal of Bacteriology*, 193(3), pp. 768–773. Available at: https://doi.org/10.1128/JB.01196-10.

Henly, E.L. (2019) *Antimicrobial Adaptation in Uropathogenic Escherichia coli*. Thesis. Sheffield Hallam University.

Henly, E.L., Dowling, J.A.R., Maingay, J.B., Lacey, M.M., Smith, T.J. and Forbes, S. (2019) 'Biocide Exposure Induces Changes in Susceptibility, Pathogenicity, and Biofilm Formation in Uropathogenic Escherichia coli', *Antimicrobial agents and chemotherapy*, 63(3). Available at: https://doi.org/10.1128/AAC.01892-18.

Henly, E.L., Norris, K., Rawson, K., Zoulias, N., Jaques, L., Chirila, P.G., Parkin, K.L., Kadirvel, M., Whiteoak, C., Smith, T.J., Lacey, M.M. and Forbes, S. (2021) 'Impact of long-term quorum sensing inhibition on uropathogenic Escherichia coli', *Journal of Antimicrobial Chemotherapy*, p. dkaa517. Available at: https://doi.org/10.1093/jac/dkaa517.

Hentzer, M., Riedel, K., Rasmussen, T.B., Heydorn, A., Andersen, J.B., Parsek, M.R., Rice, S.A., Eberl, L., Molin, S., Høiby, N., Kjelleberg, S. and Givskov, M. (2002) 'Inhibition of quorum sensing in Pseudomonas aeruginosa biofilm bacteria by a halogenated furanone compound', *Microbiology* [Preprint]. Available at: https://doi.org/10.1099/00221287-148-1-87.

Høiby, N., Bjarnsholt, T., Givskov, M., Molin, S. and Ciofu, O. (2010) 'Antibiotic resistance of bacterial biofilms', *International Journal of Antimicrobial Agents*. Elsevier, pp. 322–332. Available at: https://doi.org/10.1016/j.ijantimicag.2009.12.011.

Hollenbeak, C.S. and Schilling, A.L. (2018) 'The attributable cost of catheter-associated urinary tract infections in the United States: A systematic review', *American Journal of Infection Control*, 46(7), pp. 751–757. Available at: https://doi.org/10.1016/j.ajic.2018.01.015.

Houdt, R., Aertsen, A., Moons, P., Vanoirbeek, K. and Michiels, C.W. (2006) '*N* -acyl-l-homoserine lactone signal interception by *Escherichia coli*', *FEMS Microbiology Letters*, 256(1), pp. 83–89. Available at: https://doi.org/10.1111/j.1574-6968.2006.00103.x.

International Standards Organisation (2009) 'ISO 10993-5 Biological evaluation of medical devices-16:45:28'. International Standards Organisation.

Jacobsen, S.M., Stickler, D.J., Mobley, H.L.T. and Shirtliff, M.E. (2008) 'Complicated Catheter-Associated Urinary Tract Infections Due to Escherichia coli and Proteus mirabilis', *Clinical Microbiology Reviews*, 21(1), pp. 26–59. Available at: https://doi.org/10.1128/CMR.00019-07.

Jaiswal, S., McHale, P. and Duffy, B. (2012) 'Preparation and rapid analysis of antibacterial silver, copper and zinc doped sol–gel surfaces', *Colloids and Surfaces B: Biointerfaces*, 94, pp. 170–176. Available at: https://doi.org/10.1016/j.colsurfb.2012.01.035.

Janssens, J.C.A.A., Steenackers, H., Robijns, S., Gellens, E., Levin, J., Zhao, H., Hermans, K., De Coster, D., Verhoeven, T.L., Marchal, K., Vanderleyden, J., De Vos, D.E. and De Keersmaecker, S.C.J.J. (2008) 'Brominated Furanones Inhibit Biofilm Formation by Salmonella enterica Serovar Typhimurium', *Applied and Environmental Microbiology*, 74(21), pp. 6639–6648. Available at: https://doi.org/10.1128/AEM.01262-08.

Jia, Y.W., Huang, Z., Hu, L.X., Liu, S., Li, H.X., Li, J.L., Chen, C.E., Xu, X.R., Zhao, J.L. and Ying, G.G. (2020) 'Occurrence and mass loads of biocides in plastic debris from the Pearl River system, South China', *Chemosphere*, 246, p. 125771. Available at: https://doi.org/10.1016/J.CHEMOSPHERE.2019.125771.

Johnson, J.R., Johnston, B. and Kuskowski, M.A. (2012) 'In vitro comparison of nitrofurazone- and silver alloy-coated foley catheters for contact-dependent and diffusible inhibition of urinary tract infection-associated microorganisms', *Antimicrobial Agents and Chemotherapy*, 56(9), pp. 4969–4972. Available at: https://doi.org/10.1128/AAC.00733-12.

Johnson, J.R., Kuskowski, M.A. and Wilt, T.J. (2006) 'Systematic Review: Antimicrobial Urinary Catheters To Prevent Catheter-Associated Urinary Tract Infection in Hospitalized Patients', *Annals of Internal Medicine*, 144(2), p. 116. Available at: https://doi.org/10.7326/0003-4819-144-2-200601170-00009.

Jones, G.L., Muller, C.T., O'Reilly, M. and Stickler, D.J. (2006) 'Effect of triclosan on the development of bacterial biofilms by urinary tract pathogens on urinary catheters', *Journal of Antimicrobial Chemotherapy*, 57(2), pp. 266–272. Available at: https://doi.org/10.1093/jac/dki447.

Jones, R.W. (1989) *Fundamental Principles of Sol-Gel Technology*. London.

Kakkanat, A., Phan, M.D., Lo, A.W., Beatson, S.A. and Schembri, M.A. (2017) 'Novel genes associated with enhanced motility of Escherichia coli', *PLoS ONE*, 12(5). Available at: https://doi.org/10.1371/journal.pone.0176290.

Kampf, G. (2018) 'Biocidal agents used for disinfection can enhance antibiotic resistance in gram-negative species', *Antibiotics*. Available at: https://doi.org/10.3390/antibiotics7040110.

Kanjee, U., Ogata, K. and Houry, W.A. (2012) 'Direct binding targets of the stringent response alarmone (p)ppGpp', *Molecular microbiology*, 85(6), pp. 1029–1043. Available at: https://doi.org/10.1111/J.1365-2958.2012.08177.X.

Karchmer, T.B., Giannetta, E.T., Muto, C.A., Strain, B.A. and Farr, B.M. (2000) 'A Randomized Crossover Study of Silver-Coated Urinary Catheters in Hospitalized Patients', *Archives of Internal Medicine*, 160(21), pp. 3294–3298. Available at: https://doi.org/10.1001/ARCHINTE.160.21.3294.

Karczewska, M., Strzelecki, P., Bogucka, K., Potrykus, K., Szalewska-Pałasz, A. and Nowicki, D. (2023) 'Increased Levels of (p)ppGpp Correlate with Virulence and Biofilm Formation, but Not with Growth, in Strains of Uropathogenic Escherichia coli',

International Journal of Molecular Sciences, 24(4), p. 3315. Available at: https://doi.org/10.3390/IJMS24043315/S1.

Keren, I., Shah, D., Spoering, A., Kaldalu, N. and Lewis, K. (2004) 'Specialized persister cells and the mechanism of multidrug tolerance in Escherichia coli', *Journal of Bacteriology*, 186(24), pp. 8172–8180. Available at: https://doi.org/10.1128/JB.186.24.8172-8180.2004/ASSET/496D919A-39A9-42B5-8EA6-6F4EC1F43784/ASSETS/GRAPHIC/ZJB0240442760006.JPEG.

Kester, J.C. and Fortune, S.M. (2014) 'Persisters and beyond: Mechanisms of phenotypic drug resistance and drug tolerance in bacteria', *Critical Reviews in Biochemistry and Molecular Biology*, 49(2), pp. 91–101. Available at: https://doi.org/10.3109/10409238.2013.869543.

Kim, K., Lee, S. and Ryu, C.-M. (2013) 'Interspecific bacterial sensing through airborne signals modulates locomotion and drug resistance', *Nature Communications*, 4(1), p. 1809. Available at: https://doi.org/10.1038/ncomms2789.

Kim, K., Park, H., Yang, W. and Lee, J.H. (2011) 'Urinary concentrations of bisphenol A and triclosan and associations with demographic factors in the Korean population', *Environmental Research*, 111(8), pp. 1280–1285. Available at: https://doi.org/10.1016/j.envres.2011.09.003.

Kim, Y., Nam, N.H., You, Y.J. and Ahn, B.Z. (2002) 'Synthesis and Cytotoxicity of 3,4-Diaryl-2(5H)-furanones', *Bioorganic & Medicinal Chemistry Letters*, 12(4), pp. 719–722. Available at: https://doi.org/10.1016/S0960-894X(01)00831-9.

Kinnear, N., Barnett, D., O'Callaghan, M., Horsell, K., Gani, J. and Hennessey, D. (2020) 'The impact of catheter-based bladder drainage method on urinary tract infection risk in spinal cord injury and neurogenic bladder: A systematic review', *Neurourology and Urodynamics*, 39(2), pp. 854–862. Available at: https://doi.org/10.1002/NAU.24253.

Kloskowski, T., Szeliski, K., Fekner, Z., Rasmus, M., Dąbrowski, P., Wolska, A., Siedlecka, N., Adamowicz, J., Drewa, T. and Pokrywczyńska, M. (2021) 'Ciprofloxacin and levofloxacin as potential drugs in genitourinary cancer treatment—the effect of dose–response on 2D and 3D cell cultures', *International Journal of Molecular Sciences*, 22(21), p. 11970. Available at: https://doi.org/10.3390/IJMS222111970/S1.

Koc, H., Kilicay, E., Karahaliloglu, Z., Hazer, B. and Denkbas, E.B. (2021) 'Prevention of urinary infection through the incorporation of silver–ricinoleic acid–polystyrene nanoparticles on the catheter surface', *Journal of Biomaterials Applications*, 36(3), pp. 385–405. Available at: https://doi.org/10.1177/0885328220983552/ASSET/IMAGES/LARGE/10.1177_0885328220983552-FIG2.JPEG.

Kot, B., Wicha, J., Piechota, M., Wolska, K. and Gruzewska, A. (2015) 'Antibiofilm activity of trans-cinnamaldehyde, p-coumaric, and ferulic acids on uropathogenic Escherichia coli', *TURKISH JOURNAL OF MEDICAL SCIENCES*, 45, pp. 919–924. Available at: https://doi.org/10.3906/sag-1406-112.

Kuehl, R., Al-Bataineh, S., Gordon, O., Luginbuehl, R., Otto, M., Textor, M. and Landmann, R. (2009) 'Furanone at Subinhibitory Concentrations Enhances Staphylococcal Biofilm Formation by luxS Repression', *Antimicrobial Agents and Chemotherapy*, 53(10), pp. 4159–4166. Available at: https://doi.org/10.1128/AAC.01704-08.

Laganenka, L., Colin, R. and Sourjik, V. (2016) 'Chemotaxis towards autoinducer 2 mediates autoaggregation in Escherichia coli', *Nature Communications*, 7. Available at: https://doi.org/10.1038/ncomms12984.

Lam, T.B.L., Omar, M.I., Fisher, E., Gillies, K. and MacLennan, S. (2014) 'Types of indwelling urethral catheters for short-term catheterisation in hospitalised adults.', *The Cochrane database of systematic reviews*, 2014(9), p. CD004013. Available at: https://doi.org/10.1002/14651858.CD004013.pub4.

Leif, H., Sled, V.D., Ohnishi, T., Weiss, H. and Friedrich, T. (1995) 'Isolation and Characterization of the Proton-translocating NADH:ubiquinone Oxidoreductase from Escherichia coli', *European Journal of Biochemistry*, 230(2), pp. 538–548. Available at: https://doi.org/10.1111/j.1432-1033.1995.0538h.x.

Letica-Kriegel, A.S., Salmasian, H., Vawdrey, D.K., Youngerman, B.E., Green, R.A., Furuya, E.Y., Calfee, D.P. and Perotte, R. (2019) 'Identifying the risk factors for catheter-associated urinary tract infections: A large cross-sectional study of six hospitals', *BMJ Open*, 9(2). Available at: https://doi.org/10.1136/bmjopen-2018-022137.

Levy, S.B., McMurry, L.M. and Oethinger, M. (1998) 'Triclosan targets lipid synthesis', *Nature*, 394(6693), pp. 531–532. Available at: https://doi.org/10.1038/28970.

Li, F., Song, M., Xu, L., Deng, B., Zhu, S. and Li, X. (2019) 'Risk factors for catheter-associated urinary tract infection among hospitalized patients: A systematic review and meta-analysis of observational studies', *Journal of Advanced Nursing*. John Wiley & Sons, Ltd, pp. 517–527. Available at: https://doi.org/10.1111/jan.13863.

Li, J., Attila, C., Wang, L., Wood, T.K., Valdes, J.J. and Bentley, W.E. (2007) 'Quorum sensing in Escherichia coli is signaled by AI-2/LsrR: Effects on small RNA and biofilm architecture', *Journal of Bacteriology*, 189(16), pp. 6011–6020. Available at: https://doi.org/10.1128/JB.00014-07.

Li, W., Seal, S., Megan, E., Ramsdell, J., Scammon, K., Lelong, G., Lachal, L. and Richardson, K.A. (2003) 'Physical and optical properties of sol-gel nano-silver doped silica film on glass substrate as a function of heat-treatment temperature', *Journal of Applied Physics*, 93(12), pp. 9553–9561. Available at: https://doi.org/10.1063/1.1571215.

Ligowska-Marzęta, M., Hancock, V., Ingmer, H. and Aarestrup, F.M. (2019) 'Comparison of gene expression profiles of uropathogenic Escherichia Coli CFT073 after prolonged exposure to subinhibitory concentrations of different biocides', *Antibiotics*, 8(4), p. 167. Available at: https://doi.org/10.3390/antibiotics8040167.

Liu, T. and Wu, D. (2012) 'High-performance liquid chromatographic determination of triclosan and triclocarban in cosmetic products', *International Journal of Cosmetic Science*, 34(5), pp. 489–494. Available at: https://doi.org/10.1111/j.1468-2494.2012.00742.x.

Lo, E., Nicolle, L.E., Coffin, S.E., Gould, C., Maragakis, L.L., Meddings, J., Pegues, D.A., Pettis, A.M., Saint, S. and Yokoe, D.S. (2014) 'Strategies to Prevent Catheter-Associated Urinary Tract Infections in Acute Care Hospitals: 2014 Update', *Infection Control & Hospital Epidemiology*, 35(5), pp. 464–479. Available at: https://doi.org/10.1086/675718.

López, D., Vlamakis, H. and Kolter, R. (2010) 'Biofilms.', *Cold Spring Harbor perspectives in biology* [Preprint]. Available at: https://doi.org/10.1101/cshperspect.a000398.

Loveday, H.P., Wilson, J.A., Pratt, R.J., Golsorkhi, M., Tingle, A., Bak, A., Browne, J., Prieto, J. and Wilcox, M. (2014) 'epic3: National Evidence-Based Guidelines for Preventing Healthcare-Associated Infections in NHS Hospitals in England', *Journal of Hospital Infection*, 86(S1), pp. S1–S70. Available at: https://doi.org/10.1016/S0195-6701(13)60012-2.

Lu, J., Wang, Y., Li, J., Mao, L., Nguyen, S.H., Duarte, T., Coin, L., Bond, P., Yuan, Z. and Guo, J. (2018) 'Triclosan at environmentally relevant concentrations promotes horizontal transfer of multidrug resistance genes within and across bacterial genera', *Environment International*, pp. 1217–1226. Available at: https://doi.org/10.1016/J.ENVINT.2018.10.040.

Majeed, A., Sagar, F., Latif, A., Hassan, H., Iftikhar, A., Darouiche, R.O. and Mohajer, M. al (2019) 'Does antimicrobial coating and impregnation of urinary catheters prevent catheter-associated urinary tract infection? A review of clinical and preclinical studies', *Expert Review of Medical Devices*, 16(9), pp. 809–820. Available at: https://doi.org/10.1080/17434440.2019.1661774.

Mandakhalikar, K.D., Chua, R.R. and Tambyah, P.A. (2016) 'New Technologies for Prevention of Catheter Associated Urinary Tract Infection', *Current Treatment Options in Infectious Diseases*, 8(1), pp. 24–41. Available at: https://doi.org/10.1007/s40506-016-0069-5.

Manefield, M., Rasmussen, T.B., Henzter, M., Andersen, J.B., Steinberg, P., Kjelleberg, S. and Givskov, M. (2002) 'Halogenated furanones inhibit quorum sensing through accelerated LuxR turnover', *Microbiology*, 148(4), pp. 1119–1127. Available at: https://doi.org/10.1099/00221287-148-4-1119.

Melzer, M. and Welch, C. (2013) 'Outcomes in UK patients with hospital-acquired bacteraemia and the risk of catheter-associated urinary tract infections', *Postgraduate Medical Journal*, 89(1052), pp. 329–334. Available at: https://doi.org/10.1136/postgradmedj-2012-131393.

Menezes, F.G., Corrêa, L., Medina-Pestana, J.O., Aguiar, W.F. and Camargo, L.F.A. (2019) 'A randomized clinical trial comparing Nitrofurazone-coated and uncoated urinary catheters in kidney transplant recipients: Results from a pilot study', *Transplant Infectious Disease*, 21(2). Available at: https://doi.org/10.1111/tid.13031.

Merchel Piovesan Pereira, B., Wang, X. and Tagkopoulos, I. (2020) 'Short- and Long-Term Transcriptomic Responses of Escherichia coli to Biocides: a Systems Analysis', *Applied and environmental microbiology*, 86(14). Available at: https://doi.org/10.1128/AEM.00708-20.

Merchel Piovesan Pereira, B., Wang, X. and Tagkopoulos, I. (2021) 'Biocide-Induced Emergence of Antibiotic Resistance in Escherichia coli', *Frontiers in Microbiology*, 12, p. 335. Available at: https://doi.org/10.3389/FMICB.2021.640923/BIBTEX.

Mi, H., Muruganujan, A., Huang, X., Ebert, D., Mills, C., Guo, X. and Thomas, P.D. (2019) 'Protocol Update for large-scale genome and gene function analysis with the PANTHER classification system (v.14.0)', *Nature Protocols*, 14(3), pp. 703–721. Available at: https://doi.org/10.1038/s41596-019-0128-8.

Minuth, J.N., Musher, D.M. and Thorsteinsson, S.B. (1976) 'Inhibition of the Antibacterial Activity of Gentamicin by Urine', *Journal of Infectious Diseases*, 133(1), pp. 14–21. Available at: https://doi.org/10.1093/infdis/133.1.14.

Mobley, H.L., Green, D.M., Trifillis, A.L., Johnson, D.E., Chippendale, G.R., Lockatell, C. V., Jones, B.D. and Warren, J.W. (1990) 'Pyelonephritogenic Escherichia coli and killing of cultured human renal proximal tubular epithelial cells: Role of hemolysin in some strains', *Infection and Immunity*, 58(5), pp. 1281–1289. Available at: https://doi.org/10.1128/iai.58.5.1281-1289.1990.

Moreira, J.M.R., Teodósio, J.S., Silva, F.C., Simões, M., Melo, L.F. and Mergulhão, F.J. (2013) 'Influence of flow rate variation on the development of Escherichia coli biofilms', *Bioprocess and Biosystems Engineering*, 36(11), pp. 1787–1796. Available at: https://doi.org/10.1007/s00449-013-0954-y.

Murray, C.J., Ikuta, K.S., Sharara, F., Swetschinski, L., Robles Aguilar, G., Gray, A., Han, C., Bisignano, C., Rao, P., Wool, E., Johnson, S.C., Browne, A.J., Chipeta, M.G., Fell, F., Hackett, S., Haines-Woodhouse, G., Kashef Hamadani, B.H., Kumaran, E.A.P., McManigal, B., Agarwal, R., Akech, S., Albertson, S., Amuasi, J., Andrews, J., Aravkin, A., Ashley, E., Bailey, F., Baker, S., Basnyat, B., Bekker, A., Bender, R., Bethou, A., Bielicki, J., Boonkasidecha, S., Bukosia, J., Carvalheiro, C., Castañeda-Orjuela, C., Chansamouth, V., Chaurasia, S., Chiurchiù, S., Chowdhury, F., Cook, A.J., Cooper, B., Cressey, T.R., Criollo-Mora, E., Cunningham, M., Darboe, S., Day, N.P.J., De Luca, M., Dokova, K., Dramowski,

A., Dunachie, S.J., Eckmanns, T., Eibach, D., Emami, A., Feasey, N., Fisher-Pearson, N., Forrest, K., Garrett, D., Gastmeier, P., Giref, A.Z., Greer, R.C., Gupta, V., Haller, S., Haselbeck, A., Hay, S.I., Holm, M., Hopkins, S., Iregbu, K.C., Jacobs, J., Jarovsky, D., Javanmardi, F., Khorana, M., Kissoon, N., Kobeissi, E., Kostyanev, T., Krapp, F., Krumkamp, R., Kumar, A., Kyu, H.H., Lim, C., Limmathurotsakul, D., Loftus, M.J., Lunn, M., Ma, J., Mturi, N., Munera-Huertas, T., Musicha, P., Mussi-Pinhata, M.M., Nakamura, T., Nanavati, R., Nangia, S., Newton, P., Ngoun, C., Novotney, A., Nwakanma, D., Obiero, C.W., Olivas-Martinez, A., Olliaro, P., Ooko, E., Ortiz-Brizuela, E., Peleg, A.Y., Perrone, C., Plakkal, N., Ponce-de-Leon, A., Raad, M., Ramdin, T., Riddell, A., Roberts, T., Robotham, J.V., Roca, A., Rudd, K.E., Russell, N., Schnall, J., Scott, J.A.G., Shivamallappa, M., Sifuentes-Osornio, J., Steenkeste, N., Stewardson, A.J., Stoeva, T., Tasak, N., Thaiprakong, A., Thwaites, G., Turner, C., Turner, P., van Doorn, H.R., Velaphi, S., Vongpradith, A., Vu, H., Walsh, T., Waner, S., Wangrangsimakul, T., Wozniak, T., Zheng, P., Sartorius, B., Lopez, A.D., Stergachis, A., Moore, C., Dolecek, C. and Naghavi, M. (2022) 'Global burden of bacterial antimicrobial resistance in 2019: a systematic analysis', *The Lancet*, 399(10325), pp. 629–655. Available at: https://doi.org/10.1016/S0140-6736(21)02724-0.

Nichol, T., Callaghan, J., Townsend, R., Stockley, I., Hatton, P. V., Le Maitre, C., Smith, T.J. and Akid, R. (2021) 'The antimicrobial activity and biocompatibility of a controlled gentamicin-releasing single-layer sol-gel coating on hydroxyapatite-coated titanium', *Bone and Joint Journal*, 103 B(3), pp. 522–529. Available at: https://doi.org/10.1302/0301-620X.103B3.BJJ-2020-0347.R1.

Nicolle, L.E. (2014) 'Catheter associated urinary tract infections', *Antimicrobial resistance and infection control*, 3(1), p. 23. Available at: https://doi.org/10.1186/2047-2994-3-23.

Niu, C., Afre, S. and Gilbert, E.S. (2006) 'Subinhibitory concentrations of cinnamaldehyde interfere with quorum sensing', *Letters in Applied Microbiology*, 43(5), pp. 489–494. Available at: https://doi.org/10.1111/j.1472-765X.2006.02001.x.

Niu, C. and Gilbert, E.S. (2004) 'Colorimetric method for identifying plant essential oil components that affect biofilm formation and structure', *Applied and Environmental*

Microbiology, 70(12), pp. 6951–6956. Available at: https://doi.org/10.1128/AEM.70.12.6951-6956.2004.

Nord, S., Bylund, G.O., Lövgren, J.M. and Wikström, P.M. (2009) 'The RimP Protein Is Important for Maturation of the 30S Ribosomal Subunit', *Journal of Molecular Biology*, 386(3), pp. 742–753. Available at: https://doi.org/10.1016/j.jmb.2008.12.076.

Norton, J.P. and Mulvey, M.A. (2012) 'Toxin-Antitoxin Systems Are Important for Niche-Specific Colonization and Stress Resistance of Uropathogenic Escherichia coli', *PLoS Pathogens*, 8(10). Available at: https://doi.org/10.1371/journal.ppat.1002954.

O'Malley, L.P., Hassan, K.Z., Brittan, H., Johnson, N. and Collins, A.N. (2006) 'Characterization of the biocide polyhexamethylene biguanide by matrix-assisted laser desorption ionization time-of-flight mass spectrometry', *Journal of Applied Polymer Science*, 102(5), pp. 4928–4936. Available at: https://doi.org/10.1002/app.24915.

Orazi, G. and O'Toole, G.A. (2019) '"It Takes a Village": Mechanisms Underlying Antimicrobial Recalcitrance of Polymicrobial Biofilms', *Journal of Bacteriology*. Edited by W. Margolin, 202(1). Available at: https://doi.org/10.1128/JB.00530-19.

Orhan, G., Bayram, A., Zer, Y. and Balci, I. (2005) 'Synergy Tests by E Test and Checkerboard Methods of Antimicrobial Combinations against Brucella melitensis', *Journal of Clinical Microbiology*, 43(1), p. 140. Available at: https://doi.org/10.1128/JCM.43.1.140-143.2005.

Owens, G.J., Singh, R.K., Foroutan, F., Alqaysi, M., Han, C.-M., Mahapatra, C., Kim, H.-W. and Knowles, J.C. (2016) 'Sol–gel based materials for biomedical applications', *Progress in Materials Science*, 77, pp. 1–79. Available at: https://doi.org/10.1016/j.pmatsci.2015.12.001.

Papenfort, K. and Bassler, B.L. (2016) 'Quorum sensing signal-response systems in Gram-negative bacteria', *Nature Reviews Microbiology*, pp. 576–588. Available at: https://doi.org/10.1038/nrmicro.2016.89.

Parker, V., Giles, M., Graham, L., Suthers, B., Watts, W., O'Brien, T. and Searles, A. (2017) 'Avoiding inappropriate urinary catheter use and catheter-associated urinary tract infection (CAUTI): a pre-post control intervention study', *BMC Health Services Research*, 17(1), p. 314. Available at: https://doi.org/10.1186/s12913-017-2268-2.

Piccoli, A., Fiori, J., Andrisano, V. and Orioli, M. (2002) 'Determination of triclosan in personal health care products by liquid chromatography (HPLC)', *Farmaco*, 57(5), pp. 369–372. Available at: https://doi.org/10.1016/S0014-827X(02)01225-9.

Pratt, L.A. and Kolter, R. (1998) 'Genetic analysis of *Escherichia coli* biofilm formation: roles of flagella, motility, chemotaxis and type I pili', *Molecular Microbiology*, 30(2), pp. 285–293. Available at: https://doi.org/10.1046/j.1365-2958.1998.01061.x.

Ramstedt, M., Ribeiro, I.A.C.C., Bujdakova, H., Mergulhão, F.J.M.M., Jordao, L., Thomsen, P., Alm, M., Burmølle, M., Vladkova, T., Can, F., Reches, M., Riool, M., Barros, A., Reis, R.L., Meaurio, E., Kikhney, J., Moter, A., Zaat, S.A.J.J. and Sjollema, J. (2019) 'Evaluating Efficacy of Antimicrobial and Antifouling Materials for Urinary Tract Medical Devices: Challenges and Recommendations', *Macromolecular Bioscience*, 19(5), p. 1800384. Available at: https://doi.org/10.1002/mabi.201800384.

Rand, K.H., Houck, H.J., Brown, P. and Bennett, D. (1993) 'Reproducibility of the microdilution checkerboard method for antibiotic synergy', *Antimicrobial Agents and Chemotherapy*, 37(3), pp. 613–615. Available at: https://doi.org/10.1128/AAC.37.3.613.

Rasmussen, T.B. and Givskov, M. (2006) "Quorum-sensing inhibitors as anti-pathogenic drugs," *International Journal of Medical Microbiology*, 296(2–3), pp. 149–161. Available at: https://doi.org/10.1016/J.IJMM.2006.02.005.

Rembe, J.D., Fromm-Dornieden, C., Schäfer, N., Böhm, J.K. and Stuermer, E.K. (2016) 'Comparing two polymeric biguanides: Chemical distinction, antiseptic efficacy and cytotoxicity of polyaminopropyl biguanide and polyhexamethylene biguanide', *Journal of Medical Microbiology*, 65(8), pp. 867–876. Available at: https://doi.org/10.1099/jmm.0.000294.

Ren, D., Bedzyk, L.A., Ye, R.W., Thomas, S.M. and Wood, T.K. (2004) 'Differential gene expression shows natural brominated furanones interfere with the autoinducer-2 bacterial signaling system of Escherichia coli', *Biotechnology and Bioengineering*, 88(5), pp. 630–642. Available at: https://doi.org/10.1002/bit.20259.

Ren, D., Sims, J.J. and Wood, T.K. (2001) 'Inhibition of biofilm formation and swarming of escherichia coli by (5Z)-4-bromo-5-(bromomethylene)-3- butyl-2(5H)-furanone',

Environmental Microbiology, 3(11), pp. 731–736. Available at: https://doi.org/10.1046/j.1462-2920.2001.00249.x.

Rivero, P.J. and Goicoechea, J. (2016) 'Sol-gel technology for antimicrobial textiles', in *Antimicrobial Textiles*. Elsevier, pp. 47–72. Available at: https://doi.org/10.1016/B978-0-08-100576-7.00004-3.

Roberts, M.E. and Stewart, P.S. (2005) 'Modelling protection from antimicrobial agents in biofilms through the formation of persister cells', *Microbiology*, 151(1), pp. 75–80. Available at: https://doi.org/10.1099/MIC.0.27385-0/CITE/REFWORKS.

Roilides, E., Simitsopoulou, M., Katragkou, A. and Walsh, T.J. (2015) 'How Biofilms Evade Host Defenses', *Microbiology Spectrum*, 3(3). Available at: https://doi.org/10.1128/MICROBIOLSPEC.MB-0012-2014.

Roy, V., Adams, B.L. and Bentley, W.E. (2011) 'Developing next generation antimicrobials by intercepting AI-2 mediated quorum sensing', *Enzyme and Microbial Technology*, 49(2), pp. 113–123. Available at: https://doi.org/10.1016/j.enzmictec.2011.06.001.

Roy, V., Meyer, M.T., Smith, J.A.I., Gamby, S., Sintim, H.O., Ghodssi, R. and Bentley, W.E. (2013) 'AI-2 analogs and antibiotics: A synergistic approach to reduce bacterial biofilms', *Applied Microbiology and Biotechnology*, 97(6), pp. 2627–2638. Available at: https://doi.org/10.1007/s00253-012-4404-6.

Rubini, D., Varthan, P.V., Jayasankari, S., Vedahari, B.N. and Nithyanand, P. (2020) 'Suppressing the phenotypic virulence factors of Uropathogenic Escherichia coli using marine polysaccharide', *Microbial Pathogenesis* [Preprint]. Available at: https://doi.org/10.1016/j.micpath.2020.103973.

Russell, A.D. (2004) 'Whither triclosan?', *Journal of Antimicrobial Chemotherapy*, 53(5), pp. 693–695. Available at: https://doi.org/10.1093/jac/dkh171.

Sabir, N., Ikram, A., Zaman, G., Satti, L., Gardezi, A., Ahmed, A. and Ahmed, P. (2017) 'Bacterial biofilm-based catheter-associated urinary tract infections: Causative pathogens and antibiotic resistance', *American Journal of Infection Control*, 45(10), pp. 1101–1105. Available at: https://doi.org/10.1016/J.AJIC.2017.05.009.

Saint, S. and Chenoweth, C.E. (2003) 'Biofilms and catheter-associated urinary tract infections', *Infectious Disease Clinics of North America*, 17(2), pp. 411–432. Available at: https://doi.org/10.1016/S0891-5520(03)00011-4.

Santin, M., Motta, A., Denyer, S.P. and Cannas, M. (1999) 'Effect of the urine conditioning film on ureteral stent encrustation and characterization of its protein composition', *Biomaterials*, 20(13), pp. 1245–1251. Available at: https://doi.org/10.1016/S0142-9612(99)00026-5.

Sarigul, N., Korkmaz, F. and Kurultak, İ. (2019) 'A New Artificial Urine Protocol to Better Imitate Human Urine', *Scientific Reports*, 9(1), p. 20159. Available at: https://doi.org/10.1038/s41598-019-56693-4.

Sashital, D.G., Greeman, C.A., Lyumkis, D., Potter, C.S., Carragher, B. and Williamson, J.R. (2014) 'A combined quantitative mass spectrometry and electron microscopy analysis of ribosomal 30S subunit assembly in E. coli', *eLife*, 3. Available at: https://doi.org/10.7554/eLife.04491.

Saulou-Bérion, C., Gonzalez, I., Enjalbert, B., Audinot, J.N., Fourquaux, I., Jamme, F., Cocaign-Bousquet, M., Mercier-Bonin, M. and Girbal, L. (2015) 'Escherichia coli under ionic silver stress: An integrative approach to explore transcriptional, physiological and biochemical responses', *PLoS ONE*, 10(12). Available at: https://doi.org/10.1371/journal.pone.0145748.

Shajani, Z., Sykes, M.T. and Williamson, J.R. (2011) 'Assembly of bacterial ribosomes', *Annual Review of Biochemistry*, 80, pp. 501–526. Available at: https://doi.org/10.1146/annurev-biochem-062608-160432.

Shalom, Y., Perelshtein, I., Perkas, N., Gedanken, A. and Banin, E. (2017) 'Catheters coated with Zn-doped CuO nanoparticles delay the onset of catheter-associated urinary tract infections', *Nano Research*, 10(2), pp. 520–533. Available at: https://doi.org/10.1007/s12274-016-1310-8.

Singha, P., Locklin, J. and Handa, H. (2017) 'A review of the recent advances in antimicrobial coatings for urinary catheters', *Acta Biomaterialia*, 50, pp. 20–40. Available at: https://doi.org/10.1016/j.actbio.2016.11.070.

Smith, Y.C., Grande, K.K., Rasmussen, S.B. and O'Brien, A.D. (2006) 'Novel three-dimensional organoid model for evaluation of the interaction of uropathogenic Escherichia coli with terminally differentiated human urothelial cells', *Infection and Immunity*, 74(1), pp. 750–757. Available at: https://doi.org/10.1128/IAI.74.1.750-757.2006/ASSET/90A9CD50-34F1-456C-B8C5-836A97047DF2/ASSETS/GRAPHIC/ZII0010655890006.JPEG.

Sobota, J.M. and Imlay, J.A. (2011) 'Iron enzyme ribulose-5-phosphate 3-epimerase in Escherichia coli is rapidly damaged by hydrogen peroxide but can be protected by manganese', *Proceedings of the National Academy of Sciences of the United States of America*, 108(13), pp. 5402–5407. Available at: https://doi.org/10.1073/pnas.1100410108.

Sopirala, M.M., Mangino, J.E., Gebreyes, W.A., Biller, B., Bannerman, T., Balada-Llasat, J.-M. and Pancholi, P. (2010) 'Synergy Testing by Etest, Microdilution Checkerboard, and Time-Kill Methods for Pan-Drug-Resistant Acinetobacter baumannii', *Antimicrobial Agents and Chemotherapy*, 54(11), pp. 4678–4683. Available at: https://doi.org/10.1128/AAC.00497-10.

Sowlati-Hashjin, S., Carbone, P. and Karttunen, M. (2020) 'Insights into the Polyhexamethylene Biguanide (PHMB) Mechanism of Action on Bacterial Membrane and DNA: A Molecular Dynamics Study', *J. Phys. Chem*, 2020, pp. 4487–4497. Available at: https://doi.org/10.1021/acs.jpcb.0c02609.

Stewart, M.J., Parikh, S., Xiao, G., Tonge, P.J. and Kisker, C. (1999) 'Structural basis and mechanism of enoyl reductase inhibition by triclosan', *Journal of Molecular Biology*, 290(4), pp. 859–865. Available at: https://doi.org/10.1006/jmbi.1999.2907.

Stewart, P.S. (2002) 'Mechanisms of antibiotic resistance in bacterial biofilms', *International Journal of Medical Microbiology*, 292(2), pp. 107–113. Available at: https://doi.org/10.1078/1438-4221-00196.

Stewart, P.S. and Costerton, J.W. (2001) 'Antibiotic resistance of bacteria in biofilms', *The Lancet*, 358(9276), pp. 135–138. Available at: https://doi.org/10.1016/S0140-6736(01)05321-1.

Stobie, N., Duffy, B., McCormack, D.E., Colreavy, J., Hidalgo, M., McHale, P. and Hinder, S.J. (2008) 'Prevention of Staphylococcus epidermidis biofilm formation using a low-temperature processed silver-doped phenyltriethoxysilane sol–gel coating', *Biomaterials*, 29(8), pp. 963–969. Available at: https://doi.org/10.1016/J.BIOMATERIALS.2007.10.057.

Styles, M.J., Early, S.A., Tucholski, T., West, K.H.J., Ge, Y. and Blackwell, H.E. (2020) 'Chemical Control of Quorum Sensing in E. coli: Identification of Small Molecule Modulators of SdiA and Mechanistic Characterization of a Covalent Inhibitor', *ACS Infectious Diseases*, 6(12), pp. 3092–3103. Available at: https://doi.org/10.1021/ACSINFECDIS.0C00654/ASSET/IMAGES/LARGE/ID0C00654_0007.JPEG.

Takeoka, G.R., Dao, L.T., Wong, R.Y. and Harden, L.A. (2005) 'Identification of benzalkonium chloride in commercial grapefruit seed extracts', *Journal of Agricultural and Food Chemistry*, 53(19), pp. 7630–7636. Available at: https://doi.org/10.1021/jf0514064.

Tartof, S.Y., Solberg, O.D., Manges, A.R. and Riley, L.W. (2005) 'Analysis of a uropathogenic Escherichia coli clonal group by multilocus sequence typing', *Journal of Clinical Microbiology*, 43(12), pp. 5860–5864. Available at: https://doi.org/10.1128/JCM.43.12.5860-5864.2005.

Terlizzi, M.E., Gribaudo, G. and Maffei, M.E. (2017) 'UroPathogenic Escherichia coli (UPEC) Infections: Virulence Factors, Bladder Responses, Antibiotic, and Non-antibiotic Antimicrobial Strategies', *Frontiers in microbiology*, 8, p. 1566. Available at: https://doi.org/10.3389/fmicb.2017.01566.

Totsika, M., Beatson, S.A., Sarkar, S., Phan, M.-D., Petty, N.K., Bachmann, N., Szubert, M., Sidjabat, H.E., Paterson, D.L., Upton, M. and Schembri, M.A. (2011) 'Insights into a Multidrug Resistant Escherichia coli Pathogen of the Globally Disseminated ST131 Lineage: Genome Analysis and Virulence Mechanisms', *PLoS ONE*. Edited by D. Kaushal, 6(10), p. e26578. Available at: https://doi.org/10.1371/journal.pone.0026578.

Trautner, B.W. and Darouiche, R.O. (2004) 'Role of biofilm in catheter-associated urinary tract infection', *AJIC: American Journal of Infection Control*, 32(3), pp. 177–183. Available at: https://doi.org/10.1016/j.ajic.2003.08.005.

Wang, A., Weldrick, P.J., Madden, L.A. and Paunov, V.N. (2021) 'Biofilm-Infected Human Clusteroid Three-Dimensional Coculture Platform to Replace Animal Models in Testing Antimicrobial Nanotechnologies', *ACS Applied Materials and Interfaces*, 13(19), pp. 22182–22194. Available at: https://doi.org/10.1021/ACSAMI.1C02679/ASSET/IMAGES/LARGE/AM1C02679_0013.JPEG.

Wang, D. and Bierwagen, G.P. (2009) 'Sol-gel coatings on metals for corrosion protection', *Progress in Organic Coatings*. Elsevier, pp. 327–338. Available at: https://doi.org/10.1016/j.porgcoat.2008.08.010.

Wang, S., Yin, Y. and Wang, J. (2017) 'Enhanced biodegradation of triclosan by means of gamma irradiation', *Chemosphere*, 167, pp. 406–414. Available at: https://doi.org/10.1016/j.chemosphere.2016.10.028.

Wazait, H.D., Patel, H.R.H., Veer, V., Kelsey, M., Van Der Meulen, J.H.P., Miller, R.A. and Emberton, M. (2003) 'Catheter-associated urinary tract infections: prevalence of uropathogens and pattern of antimicrobial resistance in a UK hospital (1996-2001)', *BJU International*, 91(9), pp. 806–809. Available at: https://doi.org/10.1046/j.1464-410X.2003.04239.x.

Welch, R.A., Burland, V., Plunkett, G., Redford, P., Roesch, P., Rasko, D., Buckles, E.L., Liou, S.-R., Boutin, A., Hackett, J., Stroud, D., Mayhew, G.F., Rose, D.J., Zhou, S., Schwartz, D.C., Perna, N.T., Mobley, H.L.T., Donnenberg, M.S. and Blattner, F.R. (2002) 'Extensive mosaic structure revealed by the complete genome sequence of uropathogenic *Escherichia coli*', *Proceedings of the National Academy of Sciences*, 99(26), pp. 17020–17024. Available at: https://doi.org/10.1073/pnas.252529799.

Werneburg, G.T. (2022) 'Catheter-Associated Urinary Tract Infections: Current Challenges and Future Prospects', *Research and Reports in Urology*. Dove Press, pp. 109–133. Available at: https://doi.org/10.2147/RRU.S273663.

Westfall, C., Flores-Mireles, A.L., Robinson, J.I., Lynch, A.J.L., Hultgren, S., Henderson, J.P. and Levin, P.A. (2019) 'The Widely Used Antimicrobial Triclosan Induces High Levels of Antibiotic Tolerance In Vitro and Reduces Antibiotic Efficacy up to 100-Fold In Vivo'. Available at: https://doi.org/10.1128/AAC.02312-18.

White, R.L., Burgess, D.S., Manduru, M. and Bosso, J.A. (1996) 'Comparison of three different in vitro methods of detecting synergy: Time-kill, checkerboard, and E test', *Antimicrobial Agents and Chemotherapy*, 40(8), pp. 1914–1918. Available at: https://doi.org/10.1128/aac.40.8.1914.

Woo, K.J., Hye, C.K., Ki, W.K., Shin, S., So, H.K. and Yong, H.P. (2008) 'Antibacterial activity and mechanism of action of the silver ion in Staphylococcus aureus and Escherichia coli', *Applied and Environmental Microbiology*, 74(7), pp. 2171–2178. Available at: https://doi.org/10.1128/AEM.02001-07.

Xu, Y., Huang, C., Dang, X., Khan, M.R., Huang, H., Zhao, Y. and Wang, S. (2020) 'Preparation of Long-Term Antibacterial SiO2-Cinnamaldehyde Microcapsule via Sol-Gel Approach as a Functional Additive for PBAT Film', *Processes 2020, Vol. 8, Page 897*, 8(8), p. 897. Available at: https://doi.org/10.3390/PR8080897.

Yang, S., Abdel-Razek, O.A., Cheng, F., Bandyopadhyay, D., Shetye, G.S., Wang, G. and Luk, Y.Y. (2014) 'Bicyclic brominated furanones: A new class of quorum sensing modulators that inhibit bacterial biofilm formation', *Bioorganic & medicinal chemistry*, 22(4), p. 1313. Available at: https://doi.org/10.1016/J.BMC.2014.01.004.

Yao, Y., Martinez-Yamout, M.A., Dickerson, T.J., Brogan, A.P., Wright, P.E. and Dyson, H.J. (2006) 'Structure of the Escherichia coli Quorum Sensing Protein SdiA: Activation of the Folding Switch by Acyl Homoserine Lactones', *Journal of Molecular Biology*, 355(2), pp. 262–273. Available at: https://doi.org/10.1016/j.jmb.2005.10.041.

Yazdani-Ahmadabadi, H., Yu, K., Khoddami, S., F. Felix, D., Yeh, H.H., Luo, H.D., Moskalev, I., Wang, Q., Wang, R., Grecov, D., Fazli, L., Lange, D. and Kizhakkedathu, J.N. (2022) 'Robust Nanoparticle-Derived Lubricious Antibiofilm Coating for Difficult-to-Coat Medical Devices with Intricate Geometry', *ACS Nanoscience Au*, 3(1), p. 67. Available at: https://doi.org/10.1021/ACSNANOSCIENCEAU.2C00040/SUPPL_FILE/NG2C00040_SI_001.PDF.

Yee, A., Phan, C.M. and Jones, L. (2022) 'Uptake and release of polyhexamethylene biguanide (PHMB) from hydrogel and silicone hydrogel contact lenses using a radiolabel methodology', *Contact Lens and Anterior Eye*, 45(5), p. 101575. Available at: https://doi.org/10.1016/J.CLAE.2022.101575.

Yildiz, Z.I., Kilic, M.E., Durgun, E. and Uyar, T. (2019) 'Molecular Encapsulation of Cinnamaldehyde within Cyclodextrin Inclusion Complex Electrospun Nanofibers: Fast-Dissolution, Enhanced Water Solubility, High Temperature Stability, and Antibacterial Activity of Cinnamaldehyde', *Journal of Agricultural and Food Chemistry*, 67(40), pp. 11066–11076. Available at: https://doi.org/10.1021/acs.jafc.9b02789.

Zablotny, R. and Fraenkel, D.G. (1967) *Glucose and Gluconate Metabolism in a Mutant of Escherichia coli Lacking Gluconate-6-phosphate Dehydrase*, *JOURNAL OF BACTERIOLOGY*.

Zalewska-Piątek, B., Olszewski, M., Lipniacki, T., Błoński, S., Wieczór, M., Bruździak, P., Skwarska, A., Nowicki, B., Nowicki, S. and Piątek, R. (2020) 'A shear stress micromodel of urinary tract infection by the Escherichia coli producing Dr adhesin', *PLOS Pathogens*, 16(1), p. e1008247. Available at: https://doi.org/10.1371/JOURNAL.PPAT.1008247.

Zhang, J., Liu, L., He, Y., Kong, W. and Huang, S. (2010) 'Cytotoxic effect of trans-cinnamaldehyde on human leukemia K562 cells', *Acta Pharmacologica Sinica*, 31(7), pp. 861–866. Available at: https://doi.org/10.1038/aps.2010.76.

Zhang, S., Liang, X., Gadd, G.M. and Zhao, Q. (2020) 'Superhydrophobic Coatings for Urinary Catheters to Delay Bacterial Biofilm Formation and Catheter-Associated Urinary Tract Infection', *ACS Applied Bio Materials*, 3(1), pp. 282–291. Available at: https://doi.org/10.1021/ACSABM.9B00814/ASSET/IMAGES/LARGE/MT9B00814_0012.JPEG.

Zhang, Y., Lin, Y., Zhang, X., Chen, Liqiong, Xu, C., Liu, S., Cao, J., Zheng, X., Jia, H., Chen, Lijiang and Zhou, T. (2021) 'Combining Colistin with Furanone C-30 Rescues Colistin Resistance of Gram-Negative Bacteria in Vitro and in Vivo.', *Microbiology spectrum*. Edited by C.M. Khursigara, 9(3), p. e0123121. Available at: https://doi.org/10.1128/Spectrum.01231-21.

Zhang, Y., Liu, X., Wang, Y., Jiang, P. and Quek, S.Y. (2016) 'Antibacterial activity and mechanism of cinnamon essential oil against Escherichia coli and Staphylococcus aureus', *Food Control*, 59, pp. 282–289. Available at: https://doi.org/10.1016/j.foodcont.2015.05.032.

Zhao, W., Sachsenmeier, K., Zhang, L., Sult, E., Hollingsworth, R.E. and Yang, H. (2014) 'A new bliss independence model to analyze drug combination data', *Journal of Biomolecular Screening*, 19(5), pp. 817–821. Available at: https://doi.org/10.1177/1087057114521867.

Zheng, S., Wang, W., Aldahdooh, J., Malyutina, A., Shadbahr, T., Tanoli, Z., Pessia, A. and Tang, J. (2022) 'SynergyFinder Plus: Toward Better Interpretation and Annotation of Drug Combination Screening Datasets', *Genomics, Proteomics & Bioinformatics* [Preprint]. Available at: https://doi.org/10.1016/J.GPB.2022.01.004.

Zou, Z., Potter, R.F., William H. McCoy, 4th, Wildenthal, J.A., Katumba, G.L., Mucha, P.J., Dantas, G. and Henderson, J.P. (2023) 'E. coli catheter-associated urinary tract infections are associated with distinctive virulence and biofilm gene determinants', *JCI Insight*, 8(2). Available at: https://doi.org/10.1172/JCI.INSIGHT.161461.

8. Appendix

Table 8.1. Over and underrepresented gene ontology terms of PHMB exposed EC958 with the genes within the term which had increased or decreased expression.

GO biological process		Fold enrichment	p-value	FDR	Increased gene expression	Reduced gene expression
Hydrogen sulfide biosynthetic process	GO:0070814	15.46	3.22×10^{-5}	3.67×10^{-3}	*cysC, cysD, cysJ, cysN, cysI, cysH*	
D-glucarate catabolic process	GO:0042838	15.46	7.68×10^{-4}	3.74×10^{-2}		*garL, garR, garK, gudD*
Galactarate catabolic process	GO:0046392	15.46	7.68×10^{-4}	3.69×10^{-2}		*garL, garR, garK, garD*
Glucose import across plasma membrane	GO:0098708	15.46	7.68×10^{-4}	3.63×10^{-2}		*ptsG, manY, manX, manZ*
Arginine catabolic process to succinate	GO:0019545	15.46	1.56×10^{-4}	1.00×10^{-2}	*astB, astD, astA, astC, astE*	
Arginine catabolic process to glutamate	GO:0019544	15.46	1.56×10^{-4}	9.79×10^{-3}	*astB, astD, astA, astC, astE*	
Sulfate assimilation	GO:0000103	10.31	1.49×10^{-4}	9.98×10^{-3}	*cysC, cysD, cysJ, cysN, cysI, cysH*	
Glyoxylate metabolic process	GO:0046487	7.73	1.57×10^{-4}	9.67×10^{-3}	*aceA, hyi, aceB, aceK, otnI, glxR*	*garR*
Chemotaxis	GO:0006935	5.85	1.14×10^{-6}	2.49×10^{-4}	*dppA, acs, rbsB*	*fliG, flgG, fliP, flhA, fliM, malE, flgC, fliO, fliN, cheZ, fliH*
Tricarboxylic acid cycle	GO:0006099	5.15	9.68×10^{-5}	7.83×10^{-3}	*gltA, aceA, sdhA, sucD, fumA, aceB, fumC, aceK*	*fumB, frdB*
Bacterial-type flagellum-dependent cell motility	GO:0071973	3.53	2.40×10^{-4}	1.39×10^{-2}		*fliG, flgG, flgH, fliK, fliP, flhA, fliM, flgC, fliO, fliN, fliF, cheZ, fliH*
Nitrogen compound transport	GO:0071705	1.95	2.47×10^{-4}	1.38×10^{-2}	*narU, yhdY, ydcV, argT, mppA, ompF, cysW, cysA, dppD, yhdZ, dppA, actP, , ydcS, gadC, , gabP, yhdX, ybbW, cysP, thiB, xanP, dppB, cysU, tnaB, cstA, hofC, dppC, ybaT, gltI*	*adiC, fliP, exbB, narK, flhA, fliO, fliH, uraA*
Nucleic acid metabolic process	GO:0090304	0.48	9.70×10^{-4}	4.38×10^{-2}	*yegP, gadX, mprA, nrdF, rayT, hchA, uxuR, bolA, gadW,*	*recR, rlmJ, dnaK, ruvC, pinE, rmuC, rpoE*
Organonitrogen compound biosynthetic process	GO:1901566	0.38	3.40×10^{-5}	3.37×10^{-3}	*cysJ, thiD, cysI, acs, ybdK, gabT, ettA, glsA1, astC, tufA*	*carA, ribA, pyrB,*

Macromolecule biosynthetic process	GO:0009059	0.37	$2.64x10^{-4}$	1.42×10^{-2}	*gadX, mprA, uxuR, bolA, ettA, gadW, tufA*	*recR, kdsB, rpoE*
GO molecular function						
Cytoskeletal motor activity	GO:0003774	11.6	9.44×10^{-5}	3.38×10^{-2}		*fliG, flgH, fliM, fliN, fliF, fliH*
Carbohydrate transmembrane transporter activity	GO:0015144	3.39	2.41×10^{-5}	2.01×10^{-2}	*agaB, xylG, gatA, yiaN, ytfR, frwC, sotB, mglA, rbsC*	*malF, treB, malE, ptsG, manY, malK, fruB, manX, manZ*
Active transmembrane transporter activity	GO:0022804	2.04	1.06×10^{-4}	3.32×10^{-2}	*agaB, yadH, xylG, yhhJ, dcuC, gatA, cysW, cysA, yhdZ, actP, gadC, gabP, ybbW, codB, yjfF, ytfR, glcA, cysU, tnaB, frwC, cstA,*	*adiC, dcuB, malF, treB, narK, ttdT, ptsG, manY, gudP, malK, fruB, manX, garP, uraA, manZ*
Catalytic activity, acting on a nucleic acid	GO:0140640	0.21	5.30×10^{-5}	2.21×10^{-2}	*rayT*	*rlmJ, ruvC, pinE*
GO Cellular component						
ATP-binding cassette (ABC) transporter complex, transmembrane substrate-binding subunit-containing	GO:0035796	12.37	1.32×10^{-3}	2.36×10^{-2}	*cysW, cysA, cysP, cysU*	
Bacterial-type flagellum basal body	GO:0009425	6.54	7.06×10^{-6}	2.41×10^{-4}		*fliG, flgG, flgH, fliP, flhA, fliM, flgC, fliO, fliN, fliF, fliH*
ATP-binding cassette (ABC) transporter complex, substrate-binding subunit-containing	GO:0055052	3.01	6.61×10^{-7}	2.82×10^{-5}	*xylG, yhdY, ydcV, argT, mppA, dppD, ydcU, yhdZ, dppA, ydcT, ydcS, tauC, ugpA, yhdX, thiB, yjfF, ytfR, dppB, ytfQ, rbsB, dppC, ytfT, mglA, gltI, rbsC, xylF, ugpE*	*malE, malK,*
Intracellular non-membrane-bounded organelle	GO:0043232	< 0.01	5.40×10^{-4}	1.15×10^{-2}	None	

Table 8.2. Over and underrepresented gene ontology terms of BAC exposed EC958 with the genes within the term which had increased or decreased expression.

GO biological process		Fold enrichment	Raw p-value	FDR	Increased gene expression	Reduced gene expression
Arginine catabolic process to succinate	GO:0019545	15.25	1.66E-04	9.12E-03	*astB , astD, astA, astC, astE*	
Arginine catabolic process to glutamate	GO:0019544	15.25	1.66E-04	8.96E-03	*astB , astD, astA, astC, astE*	
Bacterial-type flagellum-dependent swimming motility	GO:0071977	15.25	1.66E-04	8.81E-03		*fliG, cheY, fliM, cheA, fliN*
Regulation of chemotaxis	GO:0050920	15.25	1.66E-04	8.52E-03		*tar, tsr, cheY, cheA, cheZ*
Protein secretion by the type III secretion system	GO:0030254	10.17	1.61E-04	8.98E-03	*fliR*	*fliP, flhA, fliO, flhB, fliH*
'De novo' IMP biosynthetic process	GO:0006189	10.17	1.23E-05	1.30E-03	*purM, purN, purK, purE, purD, purF, purT, purL*	
Chemotaxis	GO:0006935	9.48	1.77E-13	2.72E-10	*dppA, acs, fliR,*	*fliG, flgG, tar, tsr, cheR, cheY, fliP, flhA, fliM, cheA, motA, flgC, fliO, fliN, cheB, flhB, rbsB, cheZ, cheW, fliH*
Nitrate assimilation	GO:0042128	6.45	8.02E-06	9.86E-04	*nirD, nac, narK, nirB, napA, nirC*	*narU, rpoA, narY, narW, narZ*
Cytoplasmic translation	GO:0002181	6.42	3.24E-11	1.66E-08		*rpmD, rpsR, rpsQ, rpsE, rpmC, rplW, rplR, rplF, rpsF, rplQ, rpsK, rplD, rpsM, rplE, rpsC, rplB, rpsN, rplO, rpsS, rplI, rpsH, rplV, rplC, rplP*
Bacterial-type flagellum assembly	GO:0044780	5.97	8.90E-05	5.70E-03	*fliR*	*flgJ, fliG, fliS, rpoA, fliK, flhA, flhB, flgK*
Purine nucleobase metabolic process	GO:0006144	5.34	9.47E-04	3.88E-02	*allB, purM, allC, purD, ybbW, purF*	*add*
Ribosomal large subunit assembly	GO:0000027	4.92	1.35E-04	8.15E-03	*crfC*	*rpmD, rpmC, rplW, rplF, rplQ, rplE, rplB, , rplP, rplC*
DNA recombination	GO:0006310	< 0.01	8.39E-04	3.49E-02	None	
GO molecular function						
Cytoskeletal motor activity	GO:0003774	11.44	1.02E-04	3.18E-02		*fliG, flgH, fliM, fliN, fliF, fliH*
Structural constituent of ribosome	GO:0003735	6.31	4.33E-11	5.41E-08		*rpmD, rpsR, rpsQ, rpsE, rpmC, rplW, rplR, rplF, rpsF, rplQ, rpsK, rplD, rpsM, rplE,*

rRNA binding	GO:0019843	5.5	2.36E-09	1.97E-06		*rpsC, rplB, rpsN, rplO, rpsS, rplI, rpsH, rplV, rplC, rplP* *rpsR, rpsQ, rpsE, rpmC, rplW, rplR, rplF, rpsF, rpsK, rplD, rpsM, rplE, rpsC, rplB, rpsN, rplO, rpsS, rplI, rpsH, rplV, rplC, rplP*
DNA binding	GO:0003677	0.43	1.41E-04	3.93E-02	*ybdO, atoC, cspH, nac, cspA, envR, stpA, cspG, xynR*	*aidB, mlrA, ybaB, rpoA, rpoD, rplD,*
Catalytic activity, acting on DNA	GO:0140097	< 0.01	6.47E-05	2.31E-02	None	None
GO Cellular component						
Bacterial-type flagellum basal body, C ring	GO:0009433	15.25	8.07E-04	1.15E-02		*fliG, cheY, fliM, fliN*
Bacterial-type flagellum rotor complex	GO:0120107	15.25	8.07E-04	1.10E-02		*fliG, cheY, fliM, fliN*
Methyl accepting chemotaxis protein complex	GO:0098561	13.07	6.12E-05	1.04E-03		*tar, tsr, cheR, cheA, cheZ, cheW*
Type III protein secretion system complex	GO:0030257	10.17	1.61E-04	2.61E-03	*fliR*	*fliP, flhA, fliO, flhB, fliH*
Bacterial-type flagellum secretion apparatus	GO:0120102	10.17	1.61E-04	2.49E-03	*fliR*	*fliP, flhA, fliO, flhB, fliH*
Cytosolic small ribosomal subunit	GO:0022627	6.35	2.33E-05	4.41E-04		*rpsR, rpsQ, rpsE, rpsF, rpsK, rpsM, rpsC, rpsN, rpsS, rpsH*
Cytosolic large ribosomal subunit	GO:0022625	6.28	5.88E-07	1.54E-05		*rpmD, rpmC, rplW, rplR, rplF, rplQ, rplD, rplE, rplB, rplO, rplI, rplV, rplC, rplP*

Table 8.3. Over and underrepresented gene ontology terms of silver nitrate exposed EC958 with the genes within the term which had increased or decreased expression.

GO biological process		Fold enrichment	Raw p-value	FDR	Increased gene expression	Reduced gene expression
Arginine catabolic process to succinate	GO:0019545	17.22	9.61E-05	5.18E-03	*astB, astD, astA, astC, astE*	
Arginine catabolic process to glutamate	GO:0019544	17.22	9.61E-05	5.09E-03	*astB, astD, astA, astC, astE*	
D-glucarate catabolic process	GO:0042838	17.22	5.20E-04	2.16E-02		*garL, garR, garK, gudD*
Galactarate catabolic process	GO:0046392	17.22	5.20E-04	2.13E-02		*garL, garR, garK, gudD*
Glycolate catabolic process	GO:0046296	14.35	1.68E-04	8.34E-03	*gcl, glcF, glcE, glcD, glxR*	
L-threonine catabolic process to propionate	GO:0070689	12.3	2.76E-04	1.28E-02		*tdcD, tdcF, tdcG, tdcA, tdcE*
Gamma-aminobutyric acid catabolic process	GO:0009450	11.48	1.43E-03	5.05E-02	*aldA, gabP, gabD, gabT*	
'De novo' IMP biosynthetic process	GO:0006189	11.48	5.22E-06	5.73E-04	*purM, purN, purK, purE, purF, purT, purL, purC*	
Hexose import across plasma membrane	GO:0140271	11.48	8.47E-05	4.82E-03	*yjfF, ytfR, ytfQ, ytfT*	*fruB, manX*
Glyoxylate metabolic process	GO:0046487	9.84	1.20E-05	1.23E-03	*aceA, gcl, hyi, aceB, aceK, otnI, glxR*	*garR*
Tricarboxylic acid cycle	GO:0006099	7.46	2.51E-07	3.86E-05	*gltA, aceA, sucC, sdhD, sdhA, fumA, sucD, aceB, fumC, aceK, sucA*	*fumB, frdB*
Cellular respiration	GO:0045333	7.26	3.92E-07	5.24E-05	*aceA, aceB, aceK, cyoA, cyoB, cyoC, cyoD, fumA, fumC, gltA, narZ, sdhA, sdhD, sucA, sucC, sucD, ynfG*	*dmsA, frdA, frdB, fumB, glpA, hybB, hybO, torC*
Carboxylic acid transport	GO:0046942	2.41	4.22E-04	1.85E-02	*livK, argT, putP, yehY, gltK, ygbN, actP, gadC, cycA, gabP, gltJ, ytfR, glcA, cstA, sstT, ybaT, gltI*	*dcuC, adiC, dcuB, eamB*
Nitrogen compound transport	GO:0071705	2.05	1.71E-04	8.19E-03	*actP, argT, cstA, cycA, cysA, cysU, cysW, dppA, dppB, dppC, dppD, gabP, gadC, ghxP, gltI, gltJ, gltK, livK, narU, ompF, potF, putP, sstT, xanP, ybaT, ybbW, ydcS, ydcV, yehY*	*adiC, eamB, narK, nikA, uraA*
Nucleic acid metabolic process	GO:0090304	0.33	2.55E-05	2.06E-03	*gadW, gadX, nrdF, pphA, yegP*	*lysU, pinE, mrr, rmuC, ttdR*
Lipid biosynthetic process	GO:0008610	< 0.01	5.65E-04	2.29E-02	None	None

GO molecular function						
Lyase activity	GO:0016829	2.36	1.07E-04	3.84E-02	*gadW, gadX, nrdF, pphA, yegP*	*lysU, mrr, pinE, rmuC, ttdR*
Active transmembrane transporter activity	GO:0022804	2.21	2.43E-05	1.21E-02	*actP, agaB, cstA, cycA, cyoA, cyoB, cyoC, cyoD, cysA, cysU, cysW, gabP, gadC, glcA, kgtP, mdlB, putP, sstT, yadH, ybbW, yjfF, ytfR*	*adiC, dcuB, dcuC, fruB, garP, gudP, malF, malK, manX, narK, treB, ttdT, uraA*
Oxidoreductase activity	GO:0016491	1.81	1.31E-04	4.09E-02	*aidB, aldA, aldB, astD, bfr, cyoA, cyoB, cyoC, cyoD, dadA, fadB, gabD, gapA, glcD, glcE, glcF, glxR, hdhA, katE, lgoD, lhgD, ltnD, narZ, nrdF, nrdH, patD, sdhA, sdhD, sucA, ydcJ, yqjG*	*aceE, aegA, ahpC, ccmH, dmsA, frdA, frdB, garK, garR, glpA, hybA, hybO, nirB, qorB, torC*
Catalytic activity, acting on a nucleic acid	GO:0140640	0.17	4.12E-05	1.72E-02		*lysU, mrr, pinE*
GO Cellular component						
Cytochrome o ubiquinol oxidase complex	GO:0009319	17.22	5.20E-04	1.27E-02	*cyoB, cyoD, cyoC, cyoA*	
ATP-binding cassette (ABC) transporter complex, substrate-binding subunit-containing	GO:0055052	3.24	2.34E-07	1.33E-05	*argT, dppA, dppB, dppC, dppD, gltI, gltJ, gltK, livK, mglA, mglB, mglC, potF, rbsB, ugpA, ugpE, ydcS, ydcT, ydcU, ydcV, yehY, yjfF, ytfQ, ytfR, ytfT*	*malE, malK, nikA*

Table 8.4. Over and underrepresented gene ontology terms of triclosan exposed EC958 with the genes within the term which had increased or decreased expression.

GO biological process		Fold enrichment	Raw p-value	FDR	Increased gene expression	Reduced gene expression
Arginine catabolic process to succinate	GO:0019545	18.77	6.49E-05	4.87E-03	*astA, astB, astC, astD, astE*	
Arginine catabolic process to glutamate	GO:0019544	18.77	6.49E-05	4.75E-03	*astA, astB, astC, astD, astE*	
Heme import across plasma membrane	GO:1904334	18.77	6.49E-05	4.64E-03		*ccmA, ccmB, ccmC, ccmD, ccmE*
Cytochrome c biosynthetic process	GO:1903607	18.77	6.49E-05	4.43E-03		*ccmA, ccmB, ccmC, ccmD, ccmE*
L-threonine catabolic process to propionate	GO:0070689	16.09	2.00E-05	1.86E-03		*tdcA, tdcB, tdcD, tdcE, tdcF, tdcG*
Glycolate catabolic process	GO:0046296	15.64	1.14E-04	6.49E-03	*gcl, glcD, glcE, glcF, glxR*	
Hydrogen sulfide biosynthetic process	GO:0070814	15.64	1.14E-04	6.38E-03	*cysD, cysH, cysI, cysJ, cysN*	
Thiosulfate transport	GO:0015709	12.51	1.05E-03	4.09E-02	*cysA, cysP, cysU, cysW*	
Sulfate assimilation	GO:0000103	10.43	4.36E-04	1.94E-02	*cysD, cysH, cysI, cysJ, cysN*	
Cytochrome complex assembly	GO:0017004	10.01	9.63E-06	1.02E-03		*ccmA, ccmB, ccmC, ccmD, ccmE, ccmF, ccmH, dsbE*
Glyoxylate metabolic process	GO:0046487	9.38	4.90E-05	3.96E-03	*aceA, aceB, aceK, gcl, glcB, glxR, hyi*	
Ornithine metabolic process	GO:0006591	9.38	6.28E-04	2.61E-02	*argB, astC, gabT*	*speF, ygeW*
Aldehyde catabolic process	GO:0046185	5.93	1.23E-03	4.68E-02	*adhP, gcl, glcB, gloC, glxR, yhbO*	
Tricarboxylic acid cycle	GO:0006099	5.63	1.04E-04	6.14E-03	*aceA, aceB, aceK, glcB, sucB, sucC, sucD*	*fumB, prpD*
Phosphoenolpyruvate-dependent sugar phosphotransferase system	GO:0009401	4.07	5.82E-05	4.58E-03		*agaB, agaC, agaD, agaS, agaV, fruB, kbaZ, manX, manY, manZ, srlB, treB, yadI*
Nucleic acid metabolic process	GO:0090304	0.36	1.80E-04	8.93E-03	*gadW, gadX, nrdB, pphA, yegP, yhbO*	*qseB, rmuC, ttdR, valS*
GO molecular function						
Catalytic activity, acting on a nucleic acid	GO:0140640	0.06	3.73E-06	3.11E-03		*valS*
GO Cellular component						

ATP-binding cassette (ABC) transporter complex, substrate-binding subunit-containing	GO:0055052	15.02	6.57E-04	2.04E-02	*cysA, cysP, cysU, cysW*	

Table 8.5. Over and underrepresented gene ontology terms of cinnamaldehyde exposed EC958 with the genes within the term which had increased or decreased expression.

GO biological process		Fold enrichment	Raw p-value	FDR	Increased gene expression	Reduced gene expression
Glutamine family amino acid catabolic process	GO:0009065	4.73	3.21E-04	4.10E-02	*ansB, astA, astB, astD, astE, sad, yahI*	*gadA, gadB, glsA1*
Chemotaxis	GO:0006935	4.37	3.21E-06	1.64E-03	*acs, rbsB*	*cheA, cheB, cheR, cheW, cheY, cheZ, flgC, flhB, fliG, fliH, fliM, fliN, fliP, motA, tar, tsr*
Nitrate assimilation	GO:0042128	4.15	2.11E-04	3.09E-02	*nac, nrfA*	*narG, narH, narI, narJ, narK, narL, narU, narW, narY, narZ*
Bacterial-type flagellum-dependent cell motility	GO:0071973	2.99	1.21E-04	2.06E-02	*preA, ydcZ*	*cheA, cheY, cheZ, flgC, flgH, flgJ, flhB, fliD, fliF, fliG, fliH, fliK, fliM, fliN, fliP, fliS, motA*
DNA recombination	GO:0006310	0.14	3.99E-04	4.91E-02	*rayT*	*recR*
GO molecular function						
Ion binding	GO:0043167	1.29	9.78E-05	4.90E-02	*acs, allB, allC, araA, araD, astE, atoC, atoS, citC, cutC, cysA, cysC, cysD, cysI, cysJ, cysN, cysP, dgcT, entB, entC, ettA, eutP, evgS, fadH, fhuA, fixC, ftnB, fucA, fucK, gcl, glcE, glcF, glnK, gloC, glpB, glpQ, gltA, gltI, hcp, hisP, hmp, hscC, kefG, lgoD, ligA, mglA, nagA, nagE, nanK, norW, nrfA, nrfB, nrfC, ompC, php, preA, preT, psuG, psuK, purD, rbbA, rbsA, rbsK, sbp, sodB, sucA, tauD, tdcB, tdcD, uacR, uspF, uxaA, xylA, xylB, xylG, ydeM, ydeN, ydhU, ydhY, yeiL, yggF, yggR, hcH, yhfS, yidA, yidJ, yniA, yojI, yphE, yqhD, zraS*	*aceE, add, adhP, adk, ahr, amyA, apbE, appC, aspS, bfr, carA, cheA, cheY, citE, clpB, cobB, dbpA, deaD, dgcM, dnaC, dnaK, dusA, dxs, edd, fecE, fic, fumB, gabT, gadA, gadB, garL, glnS, gph, gpmI, groL, guaA, guaB, gudD, gudX, hemW, hslO, hslU, hslV, htpG, hyaA, hyaB, hyaC, ispA, ispF, katE, kbp, kdsB, kefF, lepA, lhgD, mltB, mnmA, msrP, nagK, narG, narH, narI, narL, narY, narZ, otsB, pcnB, pdeR, poxB, prpB, pta, pyrC, rclA, rdgB, recR, rffH, rhlE, rlmA, rnhB, rplB, rsxG, srmB, sufA, sufC, sufS, suhB, thiL, tktB, tmk, upp, wecE, wrbA, yahK, ybdK, ybiI, ycjX, ydcJ, ydcT, yedP, yegS, yehX, yeiR, yigB, ynfF*
Catalytic activity	GO:0003824	1.21	5.89E-05	3.69E-02	*acs, aes, agaB, agaV, agp, aldA, allB, allC, ansB, araA, araD, astA, astB, astD, astE, atoS, bglA, chbB, citC, cysA, cysC, cysD, cysH, cysI, cysJ, cysN, dadA, dgcT, dgoA, dhaK, dhaM, entB, entC, ettA, eutD, eutE, eutP, evgS, fadH,*	*aceE, acpH, add, adhP, adk, ahr, aidB, aldB, amyA, apaH, apbE, appA, appC, aspS, bfr, carA, cheA, cheB, cheR, cheY, cheZ, citE, citF, clpB, cobB, dbpA, dcm, deaD, dgcM, dnaK, dusA, dxs, edd, envC, erfK, fabD, fbaB, fecE, fic, flgJ, fumB, gabD, gabT, gadA, gadB,*

					fixC, fruA, frvA, frwC, ftnB, fucA, fucK, fumC, gatA, gcl, glcE, glcF, glgX, gloC, glpB, glpQ, gltA, glxR, grxA, hcp, hisP, hiuH, hmp, hscC, hyi, kefG, lgoD, ligA, mdh, mglA, mgsA, mtfA, nagA, nagE, nanK, norW, nrfA, nrfB, nrfC, pdeI, php, ppnP, preA, preT, pspE, psuG, psuK, purD, rayT, rbbA, rbsA, rbsD, rbsK, rihC, rutA, sad, sodB, sucA, tauD, tdcB, tdcD, tpx, ulaA, umuD, uspG, uxaA, xylA, xylB, xylG, yadI, yagE, yahI, yciK, ycjY, ydeM, ydeN, ydhR, ydhU, ydjH, yfbL, yggF, yhaM, yhcH, yhfS, yidA, yidJ, yieL, yjhG, yniA, yojI, yphE, yqhD, zraS	*galF, gapA, garL, garR, ggt, glnS, glsA1, gph, gpmI, groL, guaA, guaB, gudD, gudX, hemW, hslU, hslV, htpG, hyaA, hyaB, hyaC, ispA, ispF, katE, kdsB, kefF, ldcC, lepA, lhgD, mltB, mnmA, msrP, murA, nagK, narG, narH, narI, narY, narZ, nudJ, osmC, otsB, pcnB, pdeH, pdeR, phnO, pncC, poxB, prpB, pta, ptsG, pyrC, rclA, rdgB, rffG, rffH, rhlE, rimI, rlmA, rluE, rnhB, rnpA, rph, rplB, rsxG, srmB, sufC, sufS, suhB, talA, tam, thiL, tktB, tmk, trmH, trmL, truC, tsaB, upp, wecD, wecE, wrbA, xseA, yahK, ybdK, ycaC, ydcJ, ydcS, ydcT, yeaG, yedP, yegS, yehX, yeiR, yhbO, yigB, ynfF, yqgF, ysgA*
GO Cellular component						
ATP-binding cassette (ABC) transporter complex, transmembrane substrate-binding subunit-containing	GO:0055052	8.98	1.63E-03	2.52E-02	*cysA, cysP, cysU, cysW, sbp*	*cysA, cysP, cysU, cysW, sbp*
Methyl accepting chemotaxis protein complex	GO:0098561	7.7	9.10E-04	1.94E-02		*cheA, cheR, cheW, cheZ, tar, tsr*
Bacterial-type flagellum motor	GO:0120100	7.48	2.74E-03	3.73E-02		*cheY, fliG, fliM, fliN, motA*
Cytosolic large ribosomal subunit	GO:0022625	2.91	3.92E-03	4.96E-02	*rpmA, ykgM*	*rplB, rplD, rplF, rplI, rplO, rplR, rplV, rplW, rpmD*

Table 8.6. Over and underrepresented gene ontology terms of furanone-C30 exposed EC958 with the genes within the term which had increased or decreased expression.

GO biological process		Fold enrichment	Raw p-value	FDR	Increased gene expression	Reduced gene expression
thiosulfate transport	GO:0015709	18.3	2.62E-04	1.58E-02	*cysA, cysU, cysW, sbp,*	
'de novo' IMP biosynthetic process	GO:0006189	16.01	2.05E-06	2.18E-04	*purC, purE, purF, purK, purL, purM, purT,*	
sulfate transmembrane transport	GO:1902358	15.69	4.00E-04	2.23E-02	*cysA, cysU, cysW, sbp,*	
cytoplasmic translation	GO:0002181	14.45	5.61E-23	1.72E-19	*ykgM*	*rplB, rplC, rplD, rplE, rplF, rplI, rplO, rplP, rplQ, rplR, rplT, rplV, rplW, rpmB, rpmC, rpmD, rpsA, rpsC, rpsE, rpsF, rpsH, rpsI, rpsK, rpsM, rpsN, rpsO, rpsQ, rpsR, rpsS,*
ribosomal small subunit assembly	GO:0000028	10.98	3.34E-06	3.31E-04		*rpsA, rpsC, rpsE, rpsH, rpsN, rpsO, rpsQ, rpsS,*
ribosomal large subunit assembly	GO:0000027	10.63	1.41E-08	1.88E-06		*deaD, rplB, rplC, rplE, rplF, rplP, rplQ, rplT, rplW, rpmB, rpmC, rpmD,*
glyoxylate metabolic process	GO:0046487	9.8	3.93E-04	2.28E-02	*aceA, gcl, glxR, hyi,*	*garR*
nitrate assimilation	GO:0042128	6.33	7.28E-04	3.93E-02	*napA, nirB, nirC, nirD, nrfA,*	*rpoA*
GO molecular function						
nitrite reductase activity	GO:0098809	21.96	1.61E-04	3.37E-02	*nirB, nirD, nrfA, nrfB,*	
small ribosomal subunit rRNA binding	GO:0070181	19.61	3.27E-05	1.17E-02		*rpsF, rpsK, rpsO, rpsQ, rpsR,*
structural constituent of ribosome	GO:0003735	14.2	8.27E-23	2.07E-19	*ykgM*	*rplB, rplC, rplD, rplE, rplF, rplI, rplO, rplP, rplQ, rplR, rplT, rplV, rplW, rpmB, rpmC, rpmD, rpsA, rpsC, rpsE, rpsF, rpsH, rpsI, rpsK, rpsM, rpsN, rpsO, rpsQ, rpsR, rpsS,*
mRNA binding	GO:0003729	8.35	5.98E-05	1.66E-02		*rplD, rplT, rpsA, rpsC, rpsF, rpsO, rpsR,*
GO Cellular component						
ATP-binding cassette (ABC) transporter complex, transmembrane substrate-binding subunit-containing	GO:0055052	21.96	1.61E-04	2.50E-03	*cysA, cysU, cysW, sbp,*	
cytosolic small ribosomal subunit	GO:0022627	16.01	1.16E-11	3.04E-10	*rbbA*	*rpsA, rpsC, rpsE, rpsF, rpsH, rpsI, rpsK, rpsM, rpsN, rpsO, rpsQ, rpsR, rpsS,*

cytosolic large ribosomal subunit	GO:0022625	13.72	4.30E-13	1.47E-11	*ykgM*		*rplB, rplC, rplD, rplE, rplF, rplI, rplO, rplP, rplQ, rplR, rplT, rplV, rplW, rpmB, rpmC, rpmD,*

Table 8.7. Over and underrepresented gene ontology terms of F-DPD exposed EC958 with the genes within the term which had increased or decreased expression.

GO biological process		Fold enrichment	Raw p-value	FDR	Increased gene expression	Reduced gene expression
bacterial-type flagellum-dependent swimming motility	GO:0071977	27.97	1.01E-05	2.81E-03		*cheA, cheY, fliG, fliM, fliN,*
regulation of chemotaxis	GO:0050920	27.97	1.01E-05	2.38E-03		*cheA, cheY, cheZ, tar, tsr,*
regulation of protein modification process	GO:0031399	18.65	2.44E-04	3.57E-02		*cheA, cheW, tar, tsr,*
intracellular pH elevation	GO:0051454	15.99	3.73E-04	4.58E-02		*gadA, gadB, gadC, kefC,*
protein secretion by the type III secretion system	GO:0030254	15.54	7.15E-05	1.22E-02		*flhA, flhB, fliH, fliO, fliP,*
chemotaxis	GO:0006935	15.12	6.93E-16	1.07E-12		*aer, cheA, cheB, cheR, cheW, cheY, cheZ, flgC, flgG, flhA, flhB, fliG, fliH, fliM, fliN, fliO, fliP, motA, tar, tsr,*
bacterial-type flagellum assembly	GO:0044780	8.51	5.32E-05	9.61E-03		*flgJ, flgK, flhA, flhB, fliG, fliK, fliS,*
organic cyclic compound metabolic process	GO:1901360	0.46	3.65E-04	4.67E-02	*allB, glxR, rnt, suhB, tnaB, ybbW, yfhL,*	*cecR, chpB, crfC, dxs, rep, talA, tktB, yhbO,*
GO molecular function						
cytoskeletal motor activity	GO:0003774	20.98	3.67E-06	9.19E-03		*flgH, fliF, fliG, fliH, fliM, fliN,*
GO Cellular component						
bacterial-type flagellum basal body, C ring	GO:0009433	27.97	8.58E-05	2.93E-03		*cheY, fliG, fliM, fliN,*
bacterial-type flagellum rotor complex	GO:0120107	27.97	8.58E-05	2.66E-03		*cheY, fliG, fliM, fliN,*
methyl accepting chemotaxis protein complex	GO:0098561	23.98	2.16E-06	1.23E-04		*cheA, cheR, cheW, cheZ, tar, tsr,*
type III protein secretion system complex	GO:0030257	15.54	7.15E-05	3.05E-03		*flhA, flhB, fliH, fliO, fliP,*
bacterial-type flagellum secretion apparatus	GO:0120102	15.54	7.15E-05	2.71E-03		*flhA, flhB, fliH, fliO, fliP,*

Table 8.8 Minimum inhibitory concentrations of biocides (PHMB, BAC, silver nitrate and triclosan) and cinnamaldehyde alone and in combinations.

Strain	Independent		Combined	
	PHMB (μg/ml)	**Cinnamaldehyde (μg/ml)**	**PHMB (μg/ml)**	**Cinnamaldehyde (μg/ml)**
EC1	2	375 (176.8)	1	250
EC2	2	500	1.1 (0.1)	166.7 (58.9)
EC11	2	500	1.3	166.7
EC26	4	1000	1.3 (0.6)	333.3 (235.7)
EC28	3.7 (0.5)	458.3 (58.9)	1.1 (0.8)	229.2 (29.5)
EC34	2	375 (176.8)	0.8 (0.4)	250
EC958	2	500	0.8 (0.4)	187.5 (88.4)
CFT073	3 (1.4)	500	0.9 (0.1)	187.5 (29.5)

Strain	Independent		Combined	
	BAC (μg/ml)	**Cinnamaldehyde (μg/ml)**	**BAC (μg/ml)**	**Cinnamaldehyde (μg/ml)**
EC1	14.3 (1.8)	416.7 (117.9)	7.8	250
EC2	15.6	458.3 (58.9)	13.4 (3.2)	333.3 (117.9)
EC11	15.6	500	12.0 (1.4)	333.3 (117.9)
EC26	15.6	583.3 (117.9)	8.1 (4.1)	375 (176.8)
EC28	13.0 (3.7)	416.7 (117.9)	7.8	187.5 (88.4)
EC34	11.7 (5.5)	416.7 (117.9)	7.5 (0.5)	250
EC958	15.6 (0.0)	500	11.1 (6.4)	250
CFT073	11.7 (5.5)	416.7	7.2 (0.9)	250

Strain	Independent		Combined	
	Silver nitrate (μg/ml)	**Cinnamaldehyde (μg/ml)**	**Silver nitrate (μg/ml)**	**Cinnamaldehyde (μg/ml)**
EC1	9.8 (4.6)	500	3.9	187.5 (88.4)
EC2	**15.6**	**500**	**3.6 (0.5)**	**125**
EC11	**28.7 (3.7)**	**500**	**3.6 (0.5)**	**125**
EC26	18.2 (3.7)	500	5.5 (3.2)	145.8 (29.5)
EC28	31.3	500	15.6	145.8 (29.5)
EC34	28.7 (3.7)	500	9.8 (8.3)	125
EC958	31.3	416.7 (117.9)	13.0 (3.7)	125
CFT073	16.9 (1.8)	458.3 (58.9)	7.2 (0.9)	125

Strain	Independent		Combined	
	Triclosan (μg/ml)	**Cinnamaldehyde (μg/ml)**	**Triclosan (μg/ml)**	**Cinnamaldehyde (μg/ml)**
EC1	0.1 (0.0)	500	0.1	500
EC2	0.3 (0.1)	500	0.2 (0.0)	291.7 (117.9)
EC11	0.1	1000	0.2 (0.0)	1000
EC26	0.1 (0.0)	1000	0.3	500
EC28	0.3 (0.0)	500	0.3 (0.1)	500
EC34	0.1	500	0.1 (0.1)	416.7 (117.9)
EC958	0.1	500	0.3	500
CFT073	0.1	583.3(117.9)	0.1	291.7

All concentrations are in μg/ml and are an average of two biological repeats, each with 3 technical replicates, standard deviation represented in brackets where required. Combinations with a synergistic interaction are in bold.

Table 8.9. Minimum inhibitory concentrations of biocides (PHMB, BAC, silver nitrate and triclosan) and furanone-C30 alone and in combination.

Strain	Independent		Combined	
	PHMB (μg/ml)	**Furanone-C30 (μg/ml)**	**PHMB (μg/ml)**	**Furanone-C30 (μg/ml)**
EC1	2	145.8 (29.5)	1.2 (0.2)	72.9 (14.7)
EC2	3 (0.5)	500	2	80.7 (18.4)
EC11	2	125	0.9 (0.1)	52.1 (14.7)
EC26	2	125	1	62.5
EC28	2.3 (0.5)	187.5 (88.4)	1.2 (0.2)	44.3 (11.1)
EC34	1.8 (0.2)	125	0.8 (0.4)	72.9 (14.7)
EC958	3.7 (0.5)	250	1.3	67.7 (22.1)
CFT073	**3 (0.5)**	**125**	**0.7**	**28.7 (3.7)**

Strain	Independent		Combined	
	BAC (μg/ml)	**Furanone-C30 (μg/ml)**	**BAC (μg/ml)**	**Furanone-C30 (μg/ml)**
EC1	14.3 (1.8)	125	7.8	125
EC2	15.6	250	7.8	125
EC11	9.1 (1.8)	125	9.1 (1.8)	57.3 (7.4)
EC26	15.6	145.8 (29.5)	14.3 (1.8)	125
EC28	9.1 (1.8)	187.5 (88.4)	7.8	145.8 (29.5)
EC34	7.8	229.2 (29.5)	6.5 (1.8)	166.7 (58.9)
EC958	9.1 (1.8)	229.2 (29.5)	6.8 (1.4)	93.8 (44.2)
CFT073	7.8	125	5.7 (0.9)	93.8 (14.7)

Strain	Independent		Combined	
	Silver nitrate (μg/ml)	**Furanone-C30 (μg/ml)**	**Silver nitrate (μg/ml)**	**Furanone-C30 (μg/ml)**
EC1	15.6	375 (58.9)	10.4 (3.7)	187.5 (29.5)
EC2	9.1 (1.8)	250	3.9	62.5
EC11	28.7 (3.7)	500	9.8 (4.6)	250
EC26	31.3	354.2 (206.2)	14.3 (1.8)	145.8 (29.5)
EC28	28.5 (3.7)	250	15.6	93.8 (44.2)
EC34	15.6	187.5 (88.4)	11.7 (5.5)	93.8 (44.2)
EC958	15.6	125	8.5 (0.9)	67.7 (22.1)
CFT073	7.8	125	5.5 (2.8)	93.8 (44.2)

Strain	Independent		Combined	
	Triclosan (μg/ml)	**Furanone-C30 (μg/ml)**	**Triclosan (μg/ml)**	**Furanone-C30 (μg/ml)**
EC1	0.1 (0.0)	250	0.1	125
EC2	0.2 (0.0)	250	0.3	250
EC11	0.1 (0.0)	229.2 (29.5)	0.2 (0.1)	93.8 (44.2)
EC26	0.2 (0.0)	166.7 (58.9)	0.2	114.6 (14.7)
EC28	0.3	250	0.3	125
EC34	0.1 (0.0)	208.3 (58.9)	0.2	93.8 (14.7)
EC958	0.2 (0.1)	250	0.4 (0.1)	208.3 (58.9)
CFT073	0.1 (0.0)	187.5 (29.5)	0.2 (0.0)	125

All concentrations are in μg/ml and are an average of two biological repeats, each with 3 technical replicates, standard deviation represented in brackets where required. Combinations with a synergistic interaction are in bold.

Table 8.10. Minimum bactericidal concentrations of biocides (PHMB, BAC, silver nitrate and triclosan) and cinnamaldehyde alone and in combinations.

Strain	Independent		Combined	
	PHMB (µg/ml)	Cinnamaldehyde (µg/ml)	PHMB (µg/ml)	Cinnamaldehyde (µg/ml)
EC1	**14 (2.8)**	**1166.7 (235.7)**	**1.1 (0.1)**	**208.3 (58.9)**
EC2	**5.7 (3.3)**	**1833.3 (235.7)**	**1**	**270.8 (29.5)**
EC11	**7.3 (2.8)**	**2000**	**1.2 (0.2)**	**333.3**
EC26	**13.3 (3.8)**	**3000 (471.4)**	**2**	**333.3**
EC28	4.7 (0.9)	1166.7 (235.7)	1.3 (0.6)	333.3 (117.9)
EC34	4	1000	1.5 (0.7)	166.7 (58.9)
EC958	**7.3 (0.9)**	**1833.3 (235.7)**	**1.7 (0.9)**	**333.3 (235.7)**
CFT073	**5.3 (1.9)**	**1000**	**0.9 (0.1)**	**291.7 (58.9)**

Strain	Independent		Combined	
	BAC (µg/ml)	Cinnamaldehyde (µg/ml)	BAC (µg/ml)	Cinnamaldehyde (µg/ml)
EC1	15.6	1000	4.6 (0.9)	541.7 (58.9)
EC2	20.8 (7.4)	1333.3 (471.4)	9.1 (1.8)	750 (353.6)
EC11	18.2 (3.7)	1666.7 (471.4)	10.7 (3.2)	125 (589.3)
EC26	18.2 (3.7)	1500 (707.1)	11.7 (1.8)	1083.3 (353.6)
EC28	14.3 (1.8)	1166.7 (235.7)	9.1 (1.8)	666.7 (235.7)
EC34	15.6	1000	10.4	666.7
EC958	26.0 (14.7)	1666.7 (471.4)	15.6	750 (353.6)
CFT073	14.3 (1.8)	1000	7.2 (0.9)	208.3 (58.9)

Strain	Independent		Combined	
	Silver nitrate (µg/ml)	Cinnamaldehyde (µg/ml)	Silver nitrate (µg/ml)	Cinnamaldehyde (µg/ml)
EC1	15.0 (0.9)	1666.7	10.4 (7.4)	166.7
EC2	18.2 (3.7)	1833.3 (235.7)	11.7 (5.5)	291.7 (58.9)
EC11	**36.4**	**1333.3**	**8.5 (0.9)**	**291.7 (58.9)**
EC26	31.3 (7.4)	1000	18.9 (2.8)	291.7 (58.9)
EC28	**31.3**	**1500 (707.1)**	**11.1 (0.9)**	**187.5 (88.4)**
EC34	**31.3**	**1333.3 (471.4)**	**3.9**	**187.5 (88.4)**
EC958	**52.1 (29.5)**	**1250 (589.3)**	**9.8 (8.3)**	**187.5 (88.4)**
CFT073	18.2 (3.7)	833.3	7.2 (4.6)	145.8 (29.5)

Strain	Independent		Combined	
	Triclosan (µg/ml)	Cinnamaldehyde (µg/ml)	Triclosan (µg/ml)	Cinnamaldehyde (µg/ml)
EC1	2.2 (0.9)	1833.3 (235.7)	4	1000
EC2	1.0 (0.9)	2000	9.3 (1.9)	2000
EC11	1.2 (0.7)	2000	3 (1.4)	2000
EC26	4	2000	8	1000
EC28	4.7 (0.9)	2000	8	1000
EC34	2.8 (1.8)	2000	3 (0.5)	1000
EC958	4	2000	5.3	1000
CFT073	2.2 (0.7)	1333.3 (471.4)	2.8 (0.7)	1333.3

All concentrations are in µg/ml and are an average of two biological repeats, each with 3 technical replicates, standard deviation represented in brackets where required. Combinations with a synergistic interaction are in bold.

Table 8.11. Minimum bactericidal concentrations of biocides (PHMB, BAC, silver nitrate and triclosan) and Furanone-C30 alone and in combinations.

Strain	Independent		Combined	
	PHMB (μg/ml)	**Furanone-C30 (μg/ml)**	**PHMB (μg/ml)**	**Furanone-C30 (μg/ml)**
EC1	6.3 (2.4)	250	1.0 (0.8)	114.6 (14.7)
EC2	**21.3**	**500**	**3.7 (1.4)**	**130.2 (51.6)**
EC11	**11.3 (6.6)**	**250**	**1.6 (0.1)**	**72.9 (44.2)**
EC26	13.3 (3.8)	291.7 (58.9)	5.0 (4.7)	104.2
EC28	10.3 (8.0)	250	2.7 (0.5)	78.1 (36.8)
EC34	**11 (7.1)**	**229.2 (29.5)**	**2.5 (2.1)**	**44.3 (25.8)**
EC958	8	250	0.3	125
CFT073	6.3 (2.4)	125	0.9 (0.4)	52.1 (14.7)

Strain	Independent		Combined	
	BAC (μg/ml)	**Furanone-C30 (μg/ml)**	**BAC (μg/ml)**	**Furanone-C30 (μg/ml)**
EC1	33.9 (25.8)	208.3	9.1 (1.8)	83.3 (58.9)
EC2	18.2 (3.7)	291.7 (58.9)	15.6	218.8 (44.2)
EC11	23.4 (11.1)	250	11.8 (5.5)	72.9 (44.2)
EC26	20.8 (7.4)	229.2 (29.5)	9.1 (5.5)	99.0 (36.8)
EC28	16.9 (12.9)	250	7.5 (1.4)	117.2 (18.4)
EC34	27.3 (12.9)	250	7.2 (0.9)	88.5 (66.3)
EC958	10.4	250	9.1 (1.8)	208.3
CFT073	18.2 (14.7)	145.8 (29.5)	7.8	125

Strain	Independent		Combined	
	Silver nitrate (μg/ml)	**Furanone-C30 (μg/ml)**	**Silver nitrate (μg/ml)**	**Furanone-C30 (μg/ml)**
EC1	26.0 (7.4)	416.7 (117.9)	18.2 (3.7)	145.8 (29.5)
EC2	11.7 (1.8)	250	5.9 (2.8)	93.8 (44.2)
EC11	36.5 (7.4)	500	14.3 (1.8)	109.4 (81.0)
EC26	31.3	458.3 (58.9)	15.6	156.3 (44.2)
EC28	31.3	416.7 (117.9)	16.9 (1.8)	145.8 (29.5)
EC34	20.8 (7.4)	250	9.8 (8.3)	125
EC958	52.1 (44.2)	125	586 (2.8)	57.3 (7.4)
CFT073	17.1 (9.0)	208.3 (58.9)	7.8	78.0 (7.1)

Strain	Independent		Combined	
	Triclosan (μg/ml)	**Furanone-C30 (μg/ml)**	**Triclosan (μg/ml)**	**Furanone-C30 (μg/ml)**
EC1	2.3 (0.8)	250	1.4 (0.9)	145.8 (29.5)
EC2	5.3 (1.9)	333.3 (117.9)	6 (2.8)	229.2 (29.5)
EC11	1.3	250	2.2 (0.2)	187.5 (29.5)
EC26	2.8 (0.7)	250	2.0 (1.8)	125
EC28	6.7 (1.9)	291.7 (58.9)	6 (2.8)	229.2 (29.5)
EC34	2.4 (2.2)	250	2	208.3
EC958	6.7	500	6 (0.9)	416.7
CFT073	3.7 (0.5)	458.3 (58.9)	4	354.2 (88.4)

All concentrations are in μg/ml and are an average of two biological repeats, each with 3 technical replicates, standard deviation represented in brackets where required. Combinations with a synergistic interaction are in bold.

Table 8.12. Minimum biofilm eradication concentrations of biocides (PHMB, BAC, silver nitrate and triclosan) and cinnamaldehyde alone and in combinations.

Strain	Independent		Combined	
	PHMB (μg/ml)	Cinnamaldehyde (μg/ml)	PHMB (μg/ml)	Cinnamaldehyde (μg/ml)
EC1	**151.0 (110.5)**	**2000**	**6.5 (3.7)**	**500**
EC2	**104.2 (58.9)**	**2000**	**11.7 (9.2)**	**500**
EC11	**99.0 (22.1)**	**2000**	**10.4 (0.0)**	**500**
EC26	**125 (88.4)**	**2000**	**9.1 (5.5)**	**458.3 (58.9)**
EC28	**106.8 (25.8)**	**2000**	**16.3 (3.8)**	**458.3 (58.9)**
EC34	99.0 (36.8)	1166.7 (235.7)	41.7 (29.5)	416.7
EC958	**166.7**	**2333.3 (471.4)**	**36.5 (22.1)**	**583.3 (353.6)**
CFT073	78.1 (7.4)	1333.3 (471.4)	28.6 (25.8)	270.8 (29.5)

Strain	Independent		Combined	
	BAC (μg/ml)	Cinnamaldehyde (μg/ml)	BAC (μg/ml)	Cinnamaldehyde (μg/ml)
EC1	**114.6 (14.7)**	**1500 (707.1)**	**19.5 (12.9)**	**416.7**
EC2	114.6 (14.7)	1666.7 (471.4)	33.8 (25.8)	541.7 (176.8)
EC11	**197.9 (44.2)**	**1500 (707.1)**	**31.3 (7.3)**	**458.3 (58.9)**
EC26	166.7	1666.7	27.3 (9.2)	583.3 (117.9)
EC28	125 (58.9)	1833.3 (235.7)	32.6 (27.7)	500 (117.9)
EC34	**125**	**1333.3 (471.4)**	**14.3 (1.8)**	**375 (58.9)**
EC958	**72.9 (14.7)**	**2000**	**11.7 (1.8)**	**541.7 (294.6)**
CFT073	**46.9 (7.4)**	**1666.7 (471.4)**	**12.9 (0.2)**	**312.5 (147.3)**

Strain	Independent		Combined	
	Silver nitrate (μg/ml)	Cinnamaldehyde (μg/ml)	Silver nitrate (μg/ml)	Cinnamaldehyde (μg/ml)
EC1	**3125 (294.6)**	**1000**	**273.5 (202.5)**	**291.7 (58.9)**
EC2	**3333.33**	**1666.7 (471.4)**	**312.5**	**291.7 (58.9)**
EC11	**2083.3 (589.3)**	**1666.7 (471.4)**	**299.5 (165.7)**	**229.2 (29.5)**
EC26	**2083.3**	**1500 (235.7)**	**156.3 (73.7)**	**312.5 (147.3)**
EC28	**2031.3 (1841.4)**	**2000**	**227.9 (193.4)**	**458.3 (58.9)**
EC34	**2500 (589.3)**	**1666.7**	**136.7 (138.1)**	**583.3 (117.6)**
EC958	**2916.7 (1178.5)**	**2000**	**781.3 (662.9)**	**375 (176.8)**
CFT073	**520.8**	**1166.7 (235.7)**	**41.7 (3.7)**	**291.7 (58.9)**

Strain	Independent		Combined	
	Triclosan (μg/ml)	Cinnamaldehyde (μg/ml)	Triclosan (μg/ml)	Cinnamaldehyde (μg/ml)
EC1	4	1833.3 (235.7)	7.3 (0.9)	1333.3
EC2	13.3	2000	17.3 (1.9)	1833.3 (707.1)
EC11	7.3 (0.9)	2000	12 (5.7)	1333.3 (471.4)
EC26	8	2000	16	1666.7
EC28	4	1833.3 (235.7)	9.3 (1.9)	1500 (707.1)
EC34	1.7 (0.5)	1000	3.7 (0.5)	916.7 (117.9)
EC958	3.7 (0.5)	4666.7 (942.8)	6 (2.8)	2833.3 (1649.9)
CFT073	2.3 (0.5)	1000	2.3 (1.4)	583.3 (117.9)

All concentrations are in μg/ml and are an average of two biological repeats, each with 3 technical replicates, standard deviation represented in brackets where required. Combinations with a synergistic interaction are in bold.

Table 8.13. Minimum biofilm eradication concentrations of biocides (PHMB, BAC, silver nitrate and triclosan) and furanone-C30 alone and in combinations.

Strain	Independent		Combined	
	PHMB (μg/ml)	Furanone-C30 (μg/ml)	PHMB (μg/ml)	Furanone-C30 (μg/ml)
EC1	**312.5 (147.1)**	**500**	**5.9 (0.9)**	**125**
EC2	166.7 (176.8)	375 (58.9)	28.7 (3.7)	109.4 (22.1)
EC11	166.7 (58.9)	145.8 (29.5)	70.3 (25.8)	72.9 (44.2)
EC26	260.4 (14.7)	125	83.3 (29.5)	26.0 (7.3)
EC28	**166.7 (117.9)**	**375 (58.9)**	**14.7 (16.1)**	**96.4 (40.5)**
EC34	57.3 (22.1)	135.4 (44.2)	36.5 (22.1)	41.7 (14.7)
EC958	**104.2**	**458.3 (58.9)**	**11.1 (0.9)**	**125**
CFT073	44.3 (25.8)	250	26.0 (7.4)	57.3 (7.4)

Strain	Independent		Combined	
	BAC (μg/ml)	Furanone-C30 (μg/ml)	BAC (μg/ml)	Furanone-C30 (μg/ml)
EC1	**114.6 (14.7)**	**500**	**20.8 (11.1)**	**52.1 (14.7)**
EC2	72.9 (14.7)	416.7	31.3	57.3 (36.8)
EC11	177.1 (44.2)	145.8 (29.5)	33.9 (11.1)	52.1 (14.7)
EC26	41.7 (0)	229.2 (29.5)	13.0	72.9 (14.7)
EC28	**117.2 (18.4)**	**416.7**	**31.3**	**57.3 (7.4)**
EC34	54.7 (11.1)	125	13.0 (3.7)	36.5 (14.7)
EC958	**104.2 (29.5)**	**375 (58.9)**	**15.6**	**93.8 (44.2)**
CFT073	**88.5 (51.6)**	**250**	**12.4 (10.1)**	**54.7 (11.1)**

Strain	Independent		Combined	
	Silver nitrate (μg/ml)	Furanone-C30 (μg/ml)	Silver nitrate (μg/ml)	Furanone-C30 (μg/ml)
EC1	**1380.2 (1583.6)**	**250**	**97.7 (82.9)**	**62.5**
EC2	5000	250	925.8 (1195.1)	83.3 (29.5)
EC11	**3020.8 (2799.0)**	**208.3 (58.9)**	**52.1 (18.4)**	**39.1 (18.4)**
EC26	**2177.1 (456.7)**	**125**	**84.6 (9.2)**	**15.6**
EC28	**2500**	**333.3 (117.9)**	**195.3 (18.4)**	**52.1 (14.7)**
EC34	2916.7 (589.3)	333.3	664.1 (313.0)	114.6 (14.7)
EC958	**5833.3 (1178.5)**	**416.7**	**299.5 (165.7)**	**62.5**
CFT073	**4166.7 (1178.5)**	**166.7 (58.9)**	**455.7 (128.9)**	**41.7 (14.7)**

Strain	Independent		Combined	
	Triclosan (μg/ml)	Furanone-C30 (μg/ml)	Triclosan (μg/ml)	Furanone-C30 (μg/ml)
EC1	1.2 (0.2)	375 (58.9)	2.0	229.2 (29.5)
EC2	8.0	416.7 (117.9)	6.1 (0.8)	250
EC11	0.8	229.2 (29.5)	0.7 (0.2)	208.3 (58.9)
EC26	2.0	125	2.0	125
EC28	2.0	250	1.0 (0.7)	250
EC34	4.0	250	4.0	291.7 (58.9)
EC958	6.7 (1.9)	458.3 (58.9)	4 .0	250
CFT073	8.0	250	8.0	250

All concentrations are in μg/ml and are an average of two biological repeats, each with 3 technical replicates, standard deviation represented in brackets where required. Combinations with a synergistic interaction are in bold.

9. Secret Bonus Chapter

This secret bonus chapter showcases the Art of Science event held at Millennium Galleries in Sheffield on the 17th of March 2022 for which I obtained funding, planned, ran, evaluated and disseminated.

7.1.Grant Application

This is a copy of the application submitted for the Outreach and Engagement grant from Applied Microbiology International. The grant was submitted by me and written in collaboration with Sarah Forbes and Mel Lacey and contributed towards an artist in residence and printing of research images, a black out tent and fluorescent microbes, and many other art materials which were used on the evening. A total of £3560 was awarded.

Full Name: Kelly Capper-Parkin

Are you an SfAM member? Yes

Please provide a short summary of your experience in public engagement. If this is your first foray into public engagement, then a short summary of a mentor/partner is required

Kelly Capper-Parkin (SfAM member)

I am a microbiology PhD student, keen to increase my experience in public engagement. Within my PhD career I have entered, and came runner up, in the universities 3 Minute Thesis competition, where I had just 3 minutes to present my research to a lay audience. My previous experience in outreach includes volunteering for the Explore! event, run at Sheffield Hallam University and I am a member of the STEM ambassador programme which aims to promote STEM subjects to young people.

Dr Mel Lacey (SfAM member)

I have been actively involved in outreach since commencing my career in academic research as a PhD student and research associate. Since commencing my lectureship and BSc Biology course lead position at Sheffield Hallam University I have been part of a team tasked with managing the universities flagship event for Sheffield Festival of Science and Engineering, Explore! This event is based on promoting science within school age children and achieved over 1500 visitors in 2019. Outside of academia I am involved in promoting science within local schools through participation in science clubs and the Café Scientific programme. I have obtained previous outreach funding from the Microbiology Society to establish pioneer outreach activities in collaboration with Sheffield Museums Trust (formerly Museums Sheffield). In 2017 we ran an adult education evening at Millennium Gallery Sheffield entitled “The Horror Within” and in 2018 we followed up this event with the sequel “The Science of Science Fiction. Both of these events were attended by over 200 members of the local community. As well as running interactive public engagement exhibitions I have established a collaboration with the Steel Minions game studio after successfully obtaining a £10,000 Microbiology Education Resource grant in which we developed a website-based computer game and App entitled “Build a Bacteria” which aimed to teach school age children about bacterial structure and function. More recently I have secured funds of over £26,000 to update codesigned citizen science research projects aimed to increase this visibly and accessibility of science research in local school children.

Dr Sarah Forbes (non- SfAM member)

Throughout my academic career I have acquired substantial experience in the field of science communication. I have previously worked with the RCUK School-University Partnerships Initiative and Aim Higher Microbiology both of which aim to establish links between universities and local schools. I work as a scientific consultant for Guerrilla Science- a Wellcome Trust funded science communication group and as part of this role have designed and led large microbiology themed outreach events for UK music festivals which received more than 20,000 attendees. These events have been reviewed for articles published in Microbiology Today, New Scientist and The Guardian (1). I hold a close working relationship with Sheffield Museums Trust having collaborated on previous outreach initiatives involving the successful procurement of outreach based funding from the Microbiology Society. During these events

we have developed and managed family activity days at Western Park Museum under the theme of bacterial biofilms and antimicrobial resistance and adult education evenings as part of Millennium Galleries "live late" series. I have designed and run interactive exhibitions at both Manchester Science Festival and Sheffield Festival of Science and Engineering under the themes of infection transmission, antibiotic drug discovery and disease diagnosis. I have also participated in "Hands on Science" events at the Moor Market, an indoor farmers market at the heart of Sheffield's community.

(1) https://www.theguardian.com/science/blog/2011/jun/30/dirt-nudity-tears-glastonbury

Catherine Higham (non- SfAM member)

I am a practising artist & landscape architect. I combine landscape design consultancy work with the pursuit of my own art practice; primarily drawing and painting concerned with the materials and processes of landscape. I also take part in collaborative art projects and residencies, undertake illustration work, and I have been a Studio Tutor at the University of Sheffield's School of Landscape Architecture since 2010.

Inspired by the purchase of a telescope and an astronomy themed residency, my current art practice explores the interplay between the Earth, Sun and Moon; their materials and processes, surfaces and topography, light and space, cycles and rhythms, time and transience.

Experimenting with various media to investigate this new subject, work includes graphite, charcoal and chalk drawings on wood, drawings on scraperboard, ink and oil paintings, digital photography and solargraphs. Materials used and methods of practice continue a long-term interest in juxtaposing serendipity with intent, randomness with precision, the precious with the everyday. The work often combines tangible, everyday patterns and forms from landscapes on Earth (specifically local places with personal resonance), with more theoretical, abstract, and imagined marks, geometries and depictions.

For more information on my work, please visit cjhigham.com

Project title and start date

The Art of Science. Project start date: 01.03.22

Funding will be withdrawn, and no payment made if claims are NOT received by the Society within 12 months of the project start date. Do you need to make a special request to extend this period?

No

Target audience

Adult students and professionals from a range of subject specific backgrounds including those who would not typically attend a science event. We have attracted this audience to previous events.

Numbers

250 +

Activity description

To quote Albert Einstein; "The most beautiful thing we can experience is the mysterious. It is the source of all true art and all science. So, the unknown, the mysterious, is where art and science meet". We aim to explore the interplay between art and science by bringing together academics from Sheffield Hallam University and local artists in order to create an interactive showcase as part of the "Live Late" series hosted by Sheffield Museums Trust. The focus of this event will be to introduce the general public to the world of microbiology through the use of different forms of art, providing a visual gateway to science with the aim of appealing to new audiences that would not normally seek out a science event. We will explore artistic responses to scientific findings, educating the public on topical issues through a range of activities, installations and talks. In addition to the Sheffield Hallam University lead events below, Sheffield Museums Trust will also provide a range of activities.

Activity 1:

Beautiful but deadly; mini lecture series. Academic staff, research associates and PhD students. The Biomolecular Sciences Research Centre, Sheffield Hallam University.

The microbial world is populated by invisible predators that aim to infect and destroy their host. These microscopic hunters may be beautiful in presence, but they can have catastrophic consequences for

human life. We take a close up view of some of the world's most lethal bacteria, viruses and parasites to reveal the contrast between their elegant appearance and grotesque intentions.

Example presentations

i) Covid: the beauty behind the pandemic

ii) Crystalline symmetry: bacterial S- layers

iii) Capsid assembly: A dance with death

iv) Luminescent and life threatening: Bacterial communication.

Activity 2:

Artist in residence; innovative and collaborative artwork produced by Catherine Higham with the academic project leads. The Biomolecular Sciences Research Centre, Sheffield Hallam University.

This piece of work will explore the parallels between art and science via an extended discussion and art production between the artist in residence (CH) and the microbiology leads (KC, ML, SF). The work will focus on the novel research of the group, encompassing how bacterial colonies from a sample streak plate are investigated and analysed against a backdrop of antibiotic resistance. This piece will be unveiled at the Live Late event with CH and a member of the research team to discuss the work with the public including the research it is based on and the themes within it. The creation of the piece will be an organic process with likely themes being the commonalities between the art and science world, e.g. the aim to record what is observed and experienced, and discovery, investigation and communication of new ideas. The process leading up to the creation of the piece will be recorded and made into a short video which will play alongside the exhibition.

Activity 3:

A Picture's Worth a Thousand Words; Research Exhibition. Academic staff, research associates and PhD students. The Biomolecular Sciences Research Centre, Sheffield Hallam University.

Scientific research is often disseminated throughout the academic community by means of poster presentations to display data. We aim to showcase current advances within the field of microbiology by choosing representative images from ongoing research projects within the department. We will produce an “Art of Science” exhibition consisting of printed and framed images displayed within the art space of Millennium Gallery. Presenters will use their image to engage members of the public and discuss their current research.

In our one-of-a-kind light box, bacterial strains and species currently being studied within the Biomolecular Sciences Research Centre at Sheffield Hallam university will be showcased. Chromogenic agars will be used to bring out the artistic side of bacterial growth media.

Activity 4:

Life is Art; In conjunction with the ongoing interactive talks and exhibitions, several activities will also be available to give attending members of the public a hands-on experience with creating visual representations of microbiology.

i) Reinventing Life Drawing: The human body is a teaming ecosystem of microorganisms made up of a series of ecological niches each with distinct microbial communities. We invite the public to explore their own microbiomes by recreating the human figure on agar using the relevant members of the microbiota for each region of the body. Participants will be provided with a reference number and link to our Outreach Instagram account so that they can see their individual microbial landscapes post incubation.

ii) Building a Community: Recreating microbial communities remains one of the most challenging aspect in microbial ecology. We will discuss the concepts of microbial biofilm formation and the impact of biofilm associated infections on human health by using mixed-media sculpture to recreate the structural and textural complexities of the biofilm.

iii) Pathogen Purling: bacterial pathogens damage their human hosts in a multitude of ways. Visitors will learn about the pathogenesis of harmful bacteria by purling (or knitting) their own synthetic pathogen.

iv) Pastel pathogens: Urinary tract infection is the number one cause of healthcare associated infections and may cause serious medical sequelae and economic consequences for healthcare service providers. Visitors will be invited to explore the tones and textures of uropathogenic Escherichia coli and Proteus mirabilis using pastels and paints to recreate the shapes and colours observed down the microscope.

v) After Darkness Comes Light: Unravel the secret language of bacteria by immersion in our living light exhibition. Participants will be able to walk through the blackout chamber and observe our luminescent bacterial art created by Sheffield Hallam students and their interpretation of bacteria agar art.

vi) Everything is connected: Visitors will learn about current research linking historic metal contamination and antibiotic resistance in Yorkshire soils. By observing the colours and textures of soil samples, soil microbes, antibiotics and metal solutions, participants will be invited to make their own Jean Dubuffet inspired soil textured painting.

Individuals and/or organisations involved

Sheffield Hallam University- Biomolecular Research Centre: Kelly Capper-Parkin, Mel Lacey & Sarah Forbes, additional staff and PhD student volunteers. Catherine Higham. Sheffield Museums Trust.

Dissemination plan

The event will be advertised through Sheffield Hallam University's website, posters around campus and through social media outlets. Sheffield Museums Trust will also advertise the event through their museum sites, in print as well as their website and social media outlets. We will contact the Sheffield Star and the Sheffield Telegraph Newspapers closer to the date of the exhibition as they carry an 'up and coming' events section in their various forms of publication (e.g. https://www.museums-sheffield.org.uk/whats-on/lates).

Will PE resources that are developed be made available for SfAM community use?

All the videos created for the event will be freely available online after the event. We will also make freely available details of activities that were undertaken and the evaluation used. We will also be happy to showcase the resources and how we organised the event at future SfAM events and online.

What will your project legacy look like?

Public education on the role of microorganisms in health and disease relies heavily on professionals in healthcare, with direct patient contact often in very limited time and in difficult situations. Bridging the gap between the scientific community and the general public will facilitate improved awareness and understanding of topical scientific issues such as: antimicrobial resistance, the importance of the microbiome in health and disease and the value of microorganisms in biotechnology. Furthermore, by continuing in our collaborative outreach efforts with Sheffield Museums Trust we provide experience for doctoral students to improve their abilities as effective science communicators within the field of microbiology, opening up opportunities for future employment within this field.

Upon leaving the event, we will provide a questionnaire for participants to fill in which will cover: i) visitor demographics to determine the reach of the event and which communities are under-represented. ii) microbiology themed quizzes covering topics outlined during the course of the event to evaluate the learning of the participants, iii) questions to determine the impact of the event on visitors' science capital. Analysis of this questionnaire, along with event details, will be disseminated to the academic community through a case study style outreach journal article.

Within this event we will make use of equipment and resources purchased from previous outreach grants (e.g. the light box) alongside some materials donated from Sheffield Hallam University. With this added equipment we will have a diverse and interactive microbiology exhibit that can be tailored for all ages and all scientific backgrounds at a variety of other outreach events. We are keen to take this exhibit to other outreach events both within Sheffield Hallam University and across the city.

Please explain any relevant health and safety concerns, and how you will overcome these issues

In hands-on activities PPE will be provided, hand sanitiser available and only risk group 1 organisms will be used. All other microorganisms will be fixed or sealed in petri dishes. More info below.

If this is a face-to-face event or activity please state what measures have been put in place to ensure this event takes place in a COVID-secure environment, in line with governmental guidance.

In line with government advice, to mitigate the risks of COVID wearing of face coverings, distancing and handwashing will be encouraged. All guests and volunteers will be encouraged to take lateral flow tests prior to attending the event. All exhibitions will be spaced out to allow distancing and the space will be well ventilated.

Full risk assessments will be carried out both by Sheffield Hallam University and Sheffield Museums Trust, to ensure the event is as safe as possible and adhering to all current government guidance.

Total funding requested (£) – please also include a detailed breakdown of expenditure

Total funding: £3,560.

- Microbiology and lab consumables £1,030. (Disposable lab coats and gloves, £440, petri dishes and loops £250, Aliivibrio fischeri strain £120, agars £220.)

- Art materials £690. (Artist in residence £500, paint, brushes, pastels and paper £120, wool and fabric, £70.)

- Black tent and black light £540.

- Printing & framing £500.

- Room hire £500.

- Evaluation £300. (£20 focus group participant voucher x 10, £200, transcription £100.)

Have you applied for funds elsewhere?

No

7.2. Blog post for AMI

As a condition of the grant claim, the event had to be written up as a blog post for Applied Microbiology International. The blog is copied in full here, the online version is available at: https://appliedmicrobiology.org/resource/the-art-of-science.html

The Art of Science

Kelly Capper-Parkin used an Outreach and Engagement grant to demonstrate the art found in microbiology and beyond.

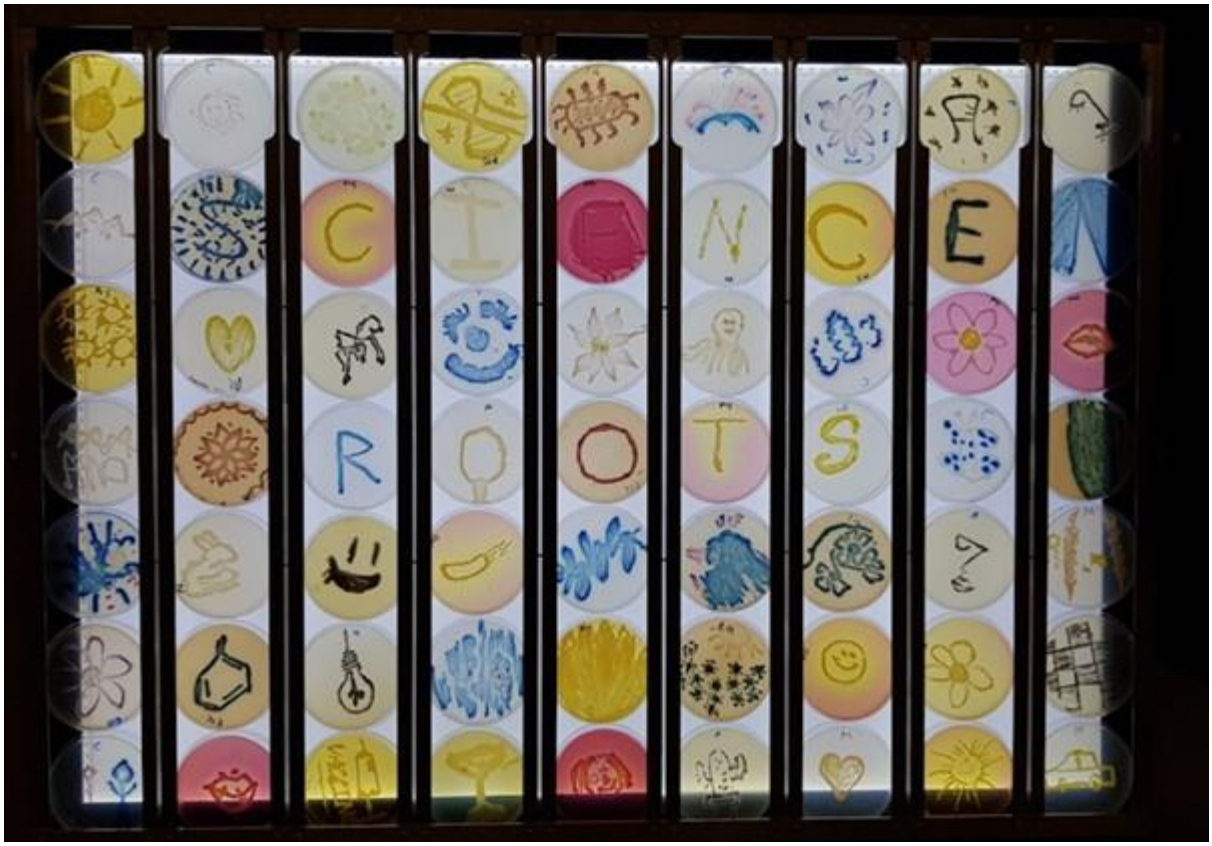

What does Science look like? Is it boring graphs, spreadsheets and stuck in the laboratories of university; or is it colourful, found everywhere anyone may be and beautiful? With support from a AMI Outreach and Engagement Grant we hosted a Live Lates event (an afterhours social event) at the Millennium Gallery, in the heart of Sheffield. Bringing science out of the lab and into the art gallery.

The aim of this event was to reach out to an adult audience from a wide range of different backgrounds, particularly those who would not normally attend a science focused event. We took the opportunity to showcase the beauty of microbiology through a range of different art forms, providing a visual gateway to science through hands on activities, a gallery of current research and a mini lecture series.

Centre stage to the event was an Artist in Residence Exhibition by Catherine Higham. In the weeks before the event Catherine had been into the microbiology research lab to

find out more about the soil microbiome project. Her visit to the lab inspired her work for the evening which was projected onto the main wall of the gallery.

In the centre of the main gallery space, PhD and Masters students presented their research in the style of paintings in a gallery. Standing next to their images for some of the evening were the "Artists", talking to guests about their work. *"It was really interesting to hear about what people thought my work was a depiction of before I explained it to them"*, Lucy Dascombe said about her micro-CT image of bones. *"It gave me a perspective on my work in wider society, much more varied than the views and opinions I would normal have at a science specific event"*.

One of the main attractions of the evening was the After Dark Tent; a black out tent which was filled with luminescent agar art of students from all levels, from undergraduate to PhD. There was a constant queue to get it and find out the mystery of what was inside. Guests were allowed in 4 at a time and told all about the natural fluorescence and bioluminescence of bacteria and their symbiotic relationships in nature. From the exit questionnaire it was a firm favourite of the activities on the night.

The night also offered many chances for people to get hands on with both Art and Science. At the Building a Community stand, guests helped to mature our microcolony of knitted and crocheted bacteria into a woolly, mature, polymicrobial biofilm. Adding to the biofilm their own pom-pom bacteria or taking them home with them. Sarah Boyce a PhD student working on biofilm joint infections ran the stand; *"It was a great evening, I got to combine my hobby of crochet with talking about biofilms and my research".*

The Reinventing Life Drawing activity allowed people to investigate their own microbiomes. Guests were encouraged to swab a part of their body and then draw onto agar plates. The agar plates were incubated and shared on social media for people to see their live drawings. The creativity of some guests was brilliant and worth checking out on the @SHU.micro Instagram page.

Many guests enjoyed the Pastel Pathogens stand, where they had the opportunity to look down a microscope at a range of pathogens, creating a pastel picture of what they observed. The soil microbiome project also had a stand, where colour paintings made of the different components of soil were made. Many people listed these as highlights of their visit on the exit questionnaires, when asked what they found interesting about the evening comments included: "U*sing the microscopes!!!*" and "*I loved learning about the living things in our soils!"*.

A mini-lecture series ran though some of the evening with talks from academic staff and PhD students. *"Explaining my research to a wide range of people was a great experience"* said Alex Williamson, who talked about 3D imaging and micro-CT techniques he uses in his PhD. Other than Microbiology, other research areas got involved, people had the opportunity to make their own blood clots, create a model of bone structures and assemble, then devour, edible DNA made of sweets. The Millennium Gallery team also put on other activities as well, including exclusive tours of the exhibits and more hands-on experiences alongside a bar and an amazing cake stand meant that everyone who attended had a great night.

Over the course of the evening more than 300 people attended, there was a great atmosphere throughout, and many people said how much they had enjoyed the event on the night as well as in the feedback questionnaires. *"It was nice to have my friends*

come along to a 'work' event and show them what I do, but in a really casual setting" said Lucy after the event. Alex said, *"It was nice to talk to such a range of people about my research, there were so many different people. I spoke to post-docs, artists, writers, people who knew nothing about science and people who knew lots".*

The evening was a success, with higher and a more diverse attendance than we have had at previous events. We showcased science as an art form and had a wonderful evening. *"Thank you very much, I've had a lovely evening :)"* – a comment on the feedback form.

Kelly Capper-Parkin

Sheffield Hallam University

Published 05/08/22

7.3. Poster

In connection to the paper, the research was presented at the Teaching Symposium at Microbiology Annual Conference 2023 – Birmingham. Replicated here is the poster presented.

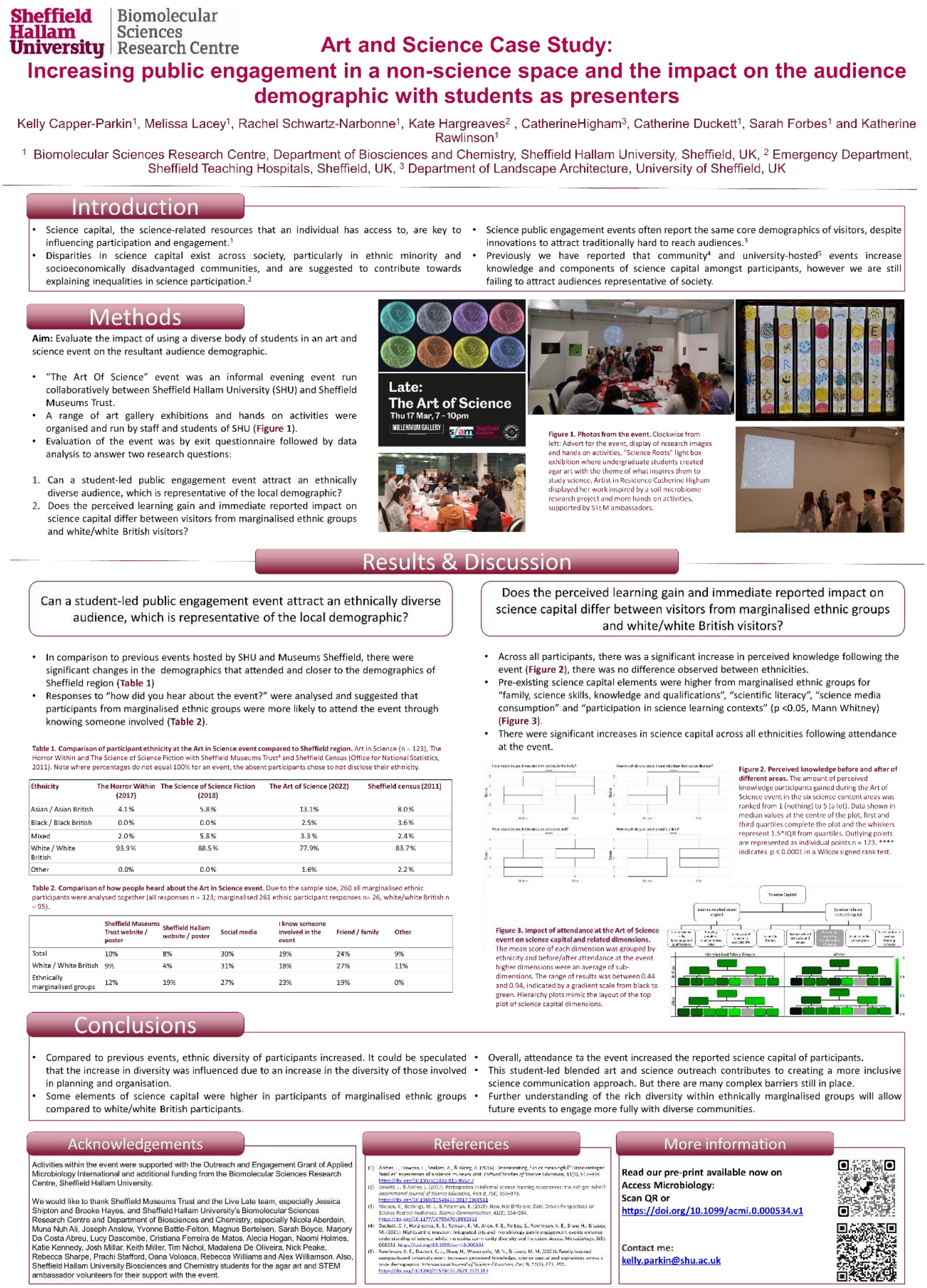

Sheffield Hallam University | Biomolecular Sciences Research Centre

Art and Science Case Study: Increasing public engagement in a non-science space and the impact on the audience demographic with students as presenters

Kelly Capper-Parkin[1], Melissa Lacey[1], Rachel Schwartz-Narbonne[1], Kate Hargreaves[2], CatherineHigham[3], Catherine Duckett[1], Sarah Forbes[1] and Katherine Rawlinson[1]

[1] Biomolecular Sciences Research Centre, Department of Biosciences and Chemistry, Sheffield Hallam University, Sheffield, UK, [2] Emergency Department, Sheffield Teaching Hospitals, Sheffield, UK, [3] Department of Landscape Architecture, University of Sheffield, UK

Introduction

- Science capital, the science-related resources that an individual has access to, are key to influencing participation and engagement.[1]
- Disparities in science capital exist across society, particularly in ethnic minority and socioeconomically disadvantaged communities, and are suggested to contribute towards explaining inequalities in science participation.[2]
- Science public engagement events often report the same core demographics of visitors, despite innovations to attract traditionally hard to reach audiences.[3]
- Previously we have reported that community[4] and university-hosted[5] events increase knowledge and components of science capital amongst participants, however we are still failing to attract audiences representative of society.

Methods

Aim: Evaluate the impact of using a diverse body of students in an art and science event on the resultant audience demographic.

- "The Art Of Science" event was an informal evening event run collaboratively between Sheffield Hallam University (SHU) and Sheffield Museums Trust.
- A range of art gallery exhibitions and hands on activities were organised and run by staff and students of SHU (**Figure 1**).
- Evaluation of the event was by exit questionnaire followed by data analysis to answer two research questions:

1. Can a student-led public engagement event attract an ethnically diverse audience, which is representative of the local demographic?
2. Does the perceived learning gain and immediate reported impact on science capital differ between visitors from marginalised ethnic groups and white/white British visitors?

Late: The Art of Science
Thu 17 Mar, 7 – 10pm
MILLENNIUM GALLERY

Figure 1. Photos from the event. Clockwise from left: Advert for the event, display of research images and hands on activities, "Science Roots" light box exhibition where undergraduate students created agar art with the theme of what inspires them to study science, Artist in Residence Catherine Higham displayed her work inspired by a soil microbiome research project and more hands on activities, supported by STEM ambassadors.

Results & Discussion

Can a student-led public engagement event attract an ethnically diverse audience, which is representative of the local demographic?

- In comparison to previous events hosted by SHU and Museums Sheffield, there were significant changes in the demographics that attended and closer to the demographics of Sheffield region (**Table 1**)
- Responses to "how did you hear about the event?" were analysed and suggested that participants from marginalised ethnic groups were more likely to attend the event through knowing someone involved (**Table 2**).

Table 1. Comparison of participant ethnicity at the Art in Science event compared to Sheffield region. Art in Science (n = 123), The Horror Within and The Science of Science Fiction with Sheffield Museums Trust[4] and Sheffield Census (Office for National Statistics, 2011). Note where percentages do not equal 100% for an event, the absent participants chose to not disclose their ethnicity.

Ethnicity	The Horror Within (2017)	The Science of Science Fiction (2018)	The Art of Science (2022)	Sheffield census (2011)
Asian / Asian British	4.1%	5.8%	13.1%	8.0%
Black / Black British	0.0%	0.0%	2.5%	3.6%
Mixed	2.0%	5.8%	3.3%	2.4%
White / White British	93.9%	88.5%	77.9%	83.7%
Other	0.0%	0.0%	1.6%	2.2%

Table 2. Comparison of how people heard about the Art in Science event. Due to the sample size, 260 all marginalised ethnic participants were analysed together (all responses n = 123; marginalised 261 ethnic participant responses n= 26, white/white British n = 95).

	Sheffield Museums Trust website / poster	Sheffield Hallam website / poster	Social media	I know someone involved in the event	Friend / family	Other
Total	10%	8%	30%	19%	24%	9%
White / White British	9%	4%	31%	18%	27%	11%
Ethnically marginalised groups	12%	19%	27%	23%	19%	0%

Does the perceived learning gain and immediate reported impact on science capital differ between visitors from marginalised ethnic groups and white/white British visitors?

- Across all participants, there was a significant increase in perceived knowledge following the event (**Figure 2**), there was no difference observed between ethnicities.
- Pre-existing science capital elements were higher from marginalised ethnic groups for "family, science skills, knowledge and qualifications", "scientific literacy", "science media consumption" and "participation in science learning contexts" ($p < 0.05$, Mann Whitney) (**Figure 3**).
- There were significant increases in science capital across all ethnicities following attendance at the event.

Figure 2. Perceived knowledge before and after of different areas. The amount of perceived knowledge participants gained during the Art of Science event in the six science content areas was ranked from 1 (nothing) to 5 (a lot). Data shown in median values at the centre of the plot, first and third quartiles complete the plot and the whiskers represent 1.5*IQR from quartiles. Outlying points are represented as individual points n = 123. **** indicates $p \leq 0.0001$ in a Wilcox signed rank test.

Science Capital
Science related social capital
Science related cultural capital
Marginalised Ethnic Groups
White
Before
After

Figure 3. Impact of attendance at the Art of Science event on science capital and related dimensions. The mean score of each dimension was grouped by ethnicity and before/after attendance at the event higher dimensions were an average of sub-dimensions. The range of results was between 0.44 and 0.94, indicated by a gradient scale from black to green. Hierarchy plots mimic the layout of the top plot of science capital dimensions.

Conclusions

- Compared to previous events, ethnic diversity of participants increased. It could be speculated that the increase in diversity was influenced due to an increase in the diversity of those involved in planning and organisation.
- Some elements of science capital were higher in participants of marginalised ethnic groups compared to white/white British participants.
- Overall, attendance ta the event increased the reported science capital of participants.
- This student-led blended art and science outreach contributes to creating a more inclusive science communication approach. But there are many complex barriers still in place.
- Further understanding of the rich diversity within ethnically marginalised groups will allow future events to engage more fully with diverse communities.

Acknowledgements

Activities within the event were supported with the Outreach and Engagement Grant of Applied Microbiology International and additional funding from the Biomolecular Sciences Research Centre, Sheffield Hallam University.

We would like to thank Sheffield Museums Trust and the Live Late team, especially Jessica Shipton and Brooke Hayes, and Sheffield Hallam University's Biomolecular Sciences Research Centre and Department of Biosciences and Chemistry, especially Nicola Aberdein, Muna Nuh Ali, Joseph Anslow, Yvonne Battle-Felton, Magnus Bertelsen, Sarah Boyce, Marjory Da Costa Abreu, Lucy Dascombe, Cristiana Ferreira de Matos, Alecia Hogan, Naomi Holmes, Katie Kennedy, Josh Millar, Keith Miller, Tim Nichol, Madalena De Oliveira, Nick Peake, Rebecca Sharpe, Prachi Stafford, Oana Voloaca, Rebecca Williams and Alex Williamson. Also, Sheffield Hallam University Biosciences and Chemistry students for the agar art and STEM ambassador volunteers for their support with the event.

References

(1) Archer, L., Dawson, E., Seakins, A., & Wong, B. (2016). Disorientating, fun or meaningful? Disadvantaged families' experiences of a science museum visit. Cultural Studies of Science Education, 11(4), 917–939. https://doi.org/10.1007/s11422-015-9667-7
(2) DeWitt, J., & Archer, L. (2017). Participation in informal science learning experiences: the rich get richer? International Journal of Science Education, Part B, 7(4), 356–373. https://doi.org/10.1080/21548455.2017.1360531
(3) Nielsen, K., Gathings, M. J., & Peterman, K. (2019). New, Not Different: Data-Driven Perspectives on Science Festival Audiences. Science Communication, 41(2), 254–264. https://doi.org/10.1177/1075547019832312
(4) Duckett, C. J., Hargreaves, K. E., Rawson, K. M., Allen, K. E., Forbes, S., Rawlinson, K. E., Shaw, H., & Lacey, M. (2021). Nights at the museum: integrated arts and microbiology public engagement events enhance understanding of science whilst increasing community diversity and inclusion. Access Microbiology, 3(5), 000231. https://doi.org/10.1099/acmi.0.000231
(5) Rawlinson, K. E., Duckett, C. J., Shaw, H., Woodcock, M. V., & Lacey, M. M. (2021). Family-focused campus-based university event increases perceived knowledge, science capital and aspirations across a wide demographic. International Journal of Science Education, Part B, 11(3), 273–291. https://doi.org/10.1080/21548455.2021.1971319

More information

Read our pre-print available now on Access Microbiology:
Scan QR or
https://doi.org/10.1099/acmi.0.000534.v1

Contact me:
kelly.parkin@shu.ac.uk

7.4.Research Paper

In the build up to the Art of Science event, the Bioscience and Chemistry students were involved in the preparation of the events and as STEM ambassadors on the evening of the event. The outcome of engaging the diverse student cohort was that the participants at the event were more representative of the demographics of Sheffield.

The paper was published in Access Microbiology on the 29th August 2023. The open access paper is available at: https://doi.org/10.1099/acmi.0.000534.v3 https://doi.org/10.1099/acmi.0.000534.v3

ACCESS MICROBIOLOGY
an open research platform

PEDAGOGY
Lacey *et al.*, *Access Microbiology* 2023;5:000534.v3
DOI 10.1099/acmi.0.000534.v3

MICROBIOLOGY SOCIETY
OPEN DATA OPEN ACCESS

University student-led public engagement event: increasing audience diversity and impact in a non-science space

Melissa M. Lacey[1,*], Kelly Capper-Parkin[1], Rachel Schwartz-Narbonne[1], Kate Hargreaves[2], Catherine Higham[3], Catherine Duckett[1], Sarah Forbes[1] and Katherine Rawlinson[1]

Abstract

There is a wealth of innovation in microbiology outreach events globally, including in the setting where the public engagement is hosted. Previous data indicate an underrepresentation of marginalized ethnic groups attending UK science-based public engagement events. This project engaged our student cohort, encompassing a diverse range of ethnic groups, to create an integrated art and science event within an existing series of adult education evenings. The study's objectives were to increase the proportion of visitors from marginalized ethnic groups and to gain a greater understanding of the impact of the event on the visitors' reported science capital. The participants' demographics, links to our students and University, and detailed impact on participants' science capital of the event were determined through analysis of exit questionnaires. There was an increase in the proportion of marginalized ethnic group visitors compared to similar previous events. A higher proportion of visitors from marginalized ethnic groups had links with our students and University compared to white/white British visitors. Elements of the exit questionnaire were mapped to the science capital framework and participants' science capital was determined. Both ethnically marginalized participants and white/white British visitors showed an increase in science capital, specifically dimensions of science-related social capital and science-related cultural capital, after the event. In conclusion, our study suggests that a student-led blended art and science public engagement can increase the ethnic diversity of those attending and can contribute towards creating more inclusive public engagement events.

DATA SUMMARY

The data presented in this study may be available on request from the corresponding author. The data are not publicly available due to ethical restrictions.

INTRODUCTION

The UK National Co-ordinating Centre for Public Engagement defines public engagement as 'the myriad of ways in which the activity and benefits of higher education and research can be shared with the public'. Engagement is by definition a two-way process, involving interaction and listening, with the goal of generating mutual benefit. The increasing narrative to take public engagement out into individual communities has led to the establishment of creative and innovative events with reported success in reaching audiences who typically would not engage with science activities [1–4].

The public's engagement in science, trust in scientists and trust in scientists' work has individual and societal benefits [5, 6]. The public engaging with science allows individuals to make informed decisions around their own lives, and more widely this decision-making impacts society as a whole. When sections of the community do not trust scientists there is often a negative impact for that group of society. For example, vaccine hesitancy amongst subgroups within the population,

Received 02 December 2022; Accepted 07 July 2023; Published 29 August 2023
Author affiliations: [1]Biomolecular Sciences Research Centre, Department of Biosciences and Chemistry, Sheffield Hallam University, Sheffield, UK; [2]Emergency Department, Sheffield Teaching Hospitals, Sheffield, UK; [3]Department of Landscape Architecture, University of Sheffield, Sheffield, UK.
***Correspondence:** Melissa M. Lacey, m.lacey@shu.ac.uk
Keywords: public engagement; science capital; marginalized ethnic groups; student-led; impact; science art.
Supplementary materials are available with the online version of this article.

University Student-led Public Engagement Event: Increasing Audience Diversity and Impact in a Non-Science Space

Melissa Lacey[1]*, Kelly Capper-Parkin[1], Rachel Schwartz-Narbonne[1], Kate Hargreaves[2], Catherine Higham[3], Catherine Duckett[1], Sarah Forbes[1] and Katherine Rawlinson[1]

[1] Biomolecular Sciences Research Centre, Department of Biosciences and Chemistry, Sheffield Hallam University, Sheffield, UK
[2] Emergency Department, Sheffield Teaching Hospitals, Sheffield, UK
[3] Department of Landscape Architecture, University of Sheffield, UK

*Corresponding author - Mel Lacey m.lacey@shu.ac.uk

Abstract

There is a wealth of innovation in microbiology public engagement events globally, including in the setting where the public engagement is hosted. Previous data indicates underrepresentation of marginalised ethnic groups attending UK science-based public engagement events. This project engaged our student cohort, encompassing a diverse range of ethnic groups, to create an integrated art and science event within an existing series of adult education evenings. The study's objectives were to increase the proportion of visitors from marginalised ethnic groups and to gain a greater understanding of the impact of the event on the visitors' reported science capital. The participants' demographics, links to our students and University, and detailed impact on participants' science capital of the event were determined through analysis of exit questionnaires. There was a 2-fold increase in the proportion of marginalised ethnic group visitors compared to similar previous events. A higher proportion (4-fold) of visitors from marginalised ethnic groups had links with our students and University compared to white/white British visitors. Elements of the exit-questionnaire were mapped to the science capital framework and participants' science capital determined. Both ethnically marginalised participants and white/white British visitors showed an increase in science capital, specifically dimensions of science-related social capital and science-related cultural capital, after the event. In conclusion, our study suggests that a student-led blended art and science public engagement can increase the ethnic diversity of those attending and can contribute towards creating more inclusive public engagement events.

Key words: public engagement, science capital, marginalised ethnic groups, student led, impact, science art.

Introduction

The UK National Co-ordinating Centre for Public Engagement defines public engagement as "the myriad of ways in which the activity and benefits of higher education and research can be shared with the public. Engagement is by definition a two-way process, involving interaction and listening, with the goal of generating mutual benefit. The increasing narrative to take public engagement out into individual communities, has led to the establishment of creative and innovative events with reported success in reaching audiences who typically would not engage with science activities (Dallas, 2006, Duckett et al., 2021, Leão & Castro, 2012, Paul & Motskin, 2016).

The publics' engagement in science, trust in scientists, and trust in scientists' work, has individual and societal benefits (Llorente et al., 2019, Stilgoe et al., 2014). The public engaging with science allows individuals to make informed decisions around their own lives, and more widely this decision-making impacts society as a whole. When sections of the community do not trust scientists there is often a negative impact for that group of society. For example, vaccine hesitancy amongst subgroups within the population, including ethnic minority communities during the Covid-19 pandemic (Ala et al., 2021), is a significant health threat globally (WHO). Whilst the science-societal relationship is complex, public engagement events give science a platform to create a dialogue between scientists and the public; however, we must ensure that events are accessible to all.

Public engagement strategies aspire to engage with groups that fully represent society (Canfield et al., 2020, Canovan, 2019). Race and ethnicity-based inaccessibility and misrepresentation is reported to be an important barrier in engagement with science events (Dawson, 2018). Communities that scientists find difficult to engage are consistently underrepresented in the visitor demographics at such events, including marginalised ethnic groups (Duckett et al., 2021, Nielsen et al., 2019). This highlights the importance of culturally appropriate platforms. Inclusive science communication can help societal progress by addressing the inequitable distribution of and engagement in science (Canfield et al., 2020). Subsequently, the development of successful and inclusive public engagement models could allow practitioners to rethink approaches to public engagement activities.

A sense of belonging

People with a strong science identity, such as those who identify themselves as a "science person", are more likely to feel a sense of belonging in and/or amongst science (Chen et al., 2021, Rainey et al., 2018). A person's sense of belonging is key to their likelihood to seek out, stay, and succeed in a space. This holds for scientific communities, where people's perception of themselves as valued community members affects their attainment and retention (Lacey et al., 2022, Lewis et al., 2016). People from underrepresented groups tend to feel a lower sense of belonging in science (Mooney & Becker, 2020, O'Brien et al., 2020, Rainey et al., 2018) and report increased accessibility barriers leading to social exclusion from engagement with science public engagement events (Dawson, 2018). Interventions which increase the sense of belonging in a member of an underrepresented or disadvantaged group can increase engagement and attainment in science (Chen et al., 2021, LaCosse et al., 2020, Murphy et al., 2020).

Role models can play key roles in establishing a sense of belonging in members of underrepresented groups (Lewis et al., 2016). Exposure to similar role models in science

helps members of underrepresented groups overcome stereotypes that science is not "for them", and thus helps develop their science identity (Dennehy & Dasgupta, 2017, Schinske et al., 2016, Shin et al., 2016). While role models can be a factor in a person's sense of belonging, this effect varies depending on the similarity of the role model, with role models perceived as relevant and compatible with a person's identity more likely to have a positive impact on that person (Rosenthal et al., 2013, Shin et al., 2016, Stout et al., 2011).

Aim

Building on our previous work undertaking public engagement of science in a non-science space, this study aims to evaluate the impact of engaging a diverse body of student organisers and presenters in a blended science and art event hosted in a public gallery on the impact of the resulting audience demographic. Through evaluation of exit questionnaires, we wanted to gain a greater understanding of the impact of attending the event across different groups of visitors through a science capital lens.

Research Question 1: Can a student-led public engagement event attract an ethnically diverse audience, which is representative of the local regional demographic?

Research Question 2: Does the perceived learning gain and immediate reported impact on science capital differ between visitors from marginalised ethnic group and white/white British visitors?

Science Capital Framework

How well an individual feels connected with science and their feelings towards science can be explored through the science capital framework. Derived from the social theory of capital, science capital is described as the "science-related resources" to which an individual has access (Archer et al., 2015). Dimensions of science capital include science-related cultural capital, an individual's engagement and participation in science, and science-related social capital, such as who you know that works in science. With positive attitudes towards science being related to higher levels of science capital, using the lens of science capital can help to explain variable rates of participation in science across society including ethnically marginalised and socioeconomically disadvantaged communities (DeWitt & Archer, 2017).

There is a drive to build and enhance science capital amongst the public to allow continued societal support for science and widened engagement across the breadth of society (PAS 2019). Previously we have reported that both community (Duckett et al., 2021) and university-hosted (Rawlinson et al., 2021) events can increase knowledge and elements of science capital amongst participants, with significantly higher reported knowledge gain in visitors from low progression to higher education postcode areas (Rawlinson et al., 2021). These findings are mirrored within the literature, with several studies showing that through engaging with informal science activities many participants report an increase in their science capital and more positive attitudes towards science (Bryan et al., 2022, Roberts & Hughes, 2022). Unfortunately, we, and much of the science community, are still failing to attract audiences to events which are ethnically diverse and representative of society and thus those communities we find

harder to reach often have lower science capital (Archer et al., 2016, Duckett et al., 2021, Nielsen et al., 2019, Rawlinson et al., 2021). Science capital will be used as a framework to address the aims of this study,

Methods

Event

The "Art in Science" event was hosted at the Millenium Galleries in Sheffield City Centre. The event was a collaboration between Sheffield Hallam University and Sheffield Museums Trust. As with previous collaborative projects (Duckett et al., 2021) the Art in Science was a multifaceted, informal, one-off event, after the normal opening times of the museum and gallery space for those 16 years old and older. The event was predominately advertised by Sheffield Museums Trust, through their newsletter and social media platforms. As with previous events, the authors invited staff and students within the Department of Biosciences and Chemistry through email via the virtual learning platform. The science and art event could be viewed as three sections, the "art gallery", hand-on art in science activities and a mini-lecture series (Table 1, Figure 1). The Millennium Galleries provided exclusive tours of the exhibits and additional hands-on experiences including print making and felt crafts, inspired by the natural history collections of the museum. Undergraduate and postgraduate students were invited to the event both as volunteers and as visitors.

Table 1: Elements and activities at the Art in Science event

Element / activity	**Overview**	**resources**	**Student-led input**
Art Gallery			
Art in Science Exhibition (Figure 1a)	Single, striking images of research were displayed in an art gallery style.	High quality printed images and display boards.	PhD students presented representative images from their work and held conversations with the

			public on their research topics.
"Science Roots" agar art (Figure 1b)	Agar art around the theme of "science roots" was displayed in a backlit box.	Nutrient agar, MacConkey agar, Mannitol salt agar, UTI brilliance agar. *Staphylococcus aureus SH1000*, *Staphylococcus epidermidis ATCC14990*, *Pseudomonas aeruginosa* PAO1 and *Escherichia coli* MG1655.	Final-year undergraduate students and MSc students from the Department of Biosciences and Chemistry were given the opportunity to make agar art under the theme of "scientific roots".
Black tent art (Figure 1c)	Luminescent agar art was displayed in a black-out tent with UV light sources.	Marine agar and *Vibrio harveyi BAA-1116*	Students helped produce luminescent agar art to display in the black out exhibition.
The Artist in Residence Exhibition (Figure 1e)	A series of projected images and short animations inspired by soil microbiology research.	AV equipment for projection. Digital drawings using iPad. Watercolour paper, acrylic inks, Indian ink, pencils, soluble graphite.	Prior to the event, the artist had visited MChem students in the microbiology research laboratories to find out more about and gain hands-on experience of the project before creating the exhibition pieces.

Hands-on activities			
Building a community (figure 1g)	Visitors helped mature the microcolony of knitted and crocheted bacteria into a woolly, mature, polymicrobial biofilm with pom poms.	Wool, scissors and cardboards.	Students volunteered to help run the stand and discuss the concept of microbial biofilms with event attendees.
Reinventing life drawing	Participants swabbed their own oral microbiome and then drew onto agar plates.	Dry, sterile swabs and nutrient agar plates (incubated overnight at 37°C after event).	Students volunteered to help run the stand and used the activity to engage members of the public on discussions around the human microbiome. They also took photos of and shared the art on social media for visitors to see after the event (Instagram, @SHU.micro).
Pastel pathogens	Visitors observed a range of pathogens under the microscope, creating a pastel picture in response.	Light microscopes and gram-stained bacterial slides. Pastels and pastel paper.	Students volunteered to help run the stand and discussed concepts in microbial pathogenesis and infection control with event attendees.
Soil microbiome project	Participants explored the impact of pollution on soil through colour-dots	Acrylic paint, small brushes, acrylics paper.	Students volunteered to help run the stand and discuss the topic of soil pollution and environmental

	paintings of soil components.		microbial communities with attendees.
Mini lecture series (Figure 1d)			
Mini lectures	The event offered a mini-lecture series of talks from academic staff and PhD students from the department of Bioscience and Chemistry focused on their areas of research interest	AV equipment.	PhD students were given the opportunity to present their research projects.

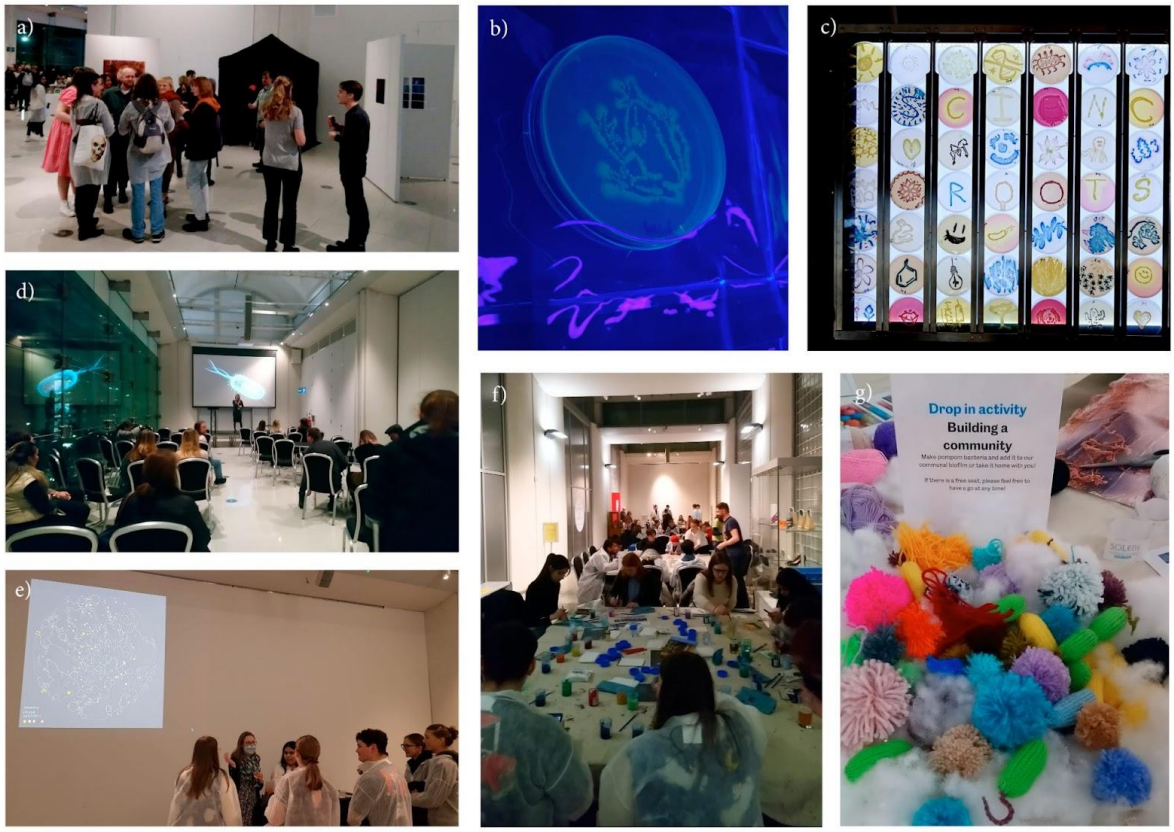

Figure 1: Elements of Art in Science event. (a) Science image exhibition area with visitors discussing research topics with doctoral students, (b) student designed fluorescent bacteria agar art housed in the blackout tent, (c) "Science Roots" light box exhibition where undergraduate students created agar art with the theme of what inspires them

to study science, (d) mini-lecture series which ran throughout evening, (e) the artist in residence created a visual projection on the main wall of the exhibition after shadowing student researchers undertaking microbiology research (f) multiple hands-on creative art activities based around microbiology research and (g) visitor-created piece of individually crafted bacteria forming a biofilm.

Data collection

Exit point feedback from visitors was collected using a modified version of our previously designed mixed-methods questionnaire (Duckett et al., 2021). The paper questionnaire (supplementary materials) was designed to be quick to complete to maximise completeness by participants. It consisted of a combination of simple profiling tick boxes, Likert-style responses, and free text comment boxes. After the event, the questionnaire data was manually transferred into Excel for analysis.

Data analysis: visitor demographic, enjoyment and perceived learning

Open coding was used to code free text responses of the question "Tell us something from your visit that you have found particularly interesting", followed by thematic analysis and categorization into themes (Byrne, 2022).

Visitors self-identified ethnicity within the categories of Asian/Asian British, black/black British, mixed ethnicity, other and white/white British. These categories of ethnicity were taken from the Sheffield 2011 Census (Office for National Statistics, 2011) to allow comparison of the ethnicity of visitors with the Sheffield region and previous collaborative events between the research team and Sheffield Museums Trust (Duckett et al, 2021). Ethnicity marginalised groups is defined within this piece of work as participants within black/black British, Asian/Asian British, mixed ethnicity and other categories.

As a measure of the perceived learning by visitors, participants were asked to rate their pre- and post-visit knowledge of the six key microbiology event topics: microbes in the body, microbes that cause disease, microbes in the soil, biofilms, antibiotics, and DNA. Scores were subsequently added to create an overall individual perceived learning score for each participant. Differences between groups was determined by Wilcoxon rank sum test, statistical analysis was performed in R.

Data analysis: science capital

Participant's existing and expected-future engagement with science were used as a measure of event impact on science capital. Nine Likert-style engagement questions were designed to cover key dimensions of science-related capital, namely scientific literacy, science-related attitudes, values and dispositions, science media consumption, participation in informal science events, and talking about science in everyday life (Archer et al., 2016). Knowledge about the transferability of science was not included in this study as it focuses on the knowledge of science qualifications linking to jobs which was not touched upon in the event. In addition, participants were asked about their highest level of science qualification and whether they and/or someone close to them worked in the science industry as additional measures of science-related social capital (Archer et al., 2015) (Table 2).

Table 2: Framework for Science Capital data collection and analysis. Individual elements of science capital were mapped to question(s) on the exit questionnaire and each element analysis to give a score from 0-1. Science related social and cultural capital scores were determined from the respective elements and given a score from 0-1 and finally overall science capital score was determined from the science related social and cultural capital score and put on a 0-1 scale.

	Question(s)	Analysis. N.B. number is initial score allocated to each question response
1 Science capital	N/A	1.1 and 1.2 scores
1.1 Science related social capital	N/A	1.1.1 - 1.1.3 scores
1.1.1 Family science skills, knowledge and qualifications	a) "Do you work in science?" b) "What is your highest qualification"	a) 1 - No, 5- Yes b) 1- GSCE/O level, 2 - A level or equivalent, 3 - BSc, 4 - Masters, 5 - PhD.
1.1.2 Knowing people in science-related roles	"Do any of your family or friends work in science?"	1 - No, 5- Yes
1.1.3 Talking about science in everyday life	"I regularly discuss science with family and friends"	Likert Scale of 1- strongly disagree to 5- strongly agree: before and after event
1.2 Science related cultural capital	N/A	1.2.1-1.2.5 scores
1.2.1 Scientific literacy	a) "How much do you know about the following, before visiting and after visiting… Microbes in the body, Biofilms, DNA, Microbes that cause disease, Microbes in the soils, antibiotic resistance" b) "I feel confident talking with others about science"	a) Likert Scale of 1- nothing to 5- A lot: before and after event for each topic. b) Likert Scale of 1- strongly disagree to 5- strongly agree: before and after event
1.2.2 Science-related attitudes, values and dispositions	a) "Science is useful to me in my daily life" b) "Science is important in society" c) "I believe science is everywhere" d) "Scientists do valuable work"	a-d) Likert Scale of 1- nothing to 5- A lot: before and after event for each question.
1.2.3 Knowledge about the transferability of science	Not included in questionnaire	N/A
1.2.4 Science media consumption	"I actively engage with/look for books/magazines/TV or internet content about science"	Likert Scale of 1- nothing to 5- A lot: before and after event for each question.
1.2.5 Participation in out-of-school science learning contexts	"I regularly (at least twice a year) visit science museums, festivals and/or science-focused events"	Likert Scale of 1- nothing to 5- A lot: before and after event for each question.

Scores of each question on the questionnaire were scaled to a value between 0 and 1. Likert scale responses were scaled to a range of 0.2 – 1, e.g., a Likert scale score of 4 translated into 0.8. "Yes" or "No" responses were given the values of 1 or 0 respectively. The mean of the scaled scores was used where multiple questions relate to a single dimension. The score of cultural and social capital was an average of the dimensions within them. Scores of each capital and dimension were used to create a heat map, the colours of which were used to colour the hierarchy graph. Dimensions were compared before and after the event by Wilcoxon signed rank tests and between ethnicity groups at each time point by Mann-Whitney tests. Data analysis was performed in Prism (GraphPad Software, USA).

Ethics

Ethics for this study were acquired through the Faculty of Health and Wellbeing and Life Sciences Ethics Committee following the Sheffield Hallam University Research Ethics Policy: ER10872482. Ethical approval was given after initial scrutiny as no identifiable, confidential or controversial information would be collected.

Results

To determine the impact of the Art in Science event on participants' science capital, as well as the uptake and impact of visitors from marginalised ethnic groups, exit questionnaires were undertaken. The event had 282 visitors with 123 completing an exit questionnaire, thus a 44% uptake.

An individual's learning is positively linked to their engagement and enjoyment of a topic or activity (Blumenfeld et al., 2005). The question "tell us something from your visit that you have found particularly interesting" was thematically analysed to determine aspects of the event that participants found engaging (Table 3).

Table 3: Qualitative analysis themes of participants' interest. Answers to the question "Tell us something from your visit that you have found particularly interesting" events were blinded, coded into each category and enumerated. Example comments are given for each theme (n = 104).

Themes	Example	Number of responses
Specific scientific/factual learning points	*"Bioluminescence", "background microbes", "antibiotic resistance"*	45
Talks/lectures	*"Oral cavity", "bone structure"*	7
Opportunity to learn something new	*"Excellent science communication to a non-scientist", "translating science"*	5
Opportunity to be creative/science inspiring art	*"Amazing shapes and patterns of the micro world", "thrush looks like grapes"*	25
Positive overall experience	*"Love the lady studying mine water", "passion from the presenters"*	7
Interactive activities	*"Using a microscope", "handling fossils"*	11

The responses identify specific scientific and factual learning as the most interesting element of the Art in Science event followed by the opportunity to be creative and artistic. There was no difference in the theme of response based on participants' ethnicity (data not shown).

Student involvement putatively increased the number of visitors from marginalised ethnic groups

An aim of the project was to increase the proportion of visitors from marginalised ethnic groups at the event. The ethnicity of participants of the Art in Science was compared to previous collaborative events with Sheffield Museums Trust and the Sheffield region (Table 4).

Table 4: Comparison of participant ethnicity at the Art in Science event compared to previous collaborative events and Sheffield region. Art in Science (n = 123), The Horror Within and The Science of Science Fiction with Sheffield Museums Trust (Duckett et al., 2021) and Sheffield Census (Office for National Statistics, 2011). Note where percentages do not equal 100% for an event, the absent participants chose to not disclose their ethnicity.

Ethnicity	Art of Science (2022) (n = 123)	The Horror Within (2017) (n = 51)	The Science of Science Fiction (2018) (n = 51)	Sheffield Census (2011) (n = 552, 698)
Asian/Asian British	13.1%	4.1%	5.8%	8.0%
Black/Black British	2.5%	0.0%	0.0%	3.6%
Mixed	3.3 %	2.0%	5.8%	2.4%
Other	1.6%	0.0%	0.0%	2.2%
White/White British	77.9%	93.9%	88.5%	83.7%

The demographic of visitors at the Art of Science event was markedly different compared to previous blended art and science evenings. The Art in Science event had an increase in the proportion of all marginalised ethnic groups apart from mixed ethnic when compared to the Science of Science Fiction event. The most marked increase was the increase in Asian/Asian British participants, increasing to 13.1% compared to 4.1% and 5.8% for the previous events. There was also an increased proportion of Asian/Asian British and mixed ethnicity participants compared to the Sheffield region, although black/black British and other ethnicities were underrepresented at the Art in Science event compared to the Sheffield region.

To determine if the increase in the proportion of participants at the Art in Science event from marginalised ethnic groups was due to the social-capital impact of increased student-led participation, the “How did you hear about the event?” question was analysed (Table 5).

Table 5: Comparison of how people heard about the Art in Science event. Due to the sample size, all marginalised ethnic participants were analysed together (all responses n = 123; marginalised ethnic participant responses n= 26, white/white British n = 95).

	Museums Sheffield Trust website/poster	Sheffield Hallam website/poster	Social media	I know someone involved in the event	Friend/family	Other
Total	12 (10%)	10 (8%)	37 (30%)	23 (19%)	30 (24%)	11 (9%)
Ethnically marginalised groups	3 (12%)	5 (19%)	7 (27%)	6 (23%)	5 (19%)	0
White/white British	9 (9%)	4 (4%)	29 (31%)	17 (18%)	25 (27%)	11 (11%)

Participants from marginalised ethnic groups were slightly less likely to hear through social media than white/white British participants (27% and 31% respectively), and slightly more likely to attend the event through someone involved (23% and 18% respectively). Participants from marginalised ethnic groups were much more likely to hear from a Sheffield Hallam University website or poster than white/white British participants (19% and 4% respectively).

Impact of attending the event was seen across all visitors, with differences observed between white/white British and marginalised ethnic group participants

The main scientific content for the Art in Science event was broadly categorised into six themes: microbes in the body, biofilms, DNA, microbes that cause disease, microbes in the soils, and antibiotic resistance. To determine perceived learning at the event, participants were asked “How much do you know about the following” for each theme, before and after the event on a scale of 1 (nothing) to 5 (a lot) (Figure 2).

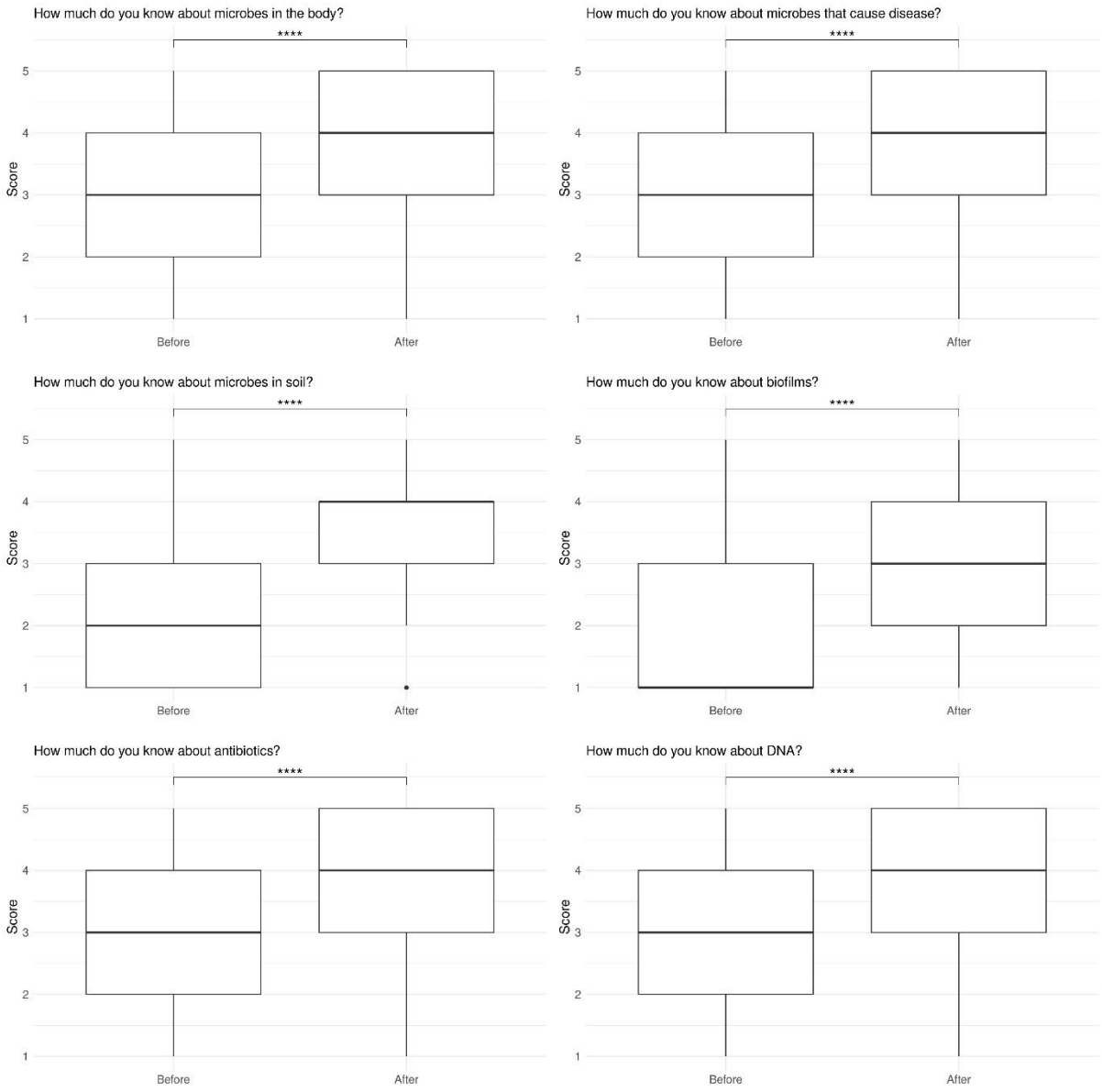

Figure 2: Perceived knowledge before and after of different areas. The amount of perceived knowledge participants gained during the Art of Science event in the six science content areas was ranked from 1 (nothing) to 5 (a lot). Data shown in median values at the centre of the plot, first and third quartiles complete the plot and the whiskers represent 1.5*IQR from quartiles. Outlying points are represented as individual points (n = 123). **** indicates $p \leq 0.0001$ in a Wilcox signed rank test.

Exit questionnaire analysis showed an increase in perceived learning by participants in all main themes of the Art in Science event. There was no difference in the perceived learning of participants from marginalised ethnic groups compared to their white/white British counterparts (data not shown). Due to the nature of data collection authors were unable to determine if participants perceived learning increases were accurate.

Perceived learning forms part of the science capital framework. Using the framework outlined in Table 1, participants' exit questionnaires were analysed to determine differences between marginalised ethnic participants and white/white British participants' science capital. The framework allows investigation of two elements of

science capital, firstly, participants pre-existing science capital and secondly, the impact of the event on participants science capital (Figure 3).

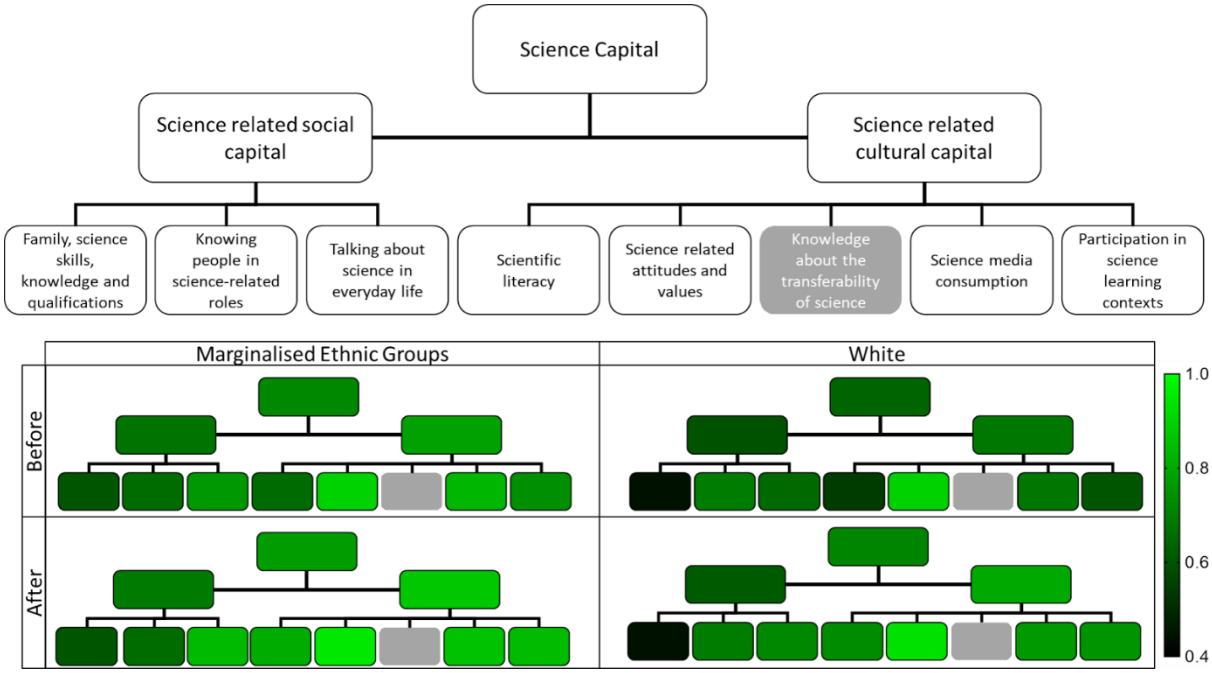

Figure 3: Impact of attendance at the Art of Science event on science capital and related dimensions. The mean score of each dimension was grouped by ethnicity and before/after attendance at the event higher dimensions were an average of sub-dimensions. The range of results was between 0.44 and 0.94, indicated by a gradient scale from black to green. Hierarchy plots mimic the layout of the top plot of science capital dimensions (n = 123).

Participants' pre-existing science capital: No difference in pre-existing overall science capital and science-related social capital was observed between marginalised ethnic participants and white/white British participants. Participants from marginalised ethnic groups had a higher pre-existing science-related cultural capital score than those from white/white British backgrounds ($p < 0.05$, Mann Whitney test). Within the individual elements of science related social capital, participants from marginalised ethnic groups had a higher score in "family, science skills, knowledge and qualifications" than those from white/white British backgrounds ($p < 0.05$, Mann Whitney test). There was no statistically significant difference in the remaining individual elements. Within the individual elements of science related cultural capital, participants from marginalised ethnic groups had a higher score in "scientific literacy", "science media consumption", and "participation in science learning contexts" than those from white/white British backgrounds ($p < 0.05$, Mann-Whitney test). There was no statistically significant difference in "science related attitudes and values" and it is worth noting that this element scored the highest across the framework analysis.

Impact of the event on participants' science capital: Participants from both marginalised ethnic backgrounds and white/white British backgrounds reported an

increase in their overall science capital after the event. They also reported an increase in both its components, science-related social capital, and science-related cultural capital ($p < 0.05$, Wilcoxon matched pairs signed rank test). Within the individual elements of science-related social capital, both groups of participants had a higher score in "talking about science in everyday life" after the event ($p < 0.05$, Wilcoxon matched pairs' signed rank test). There was no statistically significant difference in the remaining individual elements between elements based on relationships. Within the individual elements of science-related cultural capital, both groups of participants had an increase in "scientific literacy" and "participation in science learning contexts" ($p < 0.01$, Wilcoxon matched pairs signed rank test). Finally, white/white British participants reported an increase in "science-related attitudes, values and dispositions" and "science-media consumption" ($p < 0.01$, Wilcoxon matched pairs signed rank test) due to the event, whereas no difference was seen for marginalised ethnic groups.

Discussion

Drawing on the previous success of blended arts and science events, a science public engagement event was hosted in a non-science space. Our previous events, also hosted in a museum setting, engaged an "non science" audience although participants from marginalised ethnic group where underrepresented compared to the local population (Duckett et al., 2021); consistent with the UK national picture for museum attended (Department of Digital Culture, Media and Sport, 2016, Medoza, 2017). This study employed a university student-led approach to the Art in Science event, aimed to increase the ethnic diversity of those attending through exit questionnaires and qualitative data analysis. Our study also explored event impact on visitors from marginalised ethnic communities and white/white British communities.

With continued underrepresentation of visitors from marginalised ethnic groups at science public engagement events, inequality in science public engagement remains (Canfield et al., 2020). Key barriers to marginalised and minoritised individuals and communities are reported as a lack of a sense of belonging, accessible role models, and low levels of existing science capital (Chen et al., 2021, DeWitt & Archer, 2017, Lewis et al., 2016). The student body in the Department of Biosciences and Chemistry at Sheffield Hallam University has a higher representation of individuals from marginalised ethnic groups (~30%) than the Sheffield City Region population (16.3%) (Duckett et al., 2021). Our approach was to engage these students in the organisation, preparation and delivery to increase the ethnic diversity of those attending the Art in Science event. Briefly, this approach draws upon existing literature around relatable role models increasing the sense of belonging and engagement in science amongst minoritised and marginalised individuals and groups (Chen et al., 2021, Lewis et al., 2016, Shin et al., 2016).

Exit questionnaires were used to capture the demographics of participants and the immediate impact of the event. Previous similar events undertaken by the research team have echoed the national picture, which sees white individuals more likely to visit museums and science spaces than those from marginalised ethnic groups (Archer et al., 2012, Department of Digital Culture, 2016, Duckett et al., 2021). The author's previous

events (Horror Within and the Science of Science Fiction: Duckett et al., 2021) where both hosted in the same gallery space as the Art in Science, were both one off, 16+ events and both blended art and sciences. The Art in Science event observed an increase in the proportion of visitors from marginalised ethnic groups (20.5%) in comparison to our previous bended art and science events (6.1% in 2017 and 11.6% in 2018) (Duckett et al., 2021). This was also above that of the Sheffield City region at 16.3% for marginalised ethnic citizens (Office of National Statistics, 2011). The methods to generate these data was the same for all three events, a paper exit questionnaire with the same categories for ethnicity self-selection which was based on the categories within the 2011 National census. The ethnic diversity of day visitors to the Millenium Galleries in 2023 was similar to the overall Sheffield region, however data for the more comparable evening events was not collected (unpublished data curtesy of Sheffield Museums Trust).

Overall, social media led as the most common way visitors had heard about the event. However, participants from marginalised ethnic groups were more likely than white/white British participants to have heard about the event through someone involved or via Sheffield Hallam advertising. The increase in ethnic diversity was not equivalent across all ethnic groups, with Asian/Asian British having the higher representation at the event compared to the Sheffield Census. Interestingly, there is a higher proportion of Asian/Asian British students within our department than black/black British. Whether the increase in Asian/Asian British visitors is a direct result of this can only be speculated. Correlation does not equal causative, and our research of a university student-led art and science event, with a diverse student demographic and the subsequent increase in the ethnic diversity of attendees is an example of such. The comparison to previous events (Duckett et al., 2021) and the data around how different groups of visitors heard about the event adds circumstantial evidence to a causal link. It is tempting to speculate that students involved in the event, either in creating agar or as a volunteer, encouraged friends and family to attend, and those from minoritized ethnic groups with no direct link to the event team would perhaps feel more welcome as they could see their peers involved and thus the space was more accessible. To strengthen these hypothesis, further events could include short exit interviews with visitors to further explore their reasons for attending the event.

Others have reported that there can be barriers to engagement within event exhibits for minority ethnic visitors, for example due to language, which ultimately lead to the feeling of not belonging and unease (Dawson, 2018).There was no difference observed at this event in the reported knowledge gain or interests between the Art in Science minoritised ethnic and white/white British visitors. It is acknowledged our minoritised ethnic group visitors had higher existing science education, which potentially impacted on the responses to these questions. However, working with our diverse student organisers to prepare and deliver the event could have contributed towards making an inclusive accessible event and minimised any implicit biases in design which may be hindering rather than aiding in promoting inclusivity.

An individual's relationship with and attitude towards science is influenced by their science capital (Archer et al., 2015). Understanding levels of science capital amongst different groups of the population can help explain social inequalities in science participation (Archer et al., 2015, DeWitt & Archer, 2017). Through participant exit

questionnaire responses we found no difference in the overall existing (pre-event) science capital scores between marginalised ethnic groups and white/white British visitors. Further analysis of the dimensions of science capital explored in the questionnaire did identify higher cultural capital scores (across all elements) in marginalised ethnic visitors when compared to white/white British visitors. Visitors from marginalised ethnic groups also reported knowing more people working in science and holding higher level science qualifications than white/white British visitors. It is encouraging that our study suggests that students, as a diverse organisation and presenting body, can increase ethnic diversity at a science-based event, however the resulting participants from marginalised ethnic groups have a higher existing level of some elements of science capital before attending than white/white British visitors. We have previously shown that hosting a blended science and art event in a non-science space can attract and engage visitors who typically do not engage with science (Duckett et al 2021) and whilst our current study suggests an approach which can also increase ethnic diversity, these visitors are already more engaged science through their existing reported science capital. Dawson (2016) argues that science communication is not open to everyone due to social advantage and structural inequalities, meaning that events remain invisible to some groups in society. Our study suggests that whilst involving diverse multiple voices in planning and delivery through recruitment of our student body could broaden the reach of science public engagement events in non-science spaces such as museums, additional barriers are preventing societal groups of minority ethnic citizens with low levels of existing science engagement from participating.

Collective science capital scores for participants of both marginalised and white ethnic backgrounds reported as being increased after visiting the event. With participants reporting that they were more likely to talk about science in everyday life and participate in future science events, the Art in Science event successfully increased accessibility of science to all visitors. This equal impact gain across both white/white British and marginalised ethnic group participants, together with the knowledge gain and interest discussed earlier, suggests that our student-led event model is a move in the right direction of inclusive science public engagement.

Conclusion

A student-led Art in Science event was evaluated via exit-questionnaires. Ethnic diversity was increased amongst visitors compared to previous events by the group as well as the Sheffield region. A sizeable minority of participants, higher in ethnically marginalised groups, at the event reported attending due someone they knew was involved of through the university or through a university poster or website. Thus, it is tempting to speculate that the increase in ethnicity was in part due to an increase in the ethnic diversity of those involved in planning and organisation.

A science capital framework was used to gain a better understanding of the impact of the event on participants. Several pre-existing elements of science capital were higher in participants from marginalised ethnic groups than white/white British visitors. Overall reported science capital was increased in visitors irrespective of ethnicity and this increase was seen in discrete elements of science capital.

This student-led blended art and science event contributes towards creating a more inclusive science public engagement approach. However, complex barriers are still in

place surrounding participants from ethnicity marginalised groups attending public engagement events, and a greater understanding of the rich diversity within ethnicity marginalised groups will allow future events to engage more fully with diverse communities.

Funding information

Activities within the event were supported by the Society for Applied Microbiology Outreach and Engagement grant. Further activities were supported with funding from the Biomolecular Sciences Research Centre (BMRC), Sheffield Hallam University.

Acknowledgements
The authors would like to thank Sheffield Museums Trust and the Live Late team, especially Jessica Shipton and Brooke Hayes, and Sheffield Hallam University's Biomolecular Sciences Research Centre and Department of Biosciences and Chemistry, especially Nicola Aberdein, Muna Nuh Ali, Joseph Anslow, Yvonne Battle-Felton, Magnus Bertelsen, Sarah Boyce, Marjory Da Costa Abreu, Lucy Dascombe, Cristiana Ferreira de Matos, Alecia Hogan, Naomi Holmes, Katie Kennedy, Josh Millar, Keith Miller, Tim Nichol, Madalena De Oliveira, Nick Peake, Rebecca Sharpe, Prachi Stafford, Oana Voloaca, Rebecca Williams and Alex Williamson. Also, Sheffield Hallam University Biosciences and Chemistry students for the agar art and STEM ambassador volunteers for their support with the event.

Author contributions
Mel Lacey: conceptualization, funding acquisition, methodology, project administration, resources, data collection, formal analysis, writing – original draft, writing – review & editing
ORCiD 0000-0003-0997-0217 @MelMLacey

Kelly Capper-Parkin: conceptualization, funding acquisition, project administration, resources, formal analysis, writing – original draft
ORCiD 0000-0002-3831-3323 @kelly_beanzzz

Rachel Schwartz-Narbonne: resources, writing – original draft, writing – review & editing
0000-0001-9639-9252

Kate Hargreaves: formal analysis, writing – original draft
ORCiD 0000-0002-2714-0850

Catherine Higham: funding acquisition, resources, formal analysis
ORCiD 0000-0003-2489-9711
@CatherineHigham

Sarah Forbes: conceptualization, funding acquisition, project administration, resources, writing – review & editing
ORCiD 0000-0002-8361-6390 @SarahForzou

Catherine Duckett: methodology, data collection, writing – review & editing
ORCiD 0000-0002-6845-1890 @DuckettCJ

Katherine Rawlinson: conceptualization, methodology, writing – original draft, writing – review & editing
ORCiD 0000-0002-1055-6518 @KathyRawlinson

Conflicts of interest
The authors declare that there are no conflicts of interest.

Data Availability Statement

The data presented in this study may be available on request from the corresponding author. The data are not publicly available due to ethical restrictions.

References

Ala, A., Edge, C., Zumla, A., & Shafi, S. (2021). Specific COVID-19 messaging targeting ethnic minority communities. EClinicalMedicine, 35, 100862. https://doi.org/10.1016/j.eclinm.2021.100862

Archer, L., Dawson, E., DeWitt, J., Seakins, A., & Wong, B. (2015). "Science capital": A conceptual, methodological, and empirical argument for extending bourdieusian notions of capital beyond the arts. Journal of Research in Science Teaching, 52(7). https://doi.org/10.1002/tea.21227

Archer, L., Dawson, E., Seakins, A., & Wong, B. (2016). Disorientating, fun or meaningful? Disadvantaged families' experiences of a science museum visit. Cultural Studies of Science Education, 11(4), 917–939. https://doi.org/10.1007/s11422-015-9667-7

Archer, L., DeWitt, J., Osborne, J., Dillon, J., Willis, B., & Wong, B. (2012). Science Aspirations, Capital, and Family Habitus. American Educational Research Journal, 49(5), 881–908. https://doi.org/10.3102/0002831211433290

Blumenfeld, P. C., Kempler, T. M., & Krajcik, J. S. (2005). Motivation and Cognitive Engagement in Learning Environments. In The Cambridge Handbook of the Learning Sciences (pp. 475–488). Cambridge University Press. https://doi.org/10.1017/CBO9780511816833.029

Bryan, R., Gagen, M. H., Bryan, W. A., Wilson, G. I., & Gagen, E. (2022). Reaching out to the hard-to-reach: mixed methods reflections of a pilot Welsh STEM engagement project. SN Social Sciences, 2(2), 10. https://doi.org/10.1007/s43545-021-00311-6

Byrne, D. (2022). A worked example of Braun and Clarke's approach to reflexive thematic analysis. Quality & Quantity, 56(3), 1391–1412. https://doi.org/10.1007/s11135-021-01182-y

Canfield, K. N., Menezes, S., Matsuda, S. B., Moore, A., Mosley Austin, A. N., Dewsbury, B. M., Feliú-Mójer, M. I., McDuffie, K. W. B., Moore, K., Reich, C. A., Smith, H. M., & Taylor, C. (2020). Science Communication Demands a Critical Approach That Centers Inclusion, Equity, and Intersectionality. Frontiers in Communication, 5. https://doi.org/10.3389/fcomm.2020.00002

Canovan, C. (2019). "Going to these events truly opens your eyes". Perceptions of science and science careers following a family visit to a science festival. Journal of Science Communication, 18(02), A01. https://doi.org/10.22323/2.18020201

Chen, S., Binning, K. R., Manke, K. J., Brady, S. T., McGreevy, E. M., Betancur, L., Limeri, L. B., & Kaufmann, N. (2021). Am I a Science Person? A Strong Science Identity Bolsters Minority Students' Sense of Belonging and Performance in College. Personality and Social Psychology Bulletin, 47(4), 593–606. https://doi.org/10.1177/0146167220936480

Dallas, D. (2006). Café Scientifique—Déjà Vu. Cell, 126(2), 227–229. https://doi.org/10.1016/j.cell.2006.07.006

Dawson, E. (2018). Reimagining publics and (non) participation: Exploring exclusion from science communication through the experiences of low-income, minority ethnic groups. Public Understanding of Science, 27(7), 772–786. https://doi.org/10.1177/0963662517750072

Dennehy, T. C., & Dasgupta, N. (2017). Female peer mentors early in college increase women's positive academic experiences and retention in engineering. Proceedings of the National Academy of Sciences, 114(23), 5964–5969. https://doi.org/10.1073/pnas.1613117114

Department for Digital, Culture, Media & Sport Taking Part Survey 2016; Retrieved from. https://www.gov.uk/guidance/taking-part-survey#how-to-access-survey-data. Last accessed 22.11.22.

DeWitt, J., & Archer, L. (2017). Participation in informal science learning experiences: the rich get richer? International Journal of Science Education, Part B, 7(4), 356–373. https://doi.org/10.1080/21548455.2017.1360531

Duckett, C. J., Hargreaves, K. E., Rawson, K. M., Allen, K. E., Forbes, S., Rawlinson, K. E., Shaw, H., & Lacey, M. (2021). Nights at the museum: integrated arts and microbiology public engagement events enhance understanding of science whilst increasing community diversity and inclusion. Access Microbiology, 3(5), 000231. https://doi.org/10.1099/acmi.0.000231

Instagram, @SHU.micro, https://www.instagram.com/shu.micro/, last accessed 22.11.22.

Lacey, M. M., Shaw. H, Abbott. N, Dalton. C, Smith, D (2022). How students' inspirations and aspirations impact motivation and engagement in the first year of study. Education Sciences, in press

LaCosse, J., Canning, E. A., Bowman, N. A., Murphy, M. C., & Logel, C. (2020). A social-belonging intervention improves STEM outcomes for students who speak English as a second language. Science Advances, 6(40). https://doi.org/10.1126/sciadv.abb6543

Leão, M. J., & Castro, S. (2012). Science and rock. EMBO Reports, 13(11), 954–958. https://doi.org/10.1038/embor.2012.151

Lewis, K. L., Stout, J. G., Pollock, S. J., Finkelstein, N. D., & Ito, T. A. (2016). Fitting in or opting out: A review of key social-psychological factors influencing a sense of belonging for women in physics. Physical Review Physics Education Research, 12(2), 020110. https://doi.org/10.1103/PhysRevPhysEducRes.12.020110

Llorente, C., Revuelta, G., Carrió, M., & Porta, M. (2019). Scientists' opinions and attitudes towards citizens' understanding of science and their role in public engagement activities. PLOS ONE, 14(11), e0224262. https://doi.org/10.1371/journal.pone.0224262

Mendoza N. The Mendoza Review: An Independent Review of Museums in England London: Department for Digital, Culture, Media and Sport; 2017

Mooney, C., & Becker, B. A. (2020). Sense of Belonging: The Intersectionality of Self-Identified Minority Status and Gender in Undergraduate Computer Science Students.

United Kingdom & Ireland Computing Education Research Conference., 24–30. https://doi.org/10.1145/3416465.3416476

Murphy, M. C., Gopalan, M., Carter, E. R., Emerson, K. T. U., Bottoms, B. L., & Walton, G. M. (2020). A customized belonging intervention improves retention of socially disadvantaged students at a broad-access university. https://www.science.org

Nielsen, K., Gathings, M. J., & Peterman, K. (2019). New, Not Different: Data-Driven Perspectives on Science Festival Audiences. Science Communication, 41(2), 254–264. https://doi.org/10.1177/1075547019832312

O'Brien, L. T., Bart, H. L., & Garcia, D. M. (2020). Why are there so few ethnic minorities in ecology and evolutionary biology? Challenges to inclusion and the role of sense of belonging. Social Psychology of Education, 23(2), 449–477. https://doi.org/10.1007/s11218-019-09538-x

Office for National Statistics 2011 UK Census. https://www.ons.gov.uk/census/2011census/2011ukcensuses Last accessed 22.11.22.

PAS 2019. Public attitudes to science 2019. https://www.gov.uk/government/publications/public-attitudes-to-science-2019 Last accessed 22.11.22.

Paul, P., & Motskin, M. (2016). Engaging the Public with Your Research. Trends in Immunology, 37(4), 268–271. https://doi.org/10.1016/j.it.2016.02.007

Rainey, K., Dancy, M., Mickelson, R., Stearns, E., & Moller, S. (2018). Race and gender differences in how sense of belonging influences decisions to major in STEM. International Journal of STEM Education, 5(1), 10. https://doi.org/10.1186/s40594-018-0115-6

Rawlinson, K. E., Duckett, C. J., Shaw, H., Woodroofe, M. N., & Lacey, M. M. (2021). Family-focused campus-based university event increases perceived knowledge, science capital and aspirations across a wide demographic. International Journal of Science Education, Part B, 11(3), 273–291. https://doi.org/10.1080/21548455.2021.1971319

Roberts, K., & Hughes, R. (2022). Recognition Matters: The Role of Informal Science Education Programs in Developing Girls' Science Identity. Journal for STEM Education Research, 5(2), 214–232. https://doi.org/10.1007/s41979-022-00069-3

Rosenthal, L., Levy, S. R., London, B., Lobel, M., & Bazile, C. (2013). In Pursuit of the MD: The Impact of Role Models, Identity Compatibility, and Belonging Among Undergraduate Women. Sex Roles, 68(7–8), 464–473. https://doi.org/10.1007/s11199-012-0257-9

Schinske, J. N., Perkins, H., Snyder, A., & Wyer, M. (2016). Scientist Spotlight Homework Assignments Shift Students' Stereotypes of Scientists and Enhance Science Identity in a Diverse Introductory Science Class. CBE—Life Sciences Education, 15(3), ar47. https://doi.org/10.1187/cbe.16-01-0002

Shin, J. E. L., Levy, S. R., & London, B. (2016). Effects of role model exposure on STEM and non-STEM student engagement. Journal of Applied Social Psychology, 46(7), 410–427. https://doi.org/10.1111/jasp.12371

Stilgoe, J., Lock, S. J., & Wilsdon, J. (2014). Why should we promote public engagement with science? Public Understanding of Science, 23(1), 4–15. https://doi.org/10.1177/0963662513518154

Stout, J. G., Dasgupta, N., Hunsinger, M., & McManus, M. A. (2011). STEMing the tide: Using ingroup experts to inoculate women's self-concept in science, technology, engineering, and mathematics (STEM). Journal of Personality and Social Psychology, 100(2), 255–270. https://doi.org/10.1037/a0021385

WHO World Health Organisation https://www.who.int/news-room/spotlight/ten-threats-to-global-health-in-2019 Last accessed 15.5.23.